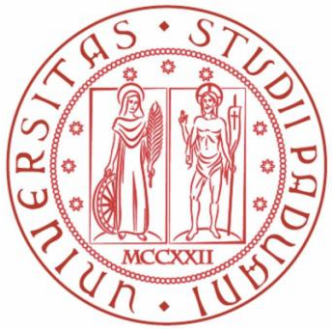

ČESKÉ VYSOKÉ UČENÍ TECHNICKÉ V PRAZE

UNIVERSITA' degli STUDI di PADOVA

Facoltà di Ingegneria

Corso di Laurea Magistrale in Ingegneria Civile

Curriculum Strutture

"Optimized design of single span steel girder railway bridges"

"Ottimizzazione di ponti ferroviari in acciaio a campata singola per piccole luci"

Supervisors: Prof. Ing. CLAUDIO MODENA

Doc. Ing. PAVEL RYJACEK

Student: ZUANNI RICCARDO 1063570

ACADEMIC YEAR 2014/2015

SUMMARY

SUMMARY OF THE FIGURES

1) State of the Art

1.1) Introduction

Engineers have been using steel in the construction of bridges since the second half of XIX century and many of these old structures are still in service, thanks to strict programs of maintenance, reinforcement and upgrade to suit changing requirements.

In modern days, a big share of the work which involves bridges is made to replace and upgrade existing structures, although some entirely new structures are being built on new railway alignments or routes.

For bridges on new alignments there's greater freedom with the design, both depth and structure typology may undergo substantial changes due to the wide range of possibilities in the choosing of track formation, clearances etc..

1.2) Requirements of the bridge profile

There are two key functional requirements for a railway bridge:

1. Provide support to the railway traffic and infrastructure throughout the life of the bridge
2. Provide adequate clearances between the structure and the traffic on and beneath it.

The first requirement can be expressed and defined by these sub-requirements:

- Strength and fatigue endurance
- Limit the deck deformation
- Robustness
- Durability

The second requirement is expressed in terms of "clearance gauges", which are defined and imposed by the authorities. There are three basic parameters that are involved to determine the form of construction of a railway bridge:

1. Available construction depth
2. Span and geometric configuration
3. Limitations which are imposed by the substructure

Construction Depth:

For some new bridges on new railway alignments, construction depth is not particularly constrained: the track level and the level and the road level beneath can be fixed at levels that suit the structure. In such cases, there are more options to choose the form of supporting girders and deck for maximum efficiency, economy and aesthetic considerations.

Replacement bridges are more likely to be constrained to a shallow construction depth, due to the need to maintain a clearance below and to avoid the lifting of the track. For short spans, deck-type structure can be entirely arranged within a shallow construction depth, but in many cases the only way to support the track is to arrange a shallow deck spanning transversely to longitudinal main girders either side of the track. This form is called "half through" construction or, for top-braced deep trusses over longer spans, "through construction".

Span and Geometric configuration:

The span has a direct influence on depth of the main girders of a bridge and thus on whether the girders can be arranged within the available construction depth. Nowadays is preferable to build continuous construction wherever it is possible, due to potential span skews to the abutments that support them.

It is obvious that considerations are needed as far as the interaction between the bridge and the track below.

Limitations which are imposed by the substructure:

In addition to the limitation in the replacement of existing bridges, replacement on an existing substructure often constrains the width of the bridge.

The strength and form of the abutments and of the intermediate supports are likely to have influence on the detailing of the bearings and beams.

SHALLOW DECK-TYPE BRIDGES

There are two forms of shallow slab construction (where the deck acts mainly as a beam spanning between abutments):

1. Solid steel slabs
2. Orthotropic decks

Solid Steel Slabs:

The simplest bridges comprise simply supported slabs spanning longitudinally between abutments. These solid steel slabs can be used to form such decks for railway bridges approximately up to 3m. The slab simply sits on the abutments on elastomeric strip bearings, it is approximately 200 or 250 mm thick and no fabrication is involved (other than cutting to size).

Their advantage is very low structure depth.

Orthotropic Deck:

For spans up to 9m, a very shallow structure depth of approximately 300 to 400mm can be achieved using a all-steel units spanning longitudinally between abutments.

This deck unit comprise a steel deck plate (20 or 25 mm thick) with T sections welded to its lower face (usually 600mm of spacing).

The deck unit is relatively flexible transversally, so robust kerbs of containment can be achieved using independent parapet walkway units located clear of the tracks; alternatively , parapets and robust kerbs can be provided by bolt-down steel units at either side of the deck (to resist the horizontal loads, transverse bracing must be provided between the T sections).

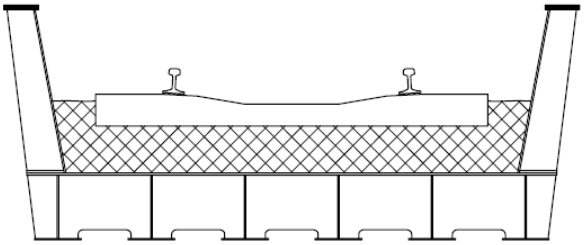

Figure 1

Example of orthotropic deck with robust kerbs.

As an example for this kind of shallow bridges, we can mention the *Eisenbahnbrücke Brunngraben* bridge, built in 2010. This structure is owned and designed by *OBB Infrastruktur AG*, and it is located in Ardning, Styria, Austria (Europe).

Total Length	16.04 m
Span	14.44 m
Girder Depth	1.253 m
Total Width	6.0 m

Figure 2 View of *Eisenbahnbrücke Brunngraben* bridge

Figure 3 View of *Eisenbahnbrücke Brunngraben* bridge

Figure 4 View of *Eisenbahnbrücke Brunngraben* bridge

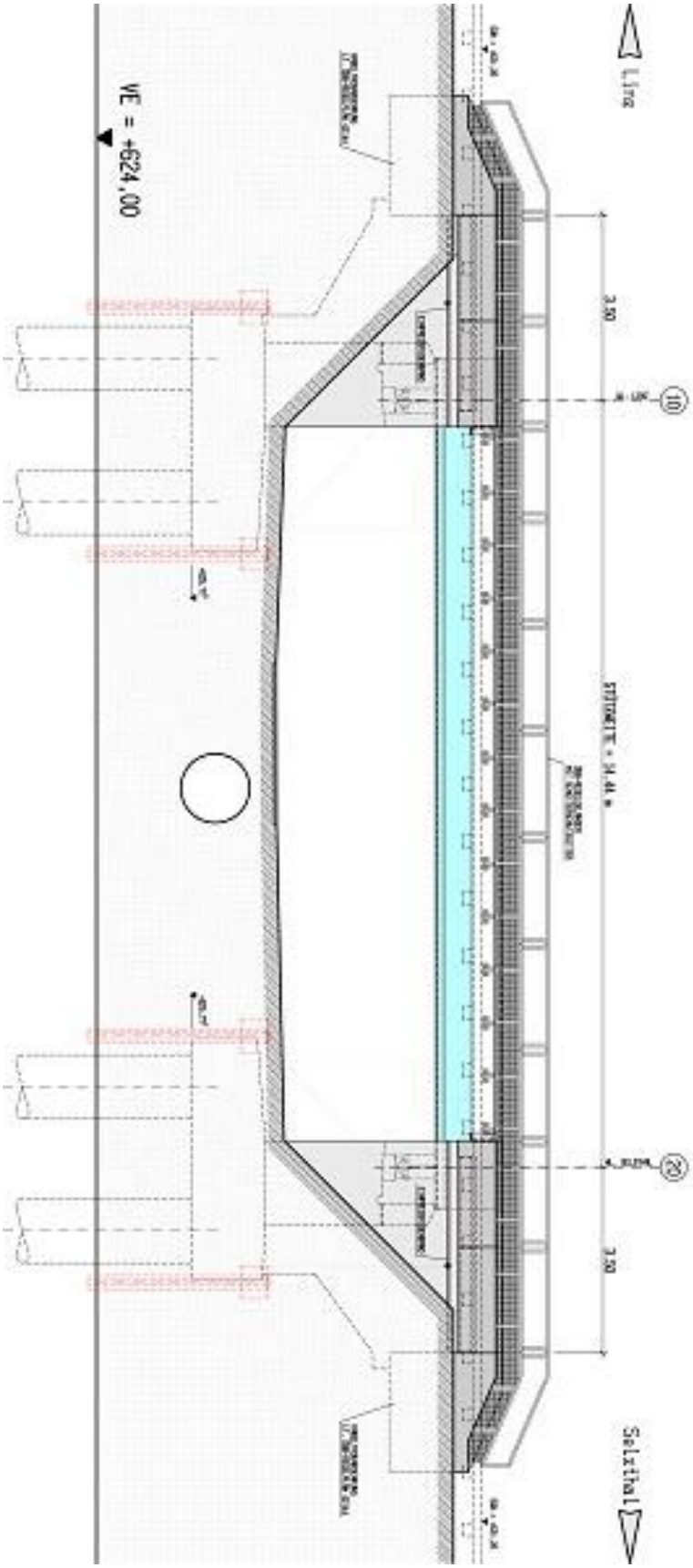

Figure 5

Lateral prospect of *Eisenbahnbrücke Brunngraben* bridge

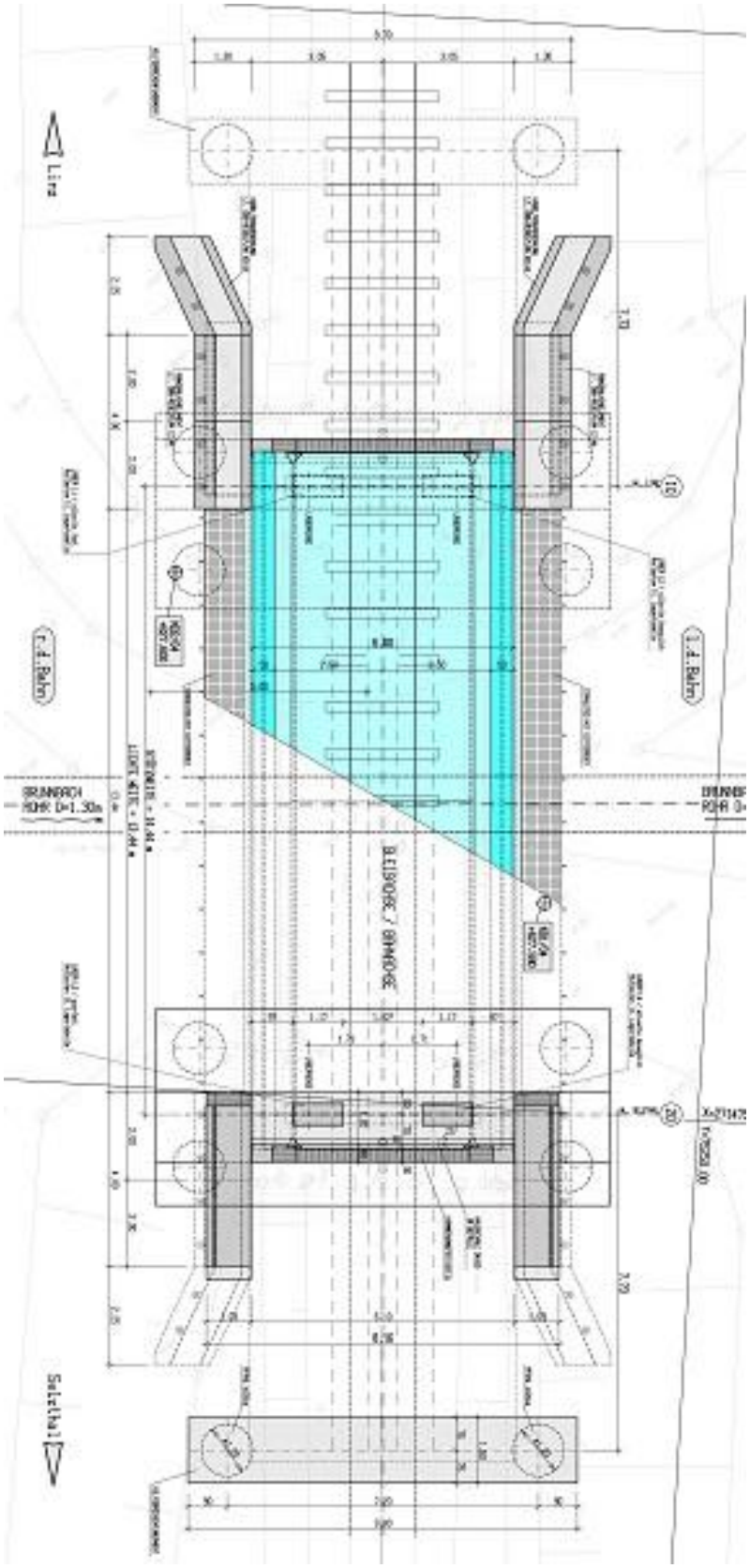

Figure 6

Top view of *Eisenbahnbrücke Brunngraben* bridge

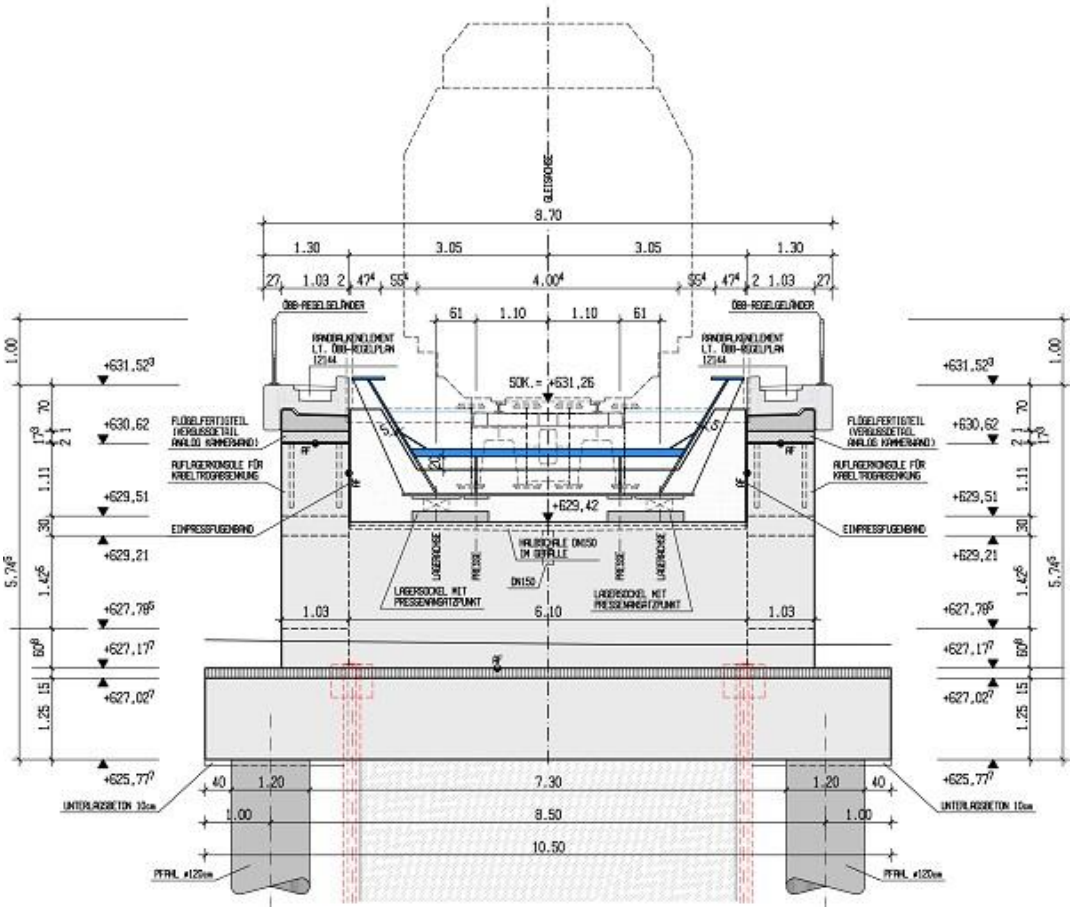

Figure 7

Cross section of *Eisenbahnbrücke Brunngraben* bridge on the supports

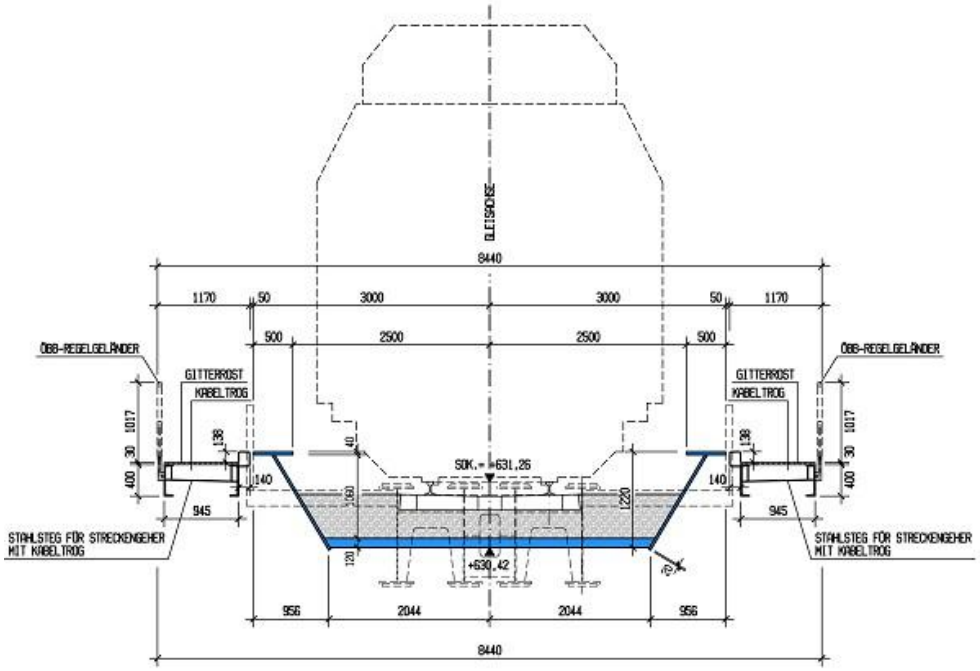

Figure 8

Cross section of *Eisenbahnbrücke Brunngraben* bridge

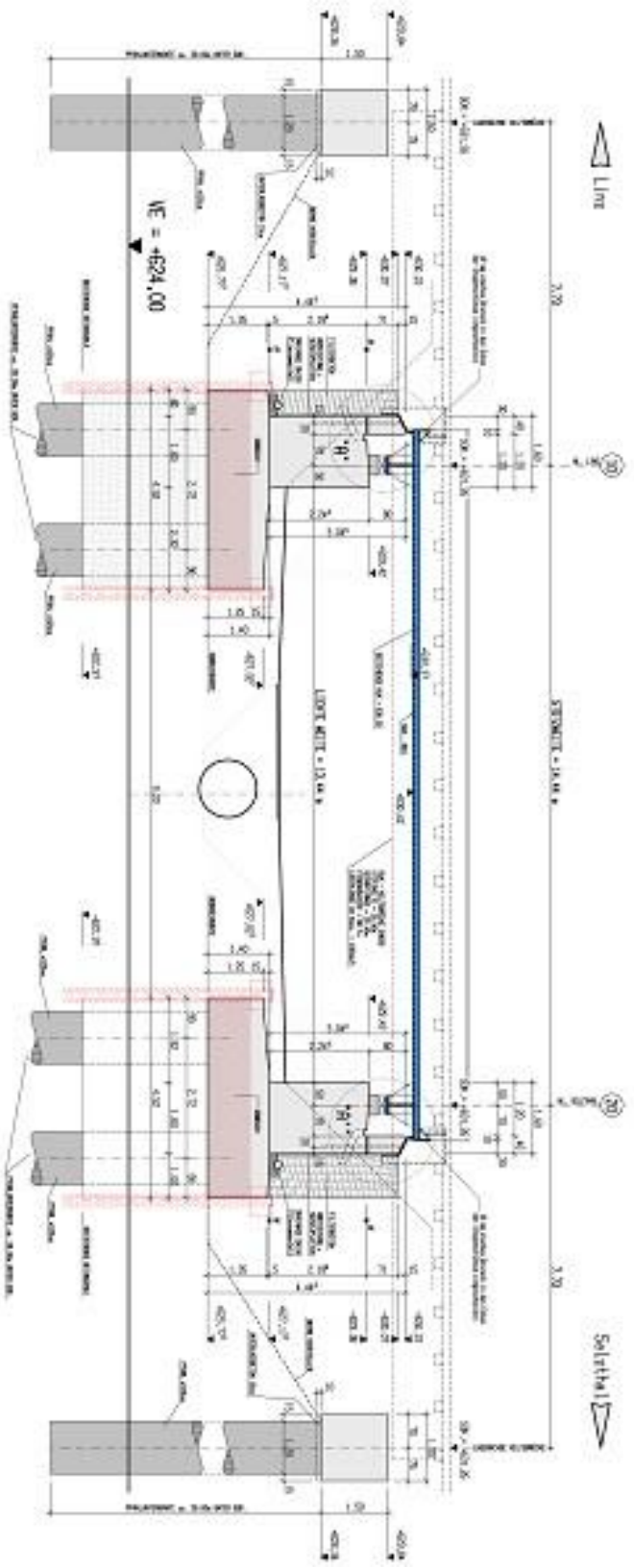

Figure 9

Lateral prospect of *Eisenbahnbrücke Brunngraben* bridge

HALF TROUGH BRIDGE

The structural configuration of a half-through bridge generally creates a linear rectangular U–shaped trough, the vertical legs being the main girders and the horizontal being the bridge deck. Design of such bridges requires consideration of the interaction between the transversely spanning action of the deck and the longitudinal spanning of the main beams.

The structure behaves essentially in a simple progress of slab spanning between cross girders, cross girders spanning between main girders and main girders spanning between supports, the key structural 'element' that requires special design consideration is the 'U-frame' that is created by a cross girder and the two vertical stiffeners to which it is connected. The need for frames is to provide intermediate lateral restraint to the top flanges, which are in compression. Such restraint is able to constrain the buckling mode of the top flanges, as shown in the picture on the right and below. The restraint provided by each 'U-frame' depends on the three components – cross girder, vertical stiffeners and the connections between cross girder and main girder. The restraint can be expressed in in terms of a flexibility under unit lateral load, as shown in the picture below.

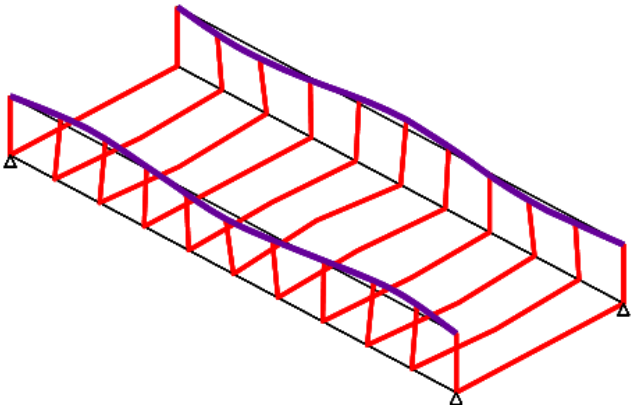

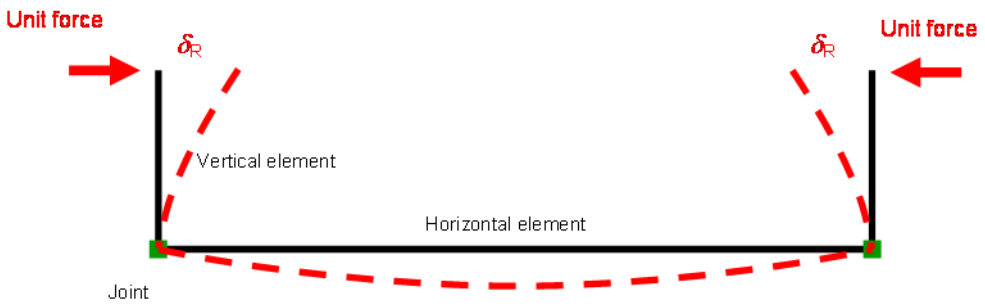

Figure 10 Example of half trough bridge design

An existing example of this type of deck can be seen in Antibes, Provence-Alpes-Cote d'Azur, France (Europe).

Figure 11

View of *Antibes Railroad Bridge*

Figure 12

View of *Antibes Railroad Bridge*

Figure 13

View of *Antibes Railroad Bridge*

Another example is Railway bridge over the Emile Mark street in Differdange, Luxembourg (Europe). The replacement of an old deck with direct track fastening by a ballasted track bridge required a structural system with minimized construction depth; a half-through
girder deck solved the problem.

Figure 14 The picture shows the assembled steel framework

Figure 15 View of *Railway bridge over the Emile Mark street in Differdange.*

1.3) Load Requirements

Several kinds of loads should be considered here:

- DL = Deal Load
- LL = Live Load
- WL = Wind Load
- IM = Dynamic Loads of vehicles

1.3.1) Dead Load

Deal Load itself can be subdivided into two subsections:

1. DC = Dead Load of structural and non-structural components
2. DW = Deal Load of the wearing surface

DC

Dead load includes the self weight of:

- Structural components such as girder, slabs, cross beams, etc…
- Nonstructural components such as medians, railings, signs, etc…

But does not include the weight of wearing surface.

We can estimate dead load from its density:

Material	Density (kg/m^3)
Concrete (Normal Weight)	2400
Concrete (Lightweight)	1775-1925
Steel	7850
Aluminium Alloy	2800
Wood	800-960
Stone Masonry	2725

DW

It is the weight of the wearing surface (usually asphalt) and utilities (pipes, lighting if needed, etc…). Different category is needed due to large variability of the weight compared with those of structural components.

1.3.2) Live Load

Live load is the force due to vehicles moving on the bridge, its impacts depends on many parameters including:

- Span length
- Weight of vehicle
- Axle loads (load per wheel)
- Axle configuration
- Position of the vehicle on the bridge (transverse and longitudinal)
- Number of vehicles on the bridge (multiple presence)
- Girder spacing
- Stiffness of structural members

When we are talking about bridges, live load is very heavy (several tons per wheel) and it can be a series of point loads (wheel loads of trains) or uniform loads; dynamic effects of live load cannot be ignored.

The strategy for analyzing live loads can be summed up this way:

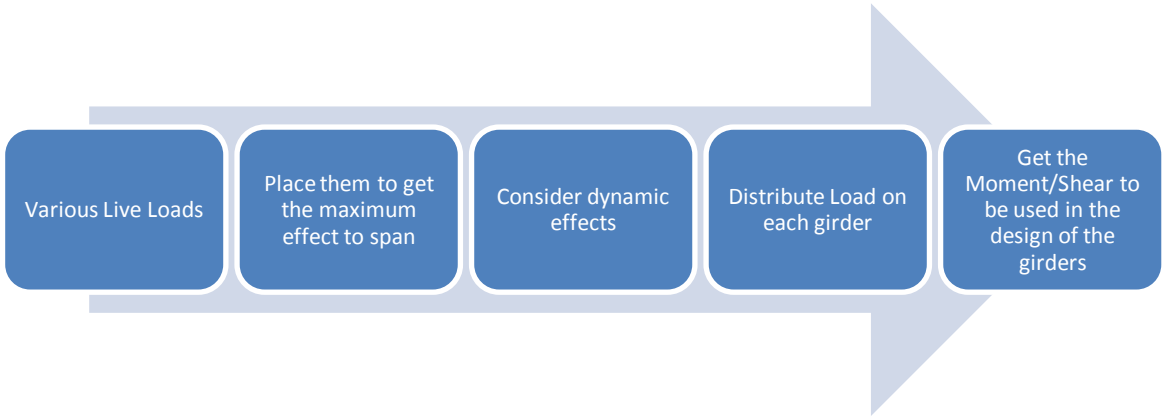

1.3.3) Dynamic Load

This kind of load will be largely explained in chapter 1.4

1.3.4) Wind Load

Wind load can be described as an horizontal load, and there are two types of wind loads on the structure:
WS = wind load on structure (Wind pressure on the structure itself)
WL = wind on vehicles on bridge (Wind pressure on the vehicles on the bridge, which the load is
transferred to the bridge superstructure).

For small and low bridges, wind load typically do not control the design. For longer span bridge over river/sea, wind load on the structure is very important; there's the need to consider the aerodynamic effect of the wind on the structure, like turbulence.
There's also the need to consider the dynamic effect of flexible long-span bridge under the wind force and we can do that by conducting dynamic analysis.

For bridges or parts of bridges more than 10 m above low ground or water level, the design wind velocity, V_{DZ}, should be adjusted according to:

$$V_{DZ} = 2.5V_0 \left(\frac{V_{10}}{V_B}\right) \ln\left(\frac{Z}{Z_0}\right)$$

Where

$$V_{DZ} = design\ wind\ velocity\ at\ design\ elevation\ (Z)$$

$$V_{10} = wind\ velocity\ at\ 10m\ above\ low\ ground\ or\ above\ design\ water\ level$$

$$V_B = base\ wind\ velocity\ of\ 160\,\frac{km}{h}\ at\ 10m$$

$$Z = height\ of\ structure\ at\ which\ wind\ loads\ are\ being\ calculated$$

$$V_0 = friction\ velocity\ depends\ on\ terrains$$

$$Z_0 = friction\ lenght\ of\ upstream\ fetch\ depends\ on\ terrain$$

After having the wind velocity it's possible to calculate the pressure on the structure

$$P_D = P_B(\frac{V_{DZ}}{V_B})^2 = P_B \frac{V_{DZ}^2}{25600}$$

We can find some references about wind force on bridges also in Eurocode 1 part 4, which shows us the simpliest method, where the wind force in direction x may be calculated using this equation:

$$F_x = \frac{1}{2}\rho v_b^2 C \qquad [\frac{KN}{m^2}]$$

Where

$$v_b = basic\ wind\ speed$$

$$C = wind\ load\ factor = C_e C_{f,x}\ where\ C_e\ is\ the\ exposure\ factor$$

$$\rho = 1{,}25\ as\ the\ density\ of\ air$$

Values of C factor can be find in the table below

b/d_{tot}	$z_e \leq 20$ m	$z_e = 50$ m
≤ 0,5	6,7	8,3
≥ 4,0	3,6	4,5

This table is based on the following assumptions :

– terrain category II according to Table 4.1

– force coefficient $c_{f,x}$ according to 8.3.1 (1)

– c_0=1,0

– k_I=1,0

For intermediate values of b/d_{tot}, and of z_e linear interpolation may be used

Values of the exposure factor can be found in the table below

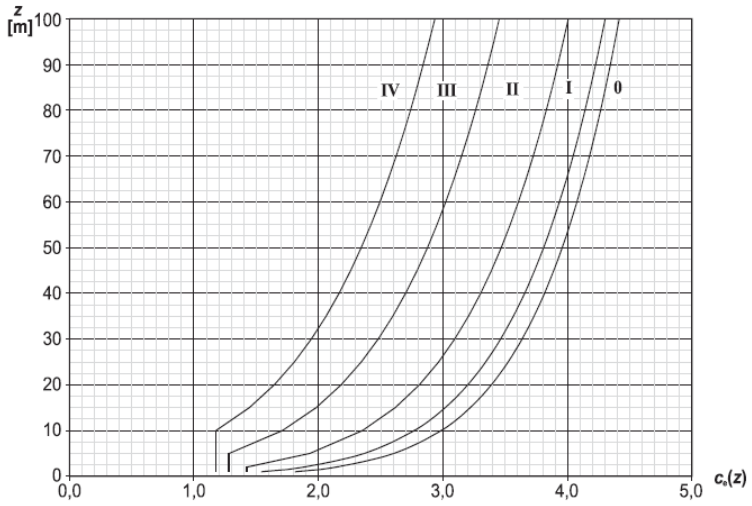

Figure 16 Table for the exposure factor

Rail traffic actions are defines by means of load models, five of them are given in the Eurocode:

1. Load Model 71 (and load model SW/0 for continuous bridges) to represent normal rail traffic on mainline railways
2. Load Model SW/2 to represent heavy loads
3. Load Model HSLM to represent the loading from passenger trains at speeds exceeding 200 km/h
4. Load Model "unloaded train" to represent the effects of an unloaded train.

1.3.5) Load Model 71

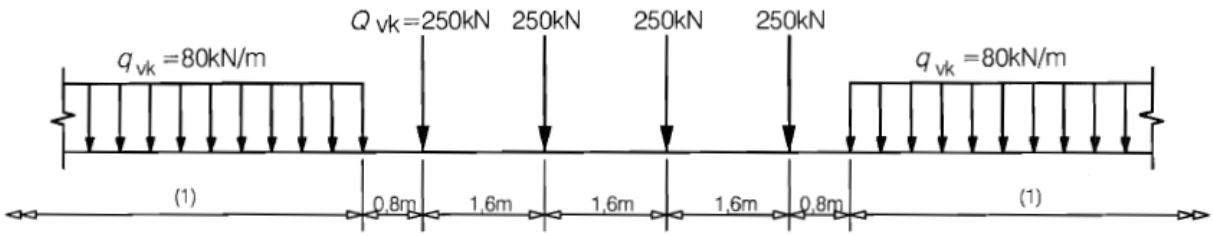

Figure 17 Load Model 71 and characteristics values for vertical loads

The characteristic values given in Figure 17 shall be multiplied by a factor α, on lines carrying rail traffic which is heavier or lighter than normal rail traffic. When multiplied by the factor α the loads are called "classified vertical loads" . This factor α shall be one of the following:

0.75 – 0.83 – 0.91 – 1.00 – 1.10 – 1.21 – 1.33 – 1.46

1.3.6) Load Model SW/0 and SW/2

Load Model SW/0 represents the static effect of vertical loading due to normal rail traffic on continuous beams; Load Model *SW/2* represents the static effect of vertical loading due to heavy rail traffic.

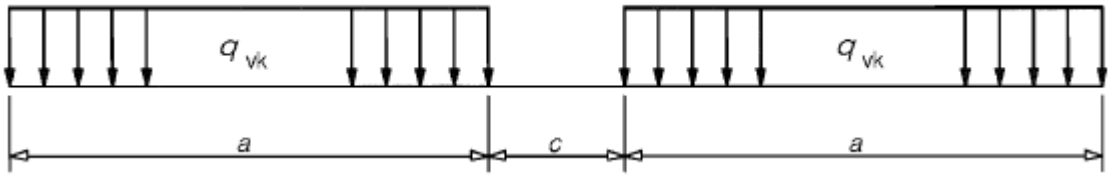

Figure 18 Characteristic values for vertical loads for Load Models SW/0 and SW/2

Load Model SW/0 shall be multiplied by the factor α as well.

Load Model	q_{vk} [kN/m]	a [m]	c [m]
SW/0	133	15,0	5,3
SW/2	150	25,0	7,0

1.3.7) Load Model unloaded train

The Load Model "unloaded train" consists of a vertical uniformly distributed load with a characteristic value of 10,0 kN/m.

1.3.8) Eccentricity of vertical loads (Load Models 71 and SW *10)*

The effect of lateral displacement of vertical loads shall be considered by taking the ratio of wheel loads on all axles as up to 1,25: 1,00 on anyone track. The resulting eccentricity *e* is shown in Figure 19.

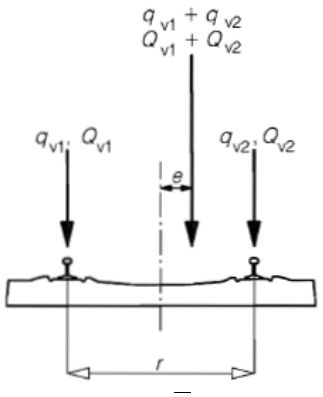

$$q_{v1}, q_{v2}, Q_{v1}, Q_{v2} \quad (1)$$

$$q_{v1} + q_{v2}, Q_{v1} + Q_{v2} \quad (2)$$

$$\frac{q_{v2}}{q_{v1}}, \frac{Q_{v2}}{Q_{v1}} \leq 1{,}25$$

$$e \leq \frac{r}{18}$$

$$r \quad (3)$$

Figure 19: Eccentricity of vertical loads

1.3.9) Distribution of the Load

The passing of the convoy on the rails produces a concentrated load through the wheels and a distributed load from the hole train itself. These two loads are transmitted first to the rails through the sleepers, then to the slab through the ballast.

From the slab the load effects are transferred to the main girders, depending on the stiffness distribution of the section. The main girders, which are simply supported, distribute the loads on the main support of the bridge.

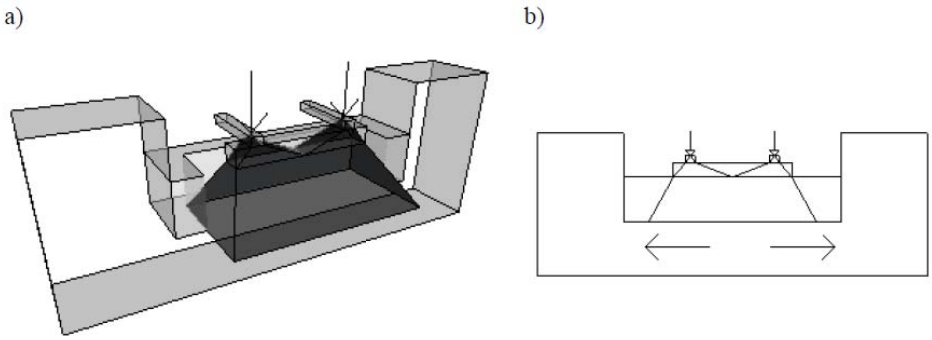

Figure 20 The shaded areas represents a possible distribution of load effects in 3D (figure a) through the sleepers to the slab, figure b shows the transmission of those loads to the main girders.

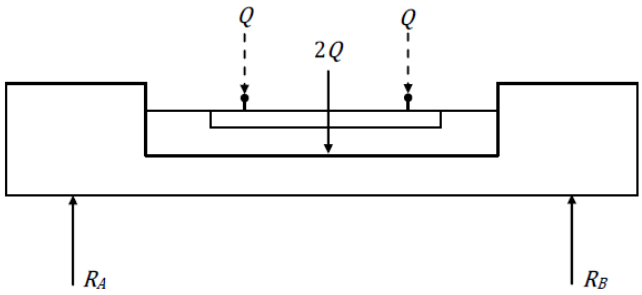

Figure 21 *The wheel loads, represented by the concentrated loads Q at the tracks, are simplified as one concentrated load 2Q acting in the middle of the cross-section, directly on the slab. The reaction forces R_A and R_B act at the supports.*

In a linear elastic analysis cracking and redistributions are neglected, which means that the slab has to behave in an isotropic way (it can distribute the load effects in all directions in the same way). However, in service state, this is unrealistic. The stiffness is influenced by transversal reinforcement that implies that the slab have an orthotropic behavior.

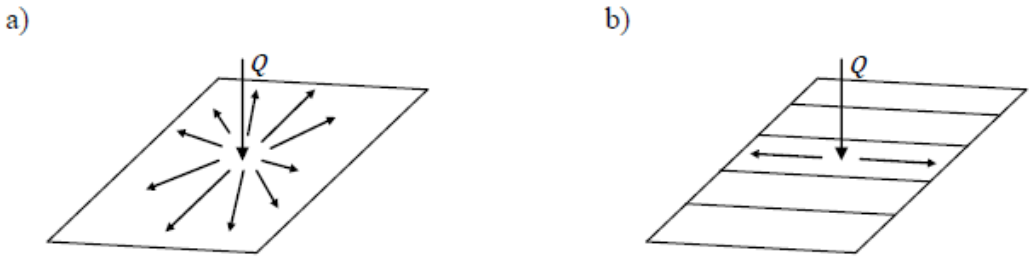

Figure 22

a) Isotropic behavior
b) Extreme scenario of orthotropic behavior, in which there's no stiffness in longitudinal direction.

1.3.10) Longitudinal distribution of wheel load by the rail

Wheel loads may be distributed onto the supports as shows in Figure 21.

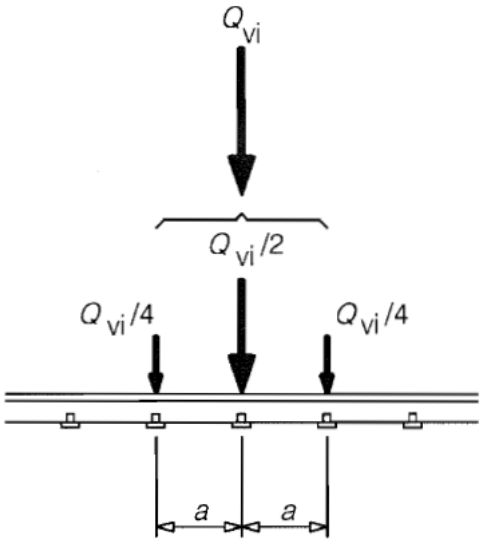

Figure 23: Distribution of wheel loads

Where

$$Q_{vi} = point\ force\ on\ each\ rail\ due\ to\ wheel\ loads$$
$$a = distance\ between\ rail\ support\ points$$

1.3.11) Longitudinal distribution of load by sleepers and ballast

Generally the point loads may be distributed uniformly in the longitudinal direction (except where local load effects are significant, *e.g.* for the design of local floor elements, etc.).

For the design of local floor elements etc. *(e.g.* longitudinal and transverse ribs, rail bearers, cross girders, deck plates, thin concrete slabs, etc.), the longitudinal distribution beneath sleepers as shown in Figure 24 should be taken into account, where the reference plane is defined as the upper surface of the deck.

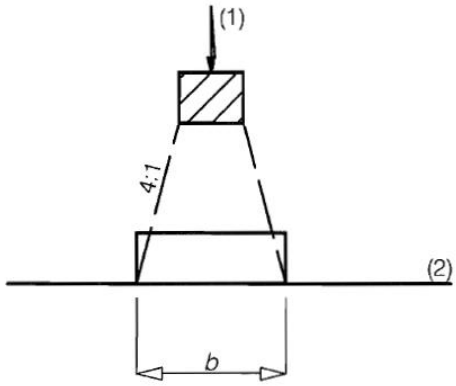

Figure 24: Longitudinal distribution of load by a sleeper and ballast

1.3.12) Transverse distribution of actions by the sleepers and ballast

On bridges with ballasted track without cant, the actions should be distributed transversely as shown in Figure 25:

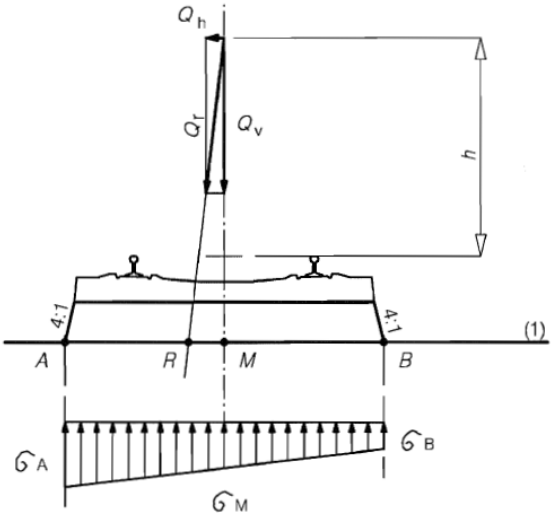

Figure 25: Transverse distribution of actions by the sleepers and ballast, track without cant (effect of eccentricity of vertical loads not shown)

1.3.13) Torsion in the main girders

When the slab is subjected to a load the slab bends in the transversal direction and as an effect of this torques are introduced in the main girders, and causes torsion. It is required that full compatibility between main girders and slab should be assumed and designed for. This means that torsion reinforcement should be designed based on the torsional moments that occur due to full compatibility.

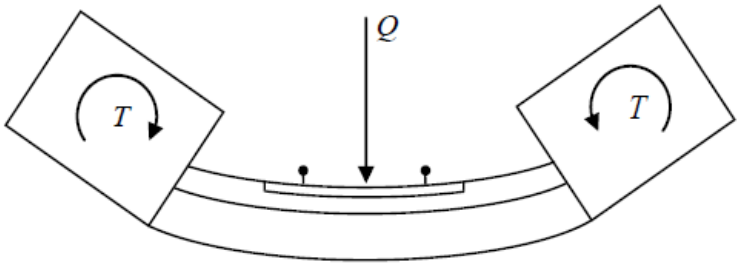

Figure 26 Torques T in the main girders caused by the load Q

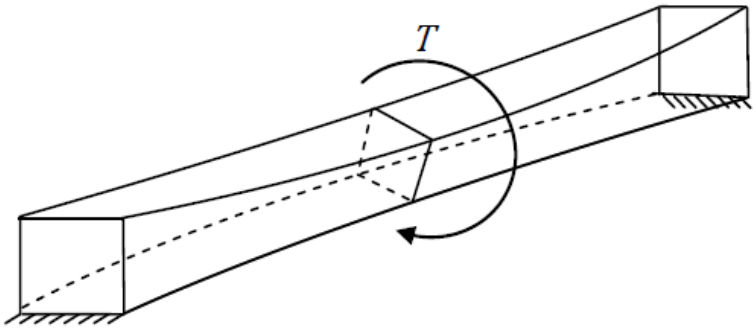

Figure 27 *Beam subjected to a torque*

.

1.4) *Dynamic behavior and load models*

All types of bridges require a specific analysis for special loads, being them footbridges, road bridges or railway ones. In particular, for railway bridges, those kind of loads can be very affecting on the entire load category; that is why there is an entire section in the Eurocodes dedicated to the matter. (Eurocode 1 – Part 2 – Section 6).

There are many factors than take part in a dynamic behavior, such as:

1) The speed of the traffic which is crossing the bridge
2) The span L
3) The mass of the structure
4) The natural frequencies of the whole structure and relevant elements
5) The number of axles, axle loads and the spacing of those
6) The damping of the structure
7) Vertical irregularities in the track
8) The unsprung/sprung mass and suspension characteristics of the vehicle
9) The presence of regularly spaced supports of the deck
10) Vehicle imperfections
11) Dynamic characteristics of the track (ballast, sleepers etc)

1.4.1) Requirements for a dynamic analysis

"The dynamic analysis shall be undertaken using characteristic values of the loading from the Real Trains specified. The selection of Real Trains shall take into account each permitted or envisaged train formation for every type of high speed train permitted or envisaged to use the structure at speeds over 200km/h.
The dynamic analysis shall also be undertaken using Load Model HSLM on bridges designed for international lines where European high speed interoperability criteria are applicable.
Load Model HSLM comprises of two separate Universal Trains with variable coach lengths, HSLM-A and HSLM-B."

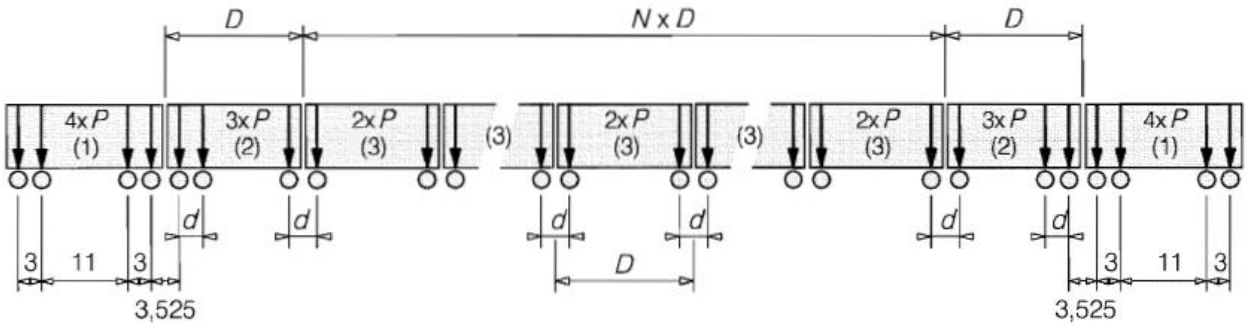

Key

(1) Power car (leading and trailing power cars identical)
(2) End coach (leading and trailing end coaches identical)
(3) Intermediate coach

Figure 28 HSLM-A

Universal Train	Number of intermediate coaches *N*	Coach length *D* [m]	Bogie axle spacing *d* [m]	Point force *P* [kN]
A1	18	18	2,0	170
A2	17	19	3,5	200
A3	16	20	2,0	180
A4	15	21	3,0	190
A5	14	22	2,0	170
A6	13	23	2,0	180
A7	13	24	2,0	190
A8	12	25	2,5	190
A9	11	26	2,0	210
A10	11	27	2,0	210

Figure 29 HSLM-A

HSLM-B comprises of *N* number point forces of 170 kN at uniform spacing *d* [In] where N and *d* are defined in Figures 30 and 31.

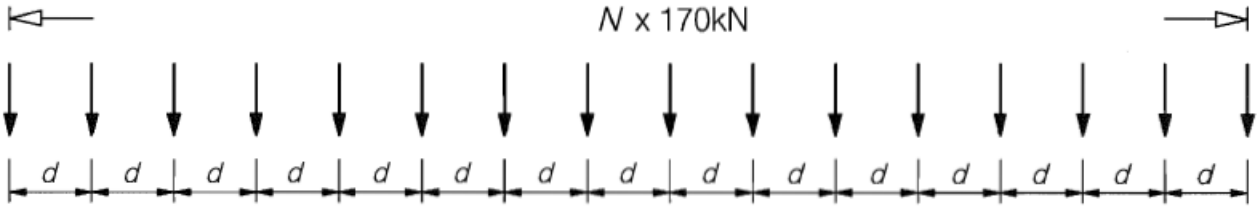

Figure 30 HSLM-B

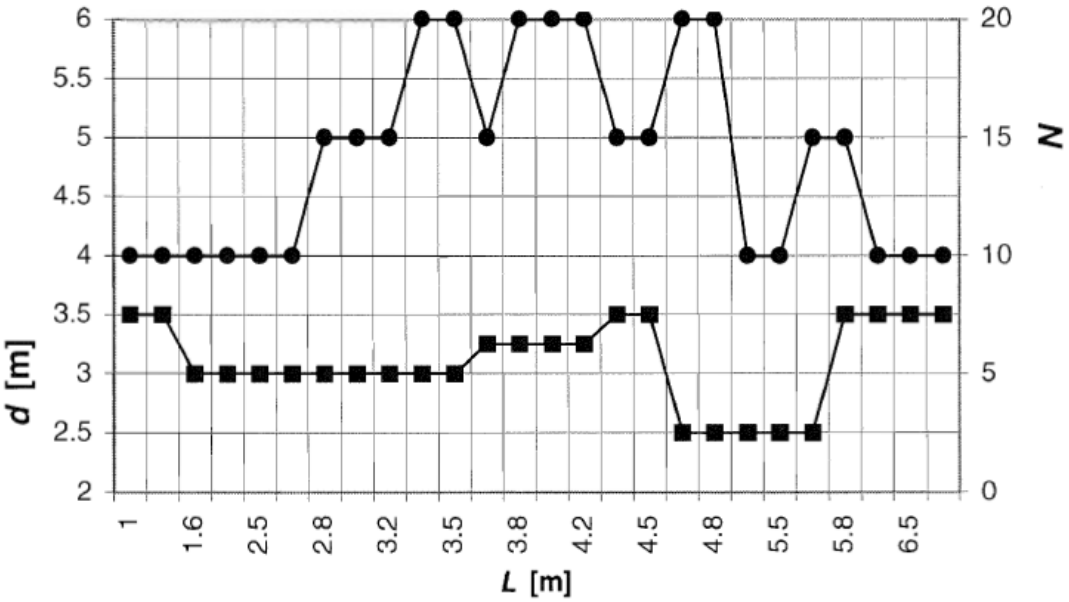

Figure 31 HSLM-B (L is the span length)

Either HSLM-A or HSLM-B should be applied in accordance with the requirements of Table 1

Structural configuration	Span	
	$L < 7$m	$L \geq 7$m
Simply supported span[a]	HSLM-B[b]	HSLM-A[c]
Continuous structure[a] or Complex structure[e]	HSLM-A Trains A1 to A10 inclusive[d]	HSLM-A Trains A1 to A10 inclusive[d]

[a] Valid for bridges with only longitudinal line beam or simple plate behaviour with negligible skew effects on rigid supports.

[b] For simply supported spans with a span of up to 7 m a single critical Universal Train from HSLM-B may be used for the analysis in accordance with 6.4.6.1.1(5).

[c] For simply supported spans with a span of 7 m or greater a single critical Universal Train from HSLM-A may be used for the dynamic analysis in accordance with annex E (Alternatively Universal trains A1 to A10 inclusive may be used).

[d] All Trains A1 to A10 inclusive should be used in the design.

[e] Any structure that does not comply with Note a above. For example a skew structure, bridge with significant torsional behaviour, half through structure with significant floor and main girder vibration modes etc. In addition, for complex structures with significant floor vibration modes (*e.g.* half through or through bridges with shallow floors) HSLM-B should also be applied.

NOTE The National Annex or the individual project may specify additional requirements relating to the application of HSLM-A and HSLM-B to continuous and complex structures.

Table 1 Application of HSLM-A and HSLM-B

Number of tracks on a bridge	Loaded track	Loading for dynamic analysis
1	one	Each Real Train and Load Model HSLM (if required) travelling in the permitted direction(s) of travel.
2 (Trains normally travelling in opposite directions) [a]	either track	Each Real Train and Load Model HSLM (if required) travelling in the permitted direction(s) of travel.
	other track	None.
[a] For bridges carrying 2 tracks with trains normally travelling in the same directions or carrying 3 or more tracks with a Maximum Line Speed at the Site exceeding 200km/h the loading should be agreed with the relevant authority specified in the National Annex.		

Table 2 Summary of additional load cases depending upon number of tracks on bridge

1.4.2) Real Trains

Here below, the schemes of the real trains from A to F.

Type A

$\Sigma Q = 6936kN \quad V = 350km/h \quad L = 350,52m \quad q = 19,8kN/m'$

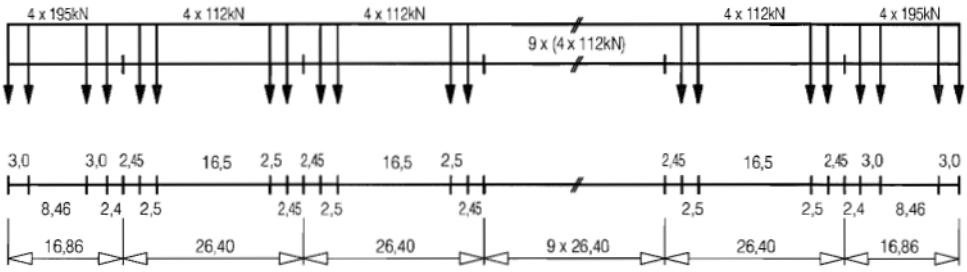

Figure 32 Real Train A

Type B

$\Sigma Q = 8784kN \quad V = 350km/h \quad L = 393,34m \quad q = 22,3kN/m'$

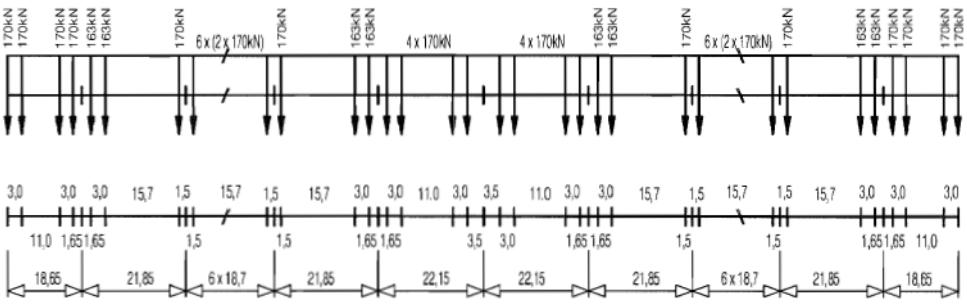

Figure 33 Real Train B

Type C

$\Sigma Q = 8160\text{kN}$ $V = 350\text{km/h}$ $L = 386{,}67\text{m}$ $q = 21{,}1\text{kN/m'}$

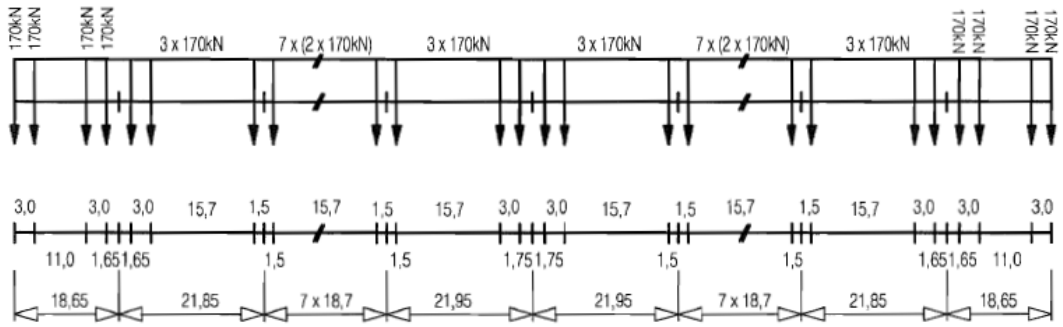

Figure 34 Real Train C

Type D

$\Sigma Q = 6296\text{kN}$ $V = 350\text{km/h}$ $L = 295{,}70\text{m}$ $q = 21{,}3\text{kN/m'}$

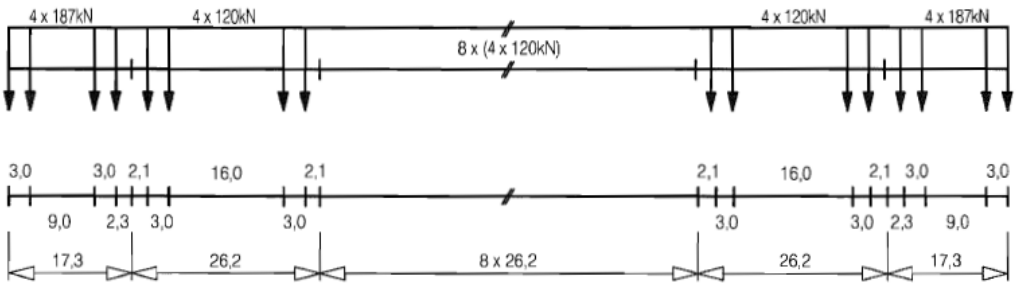

Figure 35 Real Train D

Type E

$\Sigma Q = 6800\text{kN}$ $V = 350\text{km/h}$ $L = 356{,}05\text{m}$ $q = 19{,}1\text{kN/m'}$

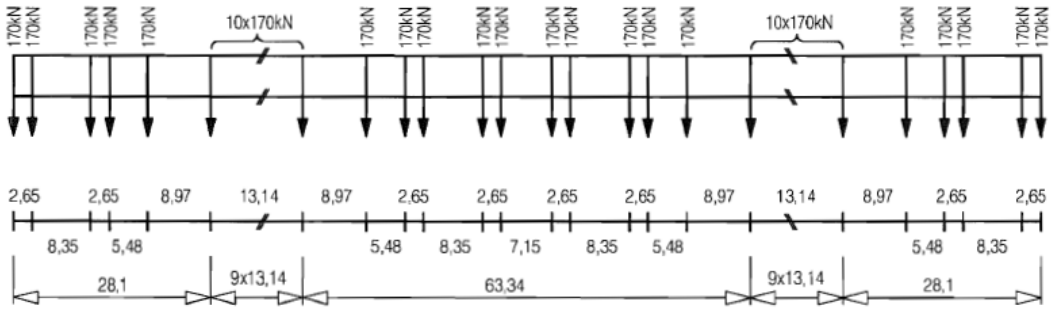

Figure 36 Real Train E

Type F

$\Sigma Q = 7480kN \quad V = 350km/h \quad L = 258{,}70m \quad q = 28{,}9kN/m'$

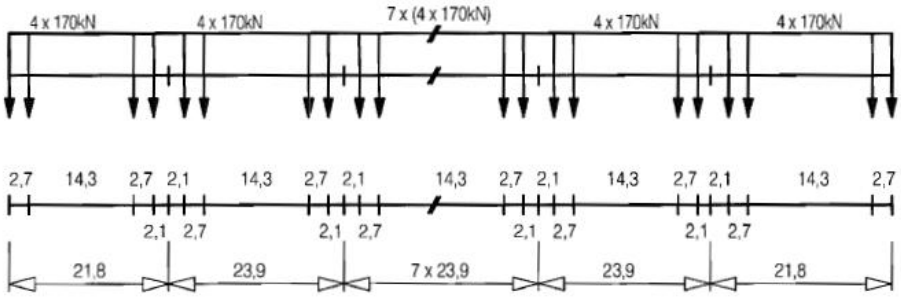

Figure 37 Real Train F

1.4.3) Speeds to be considered

"For each Real Train and Load Model HSLM a series of speeds up to the Maximum Design Speed shall be considered. The Maximum Design Speed shall be generally 1,2 x Maximun1 Line Speed at the site.

The Maximum Line Speed at the site shall be specified.

Calculations should be made for a series of speeds from 40m/s up to the Maximum Design Speed, smaller speed steps should be made in the vicinity of Resonant Speeds.

For simply supported bridges that may be modelled as a line beam the Resonant Speeds may be estimated using this equation"

$$v_i = n_0 \lambda_i \; and \; 40m/s \leq v_i \leq MDS$$

Where:

$$v_i = Resonant\ Speed\ \left[\frac{m}{sec}\right]$$

$$n_0 = First\ natural\ frequency\ of\ the\ unloaded\ structure$$

$$\lambda_i = \frac{d}{i} = Principal\ wavelenght\ of\ frequency\ of\ excitation$$

1.4.4) Bridge parameters

1) Structural Damping

"The peak response of a structure at traffic speeds corresponding to resonant loading is highly dependent upon damping. The following values of damping should be used in the dynamic analysis:"

Bridge Type	ξ Lower limit of percentage of critical damping [%]	
	Span < 20m	Span ≥ 20m
Steel and Composite	$\xi = 0{,}5 + 0{,}125(20 - L)$	$\xi = 0{,}5$
Prestressed Concrete	$\xi = 1{,}0 + 0{,}07(20 - L)$	$\xi = 1{,}0$
Filler beam and reinforced concrete	$\xi = 1{,}5 + 0{,}07(20 - L)$	$\xi = 1{,}5$

For spans less than 30m dynamic vehicle/bridge mass interaction effects tend to reduce the peak response at resonance. Account may be taken of these effects by increasing the value of damping assumed for the structure according to Figure 38.

For continuous beams, the smallest value $\Delta\xi$ (for all spans should be used. The total damping to be used is given by : $\xi_{TOTAL} = \Delta\xi + \xi$

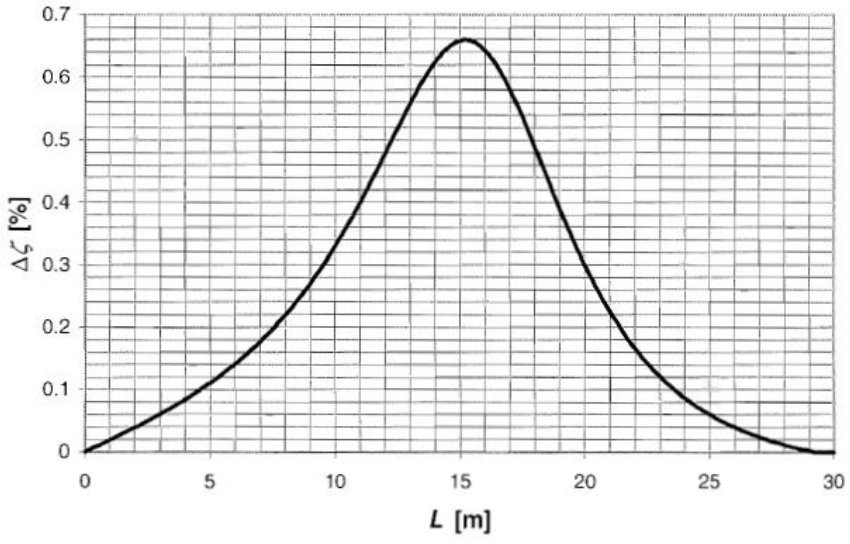

Figure 38 Additional damping as a function of span length

Where $\Delta\xi = \frac{0{,}0187L - 0{,}00064L^2}{1 - 0{,}0441L - 0{,}0044L^2 + 0.000255L^3}$ [%]

2) **Mass of the bridge**

"Maximum dynamic load effects are likely to occur at resonant peaks when a multiple of the frequency of loading and a natural frequency of the structure coincide and any underestimation of mass will overestimate the natural frequency of the structure and overestimate the traffic speeds at which resonance occurs. At resonance the maximum acceleration of a structure is inversely proportional to the mass of the structure. Two specific cases for the mass of the structure including ballast and track shall be considered:

- A lower bound estimate of mass to predict maximun1 deck accelerations using the minimum likely dry clean density and minimum thickness of ballast,

- An upper bound estimate of mass to predict the lowest speeds at which resonant effects are likely to occur using the maximum saturated density of dirty ballast

3) **Stiffness of the bridge**

Maximum dynamic load effects are likely to occur at resonant peaks when a multiple of the frequency of loading and a natural frequency of the structure coincide.

Any overestimation of bridge stiffness will overestimate the natural frequency of the structure and speed at which resonance occurs. The stiffness of the whole structure including the determination of the stiffness elements of the structure may be determined in accordance with EN 1992 to EN 1994.

Values of Young's modulus may be taken from EN 1992 to EN 1994.

1.4.5) Verifications of the limit states

"To ensure traffic safety:

- The verification of maximum peak deck acceleration shall be regarded as a traffic safety requirement checked at the serviceability limit state for the prevention of track instability.

- *The dynamic enhancement of load effects shall be allowed for by multiplying the static loading by the dynamic factor ϕ. If a dynamic analysis is necessary, the results of the dynamic analysis shall be compared with the results of the static analysis enhanced by ϕ and the most unfavourable load effects shall be used for the bridge design.*
- *If a dynamic analysis is necessary, a check shall be carried out to establish whether the additional fatigue loading at high speeds and at resonance is covered by consideration of the stresses due to load effects from ϕ x LM71. The most adverse fatigue loading shall be used in the design."*

1.4.6) Dynamic factor ϕ

The dynamic factor ϕ takes account of the dynamic magnification of stresses and vibration effects in the structure but does not take account of resonance effects. Structures carrying more than one track should be considered without any reduction of dynamic factor ϕ . Generally the dynamic factor ϕ is taken as either ϕ_2 or ϕ_3 according to the quality of track maintenance as follows:

For carefully maintained track:

$$\phi_2 = \frac{1{,}44}{\sqrt{L_\phi} - 0{,}2} + 0{,}82 \qquad with \qquad 1{,}00 \leq \phi_2 \leq 1{,}67$$

For tracks with standard maintenance:

$$\phi_3 = \frac{2{,}16}{\sqrt{L_\phi} - 0{,}2} + 0{,}73 \qquad with \qquad 1{,}00 \leq \phi_3 \leq 2{,}00$$

Being L_ϕ the length associated with ϕ.

If no dynamic factor is specified $\phi_3$shall be used. The dynamic factor ϕ shall not be used with:

- the loading due to Real Trains
- the loading due to Fatigue Trains
- Load Model HSLM
- the load model "unloaded train"

Where the maximum line speed at the site is lower than 200 km/h a dynamic analysis should be carried out. The analysis should take into account the factors that influence the dynamic behavior and consider Real Trains from A to F.

For bridge decks carrying one or more tracks the checks for the limits of deflection and vibration shall be made with the number of tracks loaded with all associated relevant traffic actions in accordance with Table 3.

Limit State and associated acceptance criteria	Number of tracks on the bridge		
	1	2	≥ 3
Traffic Safety Checks:			
– Deck twist (EN 1990: A2.4.4.2.2)	1	1 or 2 [a]	1 or 2 or 3 or more [b]
– Vertical deformation of the deck (EN 1990: A2.4.4.2.3)	1	1 or 2 [a]	1 or 2 or 3 or more [b]
– Horizontal deformation of the deck (EN 1990: A2.4.4.2.4)	1	1 or 2 [a]	1 or 2 or 3 or more [b]
– Combined response of structure and track to variable actions including limits to vertical and longitudinal displacement of the end of a deck (6.5.4)	1	1 or 2 [a]	1 or 2 [a]
– Vertical acceleration of the deck (6.4.6 and EN 1990: A2.4.4.2.1)	1	1	1
SLS Checks:			
– Passenger comfort criteria (EN 1990: A2.4.4.3)	1	1	1
ULS Checks			
– Uplift at bearings (EN 1990: A2.4.4.1(2)P)	1	1 or 2 [a]	1 or 2 or 3 or more [b]

Table 3 Number of tracks to be loaded for checking limits of deflection and vibration

1.4.7) User Comfort Criteria

Railroad traffic on bridges induces vibrations which could possibly have an adverse effect on passenger comfort. At extreme cases, vibrations from an improperly design bridge could cause derailment.

As far as the global bridge response is concerned, it is generally understood that when one of the apparent trainload excitation frequencies coincides with the fundamental natural frequency of the bridge, resonance could occur.

In order to better control excess bridge vibration, the objective is to derive a user comfort serviceability limit based on the natural frequency of the bridge.

Previous research efforts have tried to use complex modeling of bridge dynamic behavior to derive natural frequency based serviceability criteria (Wright and Walker 1971, Amaraks 1975, and DeWolf and Kou 1997). None of these previous efforts have produced acceptable criteria to place in design codes. This study will instead use a simple dynamic pluck test to obtain a dynamic property of the bridge, which, in turn, is used to formulate the proposed user comfort serviceability criteria.

In the dynamic pluck test, the bridge is loaded with the fatigue truck at the location that incurs maximum deflection. The load is then removed instantaneously, and free vibration is allowed. The response is then correlated to acceptable vibration for steel girder bridges.

$$\ddot{u}_{max} = \Delta_{max}\omega_n^2$$

Where:

$\ddot{u}_{max} = a_{max} * g$ is the maximum acceleration

Δ_{max} is the initial deflection

$\omega_n = 2\pi f_n$ is the bridge circular natural frequency, being f_n the natural frequency

The natural frequency of a simply supported, single span bridge can be calculated with:

$$f_{n,sb} = \frac{\pi}{2L^2}\sqrt{\frac{EI_b g}{W}}$$

Where

L is the span length

E is the elasticity modulus

I_b moment of inertia at midspan

g acceleration of gravity

W weight per unit length of bridge girder.

Vertical accelerations has to be controlled and compared with some limitations, as follows:

- For ballast stability, vertical accelerations of the deck to be less than 3.5m/sec/sec for frequencies up to 20Hz
- For passenger comfort, vertical acceleration within carriages of the trains to be less than 0.5m/sec/sec.

Limitations on span deflection and joint rotation are applied to control the ride quality of the track.

Limitations on twist of the track also apply, particularly at crossovers and turnouts.

Vertical deflection at midspan is also checked to ensure acceptable vertical track radii, that the structure is not significantly different in performance to existing rail bridges and also to ensure acceptable levels of vertical acceleration inside coaches corresponding to satisfactory passenger comfort.

Permitted span/deflection ratios are all those which stay below the upper limit of L/600.

1.5) Research Summary

In the past few years, engineers have been trying to improve this kind of bridge, by researching innovative solutions.

We feel like mentioning the work which has been done by Ing. Josef Fink's research group (Paul Herrmann and Lukas Juen), reguarding *"Extremely slender steel-concrete composite deck slab for railway bridges".*

The main goal in this research was to study the behavior of an innovative composite sandwich system, consisting in a concrete core in between of two steel plates, interconnected by continuos shear connectors.

This new type of deck slab is supposed to replace the thick steel slab for bridges with spans of 10 to 25 meters.

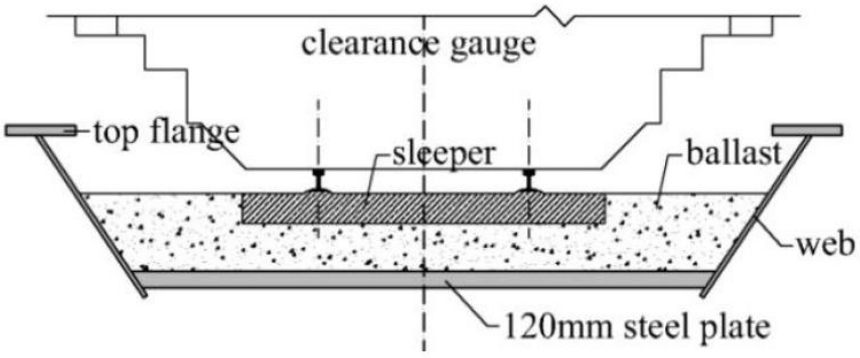

Figure 39 Trough bridge with a thick steel slab

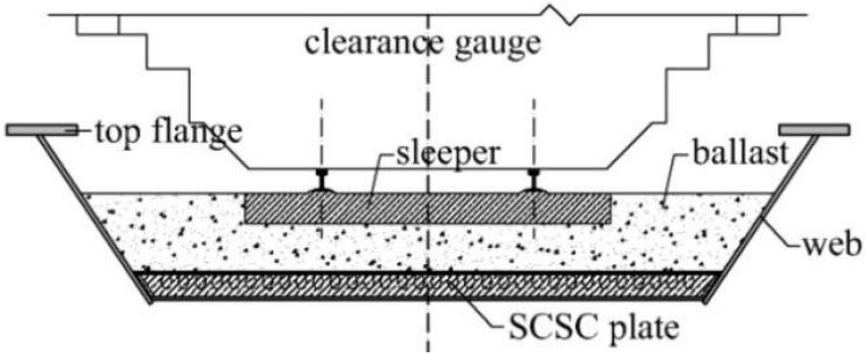

Figure 40 Trough bridge with a sandwich slab

The plate consists of two outer steel plates separated by unreinforced concrete, the height of the sandwich construction is 200mm and it mainly carries the vertical loads transversal to the main girders of the bridge.

The flexural rigidity of the SCSC system is mainly achieved by the two steel plates which participate additionally in the carrying function in longitudinal direction. The shear connection between the steel plates is generated by continuous shear connectors like crown dowels or perforated strips and the concrete filling.

Four sandwich plate specimens were tested under static load to examine load the bearing behaviour of the innovative SCSC sandwich system.

Basic Load-Bearing mechanism

The basic idea to ensure the transmission of the shear flow between the outer plates is the formation of compression struts within the concrete core, which are respectively supported by two adjoining shear connectors as shown in Figure 41 .The concrete acts with the shear connectors. This load-bearing mechanism allows the use of unreinforced concrete to reduce material and production costs compared to conventional reinforced composite structures used in bridge construction.

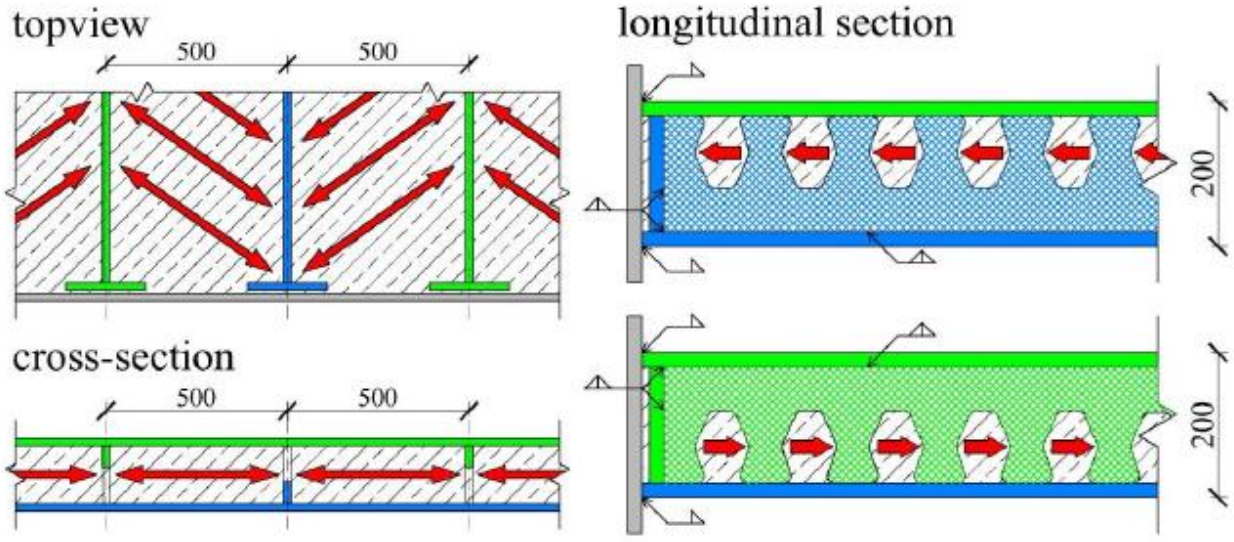

Figure 41 SCSC plate with compression diagonal within the unreinforced concrete core

Tests

Six models were investigated exemplary for one plate:

1. Rigid shear connection; constant widths (*RSC1*)
2. Rigid shear connection; effective widths due to shear lag effects (*RCS2*)
3. Elastic shear connection; constant widths; strut inclination $\alpha=45°=const.$ (*ESC1*)
4. Elastic shear connection; effective widths due to shear lag effects; strut inclination $\alpha=45°$(*ESC2*)
5. Elastic shear connection ; constant widths; strut inclination from $\alpha=30°$ to $\alpha=60°$ (*ESC3*)
6. Elastic shear connection; effective widths due to shear lag effects; strut inclination from $\alpha=30°$ to $\alpha=60°$ (*ESC4*)

The comparisons in the results are shown in Figure 42

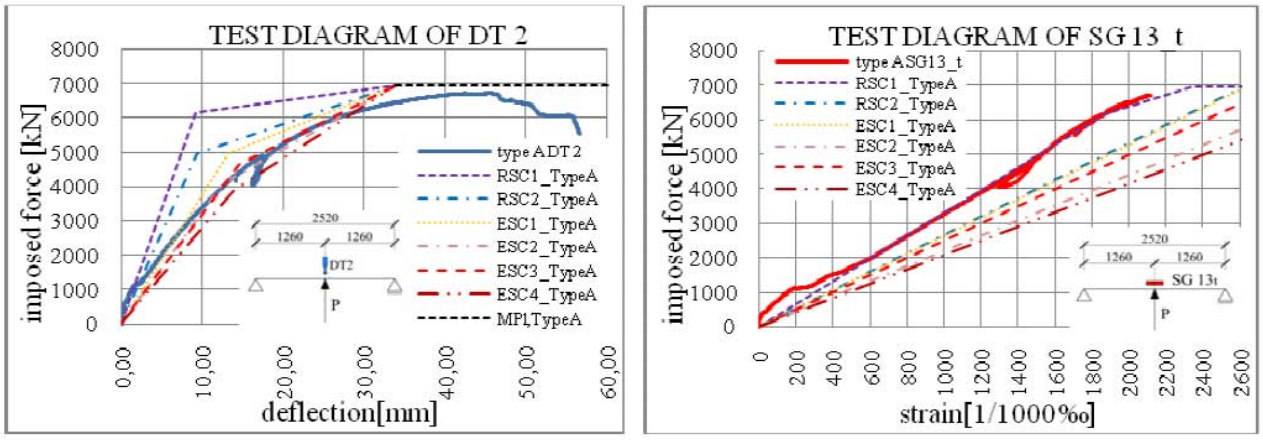

Figure 42 comparison of analytical models with test data

The model *ESC2* is the best choice to describe the structural behaviour by means of deformations. Taking the results of all strain- gauges into account, the models RSC1 and ESC1 show the best accordance with the measured test data for strain calculation.

Conclusions

The SCSC plate is a durable and cost effective element usable as deck slab for railway bridges.

Another important research was conducted by K.M.A. Sohel and J.Y. Richard Liew of the National University of Singapore. Their purpose was to study the static behavior of a SCS sandwich slab with lightweight concrete core.

To investigate the static performance of sandwich slabs, static tests for a centrally applied patch load were conducted on SCS sandwich slab specimens of different core thicknesses (80 and 100 mm) as well as different steel face plate thicknesses (4, 6 and 8 mm). Other parameters included in the investigation are the diameter of J-hook shear connectors and concrete core with and without fibres. A total number of eight SCS sandwich slabs measuring 1200 × 1200 mm2 (width × length) was prepared for the static test. All the slabs were fabricated with J-hook shear connectors. The diameter of the J-hook connectors was 10 mm for six specimens and the others contained 12 mm diameter connectors. The spacing of the connectors in both directions was 100 mm for all specimens.

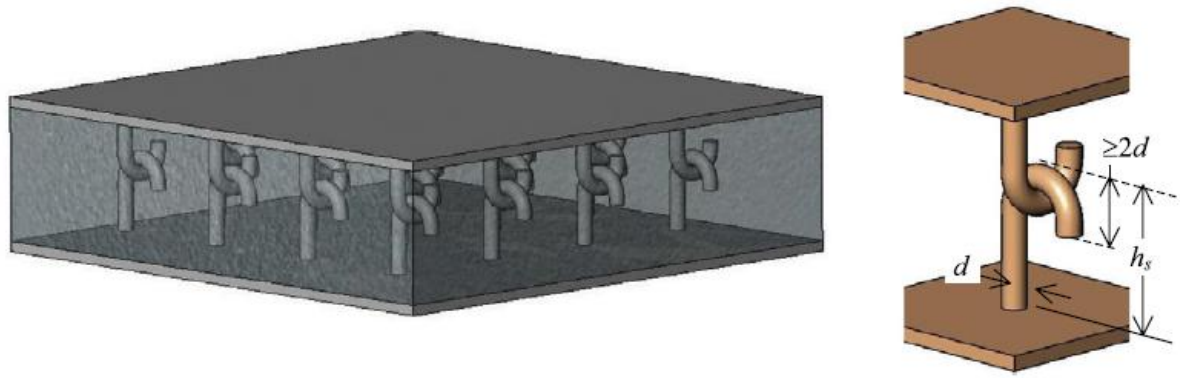

Figure 43 SCS sandwich with J-hook shear connectors.

Here below the sandwich slabs specimens

Specimen no.	t (mm)	d (mm)	h_c (mm)	S_s (mm)	L_s (mm)	Concrete type	f_c (MPa)	σ_y (MPa)
SLCS6-80	5.96	10	80	100	1200	LWC	27.0	315.0
SLFCS6-80	5.96	10	80	100	1200	LWFC	28.5	315.0
SLFCS6-100	5.96	10	100	100	1200	LWFC	28.5	315.0
SLFCS6-100(12)	5.96	12	100	100	1200	LWFC	28.5	315.0
SCS4-100	3.98	10	100	100	1200	NWC	57.2	275.5
SCS6-100	5.96	10	100	100	1200	NWC	57.2	315.0
SCFS6-100	5.96	10	100	100	1200	NWFC	59.0	315.0
SCFS8-100(12)	7.98	12	100	100	1200	NWFC	59.0	355.0

NWC = Normal weight concrete; LWC = Lightweight concrete; NWFC = Normal weight concrete with fiber (1% steel fiber); LWFC = Lightweight concrete with fiber (1% steel fiber).

Shear strength of the J-hook connectors embedded in concrete should be determined by push out tests. The failure of J-hook connectors with a lightweight concrete core of compression strength fc = 31 MPa was governed by concrete bearing failure.

Whereas, the connector with normal concrete core (compression strength > 48 MPa) failed by shear yielding of the connector occurring at about 8–10 mm slip.

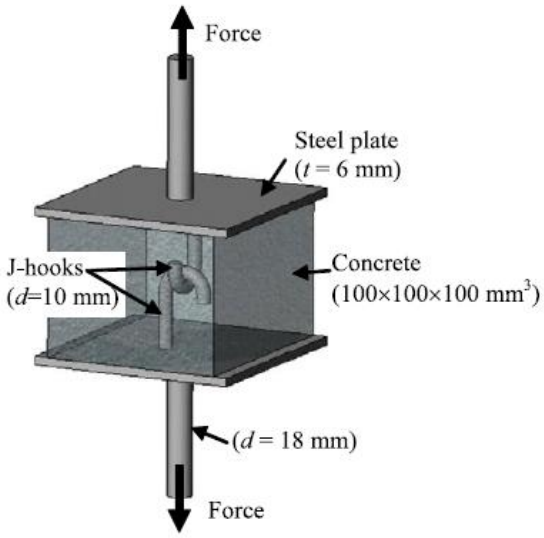

Figure 44 Direct tensile test on J-hook connectors embedded in concrete

The slab was simply supported on all four sides and subjected to a central concentrated load produced by a servo-controlled Instron hydraulic actuator of capacity 2000 kN under displacement control mode.

From the test results, the general load–deflection behavior of SCS sandwich slabs under concentrated load is illustrated in the figure below.

In the first stage, the load increased linearly with some minor tension cracking in the concrete core which was expected. In the second stage, the onset of the bottom plate slip, bucking of the top plate and possibly the failure of one or more connectors occurred.

Slab ref.	F_{cr} (kN)	F_{p-exp} (kN)	w_e (mm)	F_{60} (kN)	Failure mode
SLCS6-80	150	252	4.1	466	Flexural
SLFCS6-80	184	302	5.5	529	Flexural
SLFCS6-100	213	364	6.0	600	Flexural
SLFCS6-100(12)	235	454	7.0	611	Flexural
SCS4-100	310	518	6.4	273	Punching-shear
SCS6-100	300	620	7.1	724	Punching-shear
SCFS6-100	325	729	8.7	740	Punching-shear
SCFS8-100(12)	550	892	8.5	864	Punching-shear

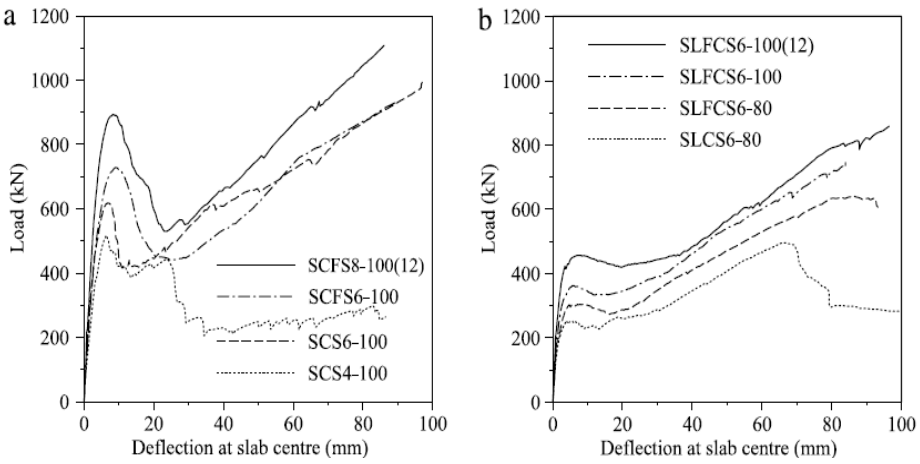

Figure 45 Experimental load–deflection curves (a) sandwich slabs with normal weight concrete core (b) sandwich slabs with lightweight concrete core.

The effect of fibres can be studied by comparing the load–deflection behavior of the slabs with and without fibres. An addition of 1% volume fraction of fibres increased the load–deflection stiffness and the first peak load.

For SCS sandwich slabs, the flexural capacity of the slab can be evaluated using the yield line theory.

Fig. 46 shows the fracture pattern of yield lines in a square slab, simply supported at four edges and subjected to a concentrated patch load. From the virtual work principle, the flexural capacity of the slab may be evaluated using the equation proposed by Rankin and Long.

$$F_p = 8m_{pl}\left(\frac{L_s}{L-c} - 0.172\right)$$

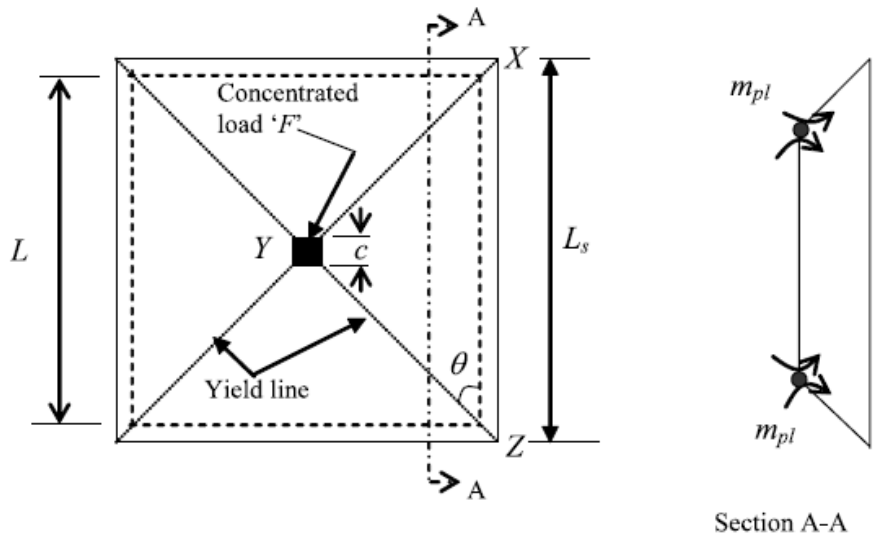

Figure 46

Formation of yield-line mechanism of sandwich slab subjected to concentrated mid-point load.

The pull-out capacity of the J-hook from the concrete core greatly affects the punching shear capacity of the slabs. Fibres within the concrete core help to increase both flexural and punching capacity of the slabs. After punching failure occurs in the concrete core, the SCS sandwich slabs continue to resist load due to the membrane action in the steel plates preventing sudden failure of the slabs and this allows the sandwich slabs to sustain a higher load at the large deflection range.

J.Y. Richard Liew conducted another investigation with X.X.Dai riguarding the SCS sandwich system, in particular the research was developed towards the static and fatigue behavior. Fatigue failure is of one of the key concerns in the design of bridge. Fatigue analysis is normally carried out

based on the S-N curve approach, as shown in the equation below, under the assumption of a linear cumulative damage law, the so called Miner's rule.

$$N_f S^m = K$$

$$\sum_{i=1}^{k} \frac{n_i}{N_i} = C$$

Where

$N_f = number\ of\ cycles\ to\ failure$

$m, K = constants$

$S = applied\ stress\ range$

$n_i = number\ of\ cycles\ applied\ by\ stress\ magnitude\ \Delta\sigma_i$

$N_i = number\ of\ cycles\ to\ failure\ of\ stress\ magnitude\ \Delta\sigma_i$

$C = constant\ usually\ considered$ 1.0

The schematic view of cyclic load or fatigue load time history is shown in Figure 47, in which the load range ΔP is defined as $\Delta P = P_{max} - P_{min}$

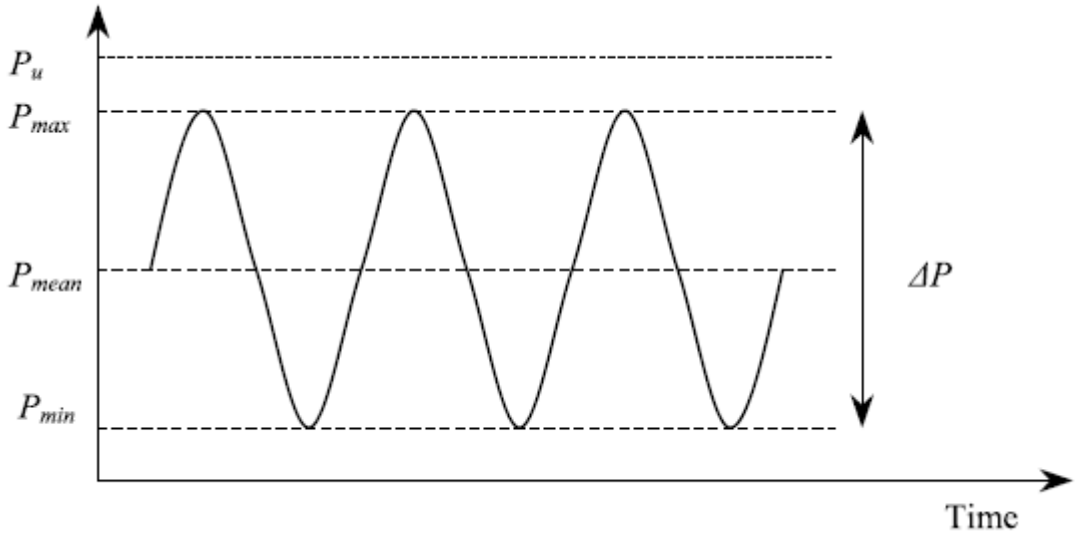

Figure 47 Fatigue load parameters

Generally the fatigue tests assume a linear relationship between log (N_f) and the stress range or load range ΔP. (where b and k are constants)

$$\log(N_f) = -k\Delta P + b$$

In the study the two researchers conducted, were used the same J-Hooks as in the study mentioned earlier

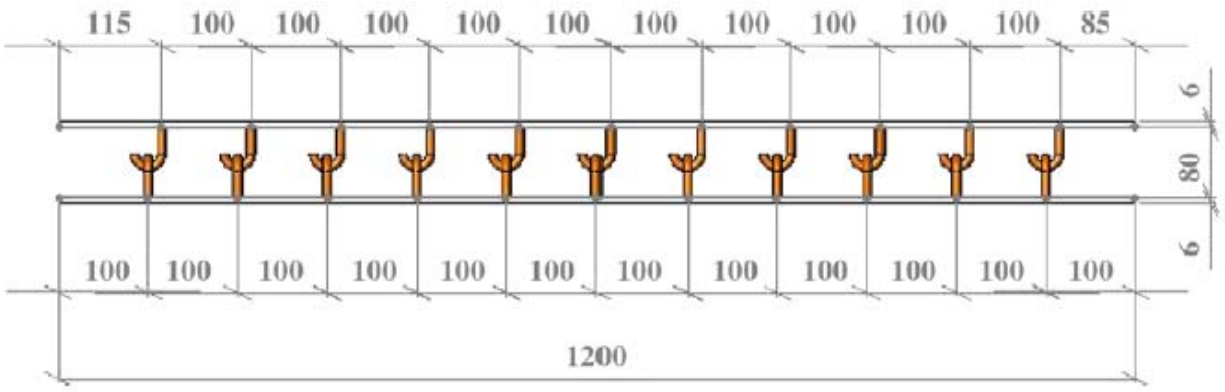

Figure 48 Design of SCS sandwich beam with J-Hooks

Test Specimens

The length, width and overall thickness of the SCS composite beam are 1200mm, 250mm and 92mm respectively, with dimensions as shown in Figure 48.

The steel plate is grade S275JR with a yield strength of 350 KN/mm^2 and ultimate tensile strength of 500 KN/mm^2. The J-Hooks are made from cold drawn round steel bar with an ultimate tensile strength of 610 KN/mm^2.

The fatigue test specimen is defined by its relative maximum applied load $\frac{P_{max}}{P_u} =$ 0.8,0.9 and relative load range $\frac{\Delta P}{P_u} = 0.4,0.5,0.7$

Static Test Results

For specimen SP, the beam deflection increased linearly with an increase of load until 20 kN, where debonding occurred at the interface between the bottom steel plate and the concrete core.

After this, the beam deflected at a slightly faster rate as shown in Figure 39. Some shear cracks (in the form of diagonal cracks) were observed starting from the loading point and gradually propagating to the beam ends when the applied loads increased from 42 to 49 kN. These cracks propagated through the concrete core at about 45 degrees across

connectors L-3, L-4 and L-5, as shown in Figure 49a. After the cracks appeared, the deflection increased at a faster rate with extension and widening of these shear cracks. Finally, the concrete core was broken into pieces of
blocks.

Larger diagonal shear cracks developed in the plain concrete core for specimen SP, as shown in Figure 49b, contributing to a larger beam deflection as compared to specimens S1 and S2 with the fibre-reinforced concrete core. Finally, significant load drops occurred in the load deflection curve indicating the failure of the connectors.

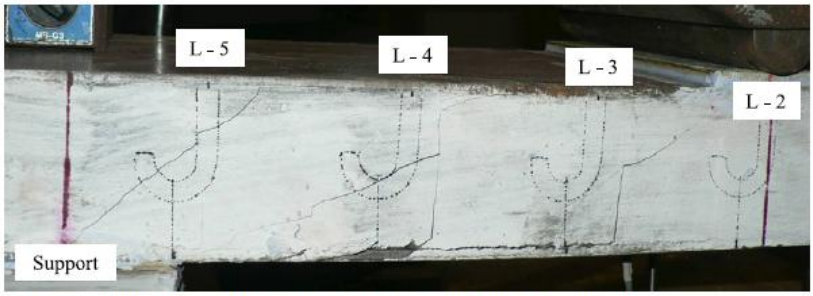

(a) Shear cracks initiate at 42 kN, 46 kN and 49 kN from load point to beam end.

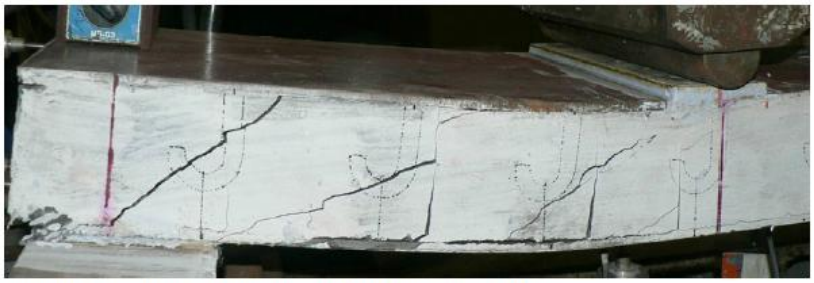

(b) Shear cracks extend and widen at 63 kN load and 31 mm deflection.

Figure 49 Shear cracks development

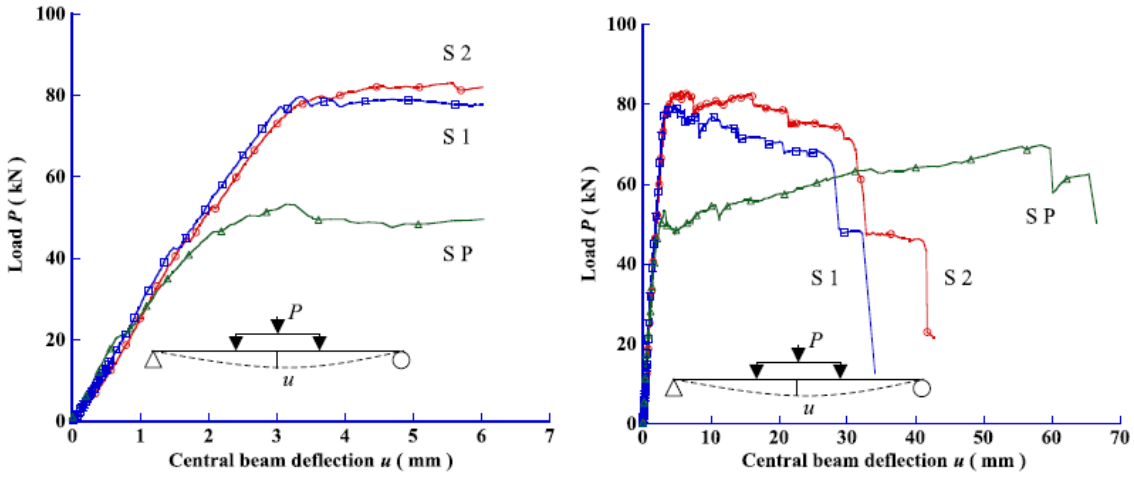

(a) At an early stage. (b) Whole range.

Figure 50 Load deflection behavior

Hysterical Responses

The hysteretic load deflection response under cyclic load is shown in Figure 40. Two static load deflection loops loaded up to the maximum applied load were recorded prior to fatigue cycling. Monotonic load cycles were conducted periodically to determine the load deflection profile of the tested specimen throughout its fatigue life. The unloading curve does not follow the loading path, which indicates some permanent deformation has occurred. The loading and unloading curves comprise a static envelope. The area covered by this envelope is the energy absorbed by the specimen inducing permanent deformation or damage. This permanent deflection increases with the increase of fatigue load cycles.

The hysteretic response of relative slip between the bottom steel face plate and the concrete core under a cyclic load show similar behavior with that of deflection, except that the slip values are smaller than the corresponding deflection values, as shown in Figure 51.

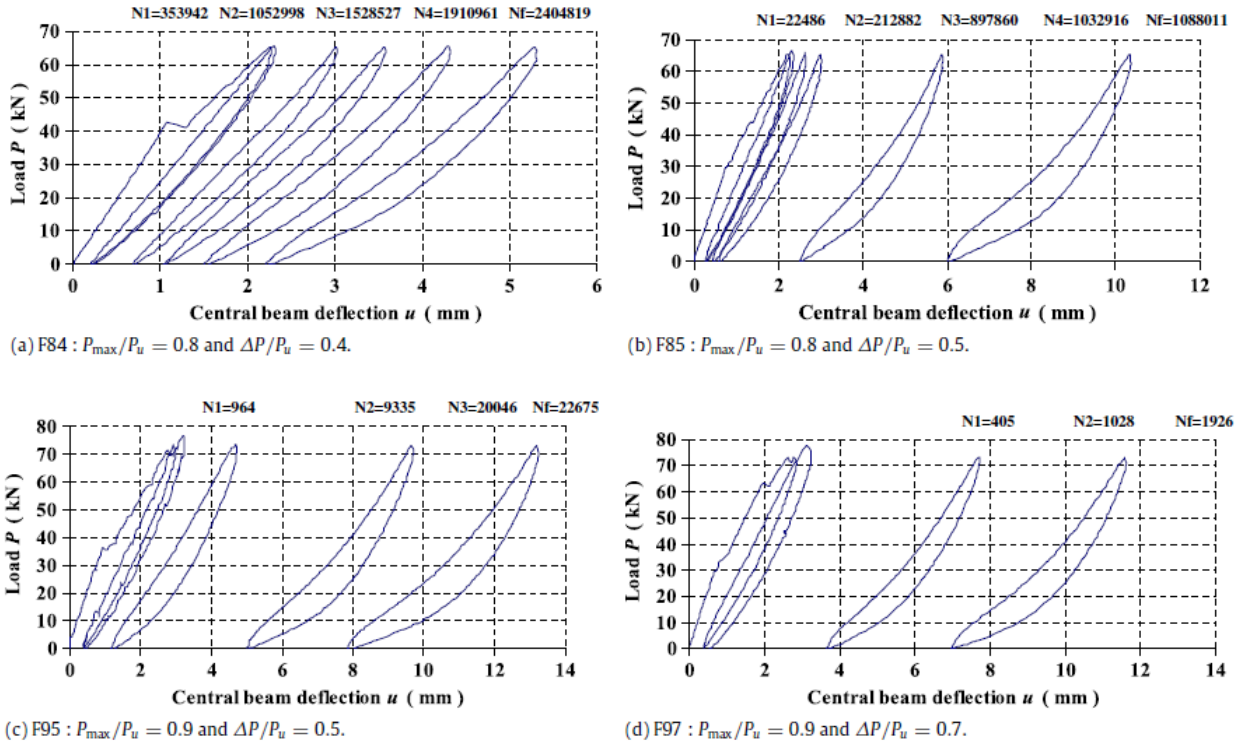

(a) F84 : $P_{max}/P_u = 0.8$ and $\Delta P/P_u = 0.4$.

(b) F85 : $P_{max}/P_u = 0.8$ and $\Delta P/P_u = 0.5$.

(c) F95 : $P_{max}/P_u = 0.9$ and $\Delta P/P_u = 0.5$.

(d) F97 : $P_{max}/P_u = 0.9$ and $\Delta P/P_u = 0.7$.

Figure 51 Hysteric response of load vs. deflection

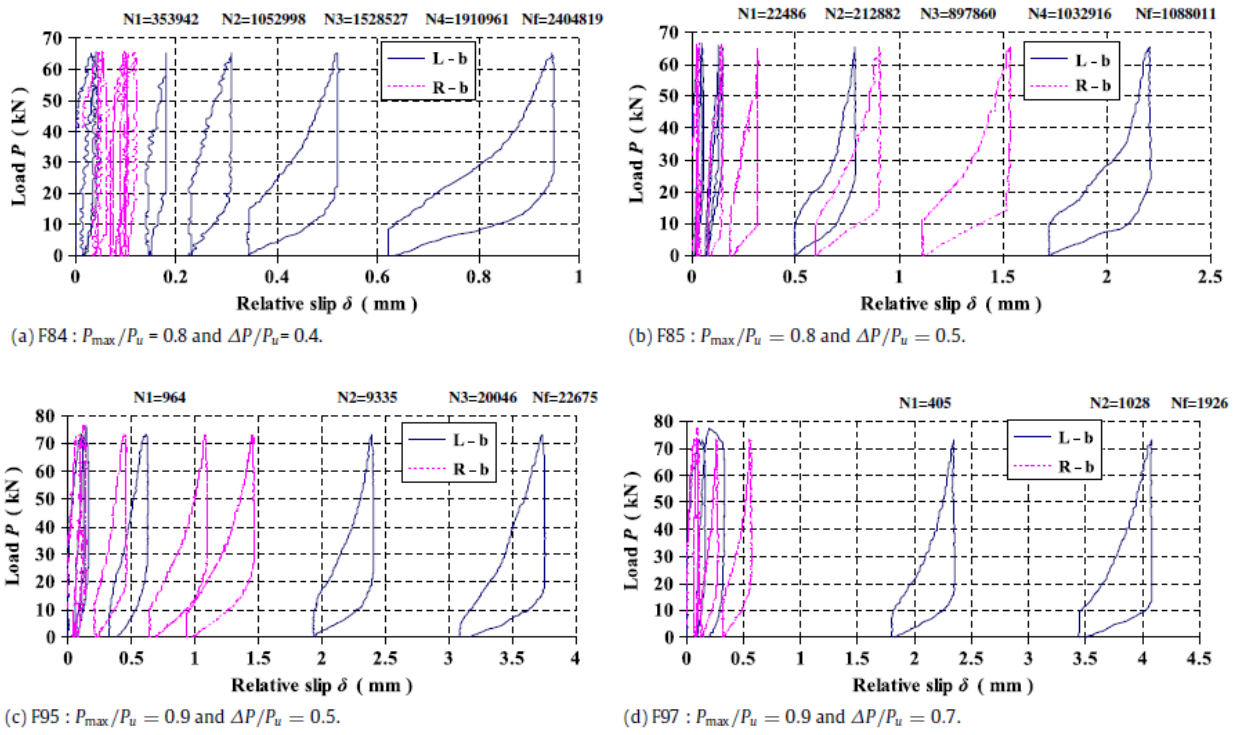

Figure 52 Hysteric response of load vs. relative slip

Permanent Deformation

The relationship between deformation, expressed by the deflection and relative slip, and the number of load cycles is shown in Figure 52, both in normal and log scale. The maximum and minimum applied load levels are 0.8 and 0.4 respectively.

The first two data points represent the permanent (plastic) deformation at the end of an unloading phase in the first two static loops before fatigue tests start. It is seen that both the deflection and relative slip increase in an accelerating manner. The slope of the line connecting the data points can be deemed as an indicator of the deformation rate with respect to the number of load cycles.

Comparing the deformation curves of F95 and F85 concludes that a larger value of maximum applied load induces more fatigue damage although the load ranges are the same.

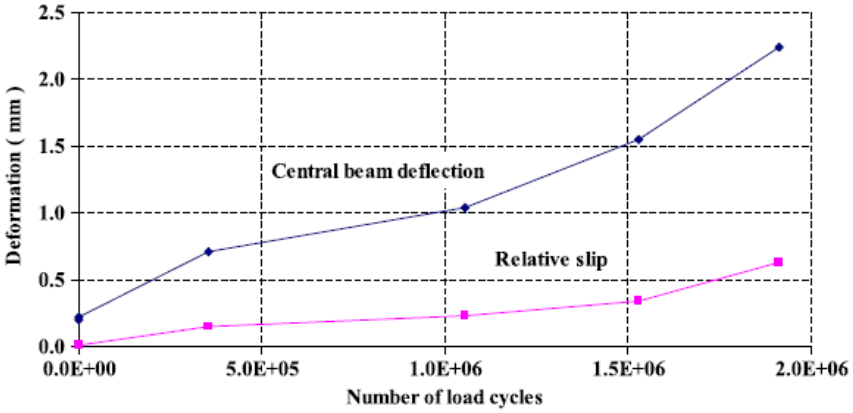

(a) F84 : $P_{max}/P_u = 0.8$ and $\Delta P/P_u = 0.4$ (in Normal scale).

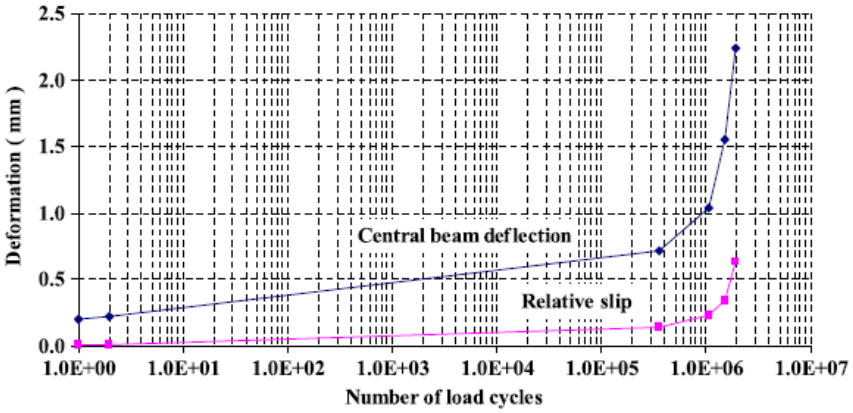

(b) F84 : $P_{max}/P_u = 0.8$ and $\Delta P/P_u = 0.4$ (in Log scale).

Figure 53 Variation of permanent deformation

Energy Dissipation

The area covered by the load displacement curve can be approximated by dividing the integral into many small trapezoids by displacement increments, such as $P_1P_2u_2u_1$ shown in Figure 54. The

unit work in this increment is thus the area of the trapezoid.

$$dW = \frac{1}{2}(P_1+P_2)(u_2 - u_1)$$

The algebraic sum of the unit work in both loading and unloading parts are thus the energy absorbed by the specimen, given as:

$$E = \sum dE = \sum \frac{1}{2}(P_1 + P_2 - P_3 - P_4)(u_2 - u_1)$$

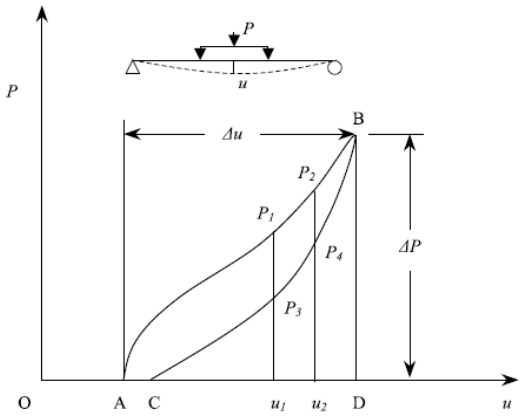

Figure 54 Permanent deformation

The variation of energy absorption capacity in the process of fatigue loading is shown in Figure 55 The absorbed energy in the first static loop for F85 and F84 are almost the same since they are subjected to the same maximum applied load. In the subsequent fatigue load cycles, specimen F85 absorbed more energy than F84.

Specimen F95 absorbed more energy than the other two in the whole process of fatigue loading due to its higher value of maximum applied load. Thus it is concluded that the variation of energy absorption capacity is affected by both the maximum applied load and load range.

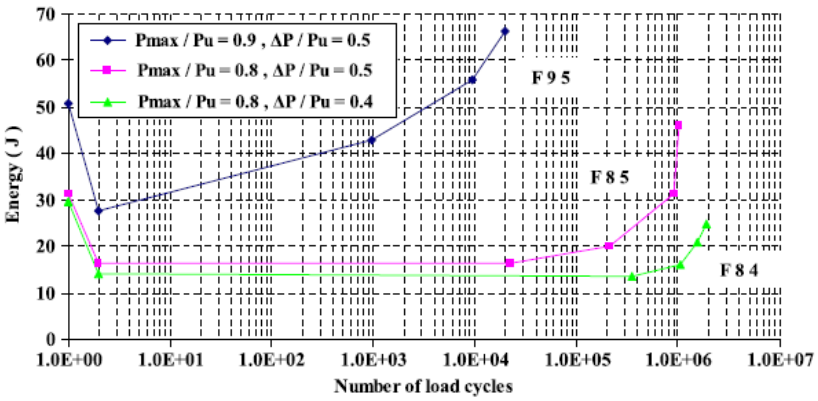

Figure 55 Variation of energy dissipation with an increasing number of load cycles

Conclusions

Test results show that J-hook connectors are effective in preventing relative slip at the steel-concrete interface and tensile separation of the steel face plates. Using a 1% volume fraction of steel fibers in the concrete core could reduce the cracks significantly and enhance the structural integrity of the sandwich beams.

Results from fatigue tests on SCS beams show that their fatigue life is affected by both the fatigue stress range and maximum applied stress; fatigue life reduces when the load range or maximum applied load increases.

The proposed SCS sandwich system with a lightweight concrete core and J-hook connectors shows good performance under fatigue loading.

2) *Bridge Design for 10 meters span with cross end beam*

2.1) Static Analysis

The main purpose of this work is to design and analyze a half trough steel bridge, suitable for railways, studying it for different bridge spans and trying to make it with the lowest building depth as possible.

Various spans will be considered, such as 6-10-15 meters supported by two types of end cross beams, also considering the possibility of three or four bearings.

This particular type of bridge is characterized by a steel deck plate, with an uniform thickness of 80 mm throughout the length of the span.

High rotational and flectional stiffness is guaranteed by the main girders, box beams with different thicknesses between the webs and the top flange, 30mm and 40mm respectively.

Additional diaphragms are positioned into the main girders to improve the stiffness of the structure, their thickness is 12mm.

2.1.1) Bridge Characteristics

Firstly, the deck supported by the end cross beam is going to be analyzed.

This beam is very stiff and presents a section as shown in Figure 56.

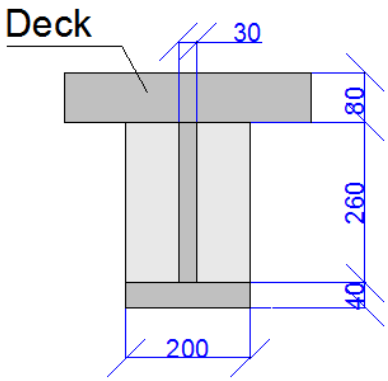

Figure 56 Section of the end cross beam

As we can see the beams web is welded directly to the bridge deck and its thickness is 30mm. This beam is going to lay on the bearings with the bottom flange, 40mm thick.

Six stiffener plates (30 mm thick) are welded transversely to the beams web, as we can se from Figure 57.

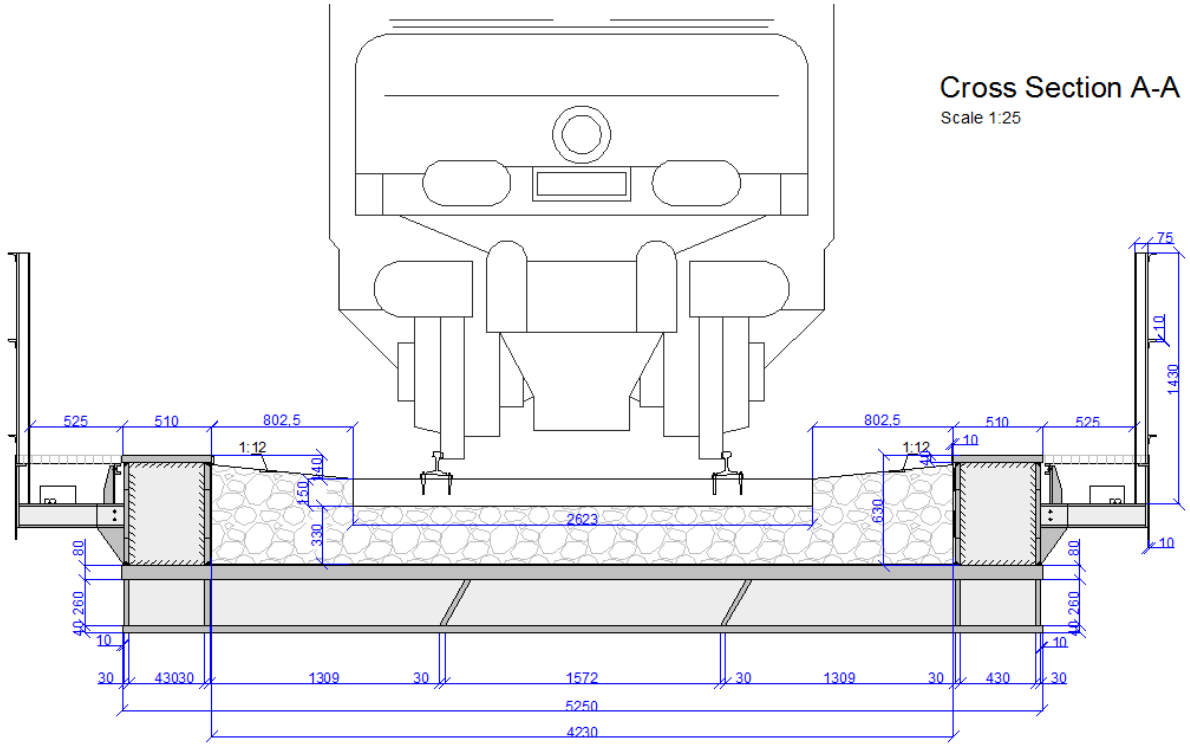

Figure 57 Bridge cross section

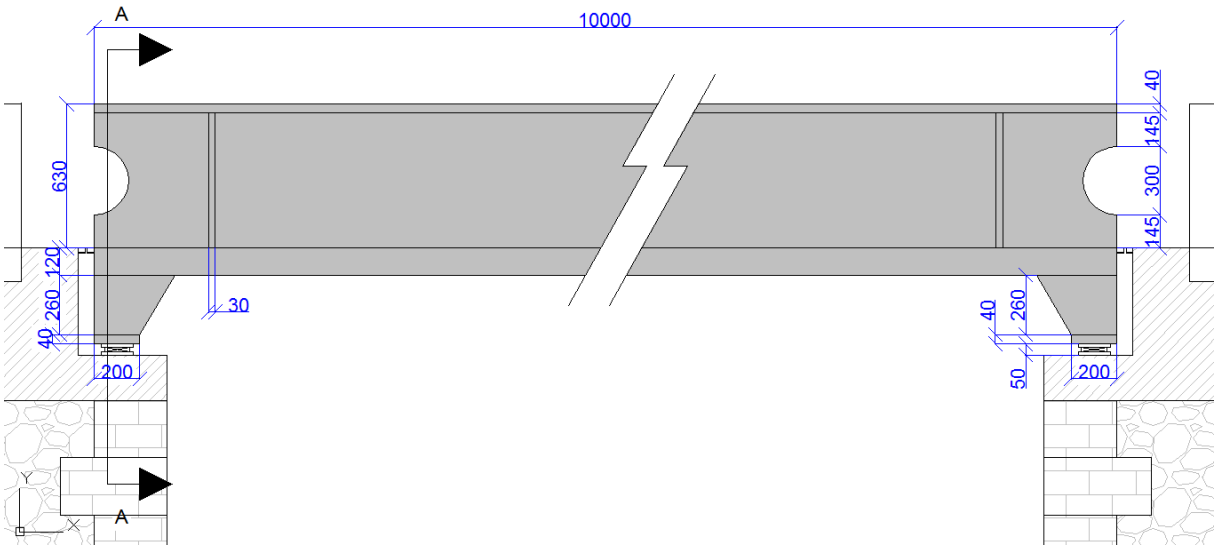

Figure 58 Bridge longitudinal view

2.1.2) Design

The bridge was modeled on the computer with the FEM software CSi Bridge, all the structure was drawn using only shells, as shown in Figure 59.

Two models will be compared to see if three bearings are enough or the loading needs a fourth bearing.

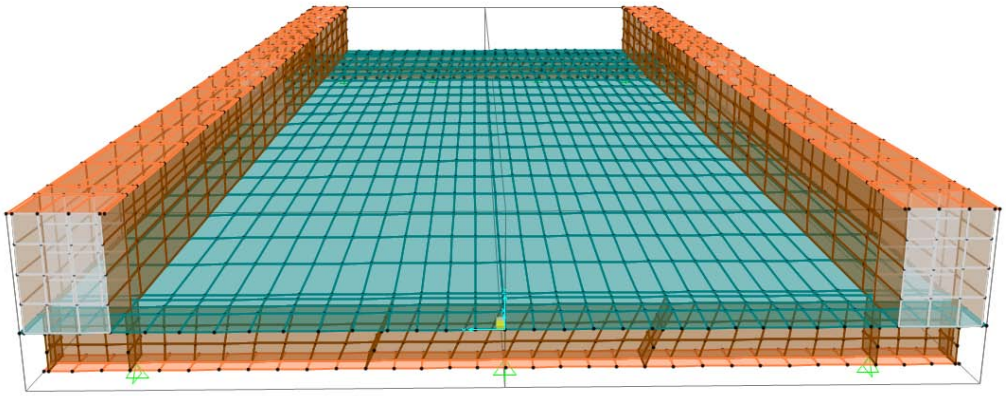

Figure 59 Bridge with end cross beam model with three bearings

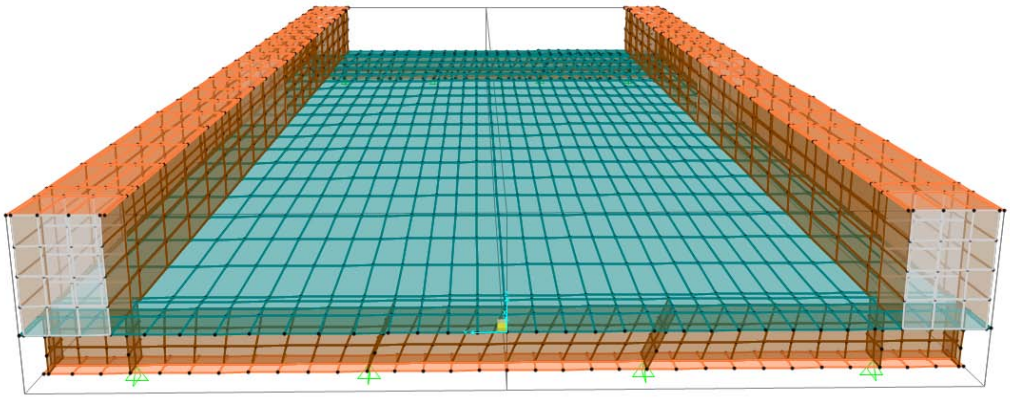

Figure 60 Bridge with end cross beam model with four bearings

2.1.3) Loading

The structure, according to the Eurocode requirements, has been loaded with all kinds of loads and those have been combined with the given coefficients:

- Dead Load
- Wind Load
- Temperature Loads (Uniform & Non Uniform)
- Vehicle Load LM 71
- Vehicle Load SW/2

DEAD LOADS:

Other than the weight of the structure itself, the ballast has also been included in the dead loads. As stated in the Eurocode 1-1-1 , the weight of the ballast has been considered increased by +30% and also with a reduction of -30% (in the combinations, the self weight multiplier won't be 1, but 1,3 to take into account the increasing of +30%, and 0,7 for the reduction)

WIND LOADS:

Using the equations given in Eurocode 1-4, the Wind forces in y and z directions were calculated, applied as a uniform pressure on the structure, considering $V_b = 27{,}5\ [\frac{m}{sec}]$.

$$F_y = \frac{\rho V_b^2 C}{2} = 0.725\ [\frac{KN}{m^2}]$$

Being $C = C_e C_{f,y} = 1.18 * 1.3 = 1.534$

And $\rho = 1.25\ [\frac{Kg}{m^3}]$

$$F_z = \frac{\rho V_b^2 C}{2} = 0.502\ [\frac{KN}{m^2}]$$

Being $C = C_e C_{f,z} = 1.18 * 0.9 = 1.062$

And $\rho = 1.25\ [\frac{Kg}{m^3}]$

Wind in x-direction may be neglected.

Coefficients $C_{f,z}$ and $C_{f,y}$ have been taken by the graph below

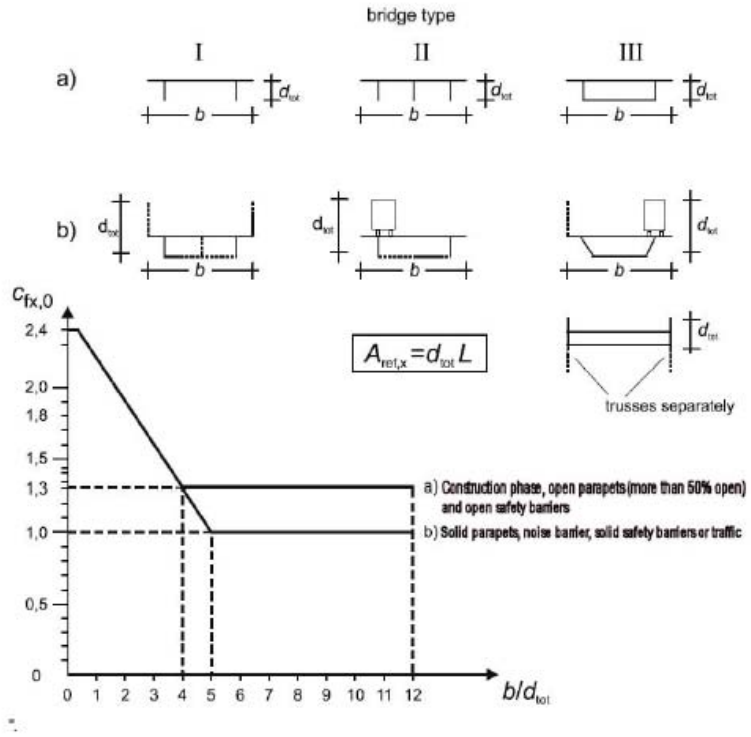

Figure 61 Graph for the determination of coefficient Cf

To take into account also the torsion moment caused by wind actions, a height of 4m for the train has been used to calculate the area on which the wind pressure takes place. This pressure has been further decomposed into two forces acting on the sleepers, as shown in figure 62.

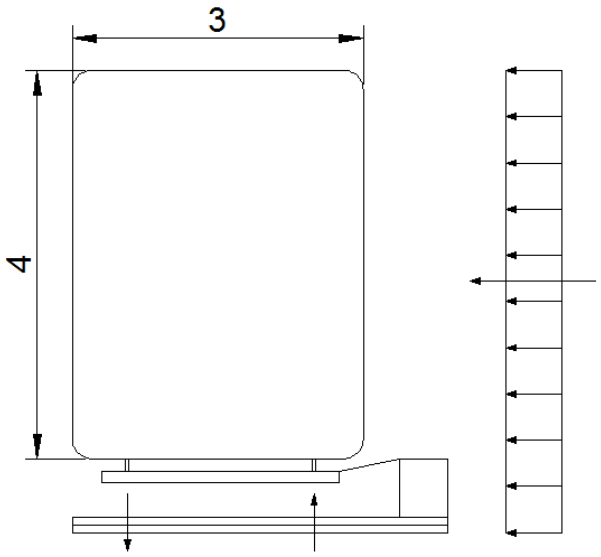

Figure 62 Wind force decomposure

The forces on the rails are calculated as follows

$$F = \frac{F_y H}{B} = \frac{0.725 * 4}{1.8} = 1.6\ [\frac{KN}{m^2}]$$

TEMPERATURE LOADS:

As stated in EC 1991-1-5 this structure can be assigned into Type 1 category, being it a steel deck bridge with box girders.

In these models, two different load cases were made to take into account the temperature leap. Characteristic values of minimum and maximum shade air temperatures for the site location shall be obtained, e.g. from national maps of isotherms.

$$T_{MAX} = +40°C$$

$$T_{MIN} = -34°C$$

Using the picture below we can detect the bridge temperatures starting from the shade air temperatures, approximately now they will be:

$$T_{MAX} = +56C$$

$$T_{MIN} = -37°C$$

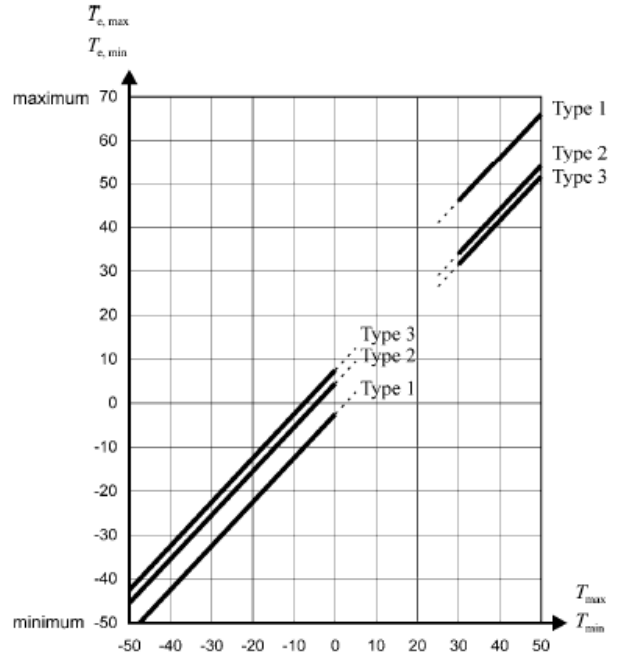

In addition to those uniform temperatures, in the model was inserted a non-uniform temperature load case, which takes into account $\pm 15°C$ on the surfaces that are exposed to the weather, $\pm 0°C$ on the shaded areas.

Figure 63 Graph for determination of structure temperatures

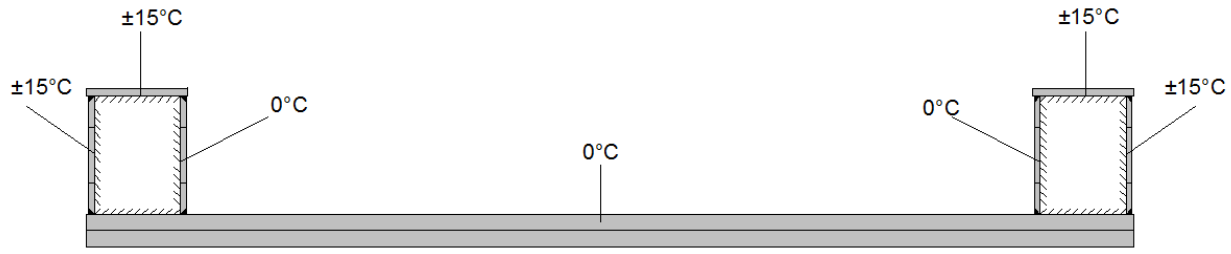

Figure 64 Non uniform temperature

VEHICLE LOADS:

In this load case two different types of load were inserted, SW/2 and LM71 (already showed in chapter 1.3). These loads were designed as shown in pictures 65 and 66.
The characteristic values given in LM71 shall be multiplied by a factor *a*, as explained before, we chose 1.10.

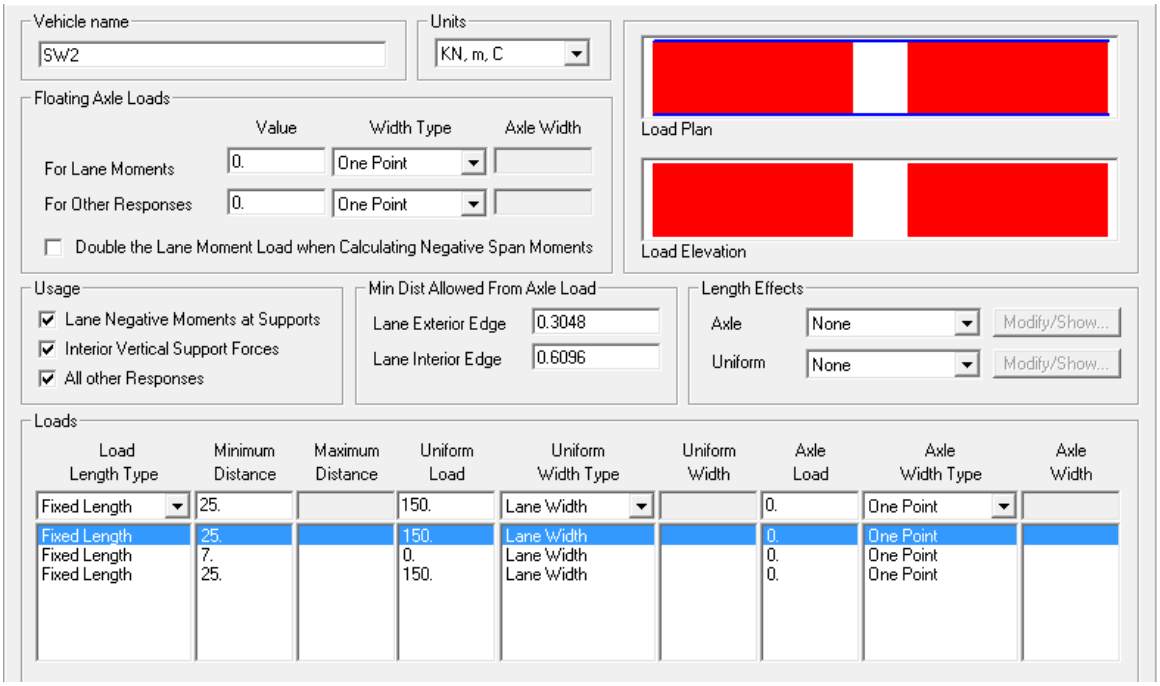

Figure 65 Input of SW/2 Load into CSi Bridge

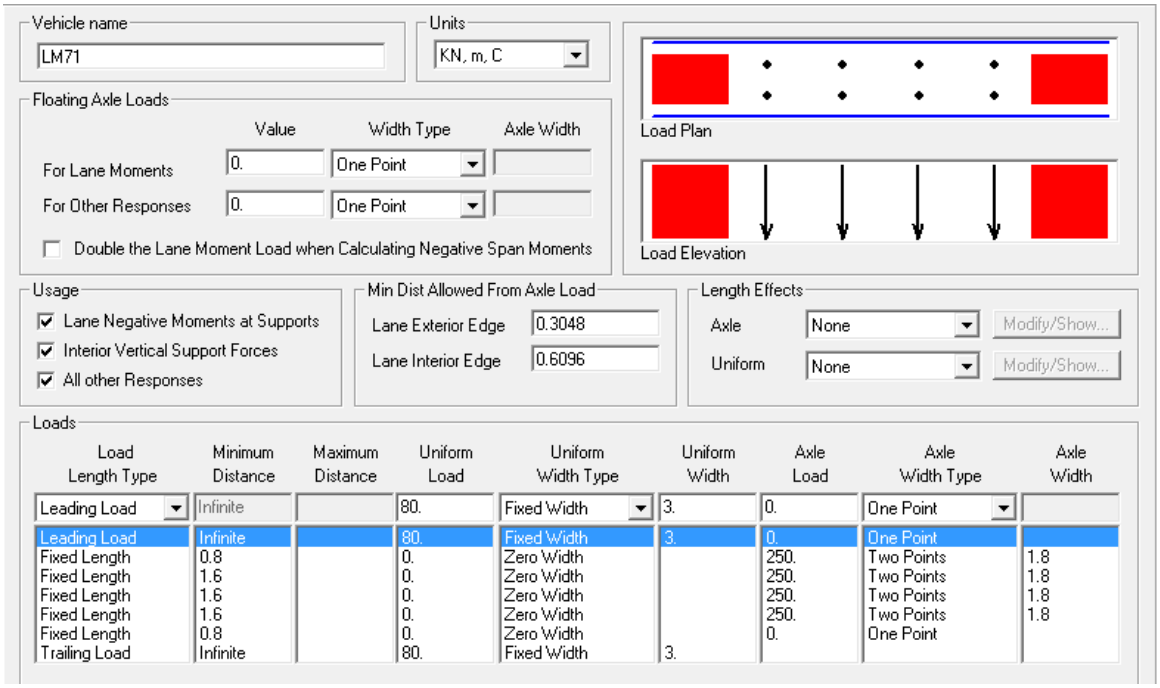

Figure 66 Input of LM71 Load into CSi Bridge

2.1.4) Distribution of the Load

Load is distributed by sleepers and ballast with a 1:4 slope like this.

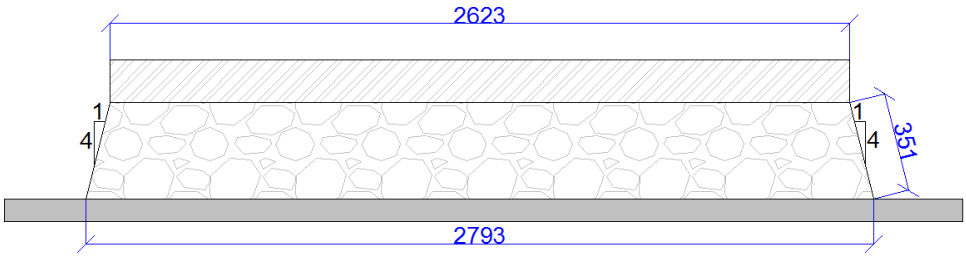

Figure 67 Distribution of the load

2.1.5) Load Combinations

The load combinations have been formed according to the rules written in Eurocode 0.
The general format of effects of actions should be:

$$E_d = \gamma_{Sd} E\{\gamma_{g,j} G_{k,j}; \gamma_p P; \gamma_{q,1} Q_{k,1}; \gamma_{q,i} \psi_{0.i} Q_{k,i}\} \quad j \geq 1; i > 1$$

Values for the coefficients can also be found in this Eurocode, As listed below.

$\gamma_{G,sup} = 1{,}35$

$\gamma_{G,inf} = 1{,}00$

$\gamma_Q = 1{,}45$, $Q\ is\ unfavourable\ actions\ due\ to\ load\ model\ LM71\ (0\ if\ favourable)$

$\gamma_Q = 1{,}20$, $Q\ is\ unfavourable\ actions\ due\ to\ load\ model\ SW2\ (0\ if\ favourable)$

Actions		ψ_0	ψ_1	ψ_2 [4]
Individual components of traffic actions [5]	LM 71	0,80	[1]	0
	SW/0	0,80	[1]	0
	SW/2	0	1,00	0
	Unloaded train	1,00	–	–
	HSLM	1,00	1,00	0
	Traction and braking Centrifugal forces Interaction forces due to deformation under vertical traffic loads	Individual components of traffic actions in design situations where the traffic loads are considered as a single (multi-directional) leading action and not as groups of loads should use the same values of ψ factors as those adopted for the associated vertical loads		
	Nosing forces	1,00	0,80	0
	Non public footpaths loads	0,80	0,50	0
	Real trains	1,00	1,00	0
		0,80	[1]	0
	Horizontal earth pressure due to traffic load surcharge	0,80	0,50	0
	Aerodynamic effects			
Wind forces [2]	F_{Wk}	0,75	0,50	0
	F_W^*	1,00	0	0
Table continued on next page				
Thermal actions [3]	T_k	0,60	0,60	0,50

These are the combinations detected, with the relative coefficients applied on each load.

				BALLAST				Non Uniform T		
	COMBINATION		DEAD	30%	-30%	WIND	SW/2	15	-15	LM/71
SW2	1		1.35	1.755		1.125		0.9		
	2		1.35	1.755			1.2	0.9		
	3		1		0.945	1.125			0.9	
	4		1.35	1.755			1.2		0.9	
	5		1.35	1.755		1.125			0.9	
	6		1.35	1.755		1.5			0.9	
	7		1.35	1.755		1.5		0.9		
	8		1		0.945	1.5		0.9		
	9		1		0.945		1.2	0.9		
	10		1		0.945		1.2		0.9	
	11		1		0.945	1.5			0.9	
	12		1		0.945	1.125		0.9		
LM71	13		1.35	1.755		1.5		0.9		1.45
	14		1.35	1.755		1.5			0.9	1.45
	15		1		0.945	1.5		0.9		1.45
	16		1		0.945	1.5			0.9	1.45
	17		1.35	1.755		1.125		0.9		1.45
	18		1.35	1.755		1.125			0.9	1.45
	19		1		0.945	1.125		0.9		1.45
	20		1		0.945	1.125			0.9	1.45
			DEAD	30%	-30%	WIND	SW/2	15	-15	LM/71

Figure 68 Load combinations

Into the loading process, something have been neglected:

- Impact forces of 1000 KN in the direction of vehicle travel of 500 KN perpendicularly
- Centrifugal forces, since this bridges are not placed into curving tracks
- Eccentricity of the track, due to different loads from the wheels. This eccentricity is so small so it doesn't affect the solution.
- Longitudinal forces

2.2) Results of the structure with three bearings

After running the analysis, these are the results provided by the post processor of the software, divided by load case and the displacement in Z is shown in Figures 69 – 70 – 71 – 72 for the three-bearings structure, Figures 73 – 74 – 75 – 76 for the four-bearings structure .

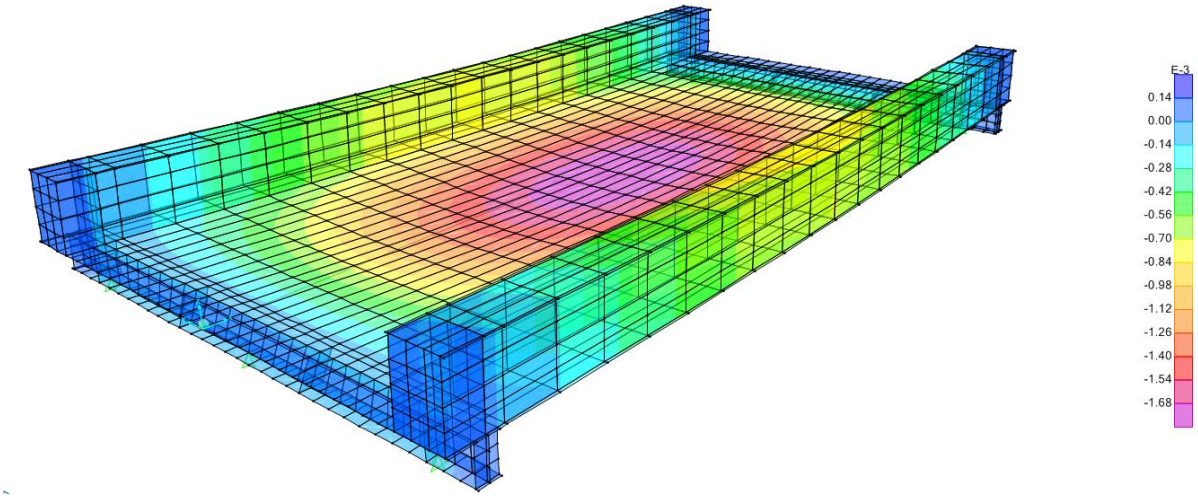

Figure 69 Dead Load z-displacement, structure with three bearings

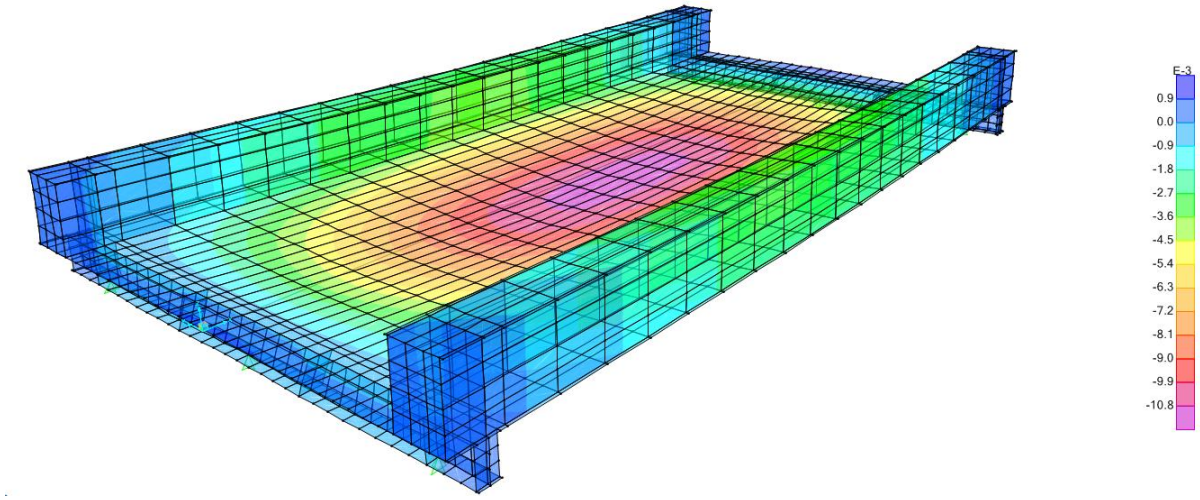

Figure 70 LM71 Load z-displacement, structure with end cross beam and three bearings

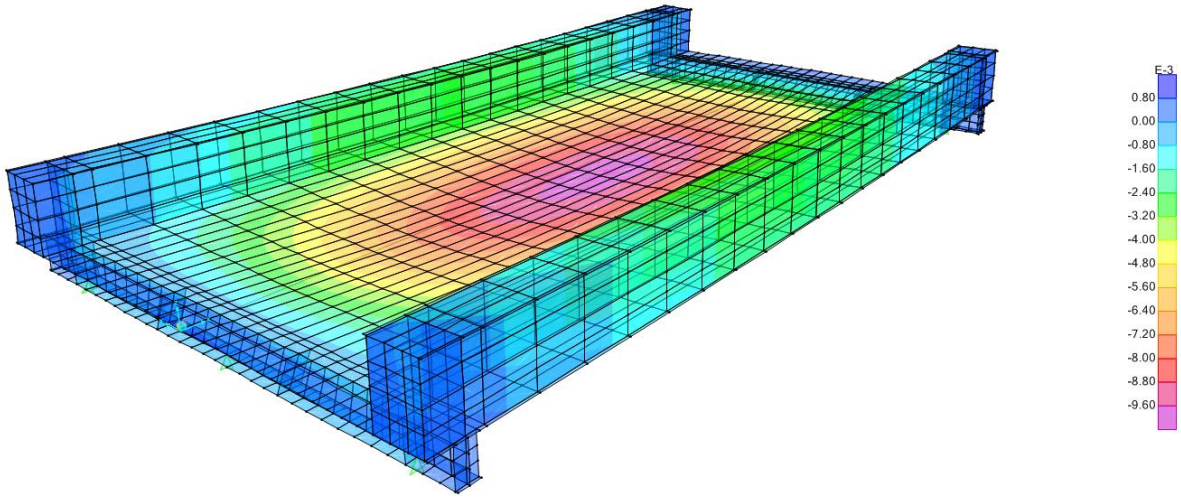

Figure 71 SW/2 Load z-displacement, structure with end cross beam and three bearings

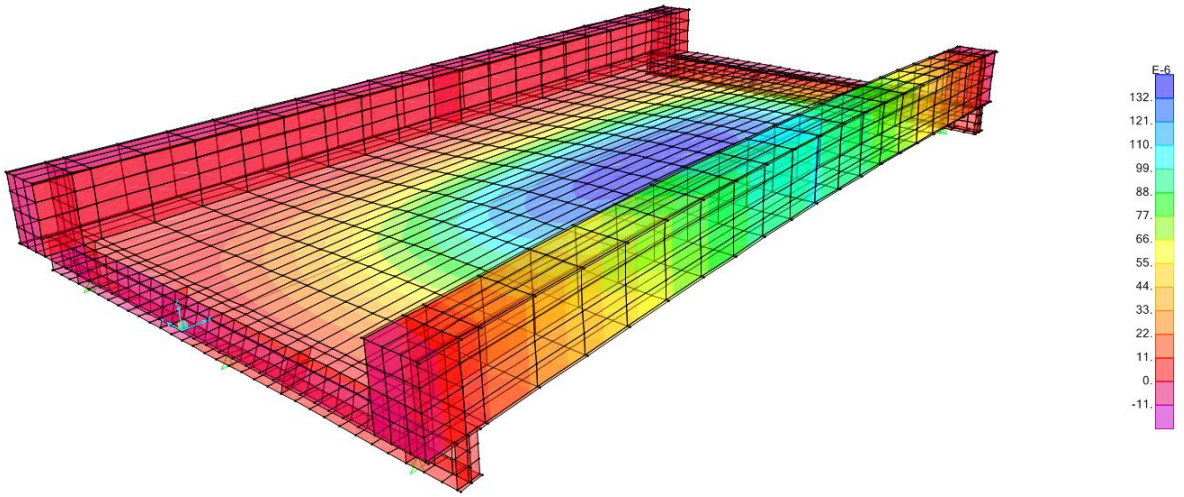

Figure 72 Wind Load z-displacement, structure with end cross beam and three bearings

2.3) Results of the structure with four bearings

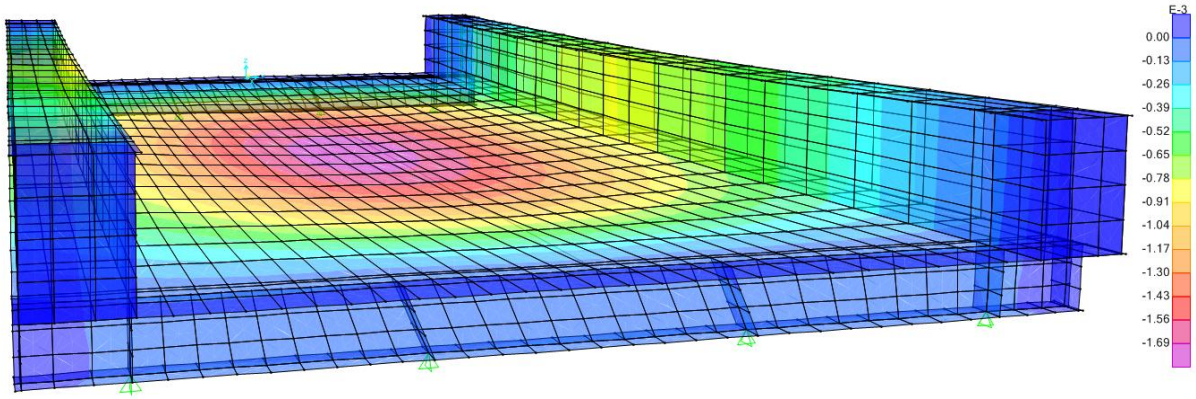

Figure 73 Dead Load z-displacement, structure with end cross beam and four bearings

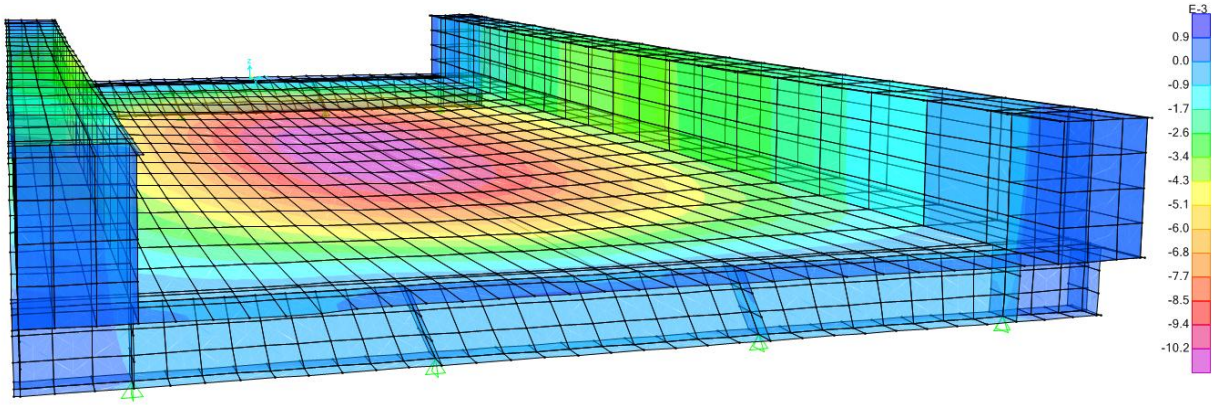

Figure 74 LM71 Load z-displacement, structure with end cross beam and four bearings

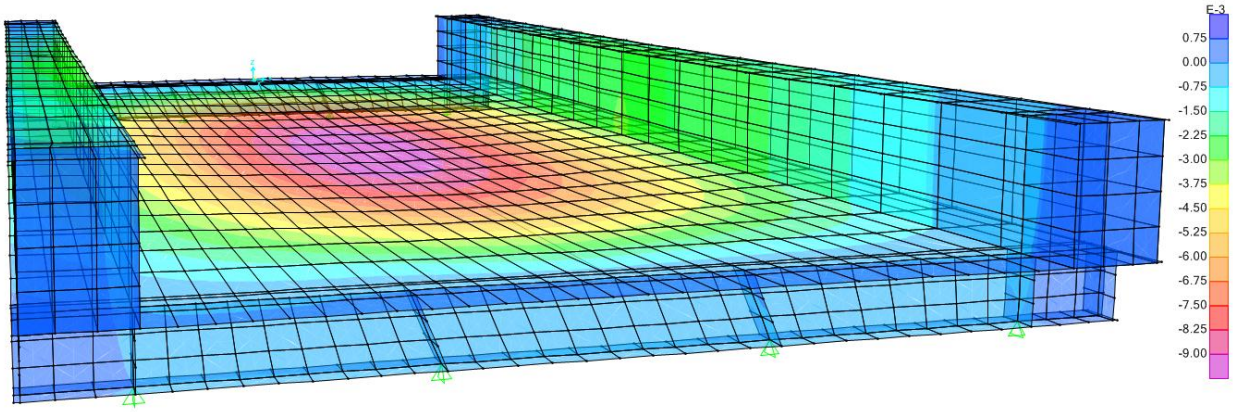

Figure 75 SW/2 Load z-displacement, structure with end cross beam and four bearings

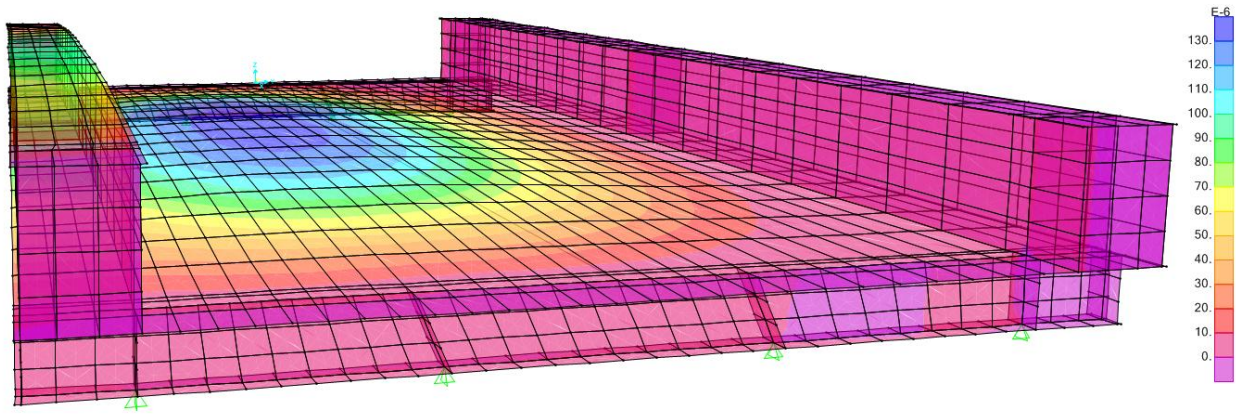

Figure 76 Wind Load z-displacement, structure with end cross beam and four bearings

If we watch the deflection gap that there's between the 3-bearings bridge and the 4-bearings one, we can see that these are the differences:

LOAD	3-BEARINGS		4-BEARINGS	
	Span Max displacement	*Deck-end Max displacement*	*Span Max displacement*	*Deck-end Max displacement*
DEAD	-1.68 [mm]	0.14 [mm]	-1.69 [mm]	0.00 [mm]
LM71	-11.88 [mm]	0.99 [mm]	-11.22 [mm]	0.99 [mm]
SW/2	-9.60 [mm]	0.80 [mm]	-9.00 [mm]	0.75 [mm]
WIND	0.13 [mm]	-0.01 [mm]	0.13 [mm]	0.00 [mm]

So, basically, displacements on the z axe are almost the same. The fourth bearing shouldn't be necessary.

3) *Bridge Design for 10 meters span without cross end beam*

3.1) Static Analysis

3.1.1) Bridge Design

If the end cross beam is considered too big and if we want to achieve a really low building depth, another solutions may be more suitable, even more practical and economical. An end cross slab, 80 mm thick like the deck, is going to replace the end cross beam; this slab may be seen in Figure 77.

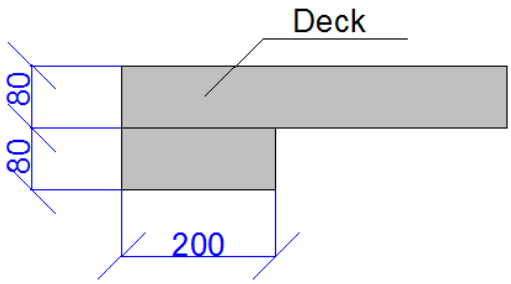

Figure 77 End cross slab

With this structural modification, the hole bridge went through some design changes, as shown in Figures 78 – 79 .

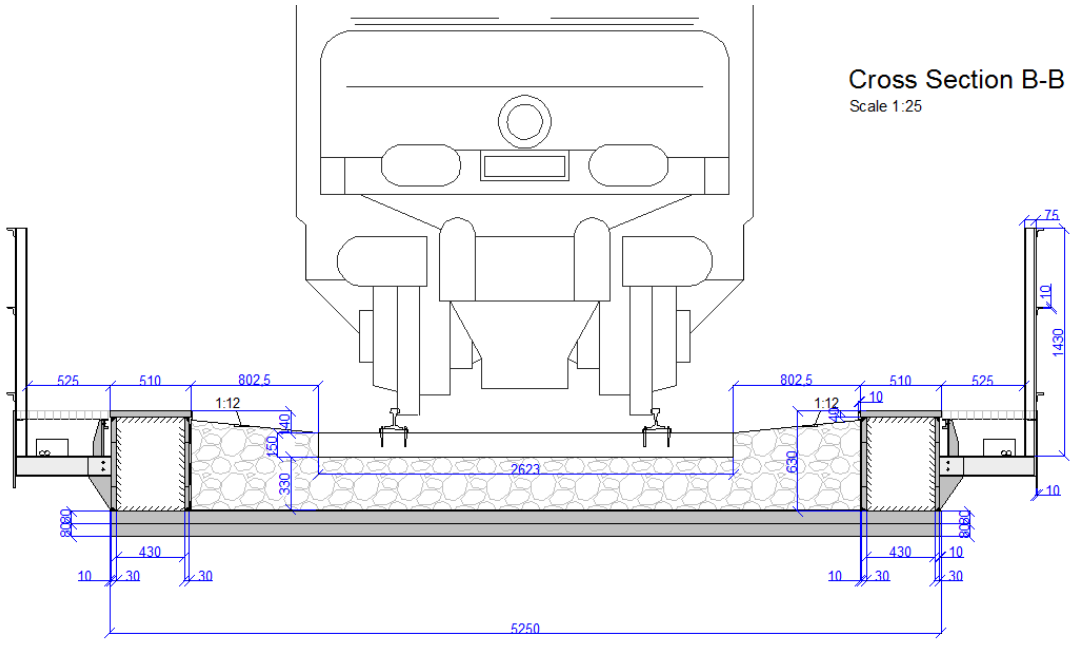

Figure 78 Bridge section with end cross slab

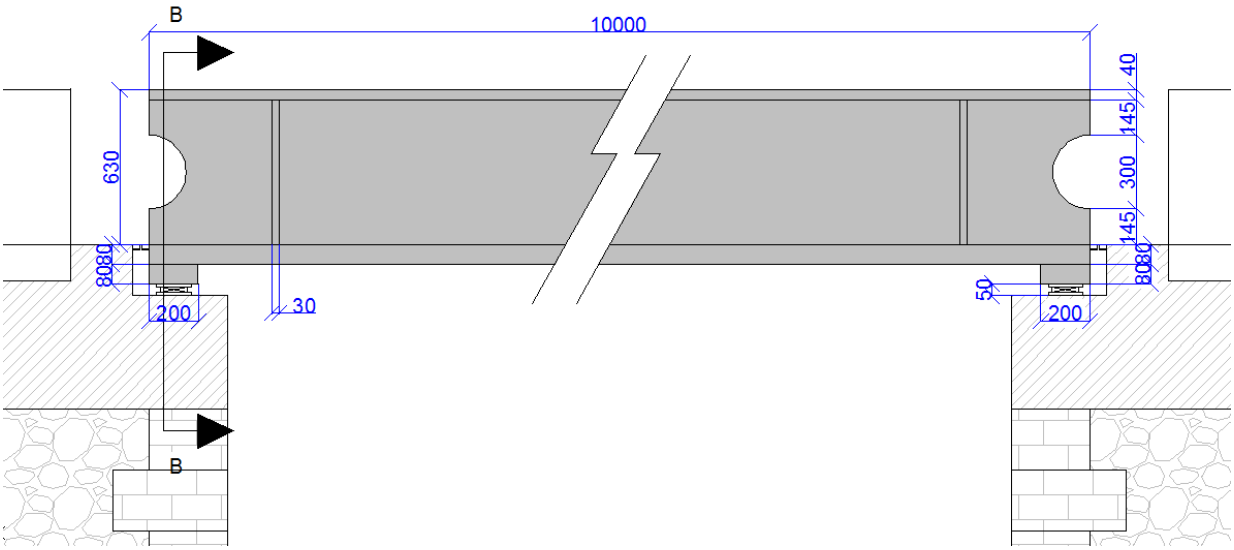

Figure 79 Bridge longitudinal view with end cross slab

Like before, this bridge was modeled with CSi Bridge, and the outcome is shown in Figure 80. Also here, the structure has been analyzed with three and four bearings, in order to make a comparison.

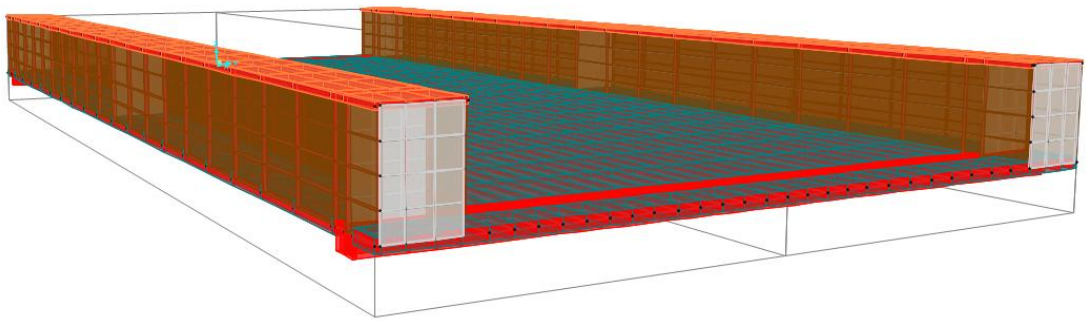

Figure 80 Bridge with end cross slab model

Below, some details of the box girder and the attachment of the diaphragms inside the main girders.

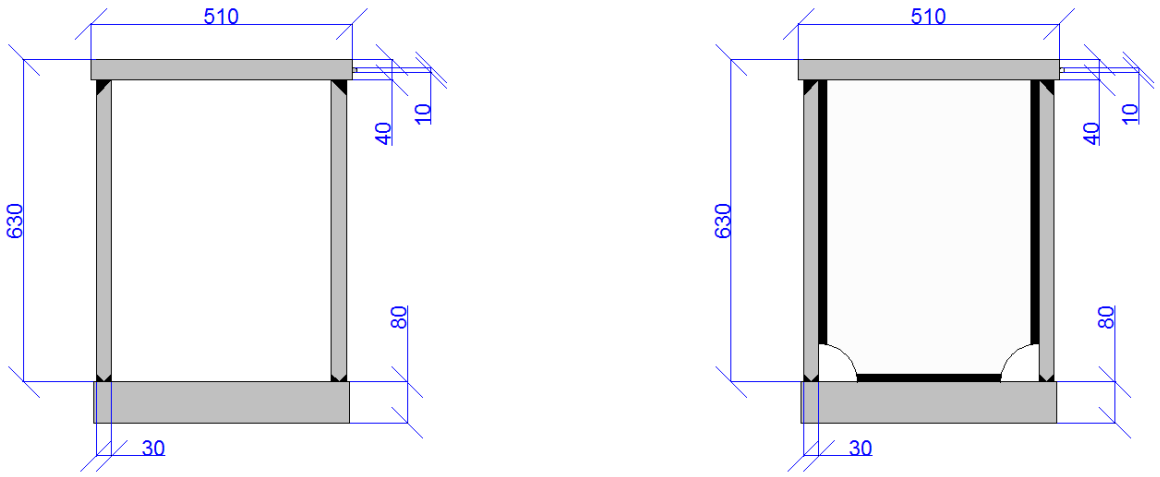

Figure 81 Details of box girder

The diaphragms at both ends of the deck will be fully penetrated all over the perimeter, because we want them to be waterproof and also can prevent external material to fall into the main girder.

3.1.2) Loading

The loading is exactly the same as in the previous description for the end cross beam bridge.

3.1.3) Results of the structure with three bearings

After running the analysis, these are the results, divided by load case and the displacement in Z is shown in Figures 82 – 83 – 84 – 85 for the three-bearings structure , Figures 86 – 87 – 88 – 89 for the four-bearings structure.

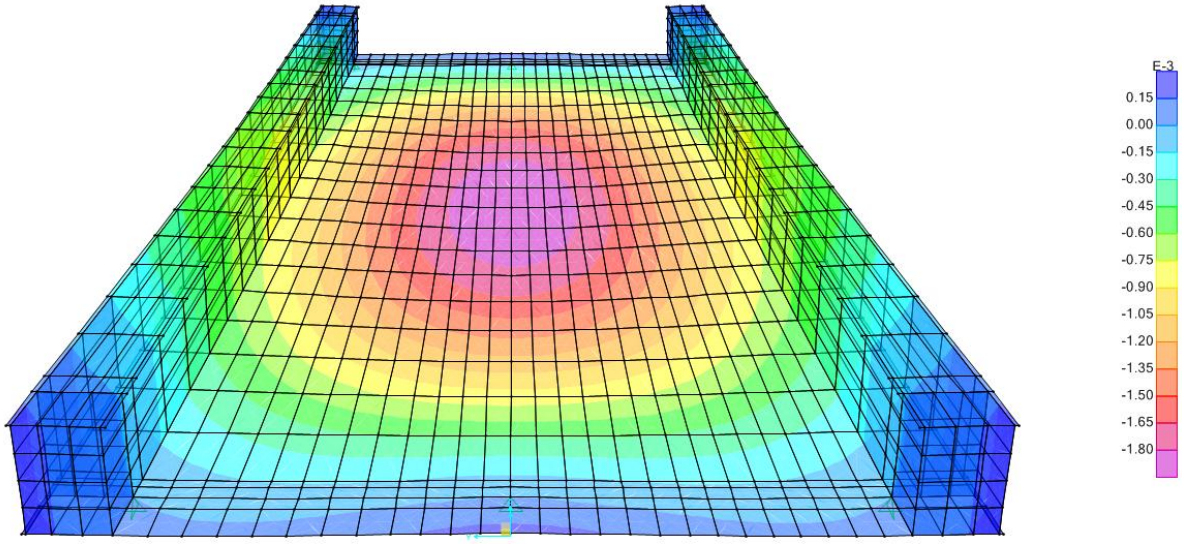

Figure 82 *Dead Load z-displacement, structure with end cross slab and three bearings*

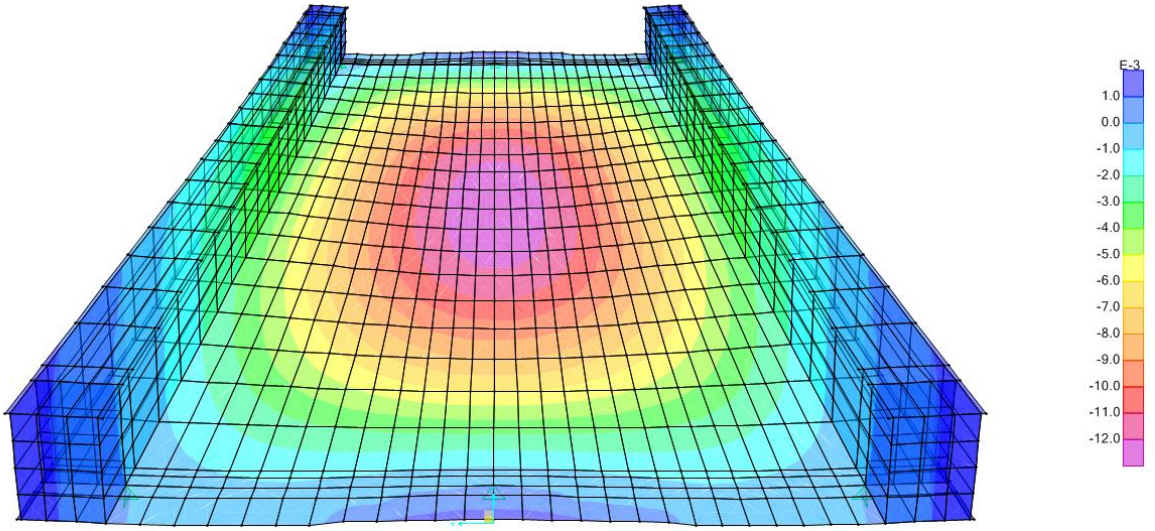

Figure 83 *LM71 Load z-displacement, structure with end cross slab and three bearings*

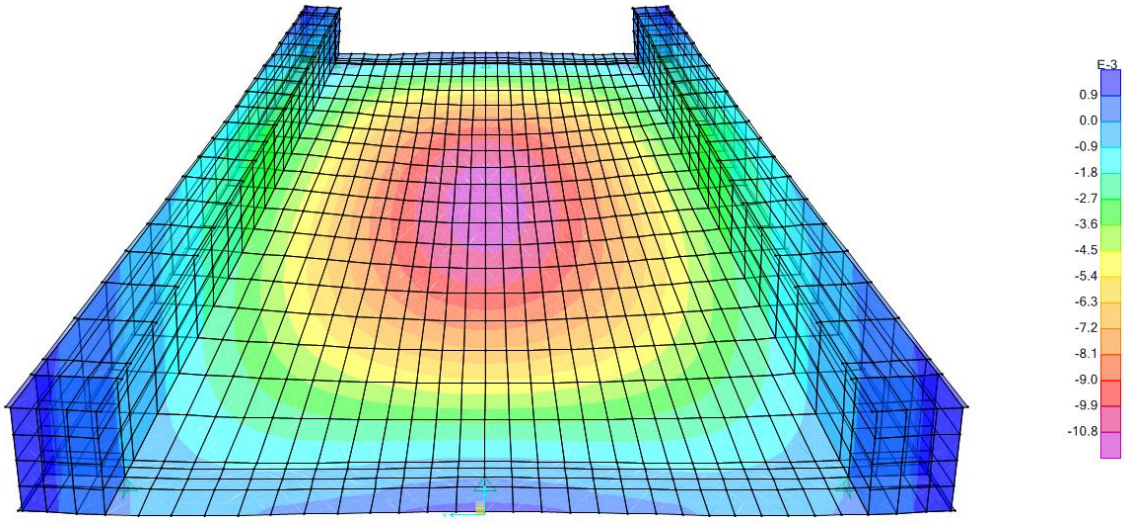

Figure 84 *SW/2 Load z-displacement, structure with end cross slab and three bearings*

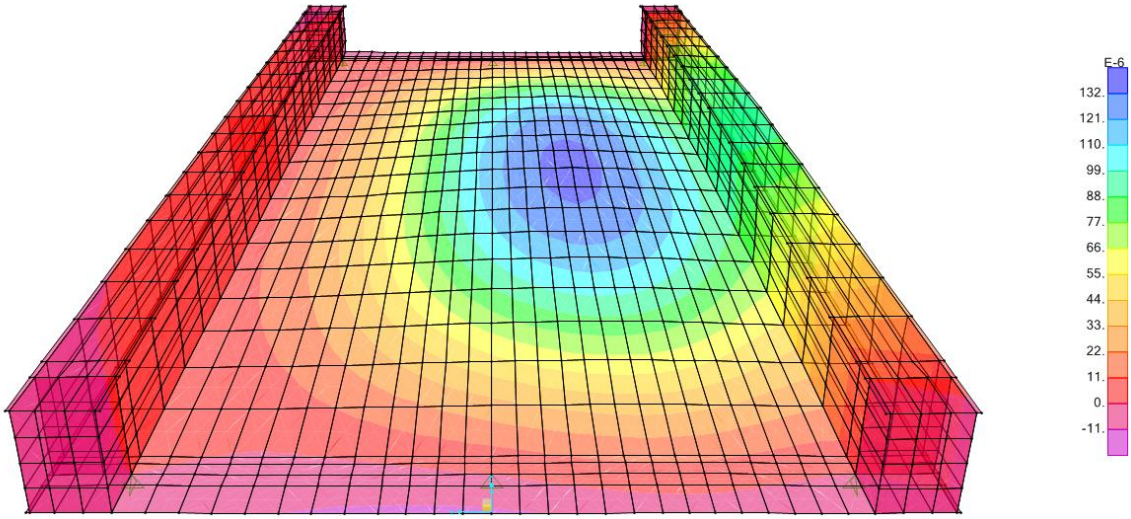

Figure 85 *Wind Load z-displacement, structure with end cross slab and three bearings*

3.1.4) Results of the structure with four bearings

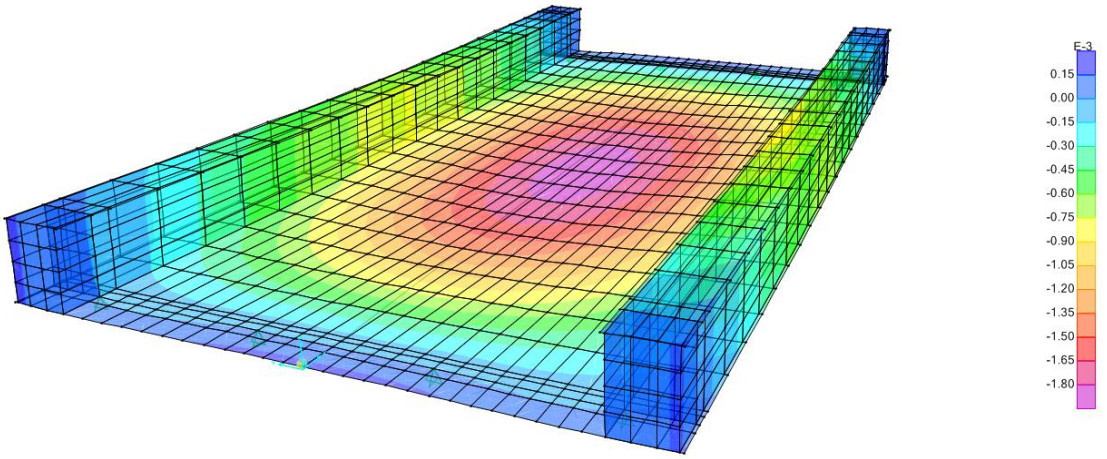

Figure 86 *Dead Load z-displacement, structure with end cross slab and four bearings*

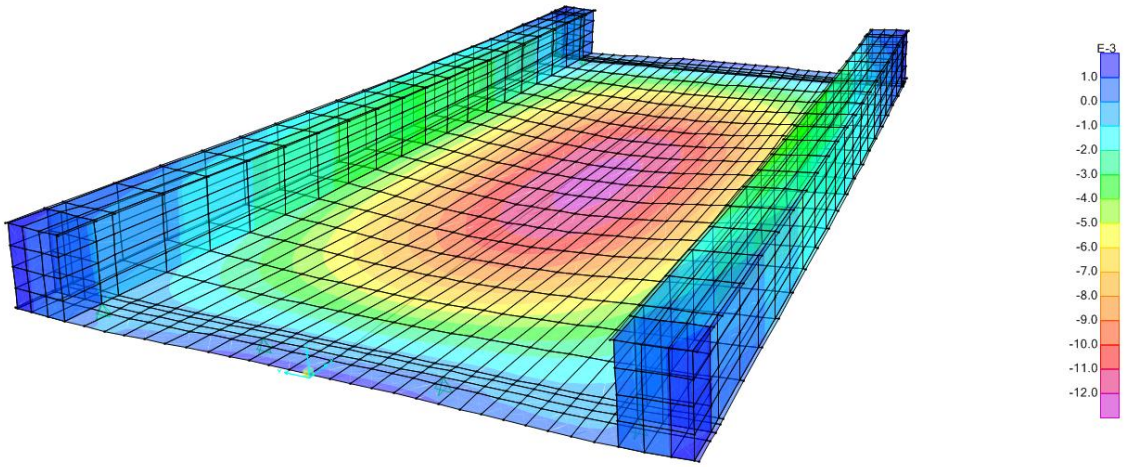

Figure 87 *LM71 Load z-displacement, structure with end cross slab and four bearings*

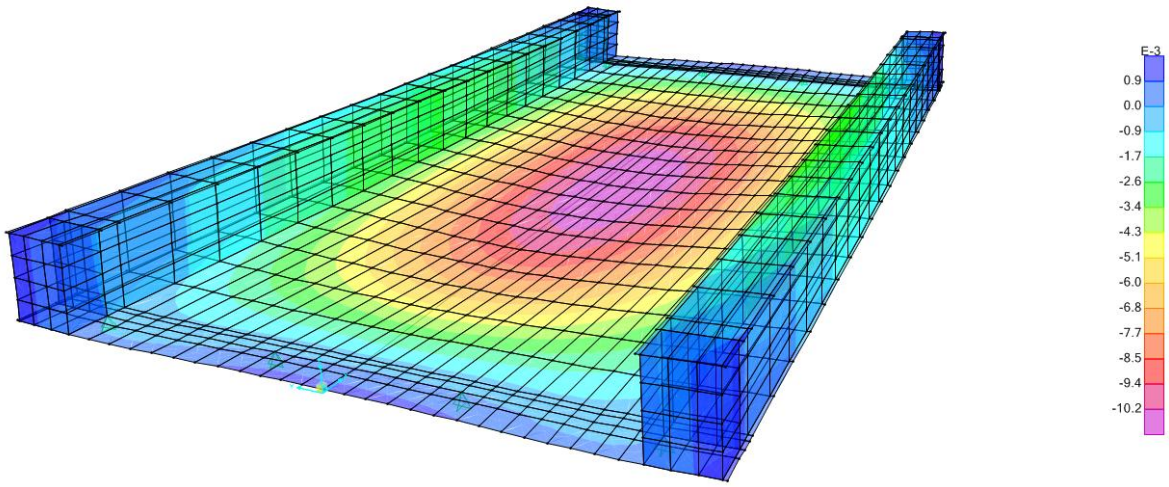

Figure 88 *SW/2 Load z-displacement, structure with end cross slab and four bearings*

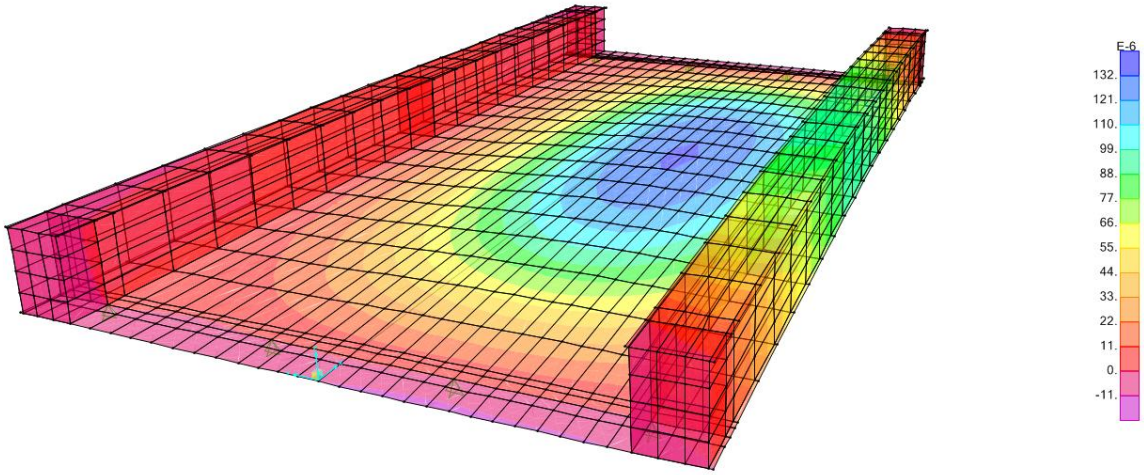

Figure 89 *Wind Load z-displacement, structure with end cross slab and four bearings*

With this structural changes, the deflections are:

LOAD	***3-BEARINGS***		***4-BEARINGS***	
	Span Max displacement	***Deck-end Max displacement***	***Span Max displacement***	***Deck-end Max displacement***
DEAD	*-1.80 [mm]*	*0.00 [mm]*	*-1.80 [mm]*	*0.00 [mm]*
LM71	*-13.20 [mm]*	*1.10 [mm]*	*-13.20 [mm]*	*1.10 [mm]*
SW/2	*-10.80 [mm]*	*0.90 [mm]*	*-10.2 [mm]*	*0.90 [mm]*
WIND	*0.13 [mm]*	*-0.01 [mm]*	*0.13 [mm]*	*0.001 [mm]*

Here also, seems that there's no need of an additional bearing, due to the little gap that there's between the two structures z-displacements. Now, stated that the 3-bearings structure is the one to be chosen, it will be interesting to compare the 3-bearing structure with end cross beam and with end cross slab.

LOAD	3-BEARINGS End Cross Beam		3-BEARINGS End Cross Slab	
	Span Max displacement	Deck-end Max displacement	Span Max displacement	Deck-end Max displacement
DEAD	-1.68 [mm]	0.14 [mm]	-1.80 [mm]	0.00 [mm]
LM71	-11.88 [mm]	0.99 [mm]	-13.20 [mm]	1.10 [mm]
SW/2	-9.60 [mm]	0.80 [mm]	-10.80 [mm]	0.90 [mm]
WIND	0.13 [mm]	-0.01 [mm]	0.13 [mm]	-0.01 [mm]

Both the structures are verified as far as the Eurocode concernes, since the limitation are:

1) 3 [mm] displacement in the deck-end
2) L/600 in middle span, which here it is 16.66 [mm]

LOAD	GAP	
	Span Max displacement	Deck-end Max displacement
DEAD	0.12 [mm]	0.14 [mm]
LM71	1.32 [mm]	0.11 [mm]
SW/2	1.20 [mm]	0.10 [mm]
WIND	0.00 [mm]	0.00 [mm]

Seen these results, 1.2 [mm] gap it's affordable, also because changing to a end cross slab structure leads to a loss of weight (this can also be seen as a money saving procedure).

$$\text{Total Weight (end cross beam)} = 44518.06 \text{ [Kg] of steel}$$
$$\text{Total Weight (end cross slab)} = 44087.94 \text{ [Kg] of steel}$$
$$\Delta W = 430.12 \text{ [Kg] of steel}$$

It is a 1% weight saving.

For a better understanding of the ratio bearings/displacement, also a two bearing structure has been analyzed, here are the related results:

LOAD	2-BEARINGS End Cross Beam		2-BEARINGS End Cross Slab	
	Span Max displacement	*Deck-end Max displacement*	*Span Max displacement*	*Deck-end Max displacement*
DEAD	-1.82 [mm]	0.00 [mm]	-2.64 [mm]	-1.20 [mm]
LM71	-12.21 [mm]	-1.87 [mm]	-17.60 [mm]	-14.30 [mm]
SW/2	-9.60 [mm]	0.80 [mm]	-16.50 [mm]	-10.50 [mm]
WIND	0.143 [mm]	0.00 [mm]	0.156 [mm]	0.065 [mm]

These numbers are not acceptable, modifications on the model are necessary. For instance, trying to higher the slab thickness might fix the displacement problem.
Instead of 8 cm, to achieve displacement verifications with the two bearings structure, we have to improve the thickness of the slab up to 20cm.

3.2) Verifications

3.2.1) Deck Twist

The twist of the bridge deck shall be calculated taking into account the characteristic values of Load Model 71 as well as SW/0 or SW/2 as appropriate multiplied by alpha.
The maximum twist t [mm/3m] of a track gauge s [m] of 1,435 m measured over a length of 3 m should not exceed the values given in Table below.

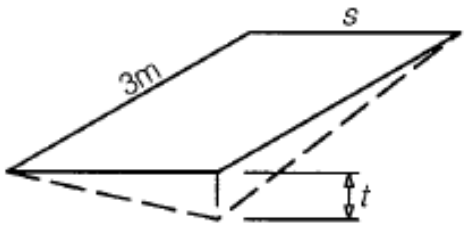

Speed range V (km/h)	Maximum twist t (mm/3m)
$V \leq 120$	$t \leq t_1$
$120 < V \leq 200$	$t \leq t_2$
$V > 200$	$t \leq t_3$

Figure 90 Deck twist

Where:

$t_1 = 4.5\ mm$

$t_2 = 3.0\ mm$

$t_3 = 1.5\ mm$

At 30 [m/sec] t= 1.023 [mm]

At 40 [m/sec] t= 1.023 [mm]

On this tracks, trains do not exceed 55.55 [m/sec]

3.2.2) Stresses

As far as stresses verification, Von Mises's stresses have to respect this limits

$$\sigma \leq f_y = 355\ [MPa]$$

The picture below shows the most unfavourable combination, the highest stress in the deck is 76.1 MPa , and around the area of the bearings where we have the singularities, the highest is 281.2 MPa.

So everything is acceptable.

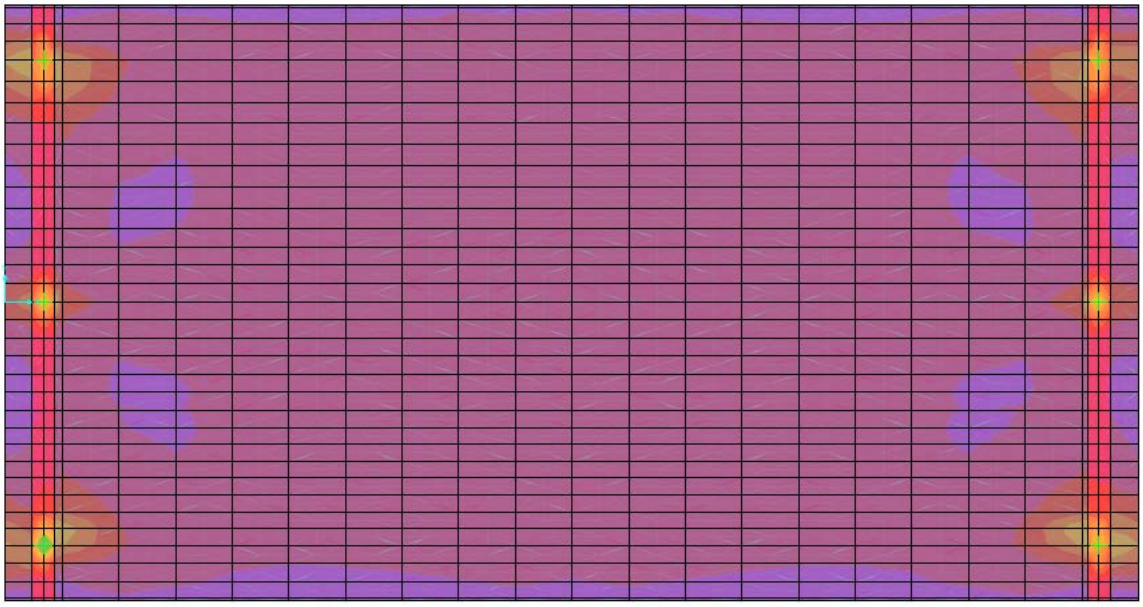

Figure 91 Von Mises diagram for 10 meters span

3.2.3) Transverse Deformation

This verification will be neglected, due to the short span length there will be no problems regarding horizontal curvatures.

4) Dynamic Analysis for 10 meters span, without cross end beam, three bearings

4.1) Introduction

Dynamic considerations are often more complex and complicated than its static counterpart, mainly due to the time varying of the dynamic problem.

Magnitude, direction and/or position of a dynamic load are also varying with time. Similarly, the structural response to a dynamic load is time varying too. Because of that, a dynamic problem does not have a single solution, as a static one does. A succession of solutions of a dynamic problem has to be established, corresponding to all times of interest in the response history. The Eurocode 1-2 also provides a flow chart to determine whether the dynamic analysis is required or not, as shown in Figure 92.

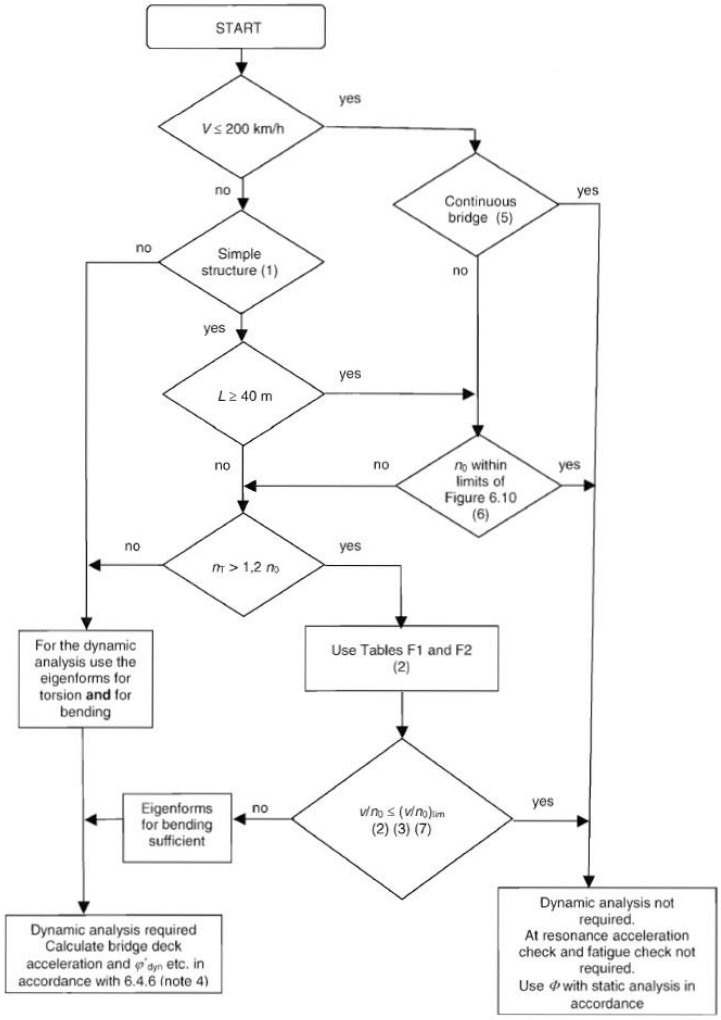

Figure 92

Flow chart to determine whether the dynamic analysis is required.

Where:

L is the span length [m]

V is the Maximum Line Speed at the site [km/h]

n_0 is the first natural bending frequency of t bridge loaded by permament actions [Hz]

n_T is the first natural torsional frequency of t bridge loaded by permament actions [Hz]

V is the maximum nominal speed [m/sec]

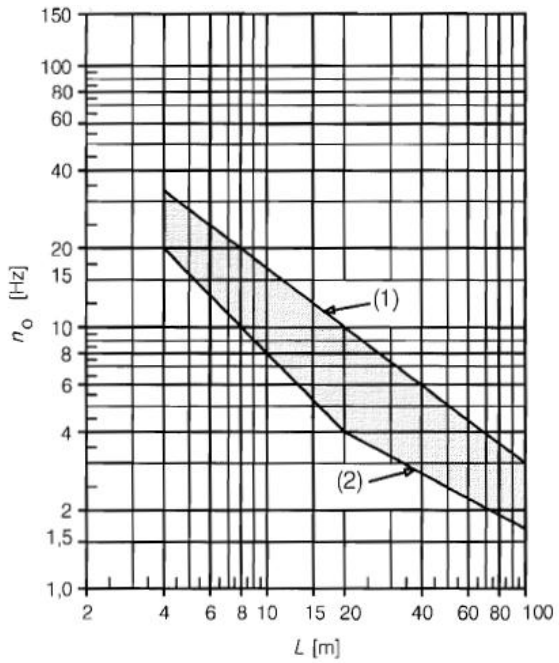

From this flow chart we can see than for this type of structure the dynamic analysis is not required, but it will be run anyways.

Also from the graph here on the left , entering with span length and natural frequency, is we end up into the "comfortable" area, the dynamic analysis is not required.

Span Length = 10m

Natural Frequency= 14.85488 Hz

So we are inside.

Figure 93 Zone which doesn't require a dynamic analysis

As written before, the EC 1-2 also states that The dynamic analysis shall be undertaken using characteristic values of the loading from the Real Trains specified, and the speeds to be considered have to be multiplied by a safety factor of 1,2 so in this case the maximum allowed speed will be:

$$160\ \left[\frac{km}{h}\right] * 1{,}2 = 192\ \left[\frac{km}{h}\right]$$

In this project six speeds will be analyzed for each of the six Real Trains:

1) 36 [km/h] = 10 [m/sec]
2) 72 [km/h] = 20 [m/sec]
3) 108 [km/h] = 30 [m/sec]
4) 144 [km/h] = 40 [m/sec]
5) 165 [km/h] = 46 [m/sec]
6) 192 [km/h] = 53 [m/sec]

Six speeds for the six real trains (from A to F), which have been inputted into the CSi software as shown in the Figures below

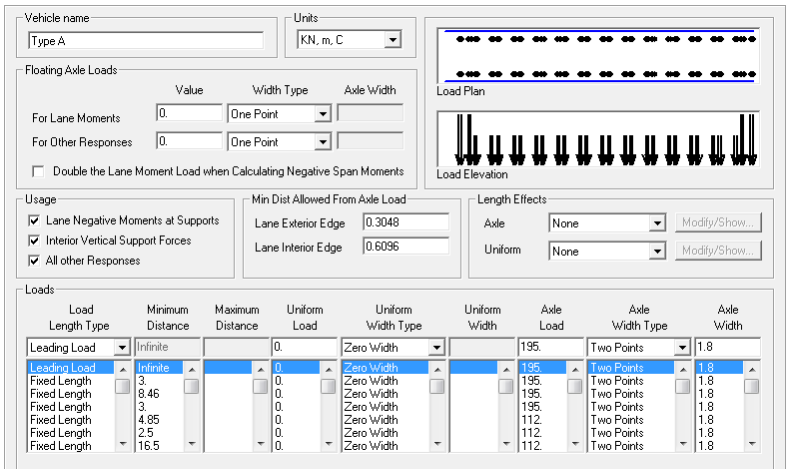

Figure 94 Train type A in CSi Bridge

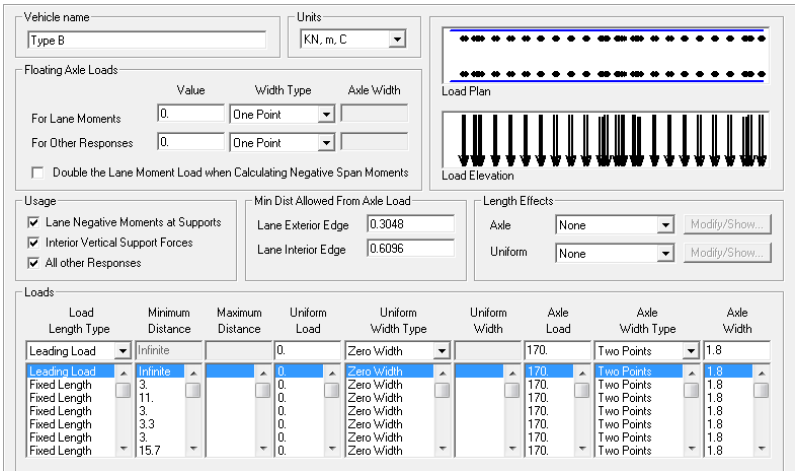

Figure 95 Train type B in CSi Bridge

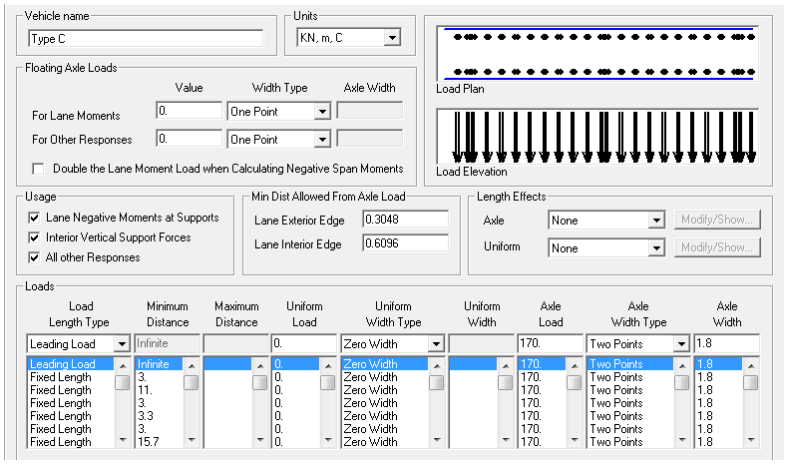

Figure 96 Train type C in CSi Bridge

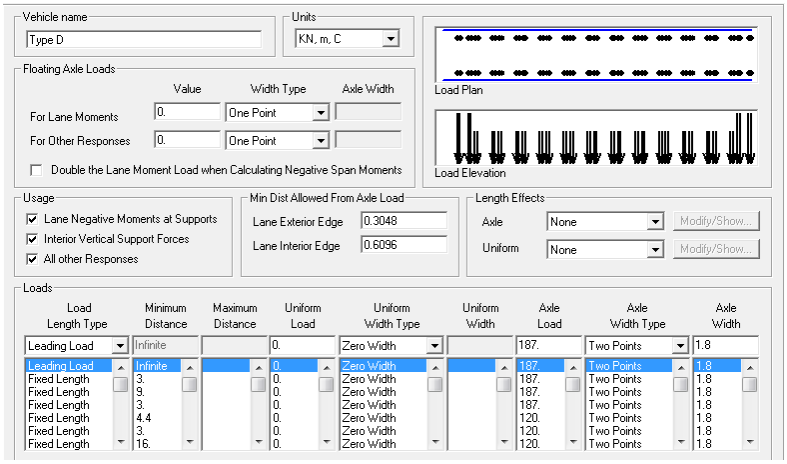

Figure 97 Train type D in CSi Bridge

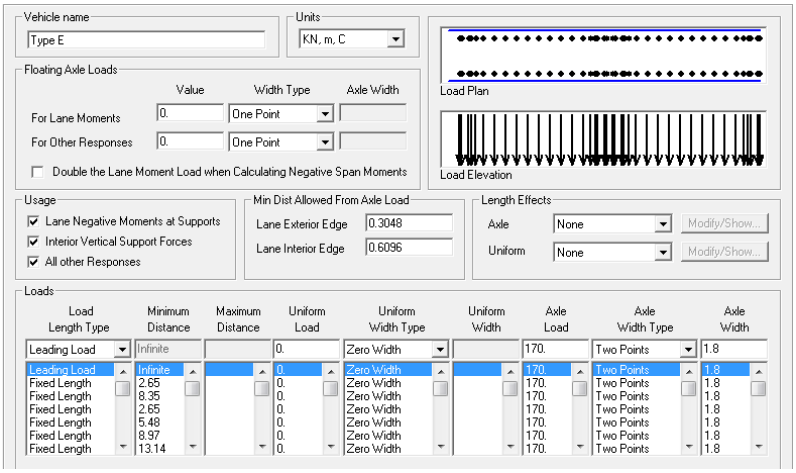

Figure 98 Train type E in CSi Bridge

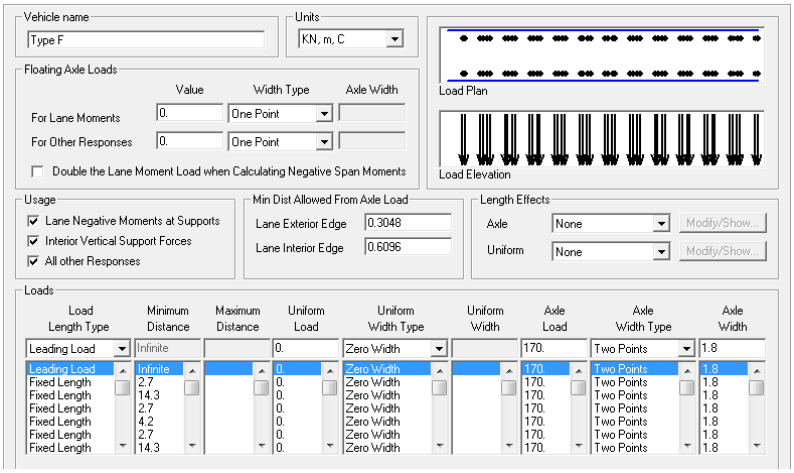

Figure 99 Train type F in CSi Bridge

As far as the introduction of the Damping Factor, a small theoretical explanation is required in addition of what has already been written before.

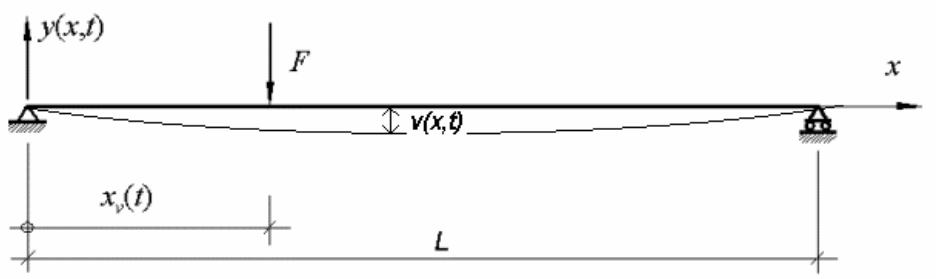

In the simplest way, the railway bridge model is supposed to be considered as a *Bernoulli-Euler beam*. This beam model considered the linear character of the bridge structure. Compared with its length, the beam has small transverse dimensions. The differential equation of the motion of a simple supported beam is formulated like this:

$$EI\frac{\partial^4 v(x,t)}{\partial x^4} + \mu\frac{\partial^2 v(x,t)}{\partial t^2} + 2\mu\omega_b\frac{\partial v(x,t)}{\partial t} = f(x,t)$$

The equation of motion is deduced on the assumption of the theory of small deformations, *Hooke's law*, *Navier's hypothesis* and *Saint-Venant's principle* can be applied. Constant cross-section and mass per unit length of the beam is assumed and the damping is considered proportional to the velocity of vibration. It is possible to divide the damping coefficient in two parts, Mass and Stiffness proportional damping coefficients, normally referred to as Rayleigh damping.

During formulation, the damping matrix is assumed to be proportional to the mass and stiffness matrices as follows:

$$C = \eta M + \delta K$$

Stiffness-proportional damping coefficient $\delta = \frac{2\xi}{\omega_i + \omega_j} = 0.002616$

Mass-proportional damping coefficient $\eta = \omega_i \omega_j \delta = 0.908$

Where

$$\xi = 0{,}05$$
$$\omega_i = \omega_1 = 14.85488\ [Hz]$$
$$\omega_j = 30\ [Hz]$$

4.1.2) Time History:

The equation of dynamic equilibrium of an elastic discretized structure is formulated in *Equation* $[M]\{\ddot{y}\} + [C]\{\dot{y}\} + [K]\{y\} = \{F(t)\}$.
Step by step integration of the equation has to be performed, in order to reproduce the complete time history response of the structure.

Direct Integration:
The equation of dynamic equilibrium is integrated, using direct integration, a numerical step by step procedure in the time domain. The method is based on following concepts:

1) The dynamic equilibrium equations are satisfied at discrete time points, within the solution time interval. These discrete points are Δt apart.
2) Within these time intervals, the variation of displacement, velocity and acceleration is assumed. This gives arise to a series of direct integration schemes, each possessing different accuracy and stability characteristics.

In this particular chapter we want to verify that the structure satisfies the EC requirements for deck acceleration, and than see the effects of some important variables of the results of dynamic analysis, such as:

- Output time
- Rampth Function
- Meshing
- Direct Integration / Modal

Like in the static analysis, both 3Bearings cross end beam structure and 3Bearings cross end slab structure have been examined, then focusing in detail only in the slab structure (it was already proven more suitable in the static analysis).
To accomplish this goal, 36 different load cases have been created in the model, one for every speed of each real train.
Using CSi Bridge, it was necessary to set up the analysis type like this, with these damping coefficients:

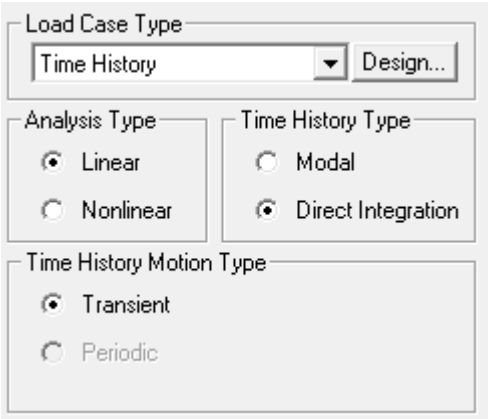

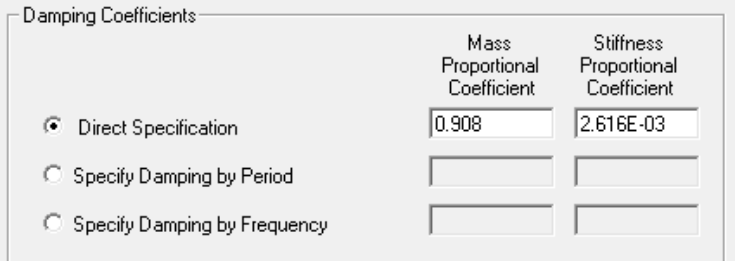

4.2) Results for 3 Bearings – Cross End Beam structure:

All the pictures with the z-displacements are shown in Annex A

4.3) Results for 3 Bearings – Cross End Slab structure:

All the pictures with the z-displacements are shown in Annex A

Since on the Eurocode there are limitations on the accelerations of the structure, we took one particular point and analyzed its accelerations under the moving loads of each train. The joint we took into account is in the middle of the span on the main girder, as shown in the picture below.

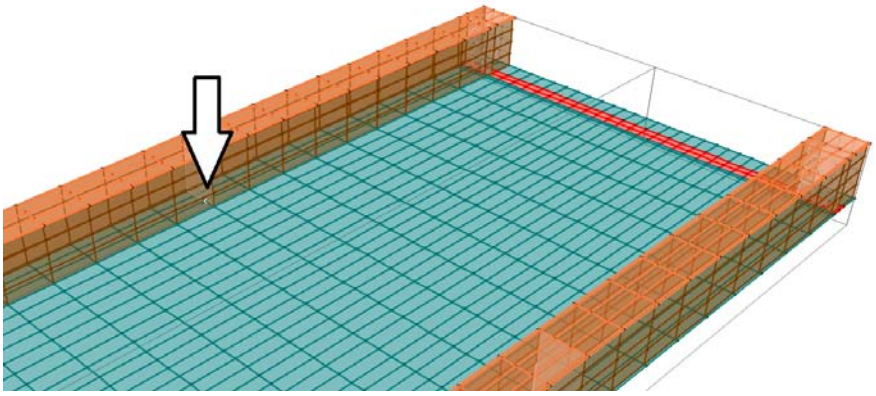

Figure 100 Joint taken into account for the acceleration verifications

The results of the primary dynamic analysis are shown in the graphs that follow.

Number of output Time Steps: 50

Output Time Step Size: 0.1 secs

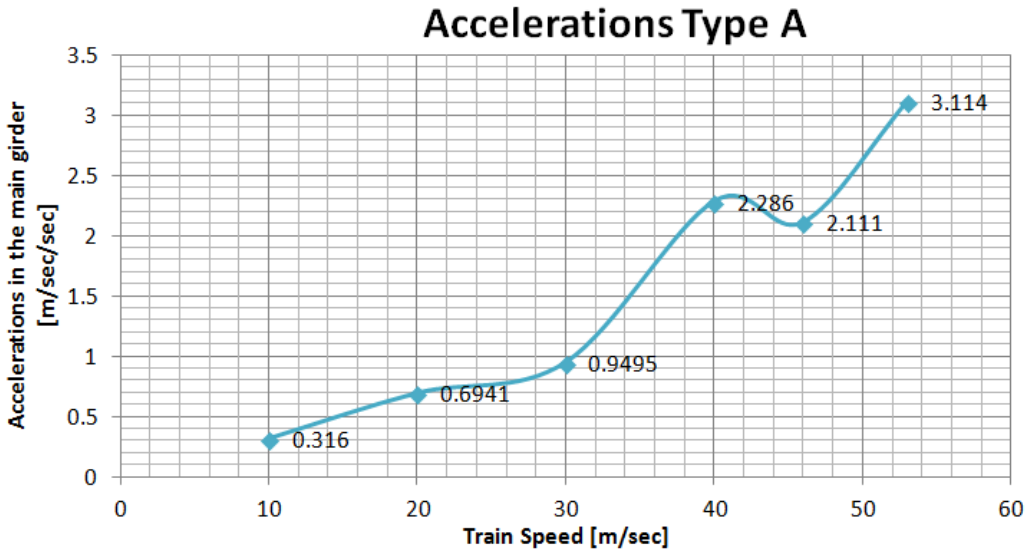
Accelerations Type A
Accelerations in the main girder [m/sec/sec]
Train Speed [m/sec]
0.316
0.6941
0.9495
2.286
2.111
3.114

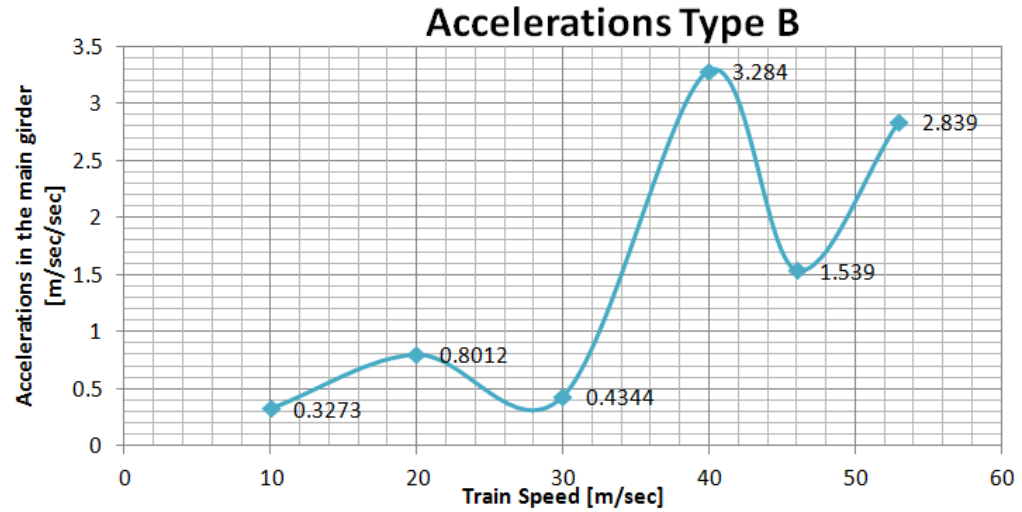
Accelerations Type B
Accelerations in the main girder [m/sec/sec]
Train Speed [m/sec]
0.3273
0.8012
0.4344
3.284
1.539
2.839

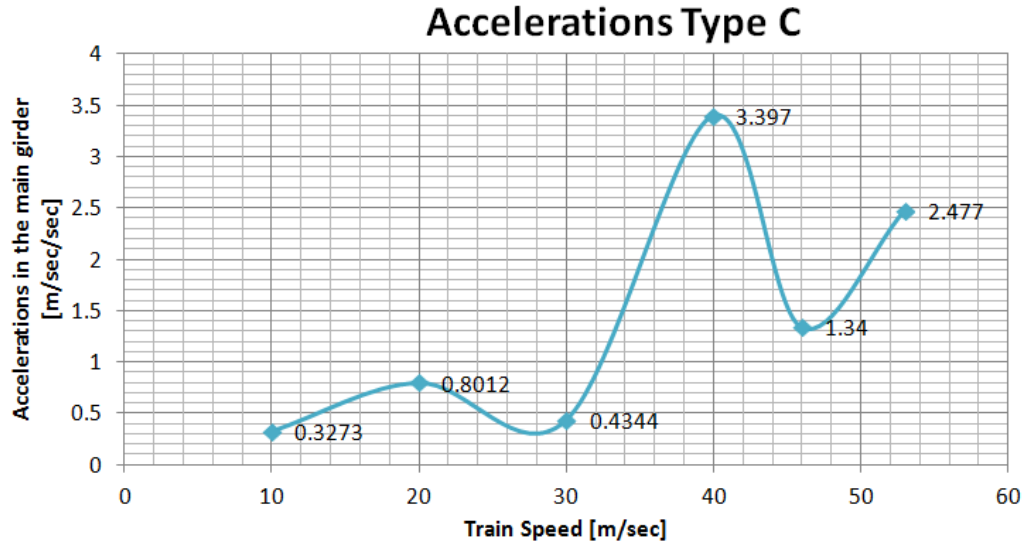
Accelerations Type C
Accelerations in the main girder [m/sec/sec]
Train Speed [m/sec]
0.3273
0.8012
0.4344
3.397
1.34
2.477

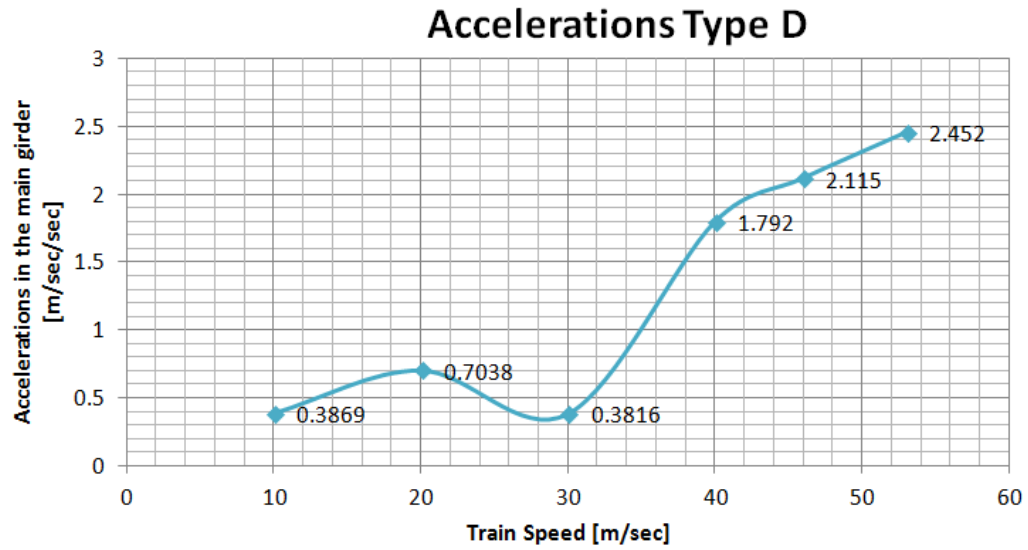
Accelerations Type D
Accelerations in the main girder [m/sec/sec]
Train Speed [m/sec]
0.3869
0.7038
0.3816
1.792
2.115
2.452

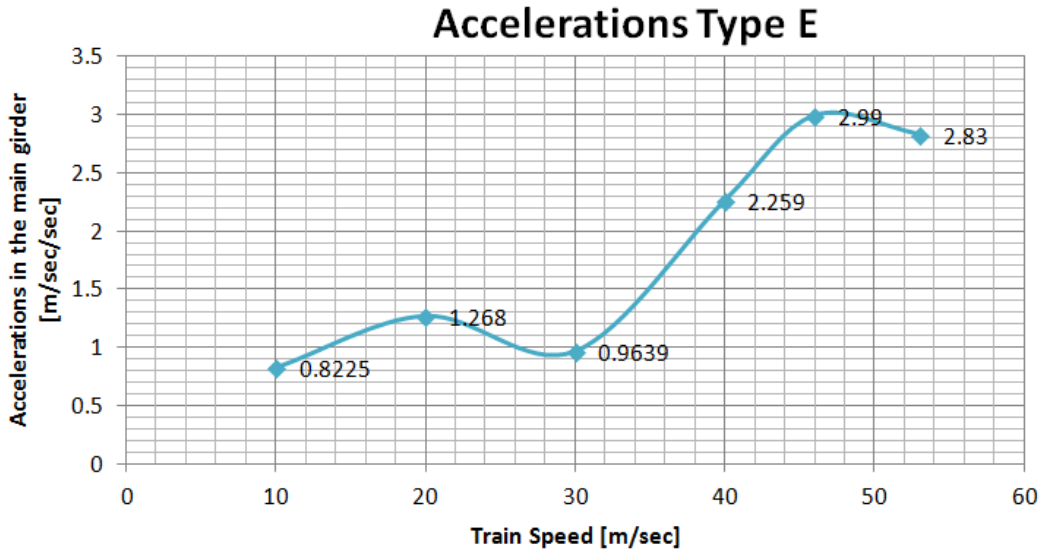
Accelerations Type E
Accelerations in the main girder [m/sec/sec]
Train Speed [m/sec]
0.8225
1.268
0.9639
2.259
2.99
2.83

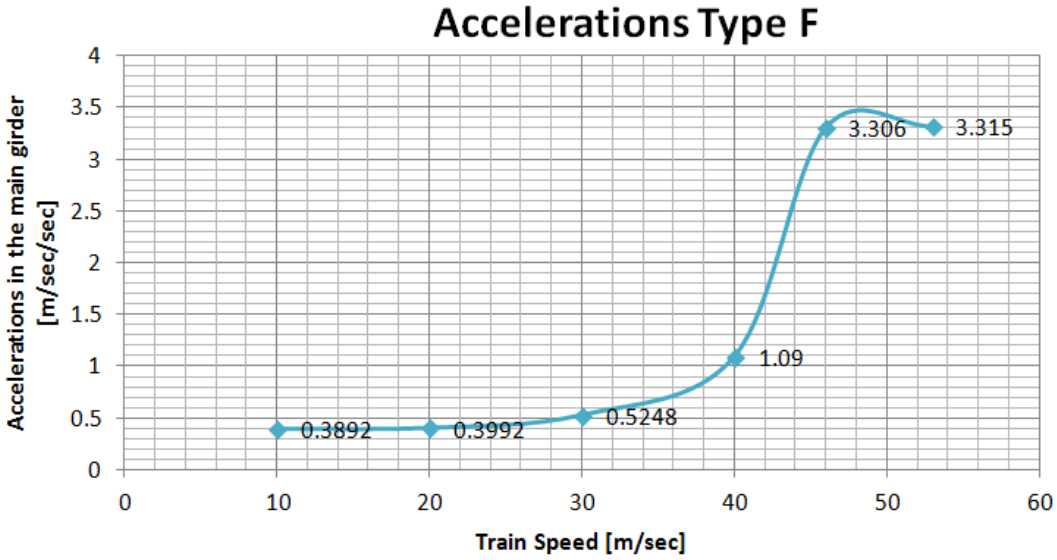
Accelerations Type F
Accelerations in the main girder [m/sec/sec]
Train Speed [m/sec]
0.3892
0.3992
0.5248
1.09
3.306
3.315

Now that all the accelerations are gathered we take the worst case scenario, which in this case is presenting itself in the Real Train C at the velocity of 40 meters per second.
Now it may be useful to understand what impact do certain variable have on the results for instance:

- Time Step Data
- Rampth Function
- Time History Type
- Meshing

4.4) Changing variables

4.4.1) Time Step Data

Time-history analysis is performed at discrete time steps. The time span over which the analysis is carried out is given by multiplying the number of time steps and their size.
For periodic analysis, the period of the cyclic loading function is assumed to be equal to this time span. Responses are calculated at the end of each time increment.

Output Time Step Size	Number Of Output Time Steps		Acceleration [m/sec/sec]
0.10	50	⇒	3.397
0.09	56	⇒	1.501
0.08	62	⇒	1.556
0.07	71	⇒	1.258
0.06	83	⇒	1.401
0.05	100	⇒	1.249
0.04	125	⇒	0.7625
0.03	166	⇒	0.741
0.02	250	⇒	0.7725
0.01	500	⇒	0.9403

Basically, if we put those results into a graph it would look like this:

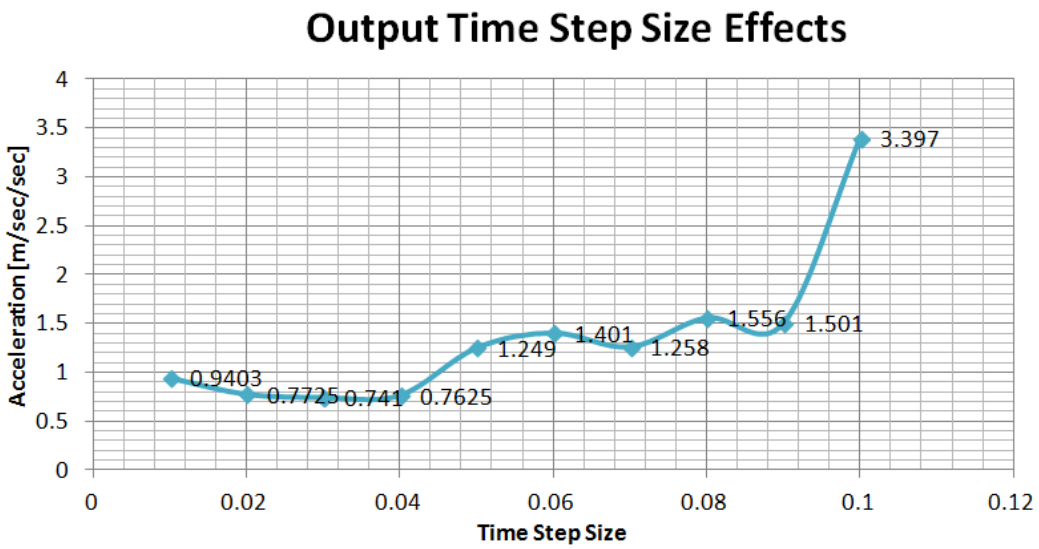

So, gradually decreasing the size of the time step, but keeping the loading time equal, it improves the solution and it kind of stabilizes between 0.02 and 0.04.

4.4.2) Ramp Function

The built-in time function in the CSi software looks like this:

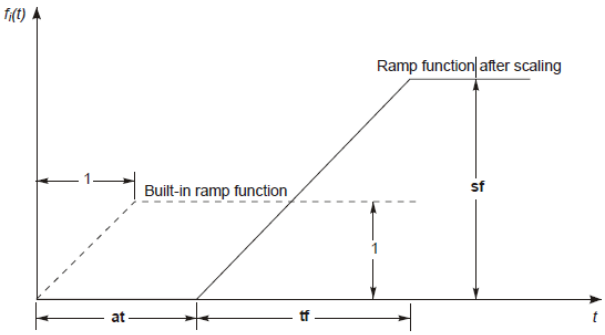

Figure 101 Ramp Function

This function can be modified in order to see if this has some effect on the results, for instance it could be like this:

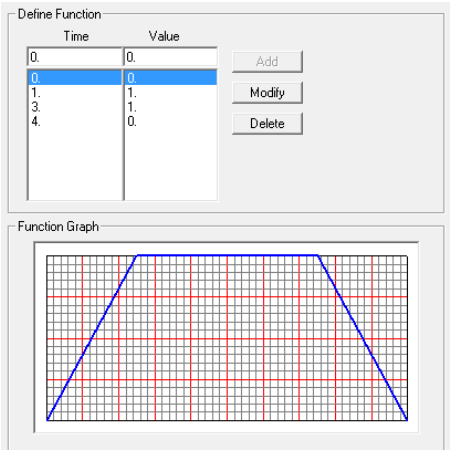

If we carry out the analysis on the Real Train C at speed of 40 m/sec , we can see that the solution is perfectly the same before and after the modification of the Rampth function.

4.4.3) Time History Type

Modal superposition provides a highly efficient and accurate procedure for performing time history analysis. Closed form integration of the modal equations is used to compute the response, assuming linear variation of the time functions, $f_i(t)$, between the input data time points. Therefore, numerical instability problems are never encountered, and the time increment may be any sampling value that is deemed fine enough to capture the maximum response values. One tenth of the time period of the highest mode is usually recommended; however, a larger value may give an equally accurate sampling if the contribution of the higher modes is small.

Direct integration of the full equations of motion without the use of modal super position is available in CSi Bridge.
While modal superposition is usually more accurate and efficient, direct integration does offer the following advantages for linear problems:
• Full damping that couples the modes can be considered
• Impact and wave propagation problems that might excite a large number of modes may be more efficiently solved by direct integration
Direct integration results are extremely sensitive to time-step size in a way that is not true for modal superposition.

We keep the same train, same speed, with the modifications done earlier. Now instead of using Linear Direct Integration as time history type, we are going to see how the results change by using the Modal one.

After running the load case analysis, the acceleration that resulted was $1.159\ [\frac{m}{sec^2}]$, previously, with the Direct Integration it was $0.741\ [\frac{m}{sec^2}]$, so a 56.4% difference.

4.4.4) Meshing

Other important share of impact on results is given by the mesh used in the model, here's the difference between a dense and non-dense meshing.

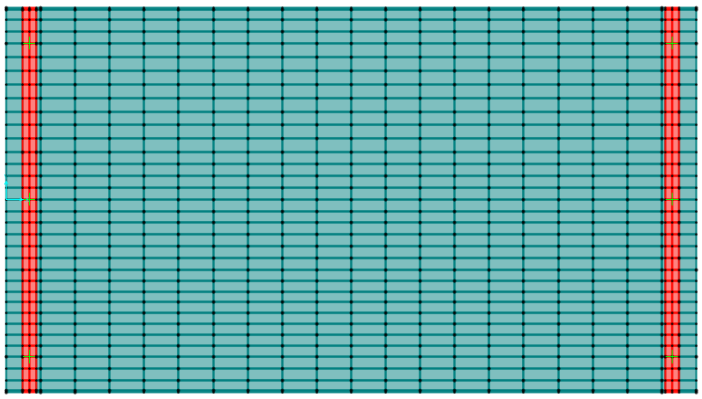

$$Joint\ Acceleration = 0.741\ \left[\frac{m}{sec^2}\right]$$

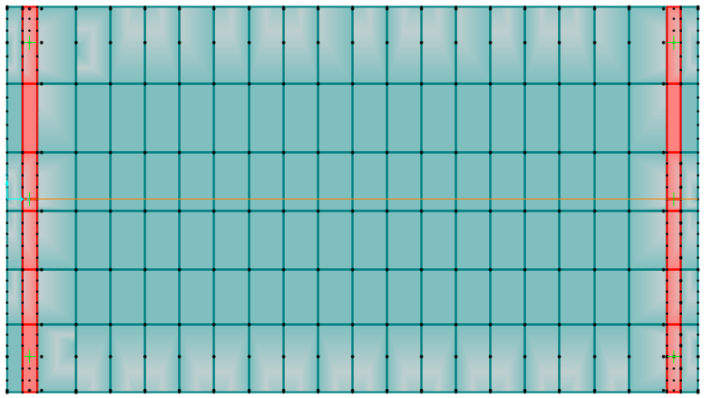

$$Joint\ Acceleration = 0.647[\frac{m}{sec^2}]$$

So here the impact of the modification is around 13%, so it is not very significant.

We can say that the changing of the output time step size has a great impact on the final results, so it will be good to see if this is happening also for low speeds, like 10 m/sec and 20 m/sec.

Real Train C : 10 m/sec

Output Time Step Size	Number Of Output Time Steps	Acceleration [m/sec/sec]
0.10	50	0.3273
0.09	56	0.2357
0.08	62	0.2581
0.07	71	0.2349
0.06	83	0.2434
0.05	100	0.2068
0.04	125	0.2002
0.03	166	0.2095
0.02	250	0.1203
0.01	500	0.1061

And graphically we can see that the results for the slowest speed is already pretty stable, so changing the output time step size has impact, but not that significant as it was for 40 m/sec.

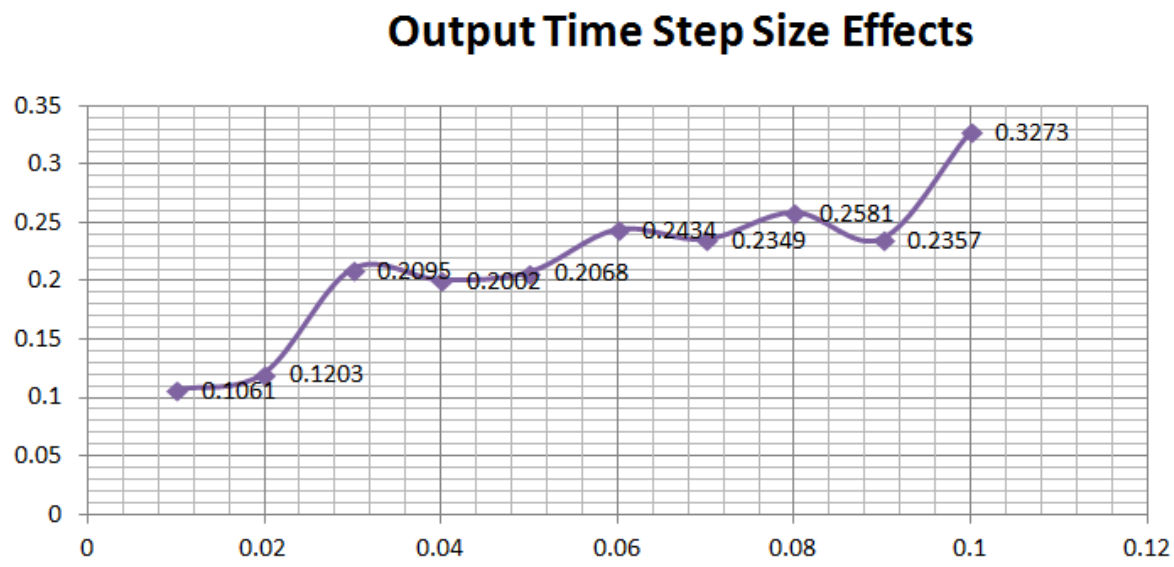

Real Train C : 20 m/sec

Output Time Step Size	Number Of Output Time Steps	Acceleration [m/sec/sec]
0.10	50	0.8012
0.09	56	0.3651
0.08	62	0.2732
0.07	71	0.406
0.06	83	0.5166
0.05	100	0.3687
0.04	125	0.6577
0.03	166	0.3459
0.02	250	0.4356
0.01	500	0.3282

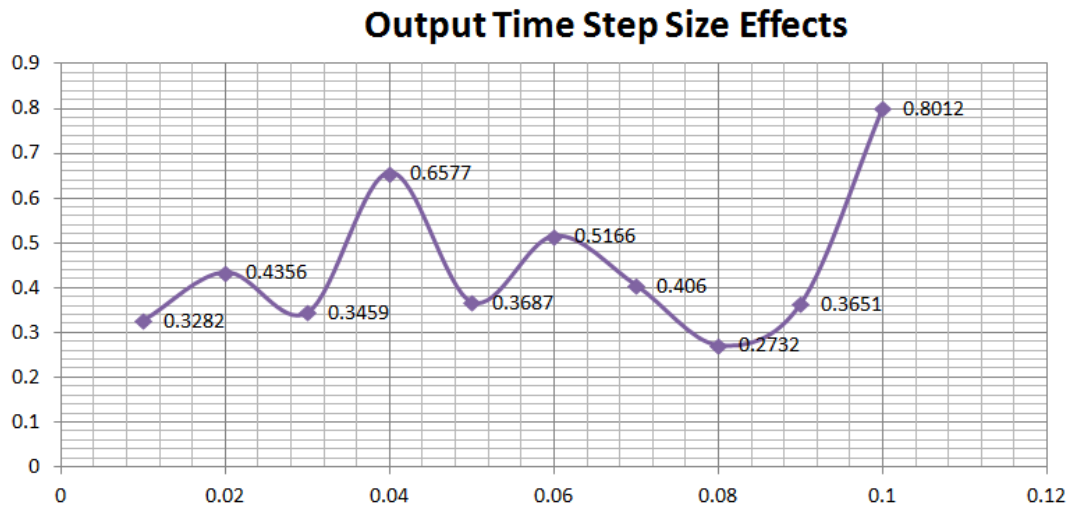

Here the results are pretty much fluctuating, never gaining a stable amount.

4.5) Acceleration Verification

In the Annex 2 chapter 4.4.2 the criteria for the deck acceleration verifications can be found:

"To ensure traffic safety, where a dynamic analysis is necessary, the verification of maximum peak deck acceleration due to rail traffic actions shall be regarded as a traffic safety requirement checked at the SLS for the prevention of track instability."

"The maximum permitted peak values of bridge deck acceleration shall not exceed the following design values:

$\gamma_{bt} = 3.5 \left[\frac{m}{s^2}\right] in\ ballasted\ tracks$

$\gamma_{df} = 5.0 \left[\frac{m}{s^2}\right]\ direct\ fasted\ decks\ with\ track\ and\ structural\ elements\ for\ HS$"

In this case, our upper limit will be 3.5 [m/sec/sec] , seeing the results presented before, every train at every speed verifies the deck acceleration limit.

Proven that the slab structure with three bearings is the most suitable for this kind of design, now the same analysis will be carried out for different spans, respectively 15 meters and then 6 meters.

5) *Bridge Design for 15 meters span*

5.1) *Static Analysis*

There are no major changes between the 10 meters and 15 meters structures, only the length and one additional diaphragm into the main girders

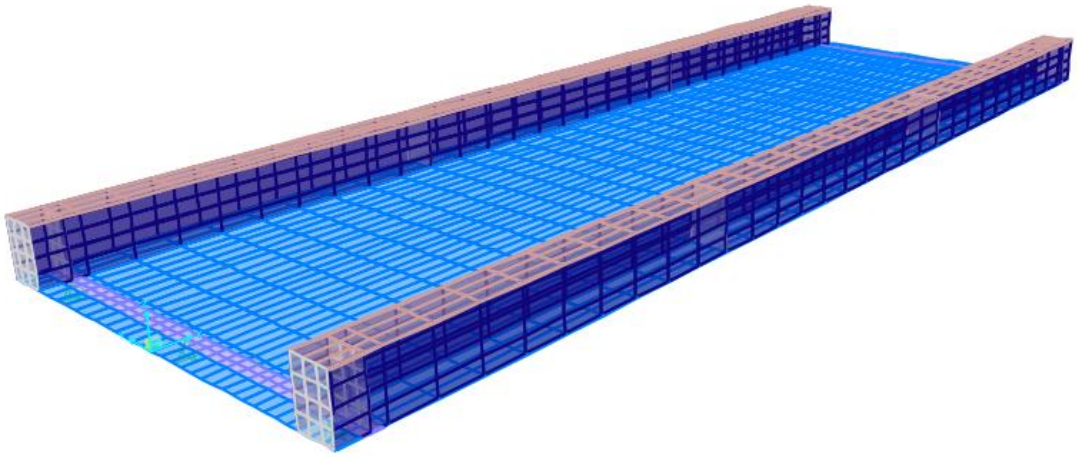

Figure 102 15 meters span bridge

5.1.1) Loading

All the loading procedure is the same as it was in the analysis of the 10 meters structure

5.1.2) Results

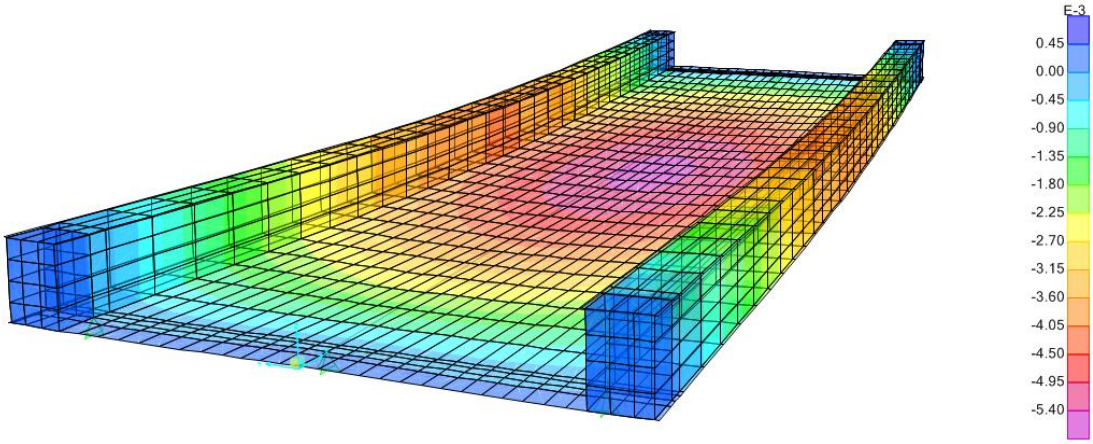

Figure 103 Dead Load z-displacement for 15 meters span

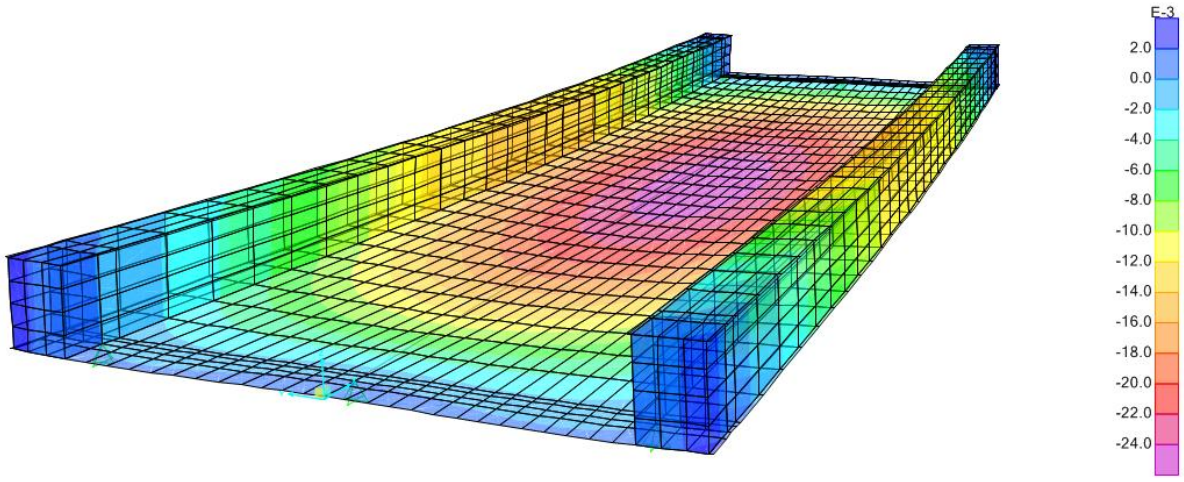

Figure 104 SW-2 z-displacement for 15 meters span

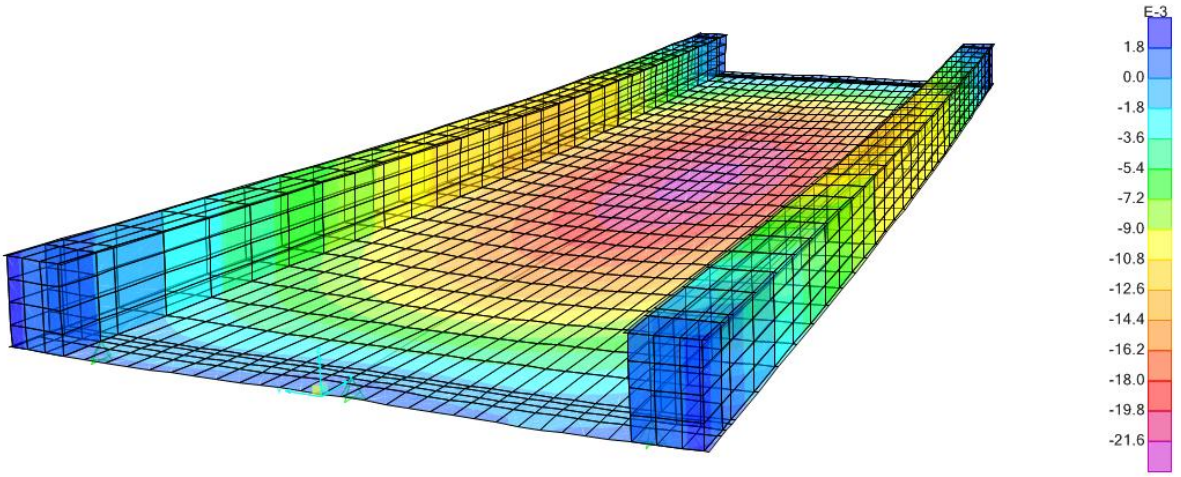

Figure 105 LM71 z-displacement for 15 meters span

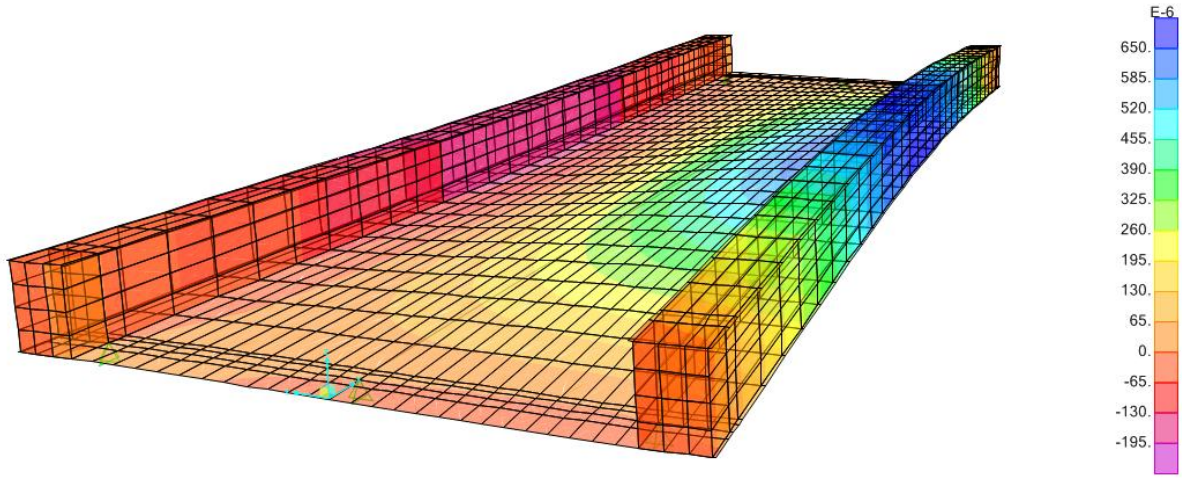

Figure 106 Wind z-displacement for 15 meters span

Load	Z-Displacement [mm]		Limits [mm]		Verification
	Deck-End	Middle Span	Deck-End	Middle Span	
Dead	+0.20	-5.40	None	None	YES
SW-2	+1.00	-24.00	3.00	25.00	YES
LM71	+0.55	-23.76	3.00	25.00	YES
Wind	-0.055	+0.65	None	None	YES

From this table we can see that the verifications that the Eurocode suggests are satisfied.

5.2) Verifications

5.2.1) Deck Twist

The twist of the bridge deck shall be calculated taking into account the characteristic values of Load Model 71 as well as SW/0 or SW/2 as appropriate multiplied by alpha.
The maximum twist *t* [mm/3m] of a track gauge *s* [m] of 1,435 m measured over a length of 3 m should not exceed the values given in Table below.

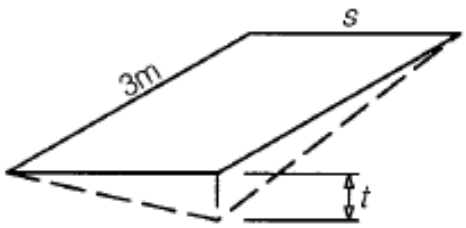

Speed range V (km/h)	Maximum twist t (mm/3m)
$V \leq 120$	$t \leq t_1$
$120 < V \leq 200$	$t \leq t_2$
$V > 200$	$t \leq t_3$

Where:

$t_1 = 4.5\,mm$

$t_2 = 3.0\,mm$

$t_3 = 1.5\,mm$

At 30 [m/sec] t=0.65 [mm]

At 40 [m/sec] t=1.09 [mm]

On this tracks, trains do not exceed 55.55 [m/sec]

5.2.2) Stresses

As far as stresses verification, Von Mises's stresses have to respect this limits

$$\sigma \leq f_y = 355\ [MPa]$$

The picture below shows the most unfavourable combination, the highest stress in the deck is 91.55 MPa , and around the area of the bearings where we have the singularities, the highest is 324.23 MPa.

So everything is acceptable.

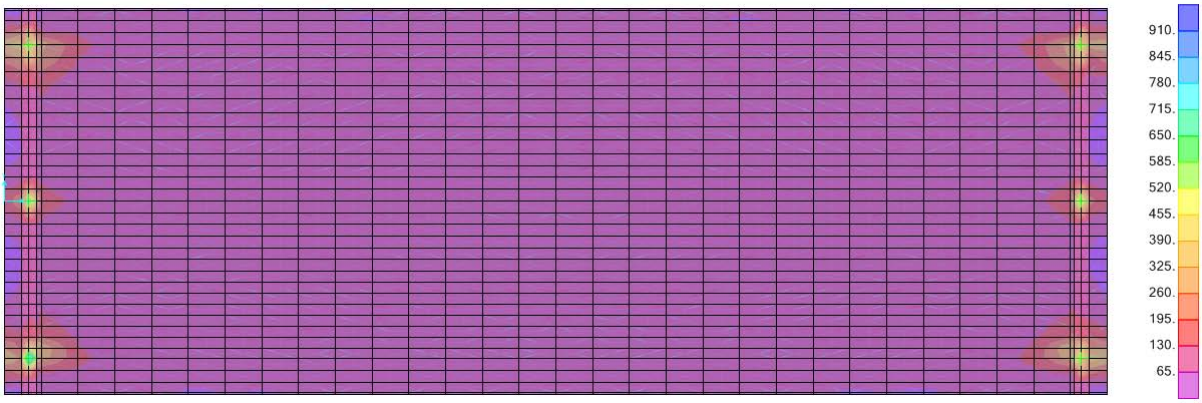

Figure 107 Von Mises diagram for 15 meters span

5.2.3) Transverse Deformation

This verification will be neglected, due to the short span length there will be no problems regarding horizontal curvatures.

5.3) Dynamic Analysis

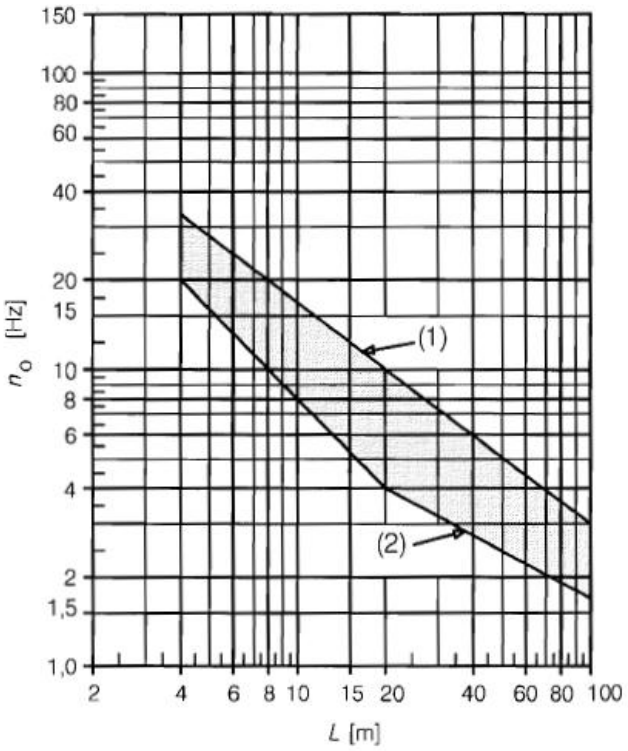

From the graph here on the left , entering with span length and natural frequency, if we end up into the "comfortable" area, the dynamic analysis is not required.

Span Length = 15m

Natural Frequency= 8.10008 Hz

So we are inside.

To run the dynamic analysis in this model, nothing basically changes from the 10 meters one. The only thing that is subject to a change is the damping coefficient since the modal analysis gives us different frequencies with which to calculate the mass-proportionl and stiffness-proportional coefficients. The equation, obviously, it's still the same:

$$C = \eta M + \delta K$$

Stiffness-proportional damping coefficient $\delta = \frac{2\xi}{\omega_i + \omega_j} = 0.0026246$

Mass-proportional damping coefficient $\eta = \omega_i \omega_j \delta = 0.637857$

Where

$$\xi = 0{,}05$$

$$\omega_i = \omega_1 = 8.10008\ [Hz]$$

$$\omega_j = 30\ [Hz]$$

5.3.1) Results

All the pictures with the z-displacements are shown in Annex A

The dynamic analysis was carried out with:

Number of output Time Steps: 166

Output Time Step Size: 0.03 secs

Pictures below show the acceleration of middle span, on the main girder, as before.

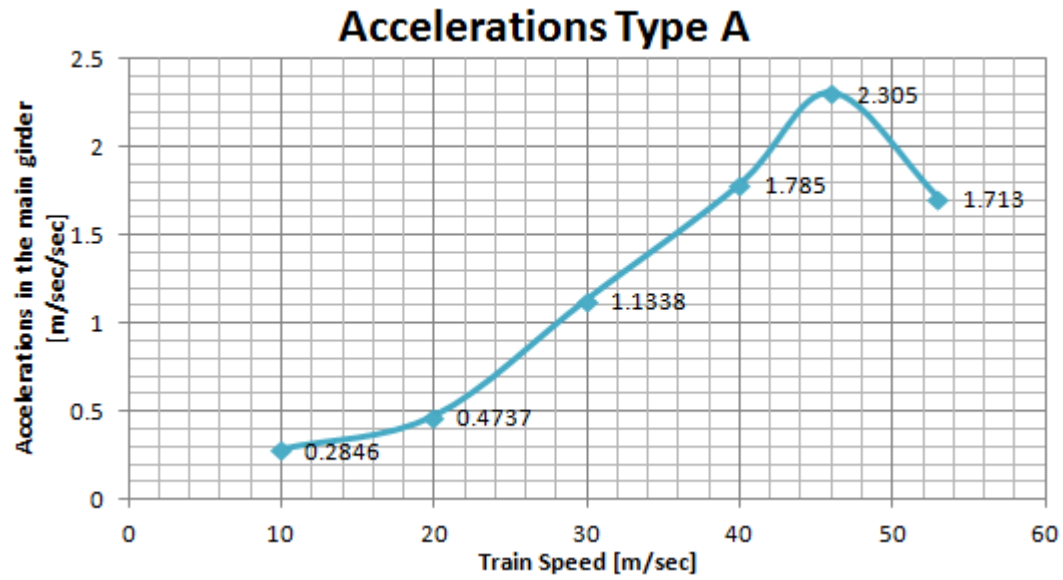
Accelerations Type A
Accelerations in the main girder [m/sec/sec]
Train Speed [m/sec]
0.2846
0.4737
1.1338
1.785
2.305
1.713

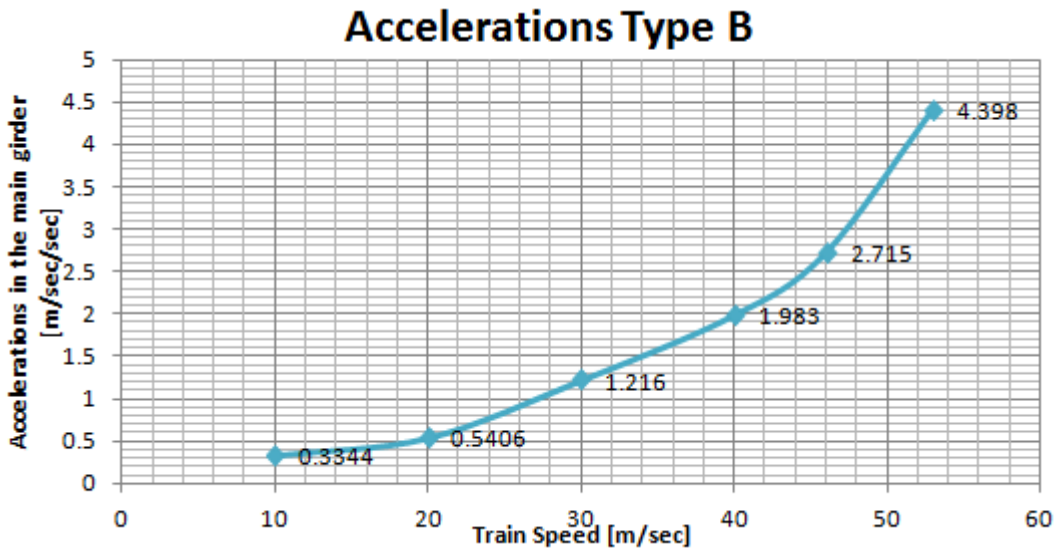
Accelerations Type B
Accelerations in the main girder [m/sec/sec]
Train Speed [m/sec]
0.3344
0.5406
1.216
1.983
2.715
4.398

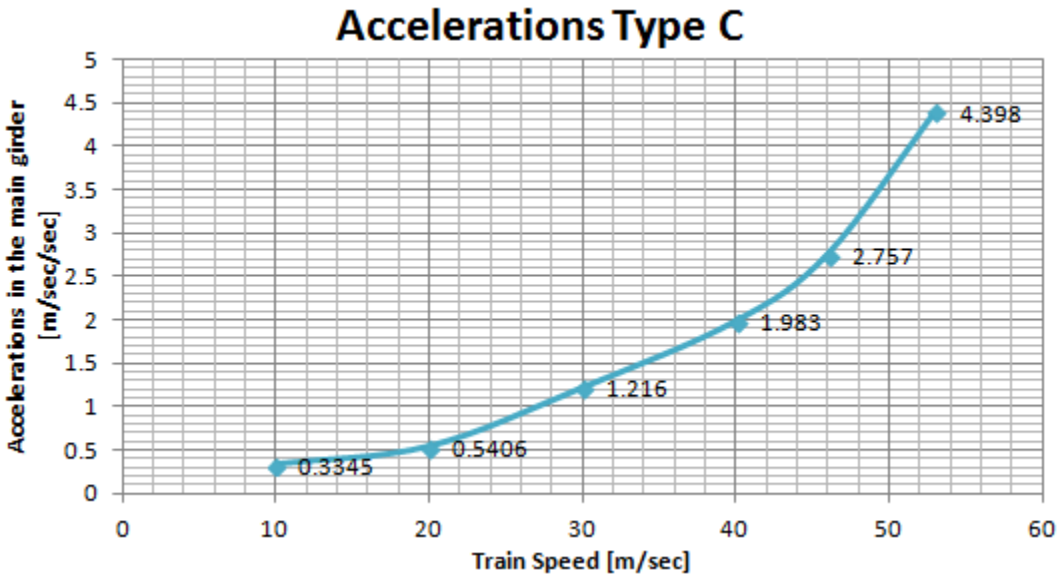
Accelerations Type C
Accelerations in the main girder [m/sec/sec]
Train Speed [m/sec]
0.3345
0.5406
1.216
1.983
2.757
4.398

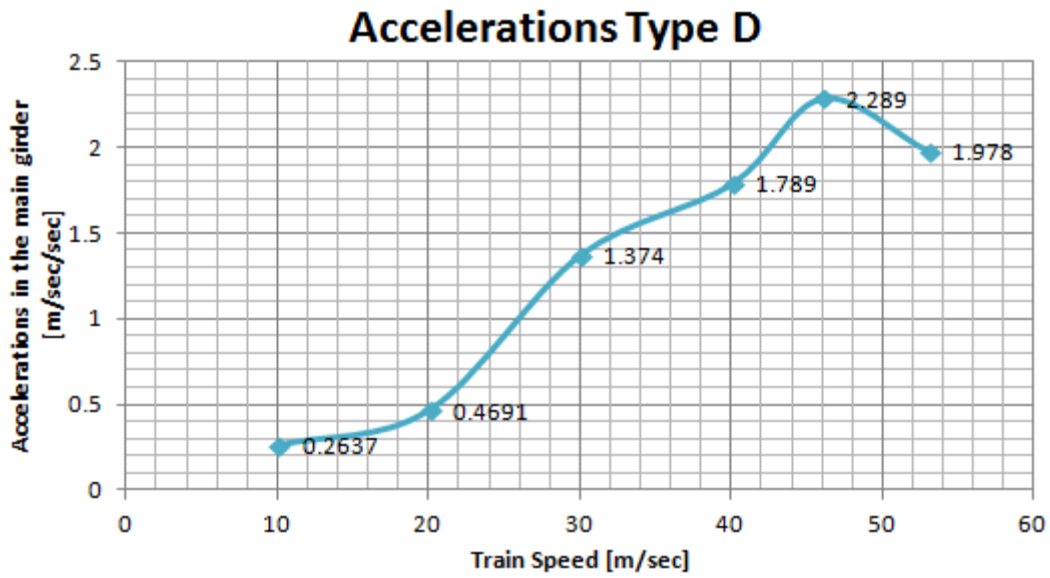
Accelerations Type D
Accelerations in the main girder [m/sec/sec]
Train Speed [m/sec]
0.2637
0.4691
1.374
1.789
2.289
1.978

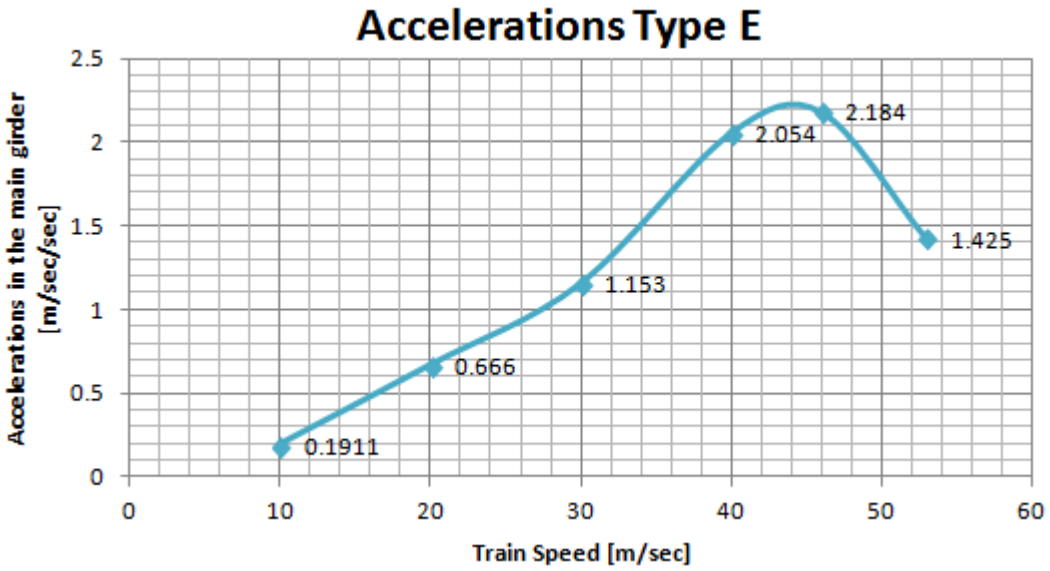
Accelerations Type E
Accelerations in the main girder [m/sec/sec]
Train Speed [m/sec]
0.1911
0.666
1.153
2.054
2.184
1.425

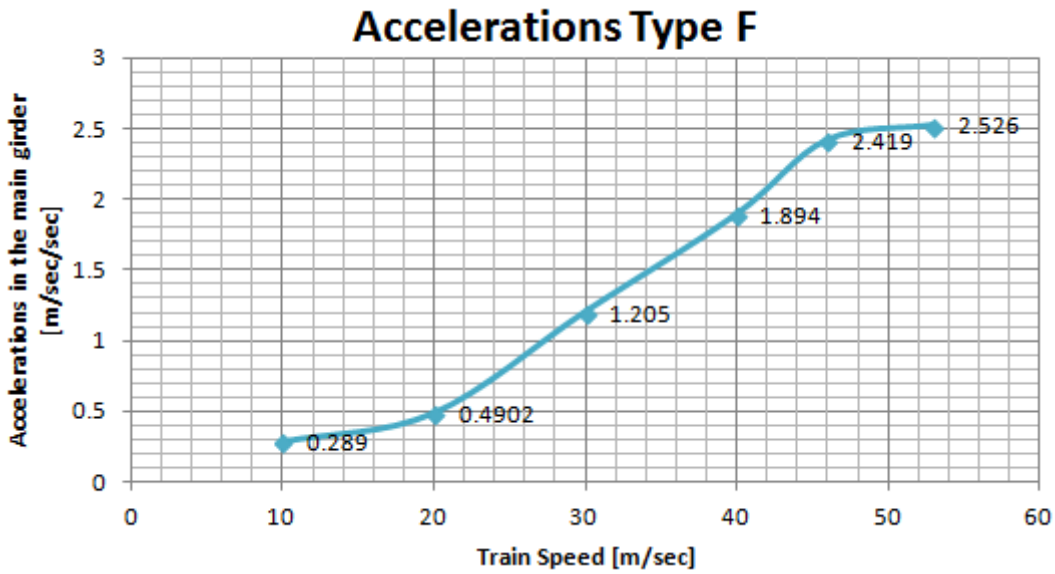
Accelerations Type F
Accelerations in the main girder [m/sec/sec]
Train Speed [m/sec]
0.289
0.4902
1.205
1.894
2.419
2.526

Since the upper limitations given by the Eurocode are 3.5 $[\frac{m}{sec^2}]$, each train in verified for every speed, apart from trains B and C at speed of 53 meters per second. (in both cases the deck acceleration is 4.398 m/sec/sec).

At this point the choices are two:

1) Limit the speed of the trains passing on the bridge with this span at the maximum of 46 meters per second.
2) Try to change the cross section of the bridge and see which modification will keep the deck acceleration below the limits.

If we higher the height of the main girders from 67 cm to 84 cm and run again the dynamic analysis for those two cases, these are the results

$$Train\ B, Speed\ of\ 53\ \left[\frac{m}{s}\right] = 1.662\left[\frac{m}{s^2}\right]$$

$$Train\ C, Speed\ of\ 53\ \left[\frac{m}{s}\right] = 1.675\left[\frac{m}{s^2}\right]$$

Proven that this little modification clearly improves the behavior of the hole structure, it's better to run the hole static and dynamic analysis once again, for each of the 36 cases.

6) *Bridge Design for 15 meters span with bigger main girders*

6.1) Static Analysis

This is how the structure with bigger main girders and an additional diaphragm looks

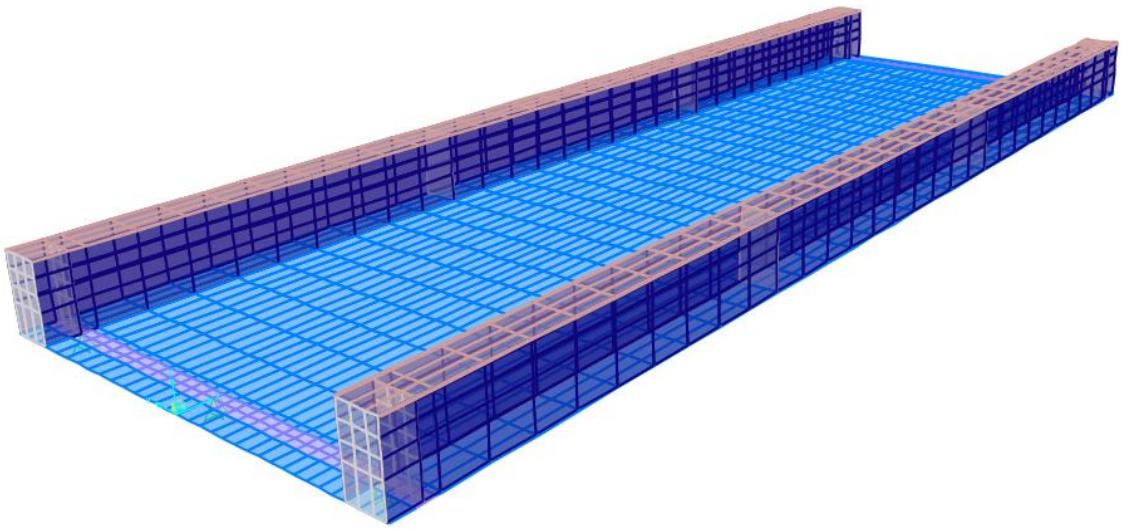

Figure 108 15 meters span bridge with bigger main girders

Cross Section and longitudinal view are presented in the next two figures.

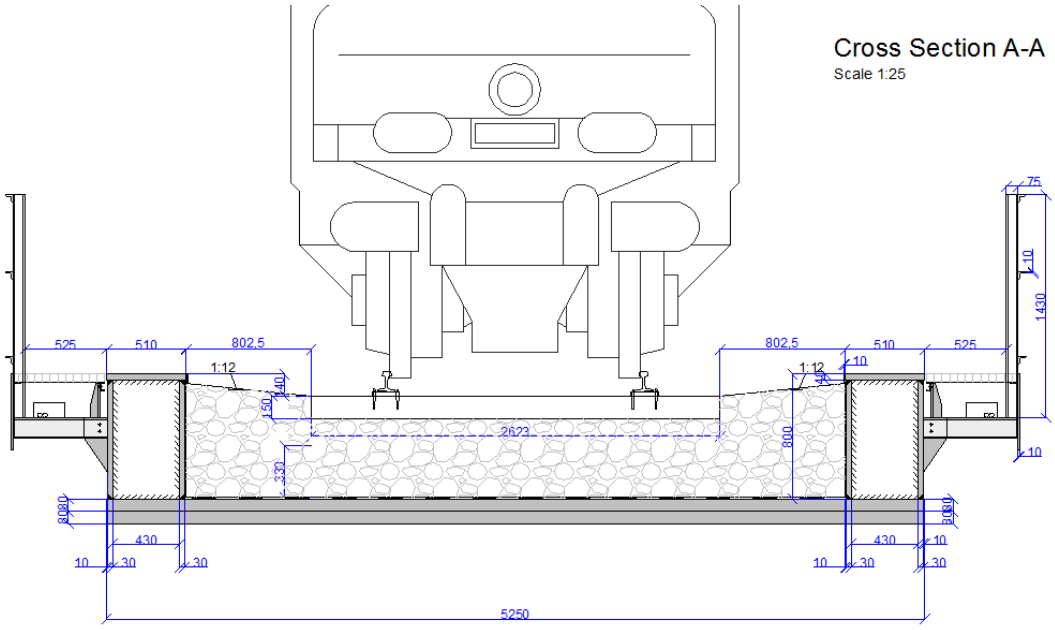

Figure 109 Cross section for 15 meters span bridge with bigger main girders

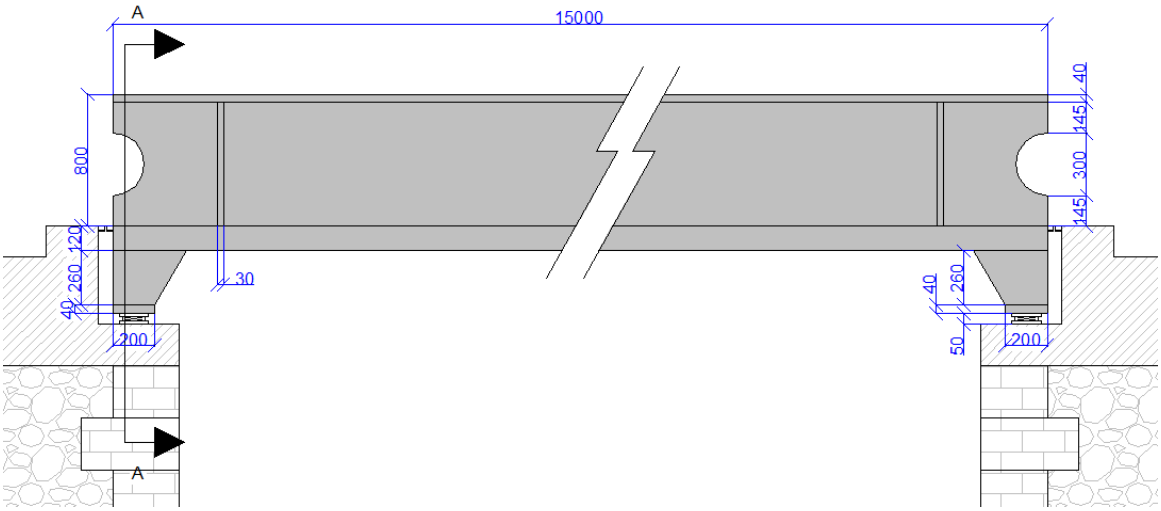

Figure 110 Longitudinal view for 15 meters span with bigger main girders

Below, some details of the box girder and the attachment of the diaphragms inside the main girders.

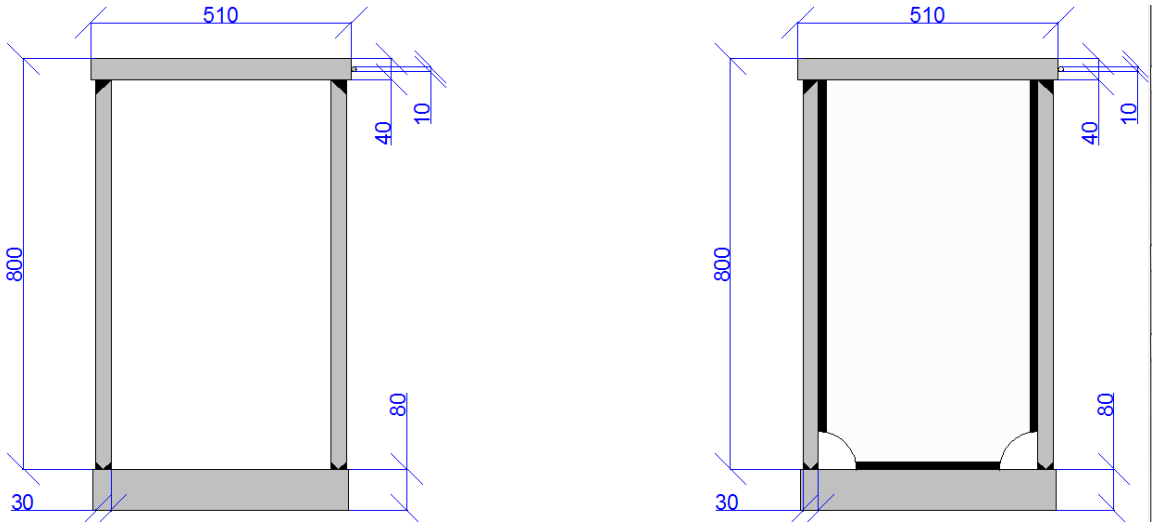

Figure 111 Detail of the bigger box girders

6.1.1) Loading

The loading of the structure is the same as before, only the damping coefficient changes.

6.1.2) Results

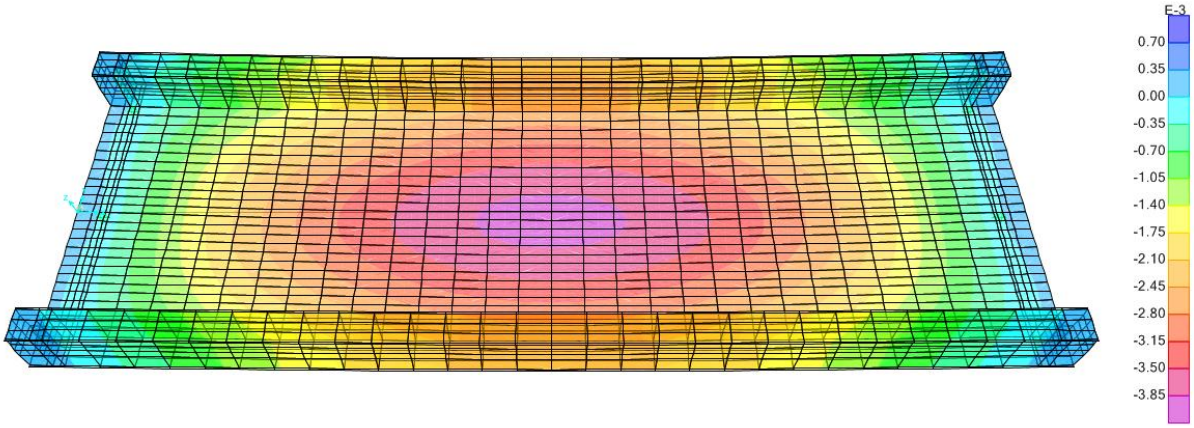

Figure 112 Dead z-displacement for 15 meters span with bigger girders

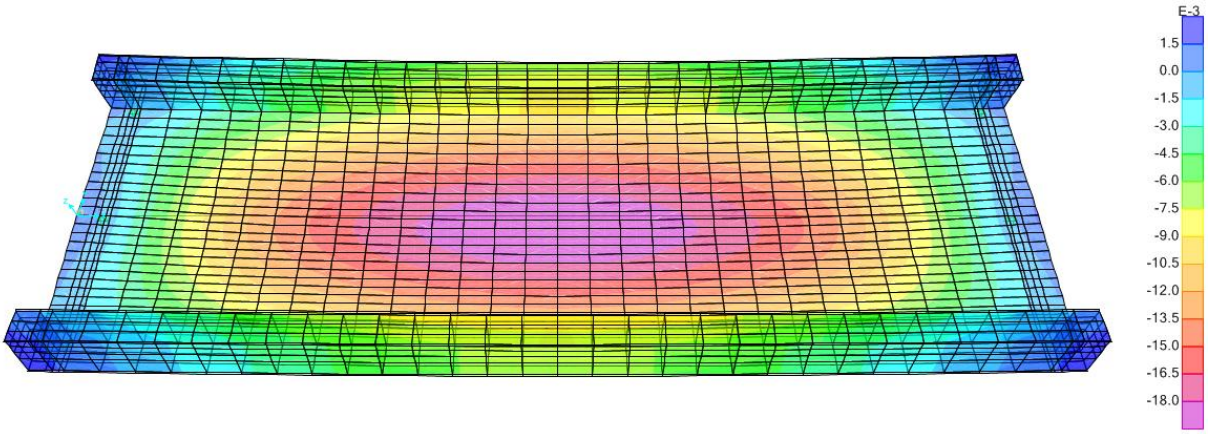

Figure 113 SW-2 z-displacement for 15 meters span with bigger girders

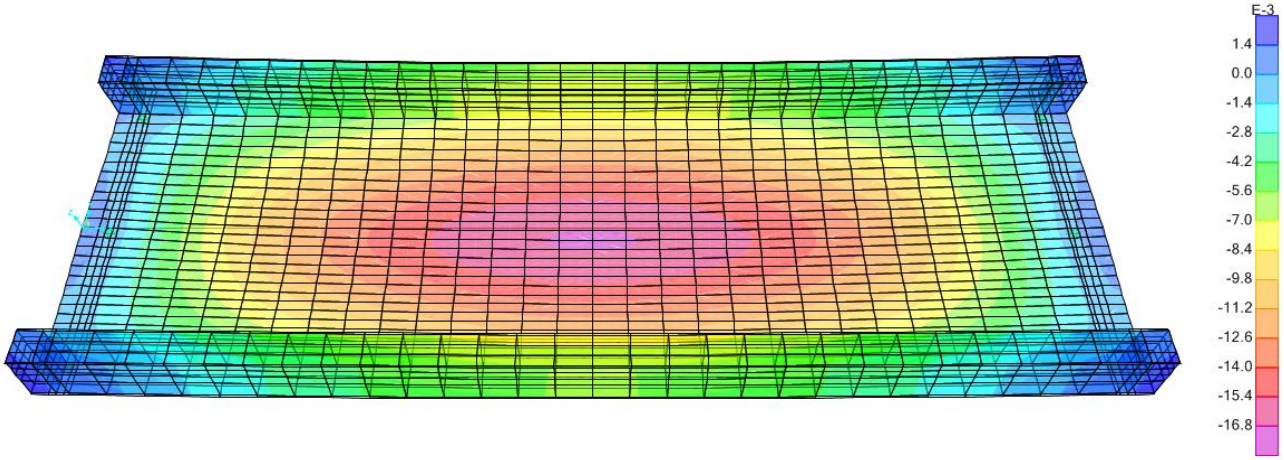

Figure 114 LM71 z-displacement for 15 meters span with bigger girders

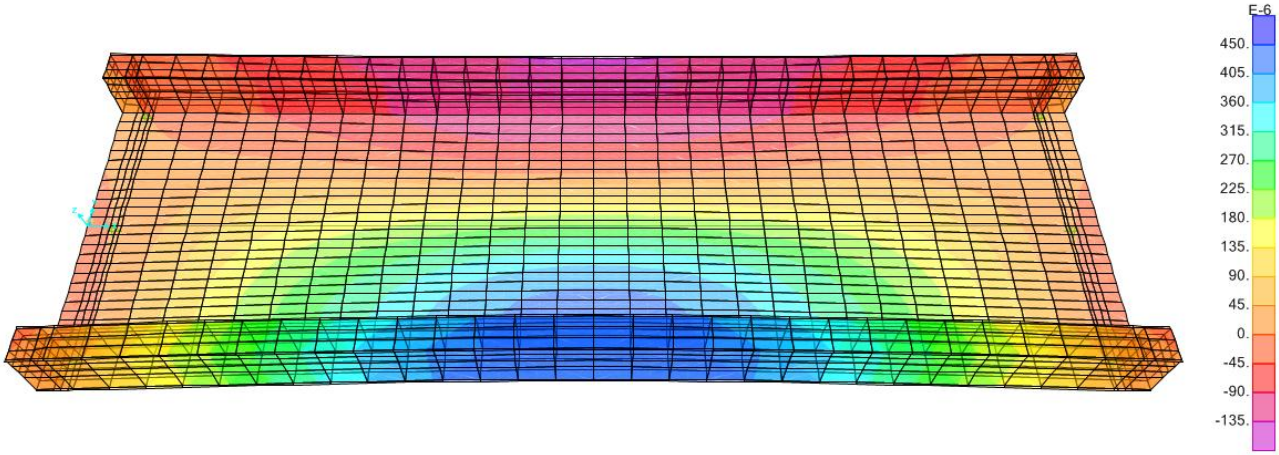

Figure 115 Wind z-displacement for 15 meters span with bigger girders

Load	Z-Displacement [mm]		Limits [mm]		Verification
	Deck-End	Middle Span	Deck-End	Middle Span	
Dead	+0.7	-3.85	None	None	YES
SW-2	+1.5	-18	3.00	25.00	YES
LM71	+1.54	-18.48	3.00	25.00	YES
Wind	-0.04	+0.45	None	None	YES

From this table we can see that the verifications that the Eurocode suggests are satisfied.

6.2) Verifications

6.2.1) Deck Twist

The twist of the bridge deck shall be calculated taking into account the characteristic values of Load Model 71 as well as SW/0 or SW/2 as appropriate multiplied by alpha.
The maximum twist *t* [mm/3m] of a track gauge *s* [m] of 1,435 m measured over a length of 3 m should not exceed the values given in Table below.

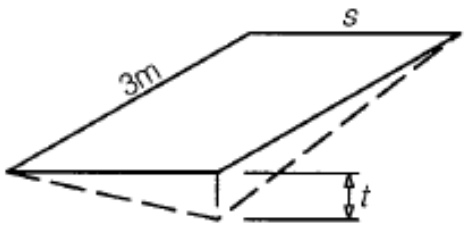

Speed range V (km/h)	Maximum twist t (mm/3m)
$V \leq 120$	$t \leq t_1$
$120 < V \leq 200$	$t \leq t_2$
$V > 200$	$t \leq t_3$

Where:

$t_1 = 4.5\ mm$

$t_2 = 3.0\ mm$

$t_3 = 1.5\ mm$

At 30 [m/sec] t=1.067[mm]

At 40 [m/sec] t=1.056 [mm]

On this tracks, trains do not exceed 55.55 [m/sec]

6.2.2) Stresses

As far as stresses verification, Von Mises's stresses have to respect this limits

$$\sigma \leq f_y = 355\ [MPa]$$

The picture below shows the most unfavourable combination, the highest stress in the deck is 100.74 MPa , and around the area of the bearings where we have the singularities, the highest is 324.23 MPa.

So everything is acceptable.

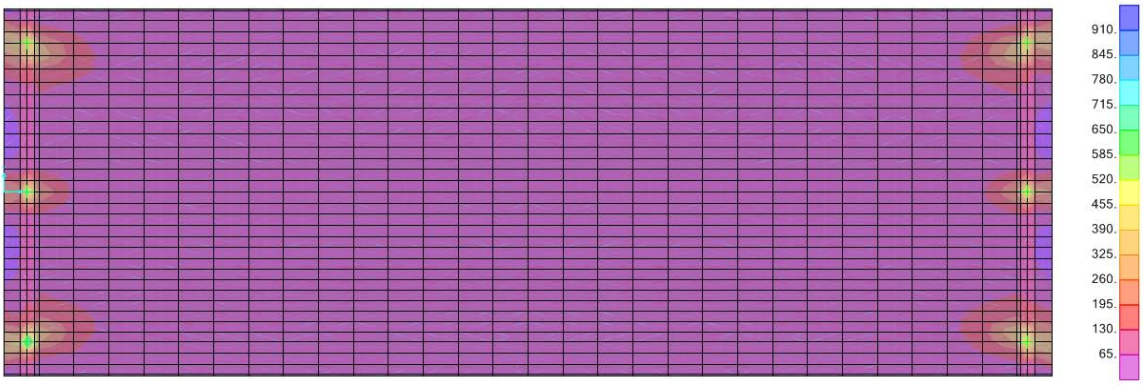

Figure 116 Von Mises diagram for 15 meters span with bigger girders

2.2.3) Transverse Deformation

This verification will be neglected, due to the short span length there will be no problems regarding horizontal curvatures.

6.3) Dynamic Analysis

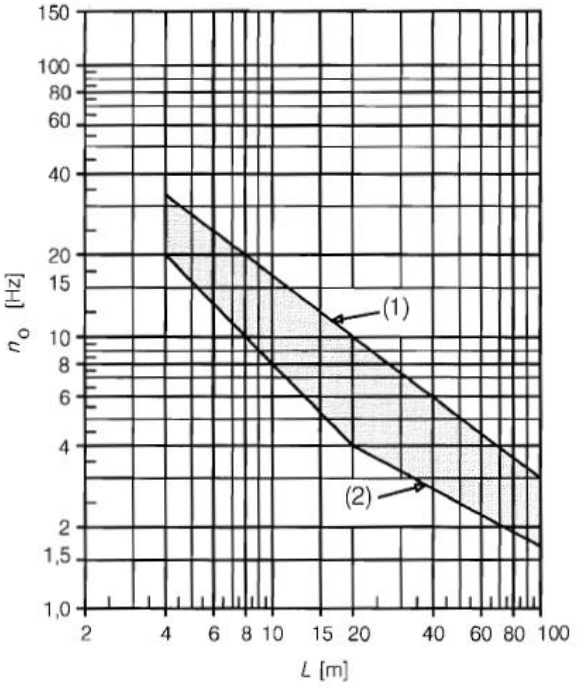

From the graph here on the left , entering with span length and natural frequency, is we end up into the "comfortable" area, the dynamic analysis is not required.

Span Length = 15m

Natural Frequency= 9.71318 Hz

So we are inside.

To run the dynamic analysis in this model, nothing basically changes from the 10 meters one. The only thing that is subject to a change is the damping coefficient since the modal analysis gives us different frequencies with which to calculate the mass-proportionl and stiffness-proportional coefficients. The equation, obviously, it's still the same:

$$C = \eta M + \delta K$$

Stiffness-proportional damping coefficient $\delta = \frac{2\xi}{\omega_i + \omega_j} = 0.002518$

Mass-proportional damping coefficient $\eta = \omega_i \omega_j \delta = 0.73375$

Where

$$\xi = 0{,}05$$
$$\omega_i = \omega_1 = 9.71318\ [Hz]$$
$$\omega_j = 30\ [Hz]$$

6.3.1) Results

All the pictures with the z-displacements are shown in Annex A

The dynamic analysis was carried out with:

Number of output Time Steps: 166

Output Time Step Size: 0.03 secs

Pictures below show the acceleration of middle span, on the main girder, as before.

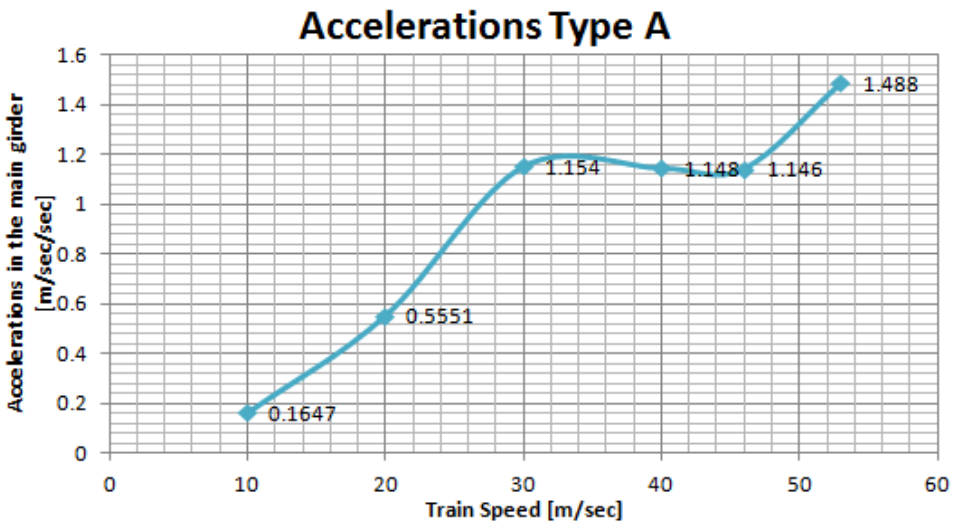
Accelerations Type A
Accelerations in the main girder [m/sec/sec]
Train Speed [m/sec]
0.1647
0.5551
1.154
1.148
1.146
1.488

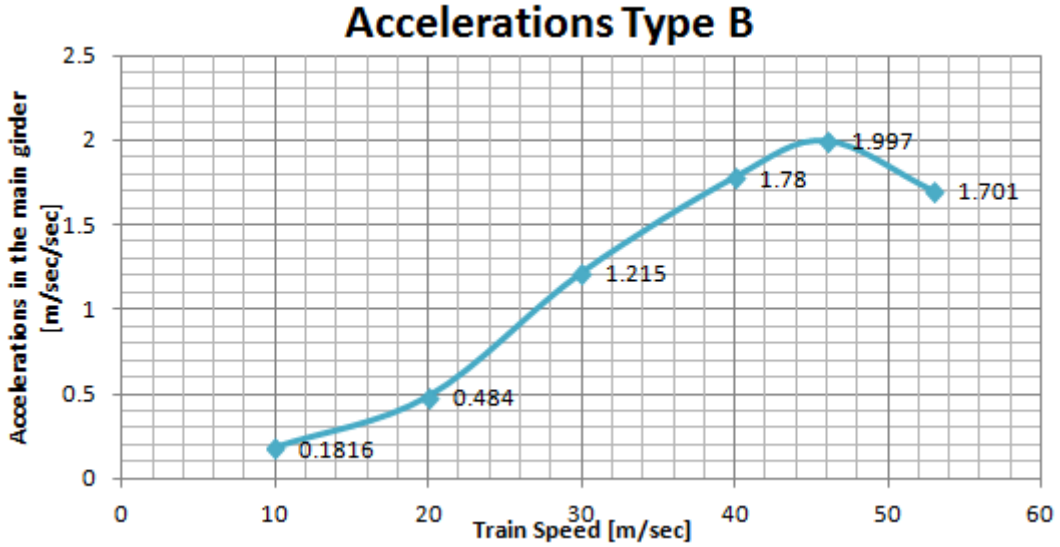
Accelerations Type B
Accelerations in the main girder [m/sec/sec]
Train Speed [m/sec]
0.1816
0.484
1.215
1.78
1.997
1.701

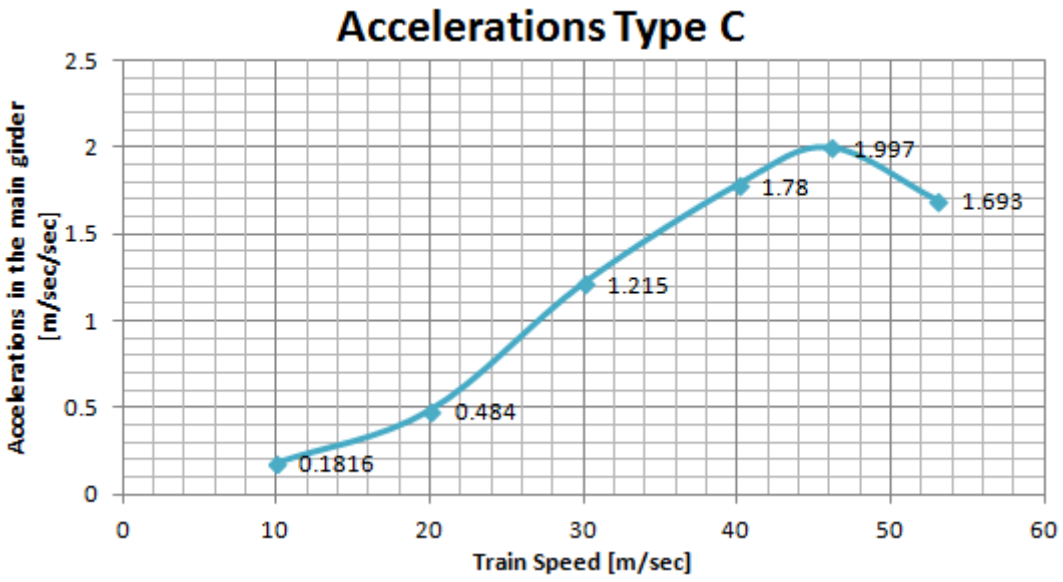
Accelerations Type C
Accelerations in the main girder [m/sec/sec]
Train Speed [m/sec]
0.1816
0.484
1.215
1.78
1.997
1.693

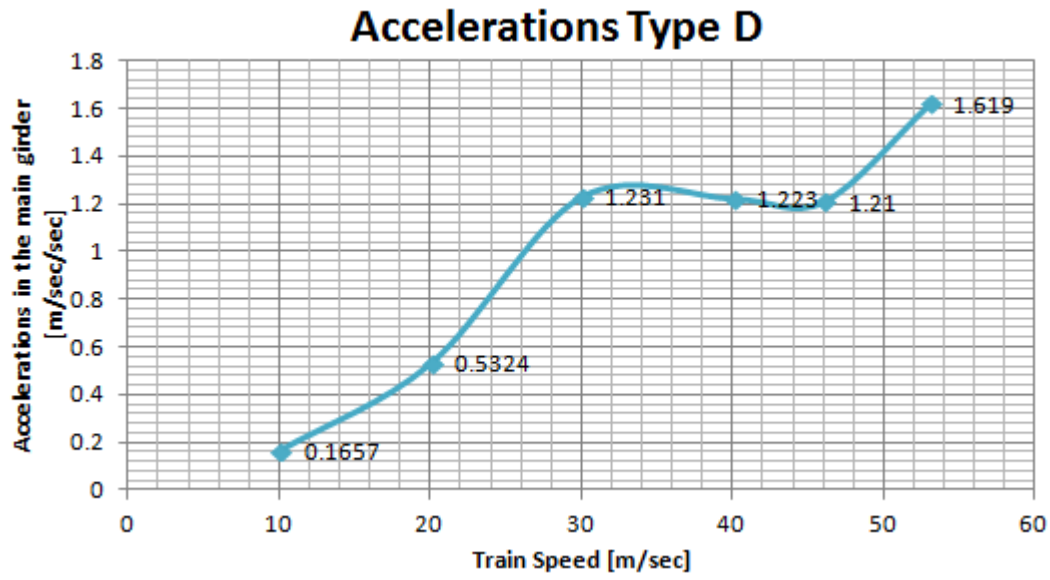
Accelerations Type D
Accelerations in the main girder [m/sec/sec]
Train Speed [m/sec]
0.1657
0.5324
1.231
1.223
1.21
1.619

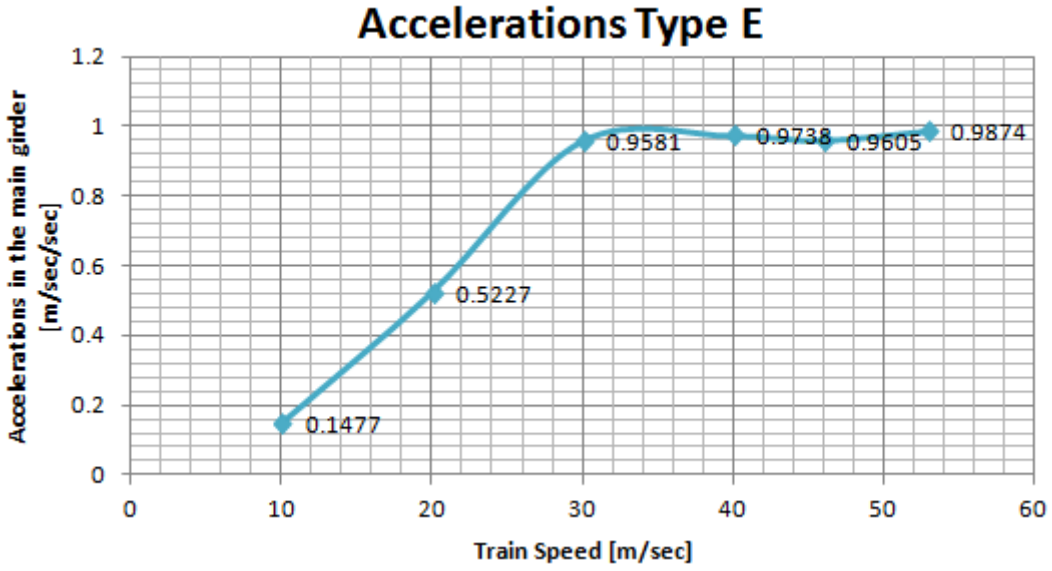
Accelerations Type E
Accelerations in the main girder [m/sec/sec]
Train Speed [m/sec]
0.1477
0.5227
0.9581
0.9738
0.9605
0.9874

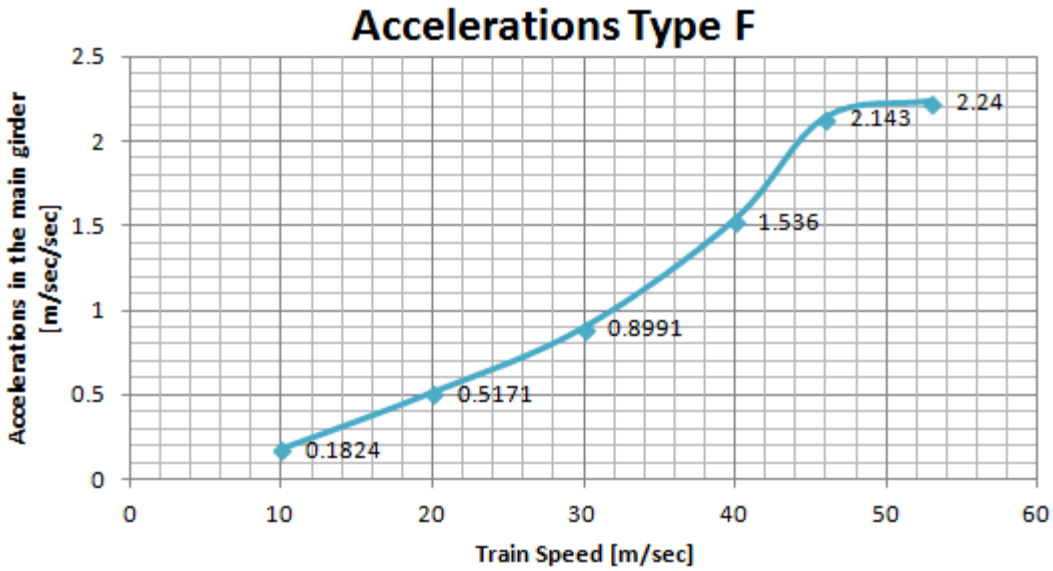
Accelerations Type F
Accelerations in the main girder [m/sec/sec]
Train Speed [m/sec]
0.1824
0.5171
0.8991
1.536
2.143
2.24

This results show that the modification made in the main girders has a huge effect on the deck accelerations.

All 36 cases is verified by Eurocode standards.

7) Bridge Design for 6 meters span

7.1) Static Analysis

Cross Section and longitudinal view are presented in the next two figures.

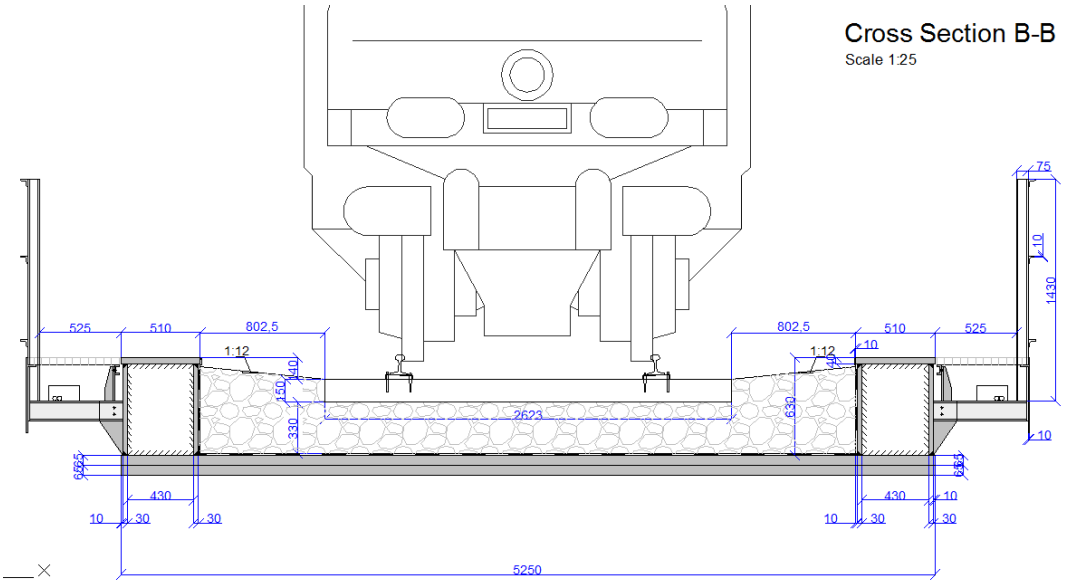

Figure 117 Cross Section 6 meters span

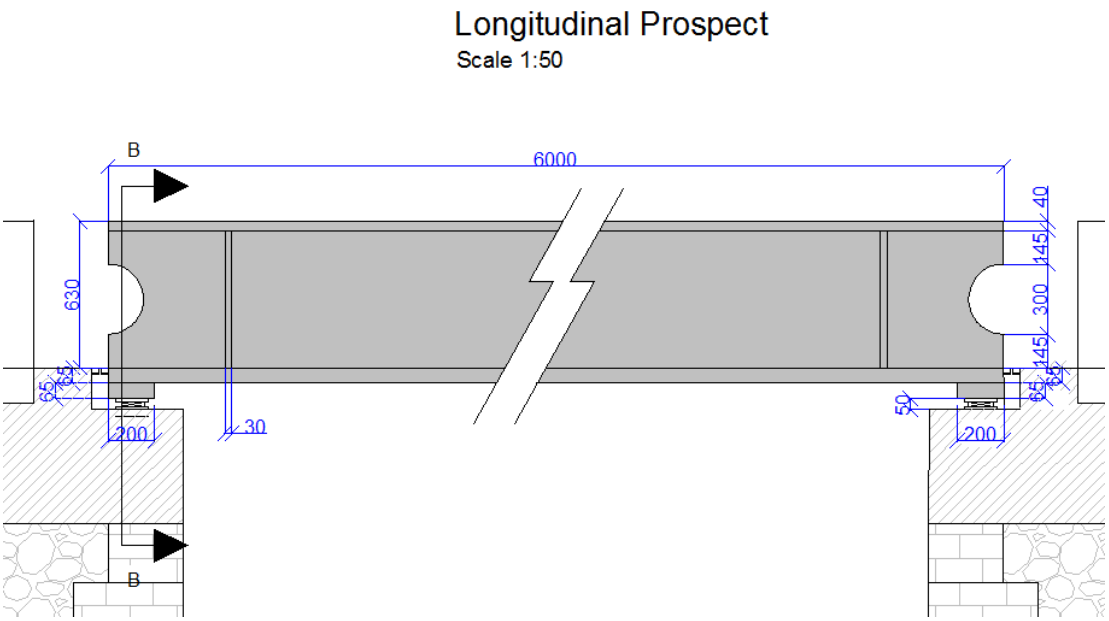

Figure 118 Longitudinal view for 6 meters span

Everything is kept the same, only the span length will change, which will affect only the damping used in the dynamic analysis.

7.1.1) Results

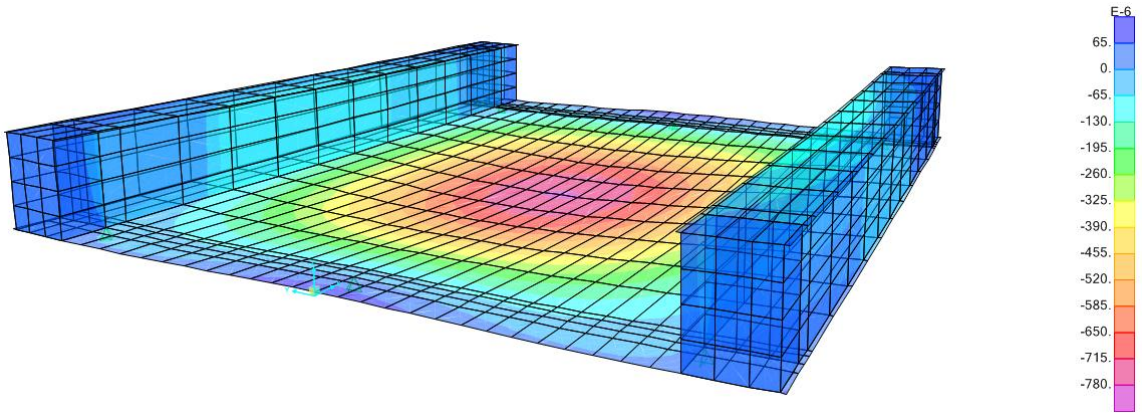

Figure 119 Dead z-displacement for 6 meters span

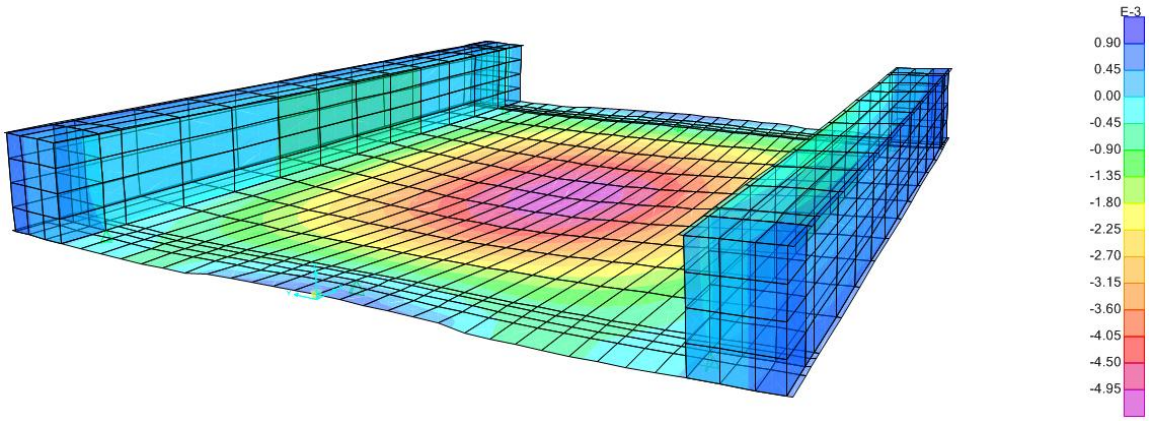

Figure 120 LM71 z-displacement for 6 meters span

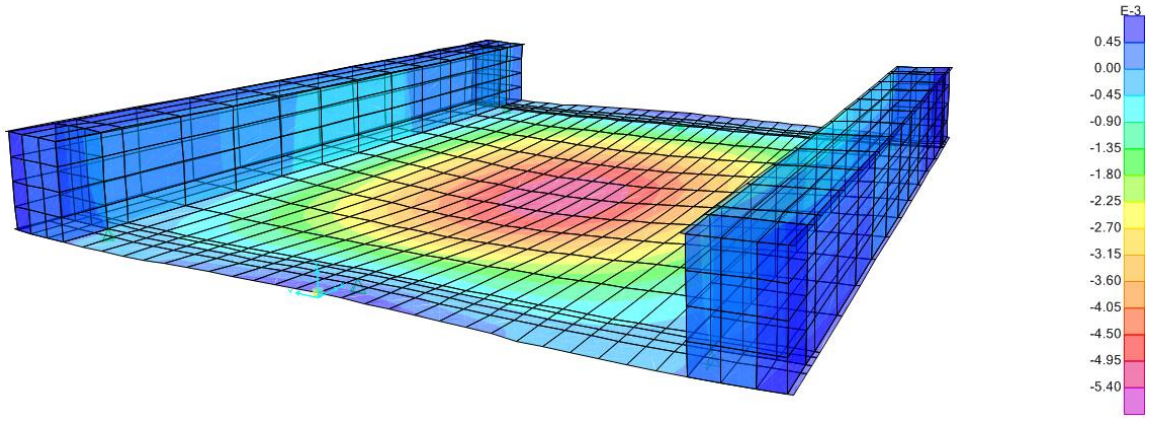

Figure 121 SW-2 z-displacement for 6 meters span

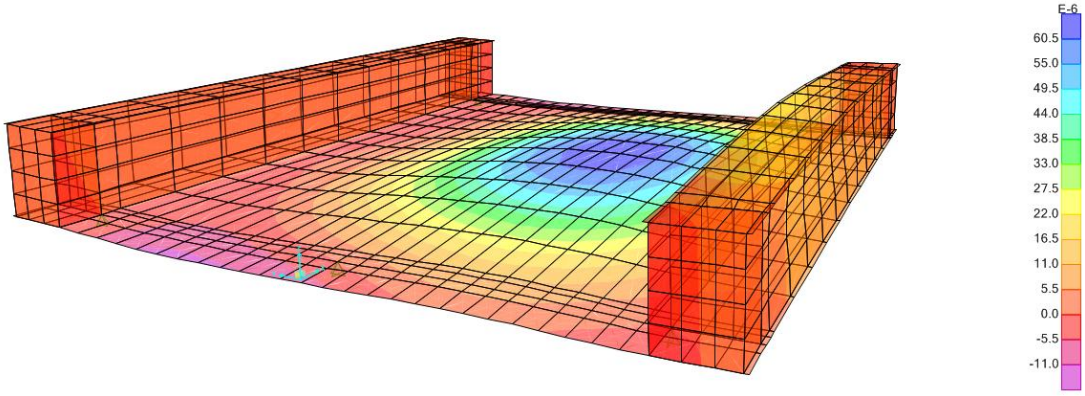

Figure 122 Wind z-displacement for 6 meters span

Load	Z-Displacement [mm]		Limits [mm]		Verification
	Deck-End	Middle Span	Deck-End	Middle Span	
Dead	+0.063	-0.78	None	None	YES
SW-2	+0.45	-5.40	3.00	10.00	YES
LM71	+0.99	-5.45	3.00	10.00	YES
Wind	-0.011	+0.06	None	None	YES

7.2) Verifications

7.2.1) Deck Twist

The twist of the bridge deck shall be calculated taking into account the characteristic values of Load Model 71 as well as SW/0 or SW/2 as appropriate multiplied by alpha.
The maximum twist *t* [mm/3m] of a track gauge *s* [m] of 1,435 m measured over a length of 3 m should not exceed the values given in Table below.

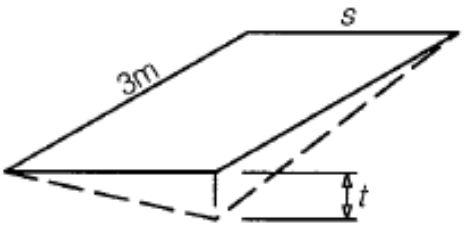

Speed range V (km/h)	Maximum twist t (mm/3m)
$V \leq 120$	$t \leq t_1$
$120 < V \leq 200$	$t \leq t_2$
$V > 200$	$t \leq t_3$

Where:

$t_1 = 4.5\ mm$

$t_2 = 3.0\ mm$

$t_3 = 1.5\ mm$

At 30 [m/sec] t=0.748 [mm]

At 40 [m/sec] t=0.753 [mm]

On this tracks, trains do not exceed 55.55 [m/sec]

7.2.2) Stresses

As far as stresses verification, Von Mises's stresses have to respect this limits

$$\sigma \leq f_y = 355\ [MPa]$$

The picture below shows the most unfavourable combination, the highest stress in the deck is 86.23 MPa , and around the area of the bearings where we have the singularities, the highest is 266.93 MPa.

So everything is acceptable.

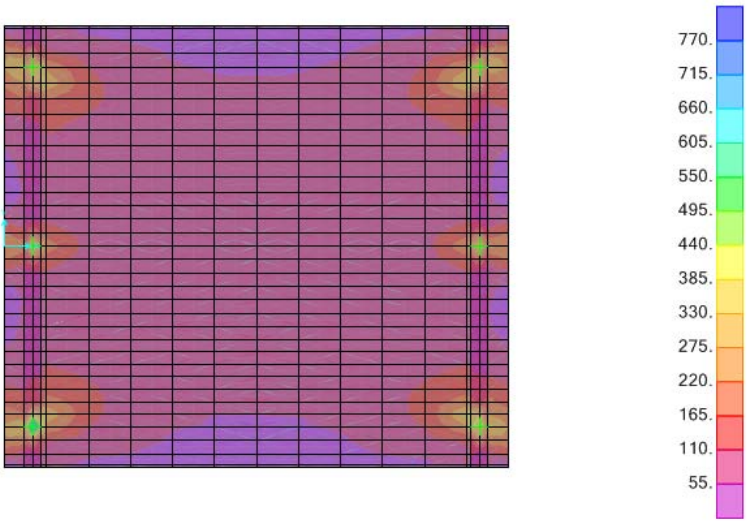

Figure 123 Von Mises diagram for 6 meters span

7.2.3) Transverse Deformation

This verification will be neglected, due to the short span length there will be no problems regarding horizontal curvatures.

Since the displacements seem to be highly verified, the deck has been modeled a bit thinner (65mm instead of 80mm) in order to save some steel if the analysis will be verified.

7.3)Static Analysis with 65mm deck

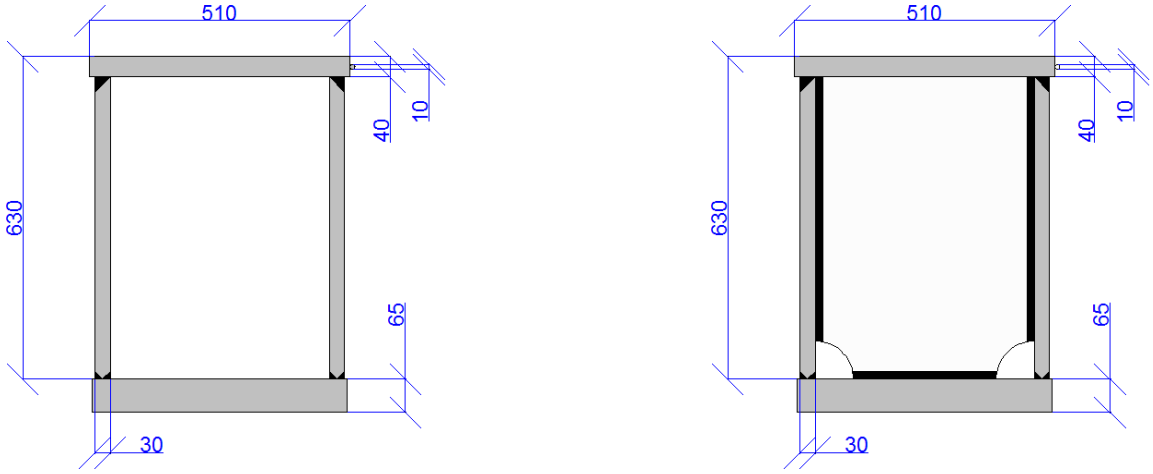

Figure 124 Box girders for 6 meters span with 65 mm deck

7.3.1) Results

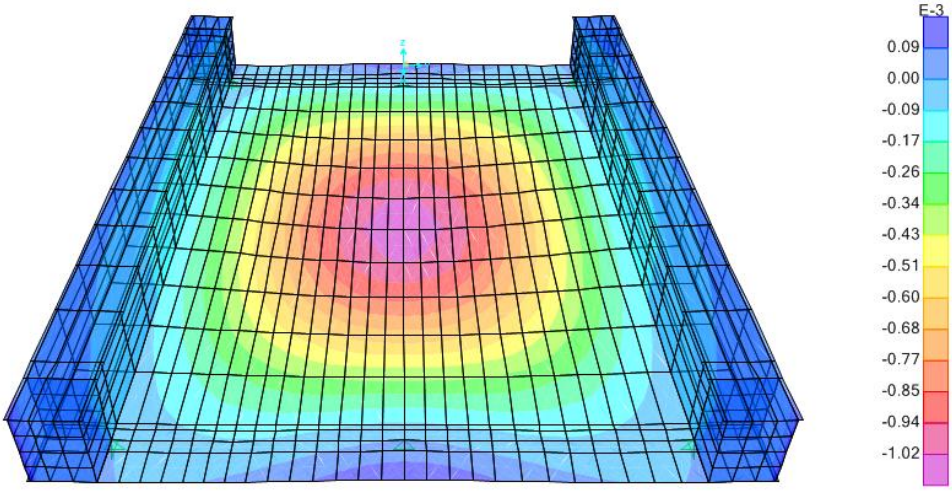

Figure 125 Dead z-displacement for 6 meters span with 65 mm deck

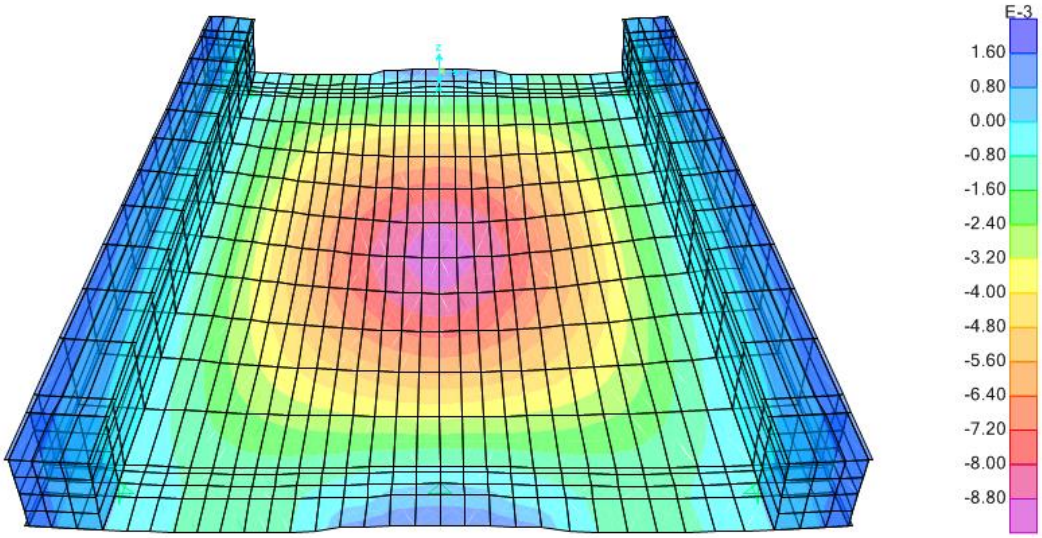

Figure 126 LM71 z-displacement for 6 meters span with 65 mm deck

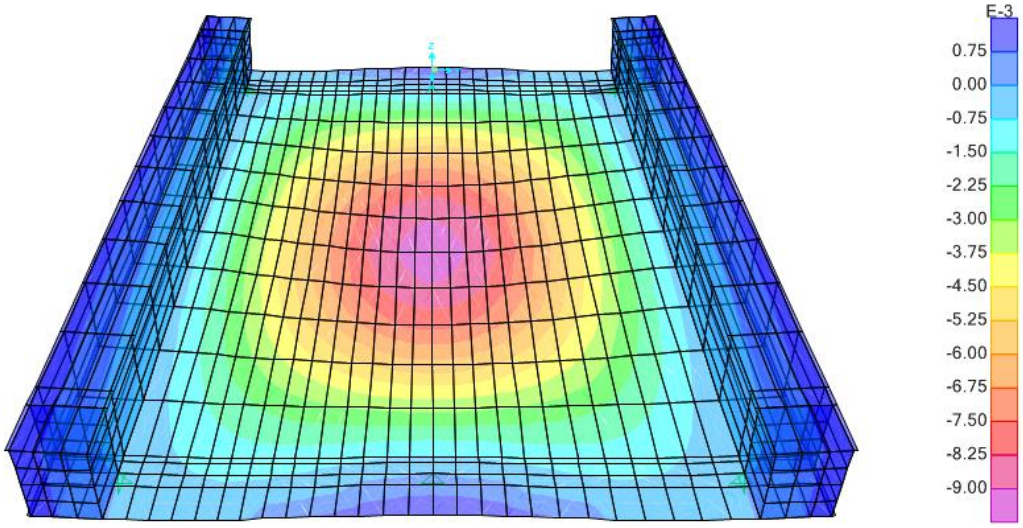

Figure 127 SW-2 z-displacement for 6 meters span with 65 mm deck

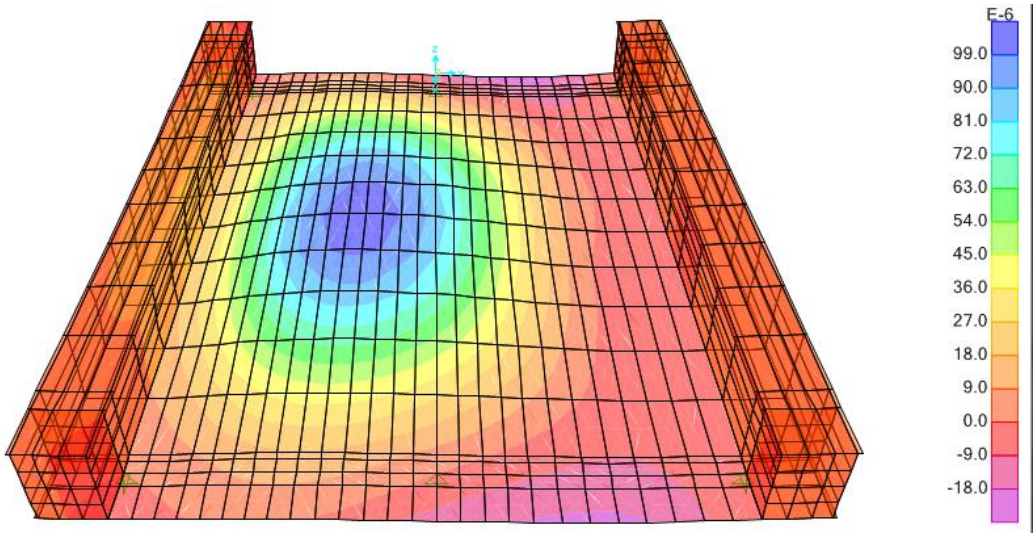

Figure 128 Wind z-displacement for 6 meters span with 65 mm deck

Load	Z-Displacement [mm]		Limits [mm]		Verification
	Deck-End	Middle Span	Deck-End	Middle Span	
Dead	+0.09	-1.02	None	None	YES
SW-2	+0.75	-9.00	3.00	10.00	YES
LM71	+1.76	-9.68	3.00	10.00	YES
Wind	-0.018	+0.099	None	None	YES

Since everything is verified, we can use this structure to carry on the dynamic analysis.

7.3.2) Verifications

7.3.2.1) Deck Twist

The twist of the bridge deck shall be calculated taking into account the characteristic values of Load Model 71 as well as SW/0 or SW/2 as appropriate multiplied by alpha.
The maximum twist *t* [mm/3m] of a track gauge *s* [m] of 1,435 m measured over a length of 3 m should not exceed the values given in Table below.

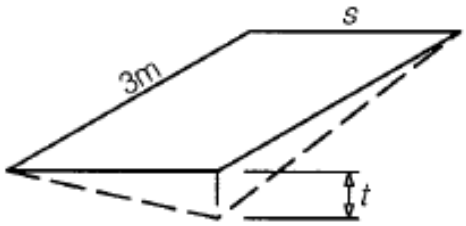

Speed range V (km/h)	Maximum twist t (mm/3m)
$V \leq 120$	$t \leq t_1$
$120 < V \leq 200$	$t \leq t_2$
$V > 200$	$t \leq t_3$

Where:

$t_1 = 4.5\,mm$

$t_2 = 3.0\,mm$

$t_3 = 1.5\,mm$

At 30 [m/sec] t=1.373 [mm]

At 40 [m/sec] t=1.369 [mm]

On this tracks, trains do not exceed 55.55 [m/sec]

7.3.2.2) Stresses

As far as stresses verification, Von Mises's stresses have to respect this limits

$$\sigma \leq f_y = 355\ [MPa]$$

The picture below shows the most unfavourable combination, the highest stress in the deck is 88.82 MPa , and around the area of the bearings where we have the singularities, the highest is 267.83 MPa.

So everything is acceptable.

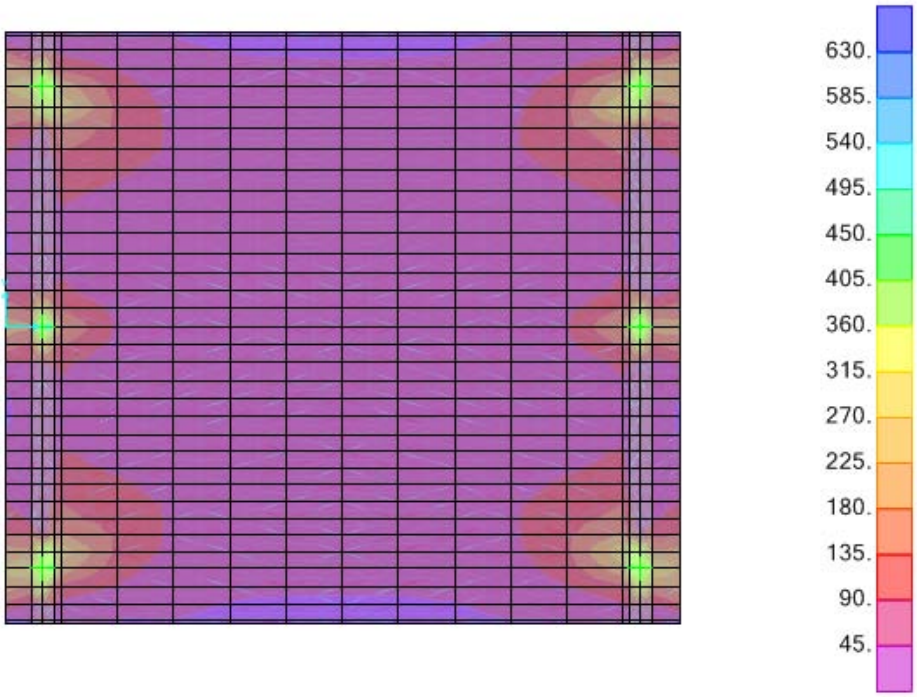

Figure 129 Von Mises diagram for 6 meters span with 65mm deck

7.3.2.3) Transverse Deformation

This verification will be neglected, due to the short span length there will be no problems regarding horizontal curvatures.

7.4) Dynamic Analysis

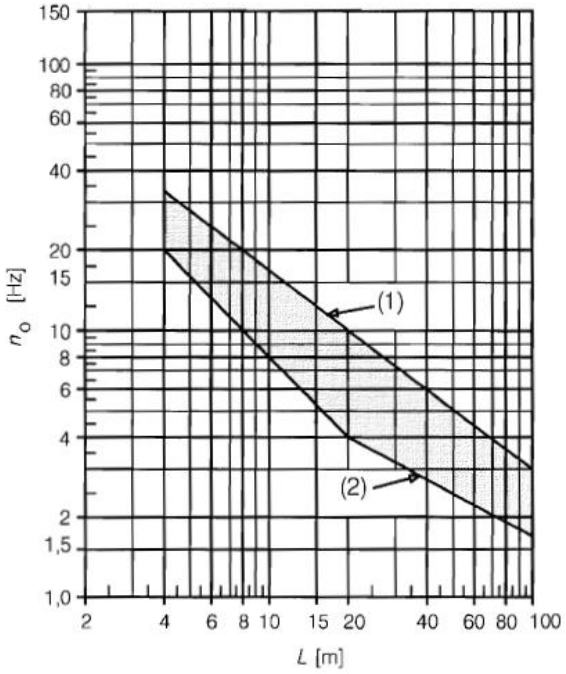

From the graph here on the left , entering with span length and natural frequency, is we end up into the "comfortable" area, the dynamic analysis is not required.

Span Length = 6m

Natural Frequency= 18.20517 Hz

So we are inside.

To run the dynamic analysis in this model, nothing basically changes from the 10 meters one. The only thing that is subject to a change is the damping coefficient since the modal analysis gives us different frequencies with which to calculate the mass-proportionl and stiffness-proportional coefficients. The equation, obviously, it's still the same:

$$C = \eta M + \delta K$$

Stiffness-proportional damping coefficient $\delta = \frac{2\xi}{\omega_i + \omega_j} = 0.0020744$

Mass-proportional damping coefficient $\eta = \omega_i \omega_j \delta = 1.13298$

Where

$$\xi = 0{,}05$$
$$\omega_i = \omega_1 = 18.20517\ [Hz]$$
$$\omega_j = 30\ [Hz]$$

7.4.1) Results

All the pictures with the z-displacements are shown in Annex A

The dynamic analysis was carried out with:

Number of output Time Steps: 166

Output Time Step Size: 0.03 secs

Pictures below show the acceleration of middle span, on the main girder, as before.

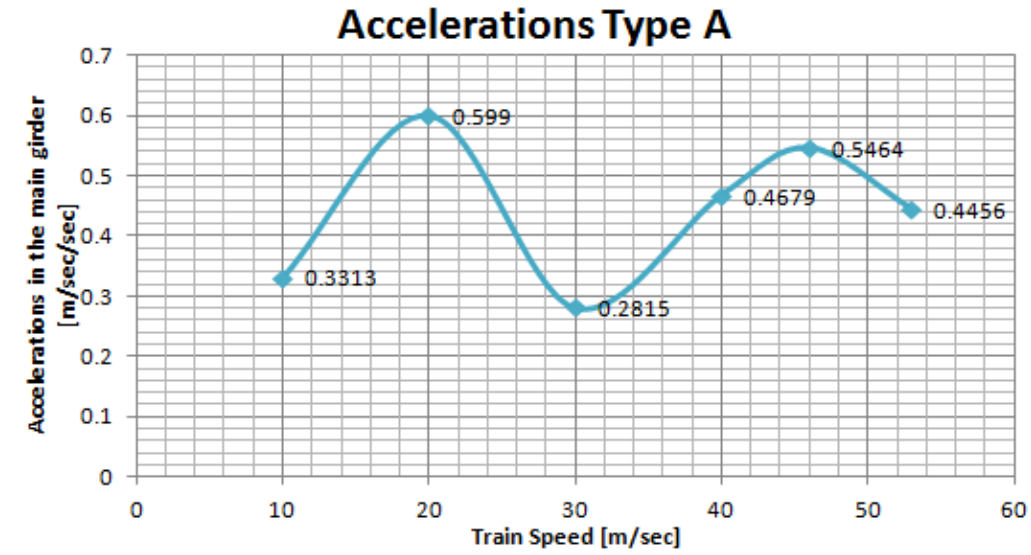
Accelerations Type A
Accelerations in the main girder [m/sec/sec]
Train Speed [m/sec]
0.3313
0.599
0.2815
0.4679
0.5464
0.4456

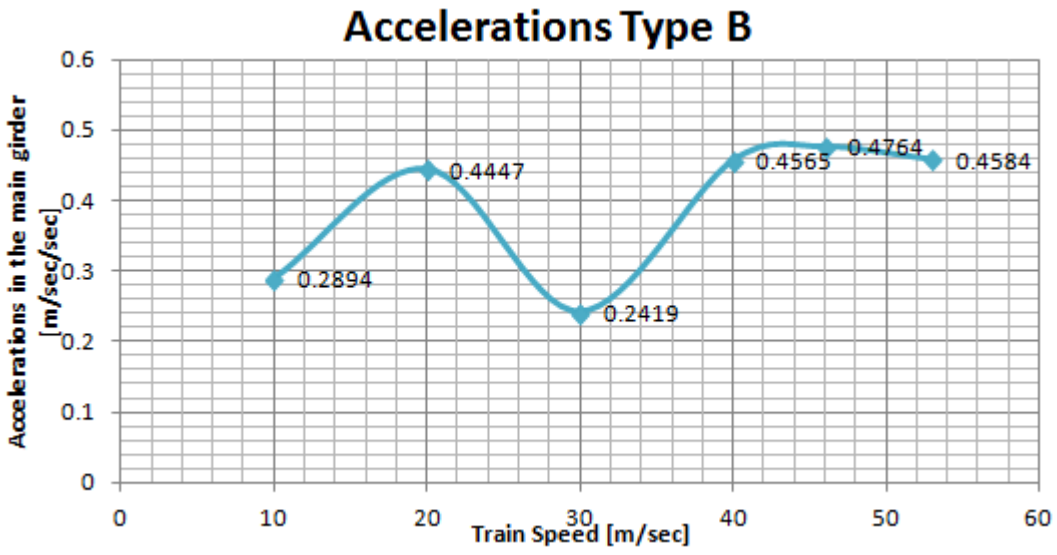
Accelerations Type B
Accelerations in the main girder [m/sec/sec]
Train Speed [m/sec]
0.2894
0.4447
0.2419
0.4565
0.4764
0.4584

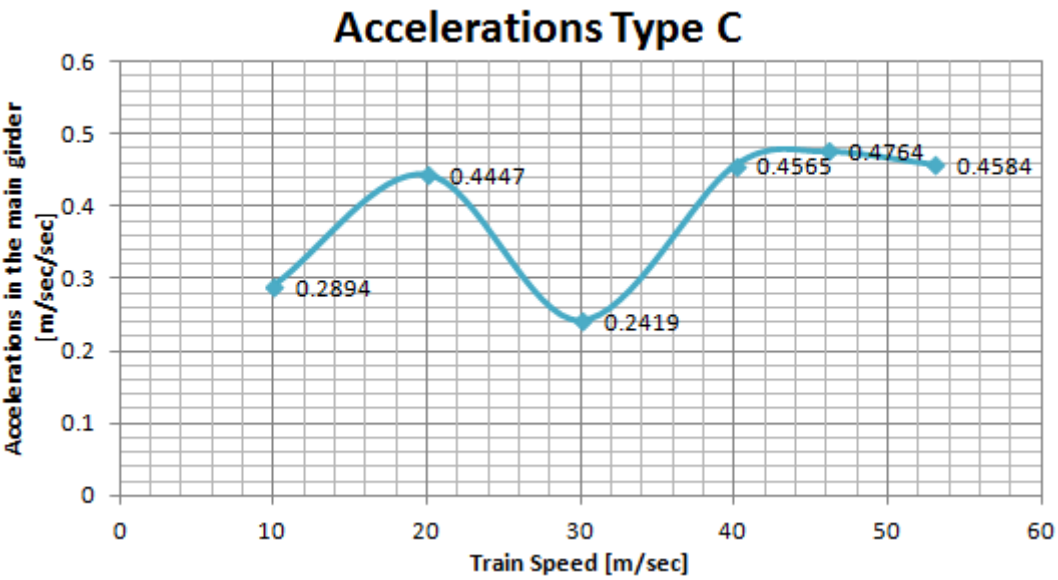
Accelerations Type C
Accelerations in the main girder [m/sec/sec]
Train Speed [m/sec]
0.2894
0.4447
0.2419
0.4565
0.4764
0.4584

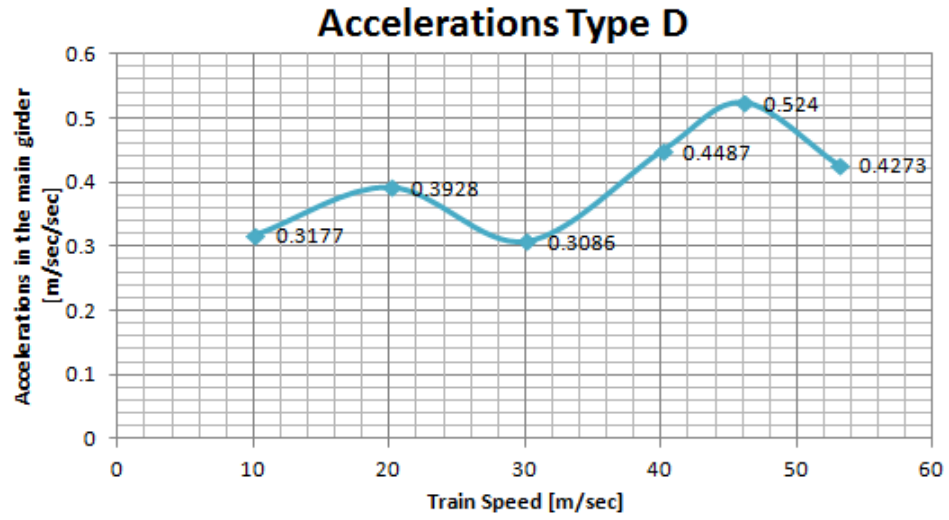

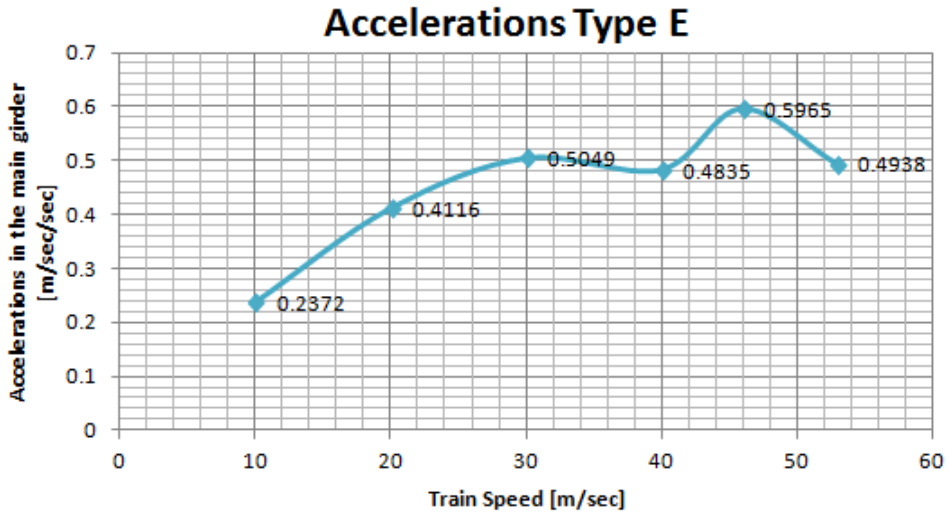

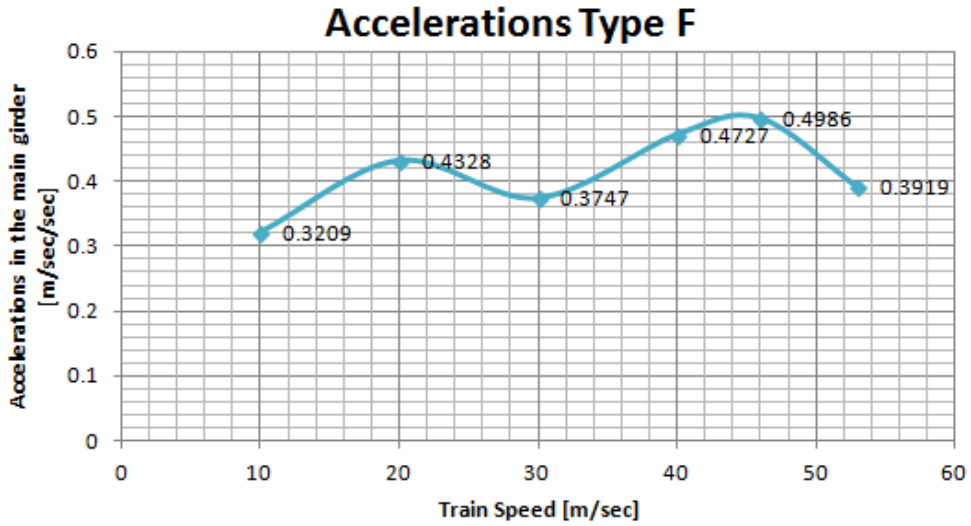

Since the upper limitations given by the Eurocode are 3.5 $[\frac{m}{sec^2}]$, each train in verified for every speed.

8)Fatigue Checks

Fatigue in metals is the process of initiation and growth of cracks under the action of repetitive tensile loads. If crack growth is allowed to go on long enough, failure of the member can result when the non cracked cross-section is sufficiently reduced such that the member can no longer carry the internal forces for the crack extends in an unstable mode. The fatigue process can take place at stress levels (calculated on the initial cross-section) that are substantially less than those associated with failure under static loading conditions. The usual condition that produces fatigue cracking is the application of a large number of load cycles. Consequently, the types of civil engineering applications that are susceptible to fatigue cracking include structures such as bridges, crane support structures, stacks and masts, and offshore structures.

Crack growth in metals requires two existing conditions: existing flaws and tensile stresses. This crack growth can be delineated into three distinct regimes: initiation, steady-state propagation and unstable fracture, like in the next figure.

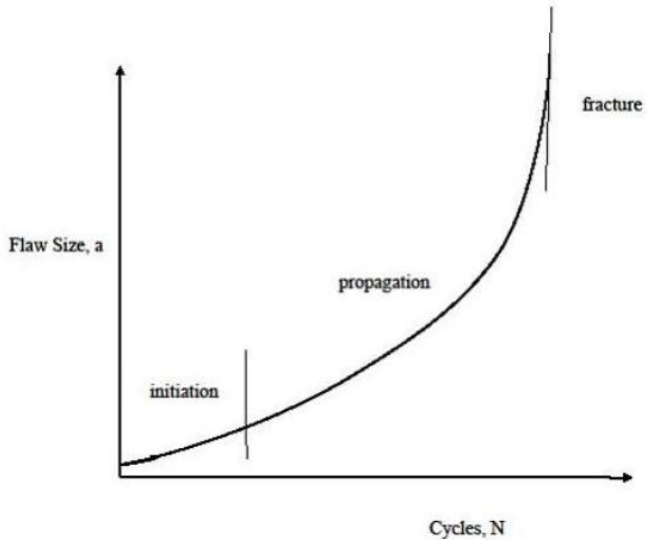

Figure 130 Crack growth chart

As has already been noted, the initiation portion of general crack growth in which existing flaws are sharpened into cracks is essentially non-existent for all fabricated steel structures and can conservatively be ignored.

8.1) Verification of the structural steel bridge part

For the fatigue calculations in the structural steel bridge part EN1994-2 allows the use of the equivalent stress ranges simplified method. The stress variations in a given structural detail is thus obtained by the single crossing of the bridge of Load Model 71.
All in all the verification format of the equivalent stress ranges simplified method is as follows:

$$\gamma_{Ff}\Delta\sigma_{E,2} \leq \frac{\Delta\sigma_C}{\gamma_{Mf}}$$

Where:

$\gamma_{Ff} = 1.00$ partial factor applied to the load models

$\Delta\sigma_{E,2} = \lambda\phi\Delta\sigma_C = \lambda\phi(\sigma_{max,f} - \sigma_{min,f})$ is the equivalent constant amplitude stress range related to 2 millions cycles

$\Delta\sigma_C$ is the reference value of the fatigue strength at 2 millions cycles (detail category)

$\gamma_{Mf} = 1.35$ partial factor for the fatigue strength

$\lambda =$ damage equivalent factor

$\phi = \frac{1.44}{\sqrt{L}-0.2} + 0.82$ dynamic factor

How to calculate the damage equivalent factor is given by this combination of sub-factors.

$\lambda = \lambda_1\lambda_2\lambda_3\lambda_4 \leq \lambda_{max}$

Where:

λ_1 is the factor for the damage effect of traffic and depends on the length of the influence line

λ_2 in the factor for traffic volume

λ_3 is the factor for the design life of the bridge

λ_4 is the factor for the structural element is loaded by more than one track

λ_{max} is the maximum factor value taking into account the fatigue limit

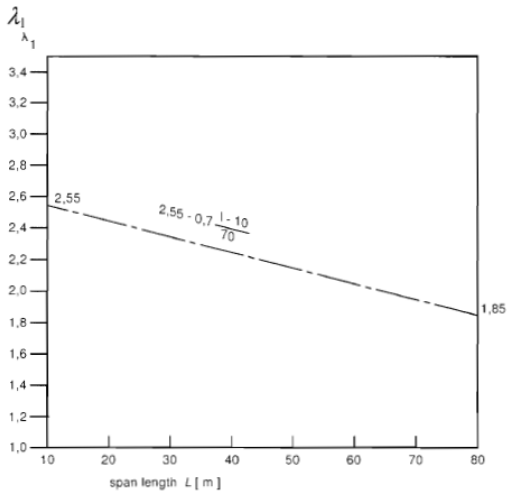

span length L [m]

at midspan

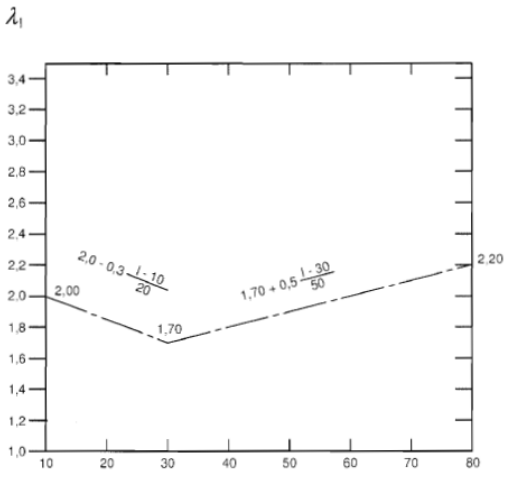

span length L [m]

at support

Q_{m1}	N_{Obs}							
	$0{,}25\times10^6$	$0{,}50\times10^6$	$0{,}75\times10^6$	$1{,}00\times10^6$	$1{,}25\times10^6$	$1{,}50\times10^6$	$1{,}75\times10^6$	$2{,}00\times10^6$
200	0,362	0,417	0,452	0,479	0,500	0,519	0,535	0,550
300	0,544	0,625	0,678	0,712	0,751	0,779	0,803	0,825
400	0,725	0,833	0,904	0,957	1,001	1,038	1,071	1,100
500	0,907	1,042	1,130	1,197	1,251	1,298	1,338	1,374
600	1,088	1,250	1,356	1,436	1,501	1,557	1,606	1,649

Design life in years	50	60	70	80	90	100	120
Factor λ_3	0,871	0,903	0,931	0,956	0,979	1,00	1,037

$$\lambda_4 = [1 + \frac{N_2}{N_1}\left(\frac{\eta_2 Q_{m2}}{\eta_1 Q_{m1}}\right)^5 + \frac{N_3}{N_1}\left(\frac{\eta_3 Q_{m3}}{\eta_1 Q_{m1}}\right)^5 + \cdots + \frac{N_2}{N_1}\left(\frac{\eta_k Q_{mk}}{\eta_1 Q_{m1}}\right)^5]^{1/5}$$

$k = number\ of\ lanes\ with\ heavy\ traffic$

$N_j = number\ of\ trains\ per\ year\ in\ lane\ j$

$Q_{mj} = average\ gross\ weight\ of\ the\ trains\ in\ lane\ j$

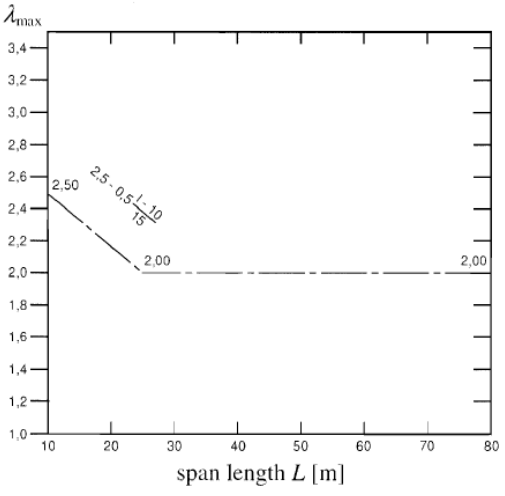

at midspan

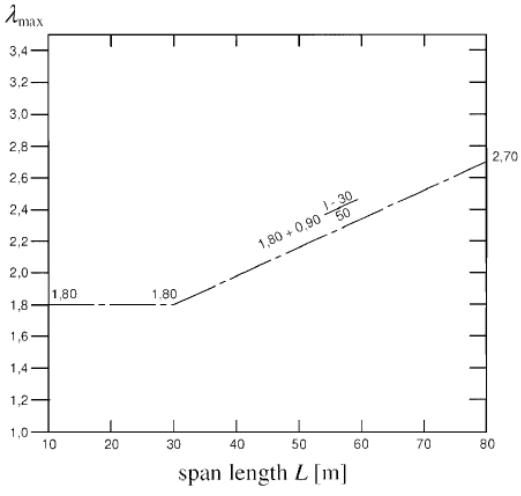

at support

8.2) Results

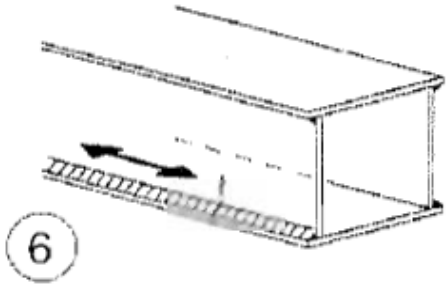

Here are the details that are subject to fatigue checks divided into spans, first in x-direction, than in y-direction.

The detail which is going to be verified for fatigue now is the welded connection between the web and deck on the main girder .

Longitudinal Direction

6 Meters

Δσp	σmax	σmin	ΔσE2	γFf	γMf	ϕ2	λ	ΔσC	λ1	1.03
9.49	12.32	2.83	14.8434	1	1.35	1.46015	1.0712	100	λ2	1
									λ3	1.04
									λ4	1

Verification			
14.8434	<	74.0741	OK!

10 Meters

Δσp	σmax	σmin	ΔσE2	γFf	γMf	ϕ2	λ	ΔσC	λ1	0.85
8.32	10.06	1.74	9.6063	1	1.35	1.30611	0.884	100	λ2	1
									λ3	1.04
									λ4	1

Verification			
9.6063	<	74.0741	OK!

15 Meters

Δσp	σmax	σmin	ΔσE2	γFf	γMf	ϕ2	λ	ΔσC	λ1	0.76
17.95	27.4	9.45	17.1962	1	1.35	1.21205	0.7904	100	λ2	1
									λ3	1.04
									λ4	1

Verification			
17.1962	<	74.0741	OK!

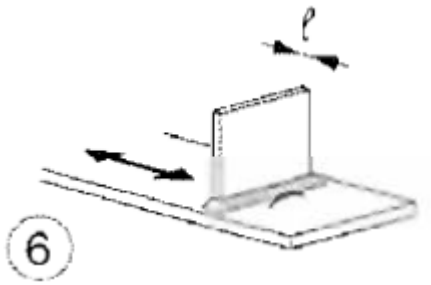

Transversal Direction

6 Meters										
Δσp	σmax	σmin	ΔσE2	γFf	γMf	Φ2	λ	ΔσC	λ1	1.03
26.38	35.2	8.82	42.67	1	1.35	1.51	1.0712	80	λ2	1
									λ3	1.04
									λ4	1

Verification			
42.67	<	59.2593	OK!

10 Meters										
Δσp	σmax	σmin	ΔσE2	γFf	γMf	Φ2	λ	ΔσC	λ1	0.85
26.29	32.21	5.92	35.0929	1	1.35	1.51	0.884	80	λ2	1
									λ3	1.04
									λ4	1

Verification			
35.0929	<	59.2593	OK!

15 Meters										
Δσp	σmax	σmin	ΔσE2	γFf	γMf	Φ2	λ	ΔσC	λ1	0.76
27.11	35.85	8.74	32.3559	1	1.35	1.51	0.7904	80	λ2	1
									λ3	1.04
									λ4	1

Verification			
32.3559	<	59.2593	OK!

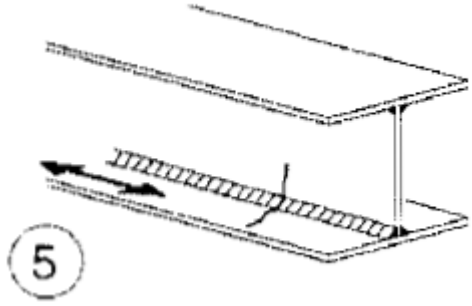

This is the detail of the web welded to the upper flange

Longitudinal Direction

6 Meters

Δσp	σmax	σmin	ΔσE2	γFf	γMf	ϕ2	λ	ΔσC	λ1	1.03
9.49	12.32	2.83	14.8434	1	1.35	1.46015	1.0712	100	λ2	1
									λ3	1.04
									λ4	1

Verification			
14.8434	<	74.0741	OK!

10 Meters

Δσp	σmax	σmin	ΔσE2	γFf	γMf	ϕ2	λ	ΔσC	λ1	0.85
8.32	10.06	1.74	9.6063	1	1.35	1.30611	0.884	100	λ2	1
									λ3	1.04
									λ4	1

Verification			
9.6063	<	74.0741	OK!

15 Meters

Δσp	σmax	σmin	ΔσE2	γFf	γMf	ϕ2	λ	ΔσC	λ1	0.76
17.95	27.4	9.45	17.1962	1	1.35	1.21205	0.7904	100	λ2	1
									λ3	1.04
									λ4	1

Verification			
17.1962	<	74.0741	OK!

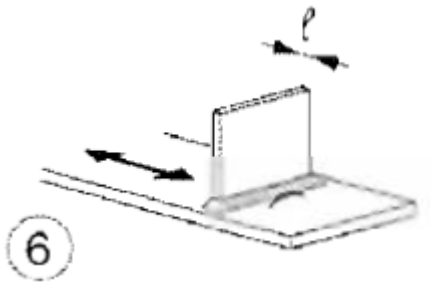

Transversal Direction

6 Meters

Δσp	σmax	σmin	ΔσE2	γFf	γMf	Φ2	λ	ΔσC	λ1	1.03
11.15	11.86	0.71	18.0353	1	1.35	1.51	1.0712	80	λ2	1
									λ3	1.04
									λ4	1

Verification			
18.0353	<	59.2593	OK!

10 Meters

Δσp	σmax	σmin	ΔσE2	γFf	γMf	Φ2	λ	ΔσC	λ1	0.85
13.35	14.14	0.79	17.8201	1	1.35	1.51	0.884	80	λ2	1
									λ3	1.04
									λ4	1

Verification			
17.8201	<	59.2593	OK!

15 Meters

Δσp	σmax	σmin	ΔσE2	γFf	γMf	Φ2	λ	ΔσC	λ1	0.76
14.03	15.37	1.34	16.7449	1	1.35	1.51	0.7904	80	λ2	1
									λ3	1.04
									λ4	1

Verification			
16.7449	<	59.2593	OK!

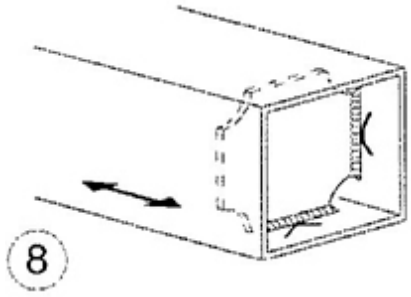

Here the detail of the diaphragms into the main girders is checked

The class of the detail is 80 because the thickness of the diaphragms is lower than 50 mm

Longitudinal Direction

6 Meters

Δσp	σmax	σmin	ΔσE2	γFf	γMf	ϕ2	λ	ΔσC	λ1	1.03
9.21	9.92	0.71	14.4054	1	1.35	1.46015	1.0712	80	λ2	1
									λ3	1.04
									λ4	1

Verification			
14.4054	<	59.2593	OK!

10 Meters

Δσp	σmax	σmin	ΔσE2	γFf	γMf	ϕ2	λ	ΔσC	λ1	0.85
9.23	9.75	0.52	10.657	1	1.35	1.30611	0.884	80	λ2	1
									λ3	1.04
									λ4	1

Verification			
10.657	<	59.2593	OK!

15 Meters

Δσp	σmax	σmin	ΔσE2	γFf	γMf	ϕ2	λ	ΔσC	λ1	0.76
13.53	14.18	0.65	12.9618	1	1.35	1.21205	0.7904	80	λ2	1
									λ3	1.04
									λ4	1

Verification			
12.9618	<	59.2593	OK!

9)Annex A

Here are presented all the results of the displacements of the dynamic analysis carried out previously.

9.1) Results for 3 Bearings – Cross End Beam structure:

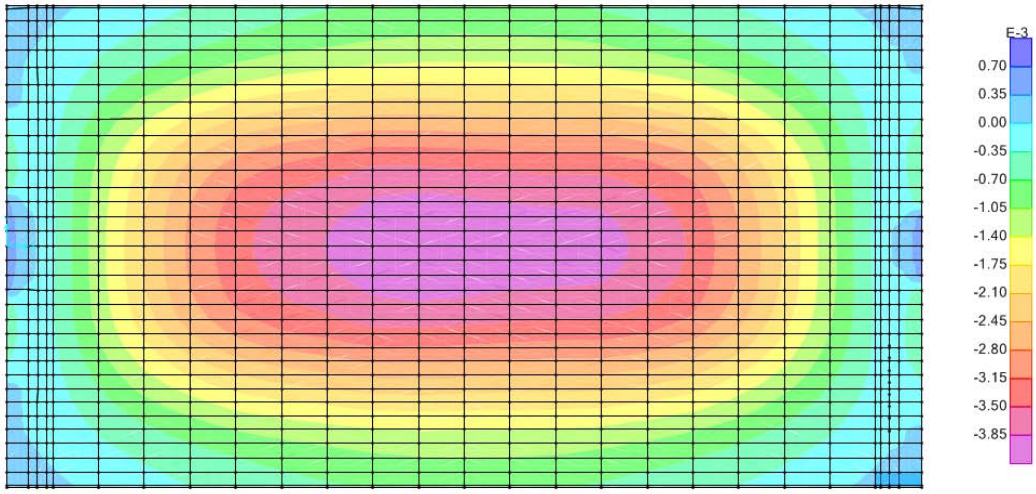

Type A: Speed 10 [m/sec]

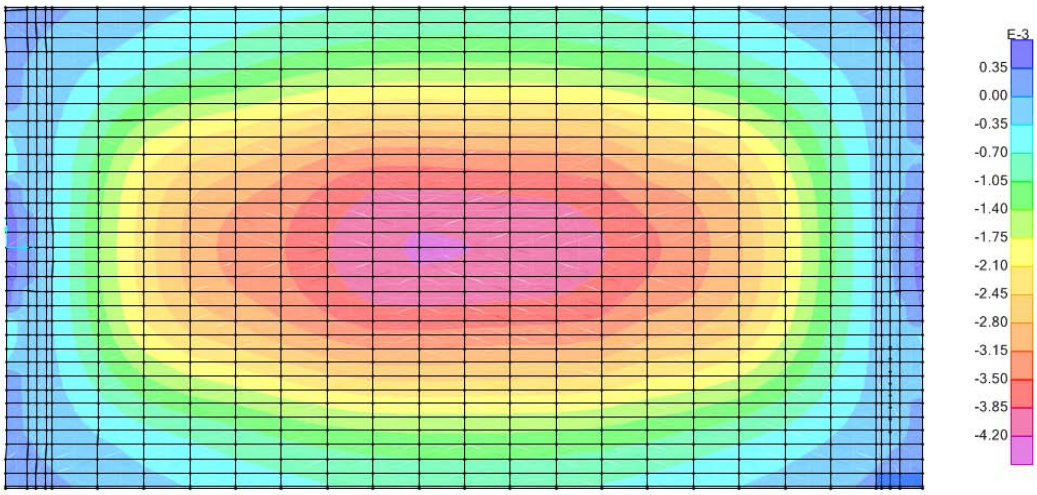

Type A: Speed 20 [m/sec]

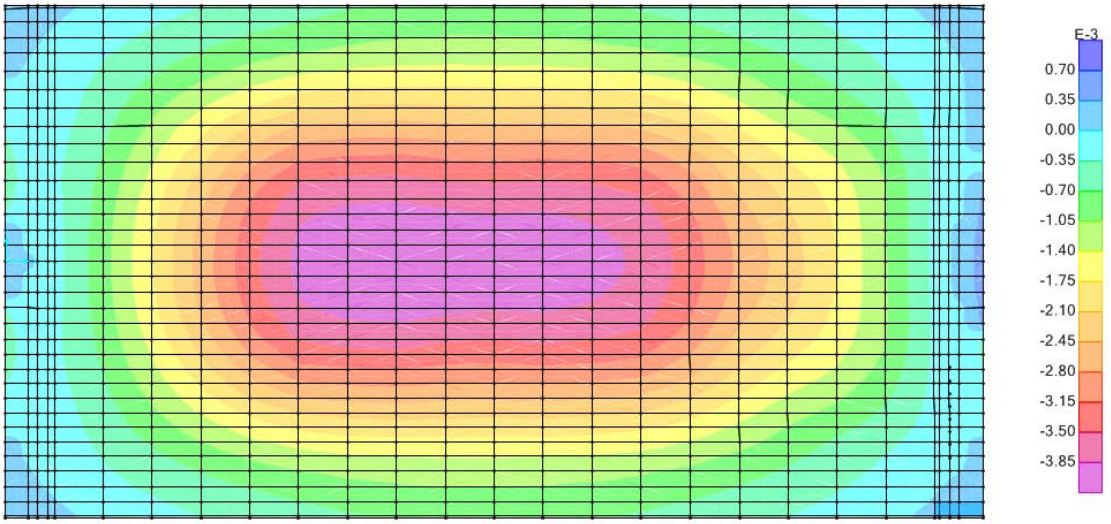

Type A: Speed 30 [m/sec]

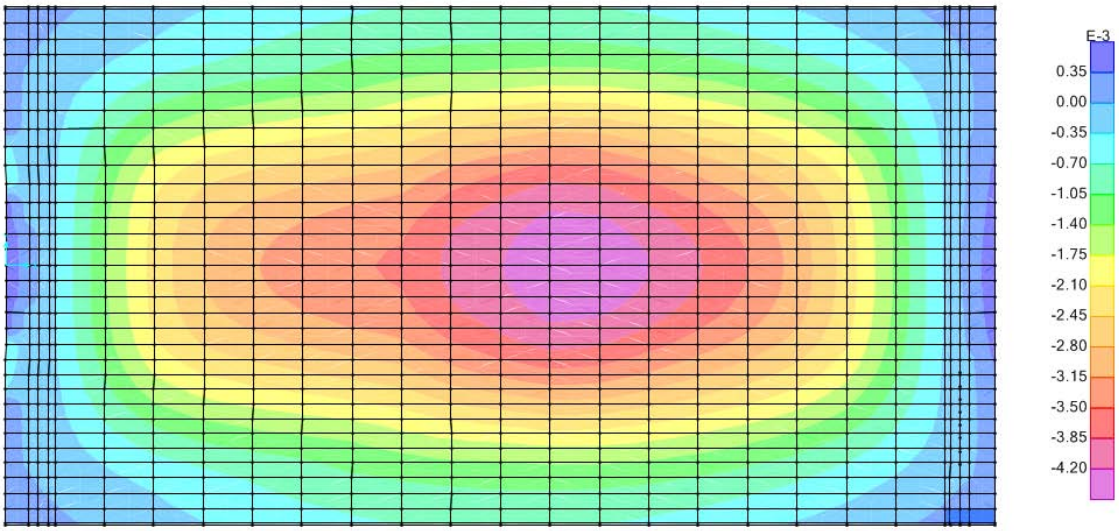

Type A: Speed 40 [m/sec]

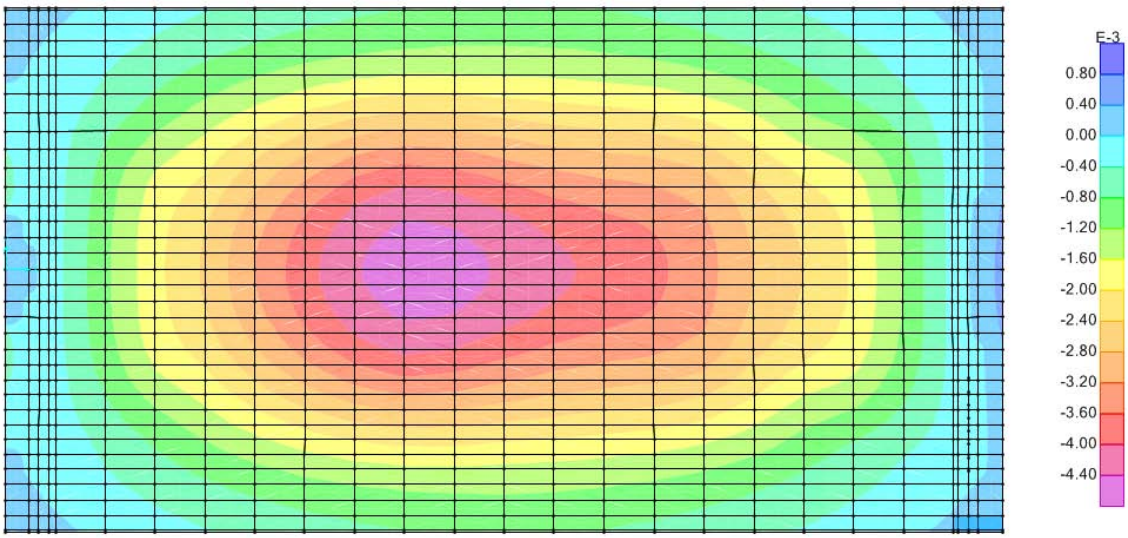

Type A: Speed 46 [m/sec]

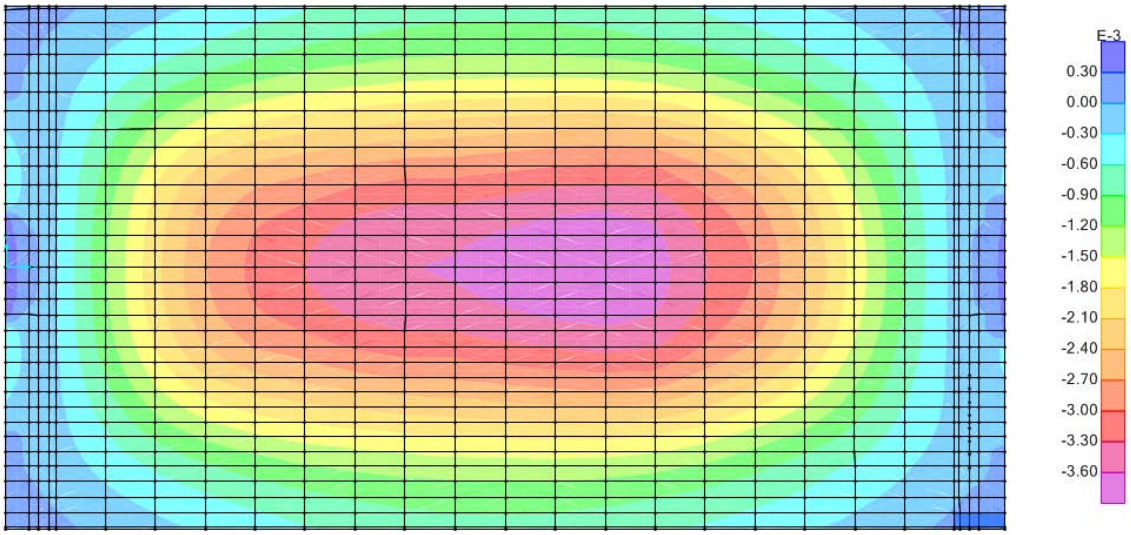

Type A: Speed 53 [m/sec]

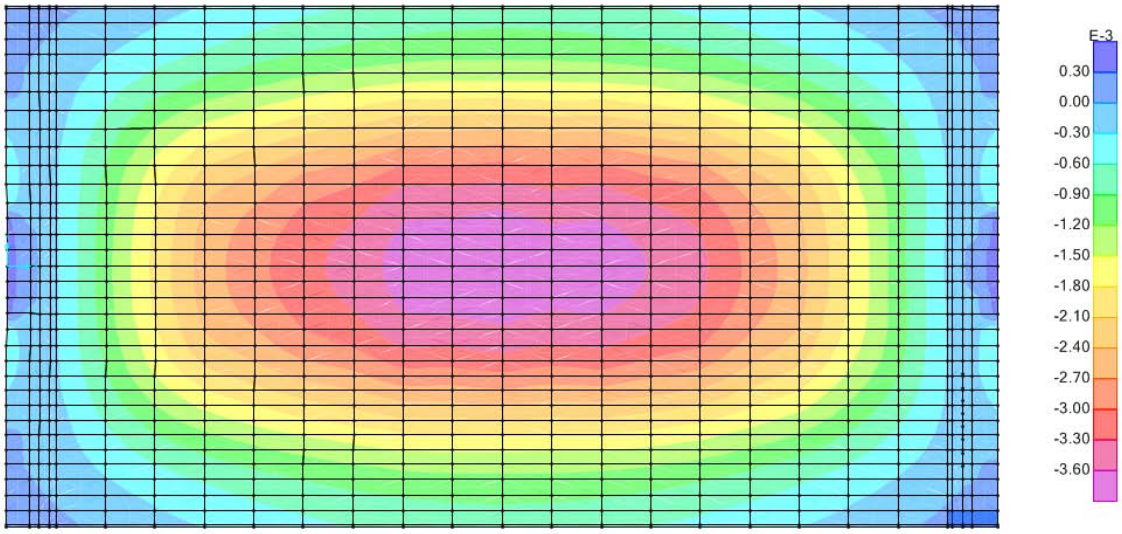

Type B: Speed 10 [m/sec]

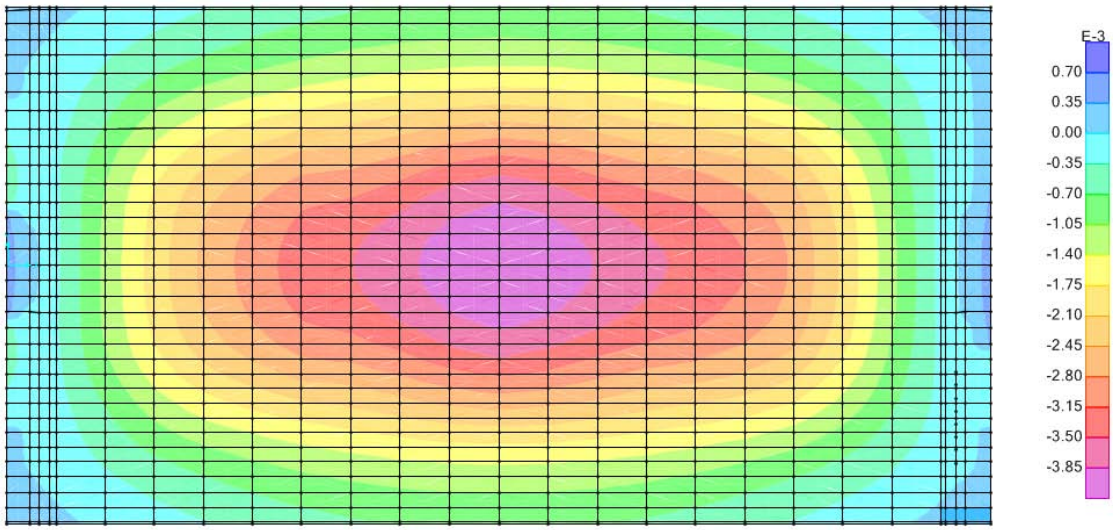

Type B: Speed 20 [m/sec]

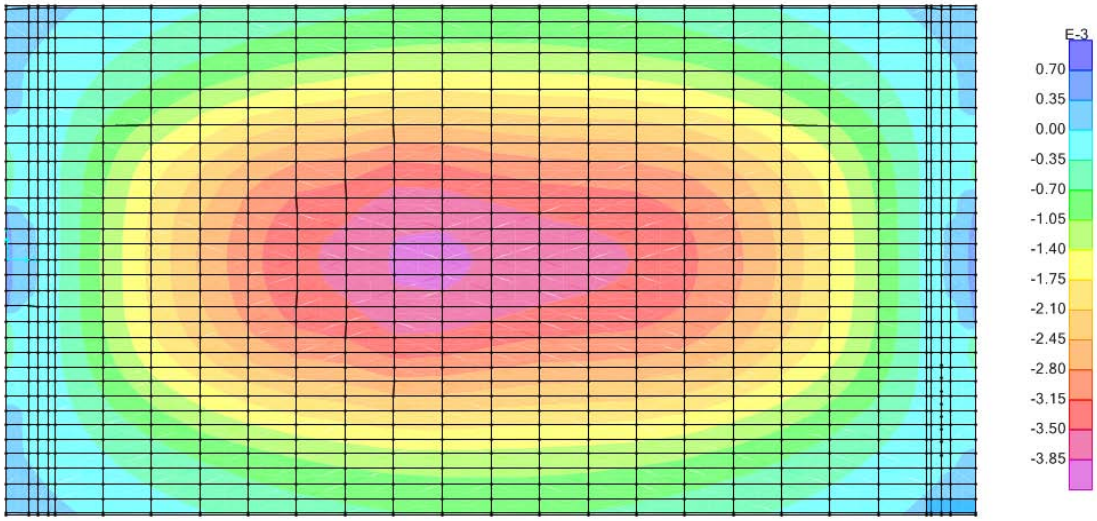

Type B: Speed 30 [m/sec]

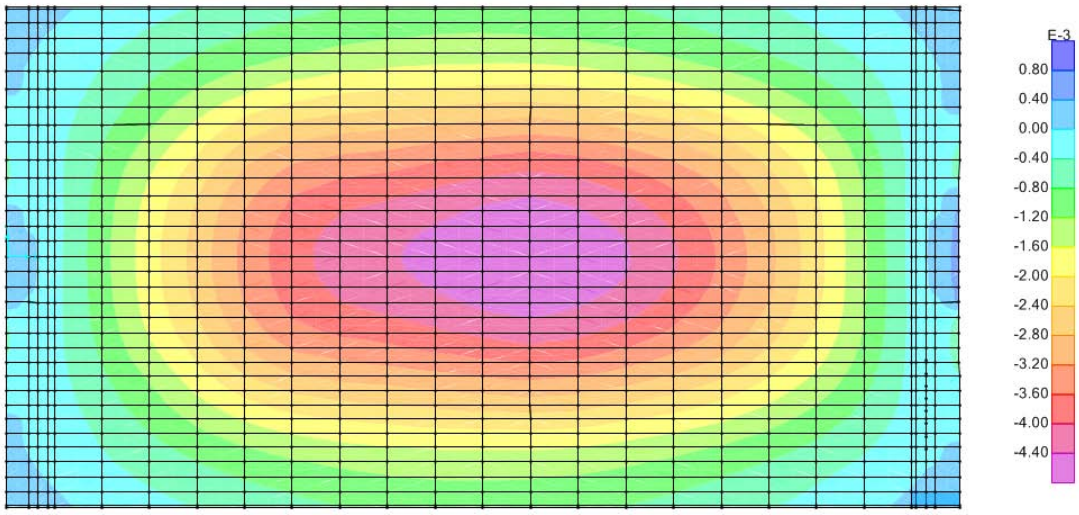

Type B: Speed 40 [m/sec]

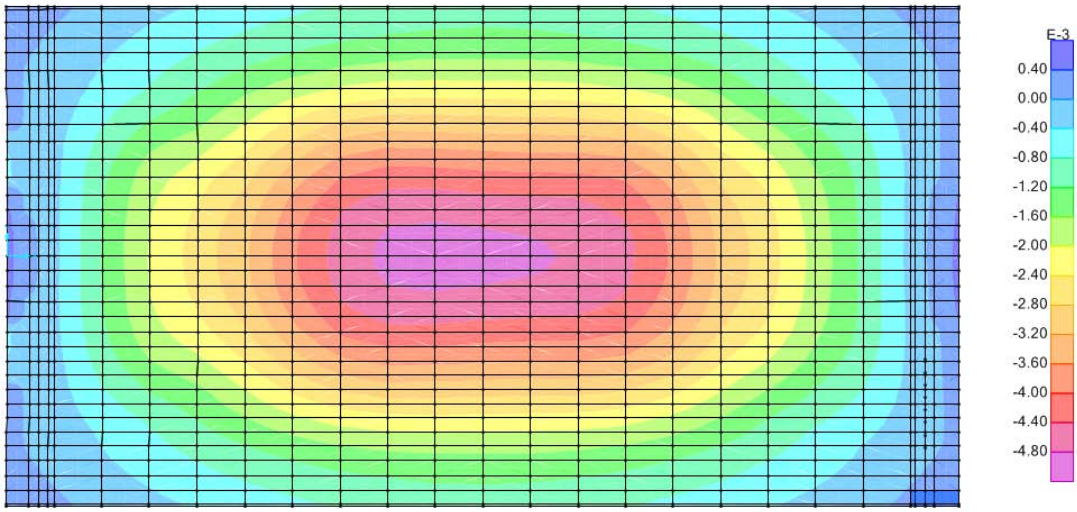

Type B: Speed 46 [m/sec]

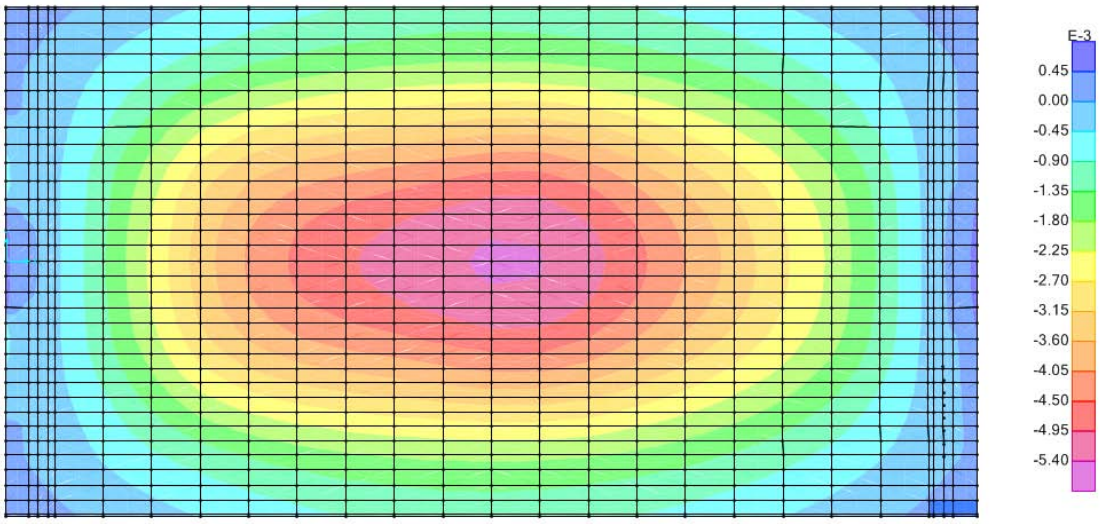

Type B: Speed 53 [m/sec]

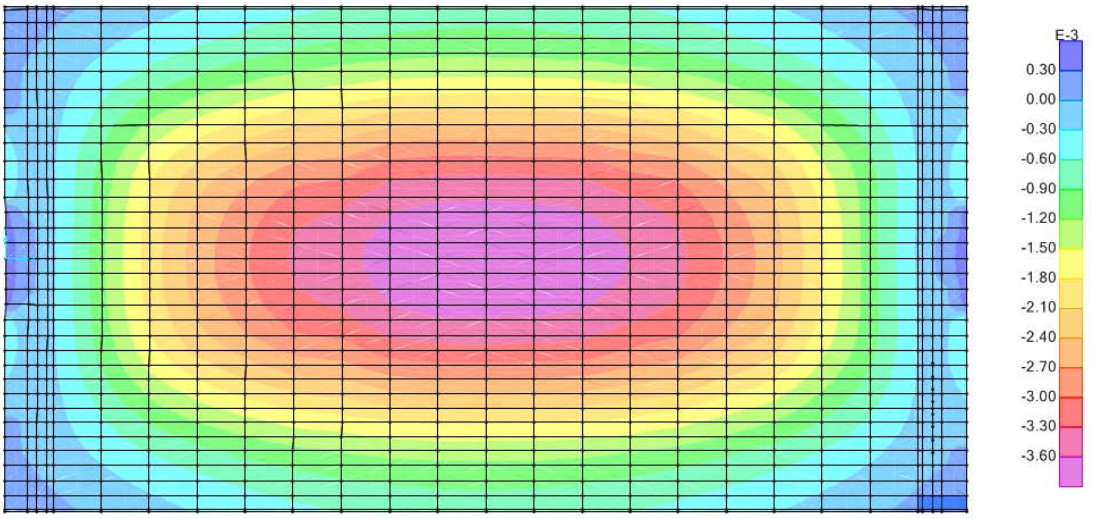

Type C: Speed 10 [m/sec]

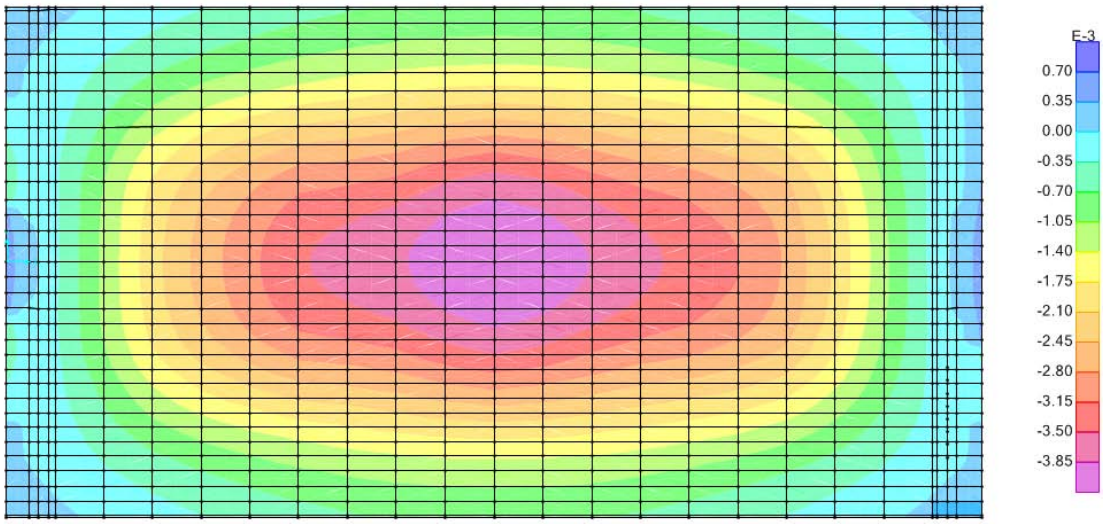

Type C: Speed 20 [m/sec]

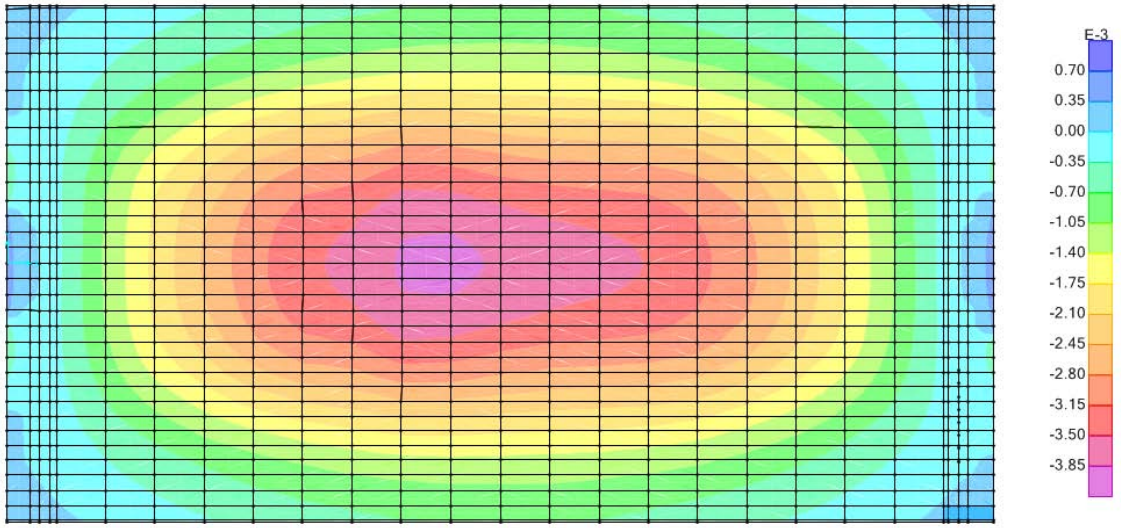

Type C: Speed 30 [m/sec]

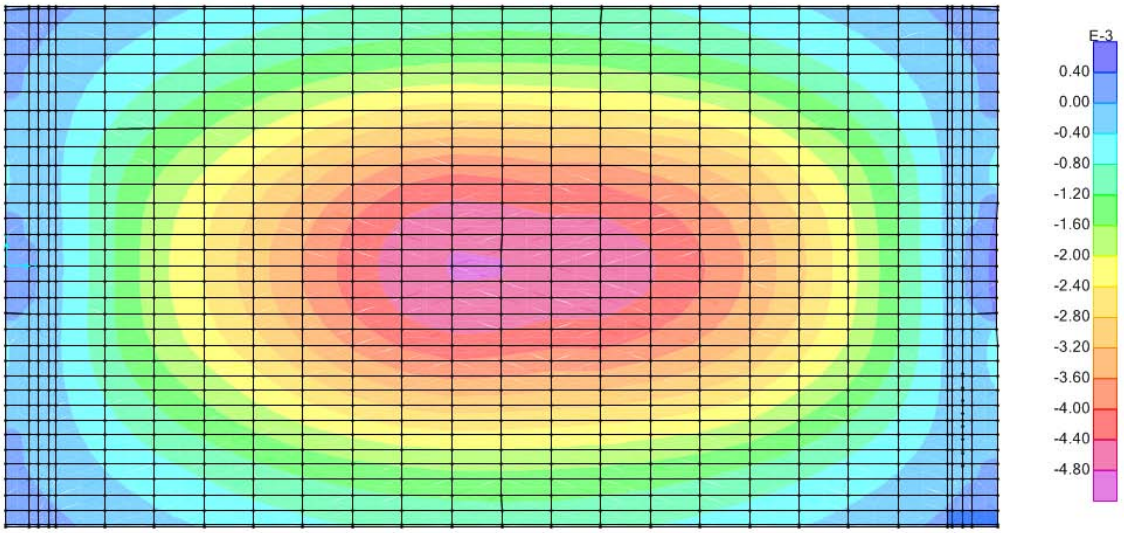

Type C: Speed 40 [m/sec]

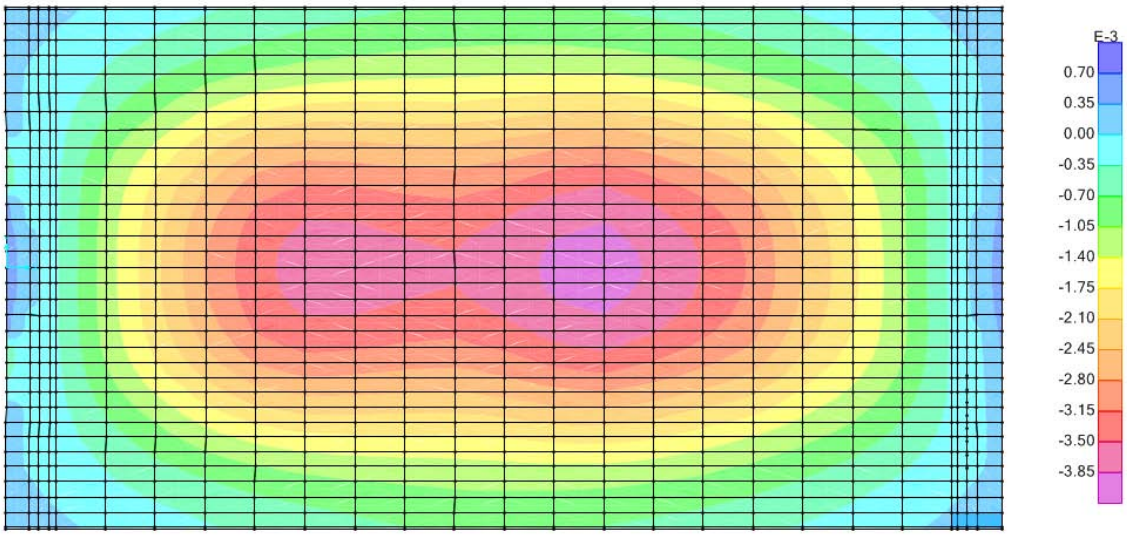

Type C: Speed 46 [m/sec]

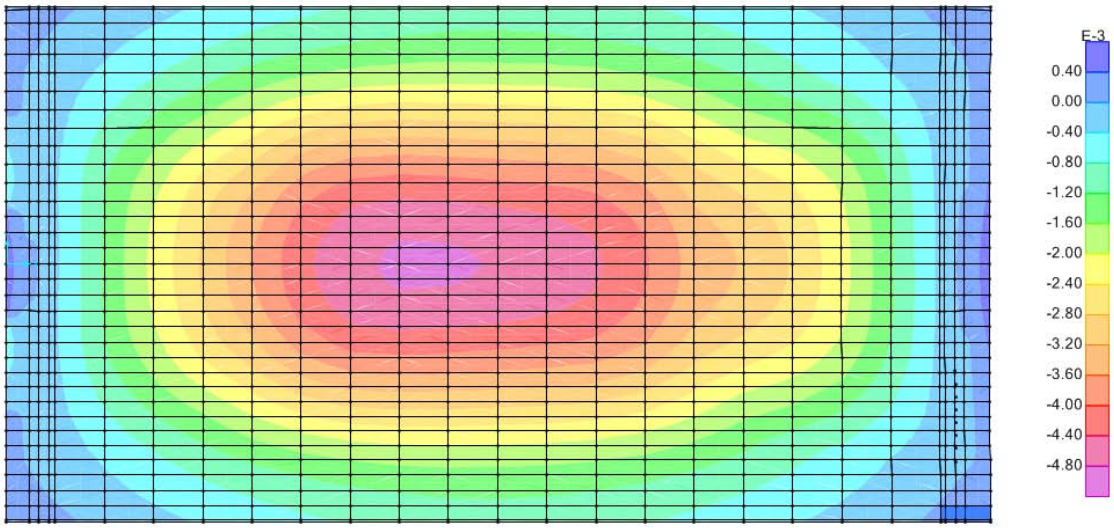

Type C: Speed 53 [m/sec]

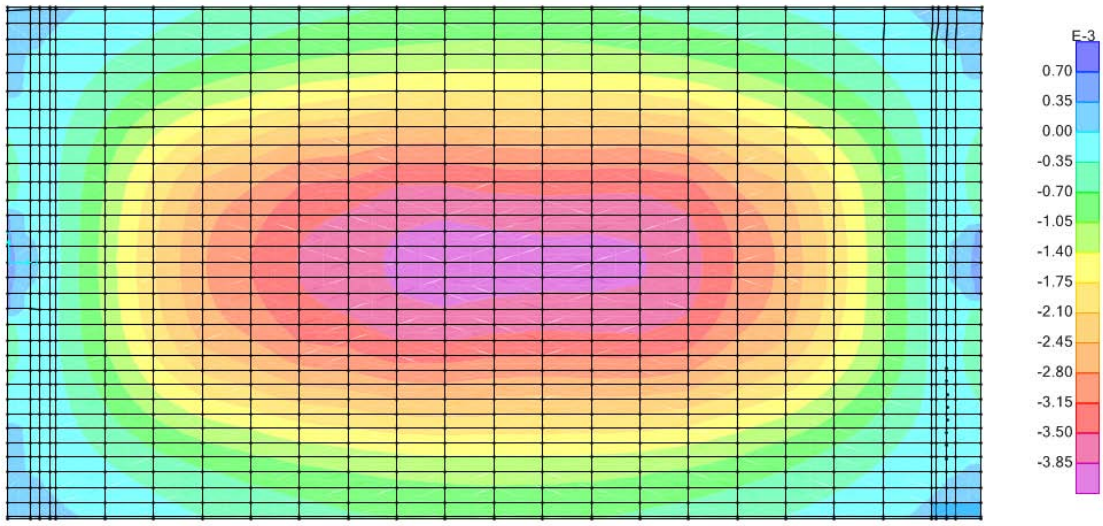

Type D: Speed 10 [m/sec]

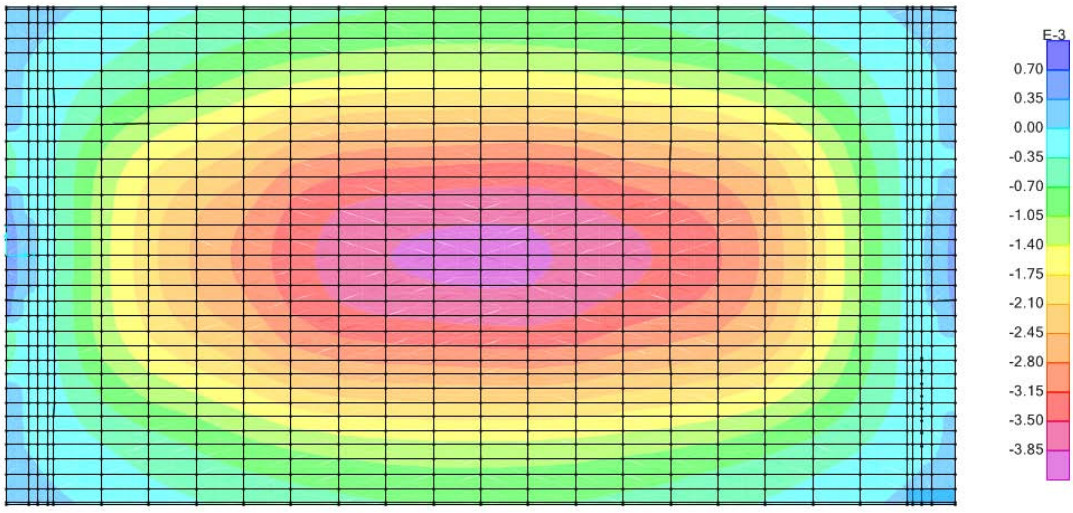

Type D: Speed 20 [m/sec]

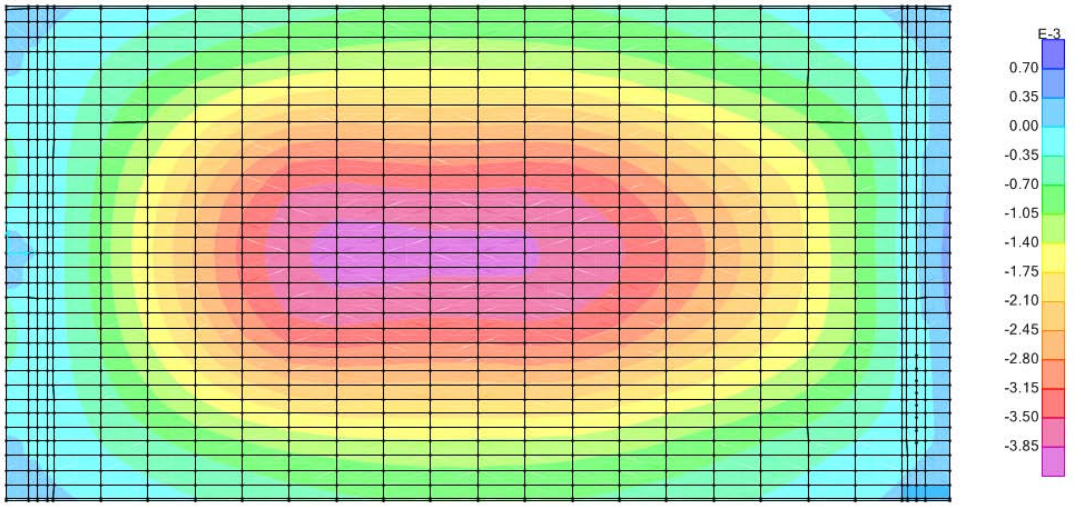

Type D: Speed 30 [m/sec]

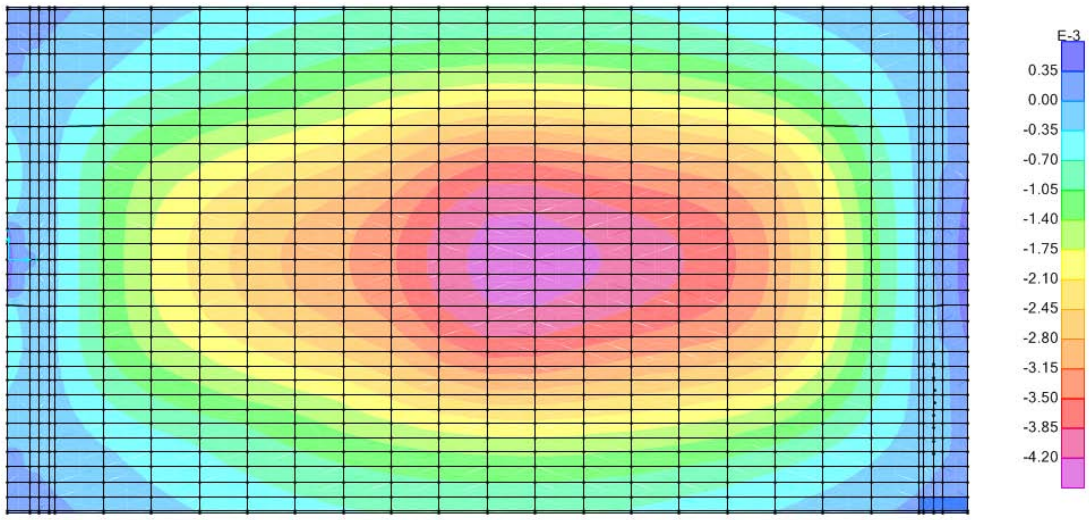

Type D: Speed 40 [m/sec]

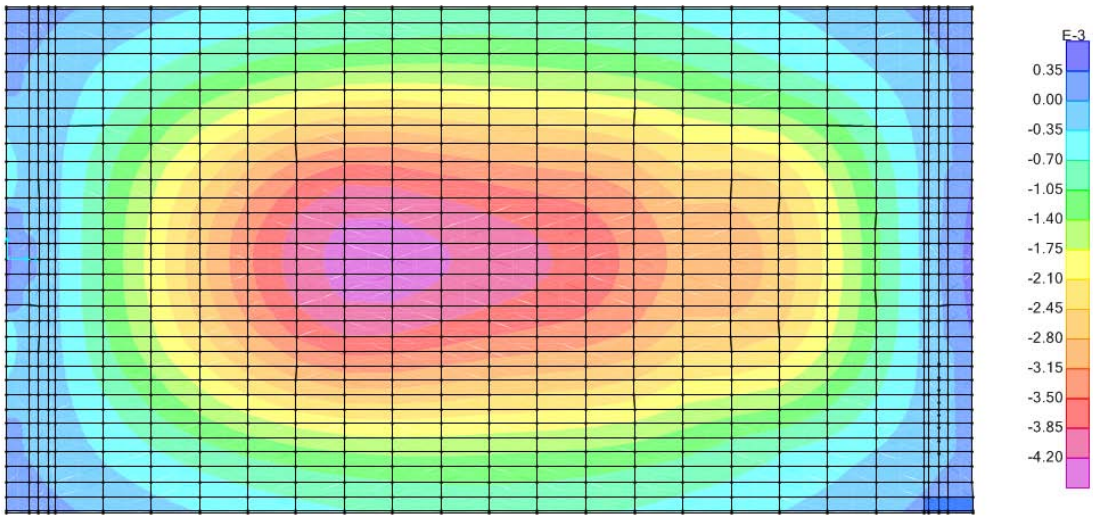

Type D: Speed 46 [m/sec]

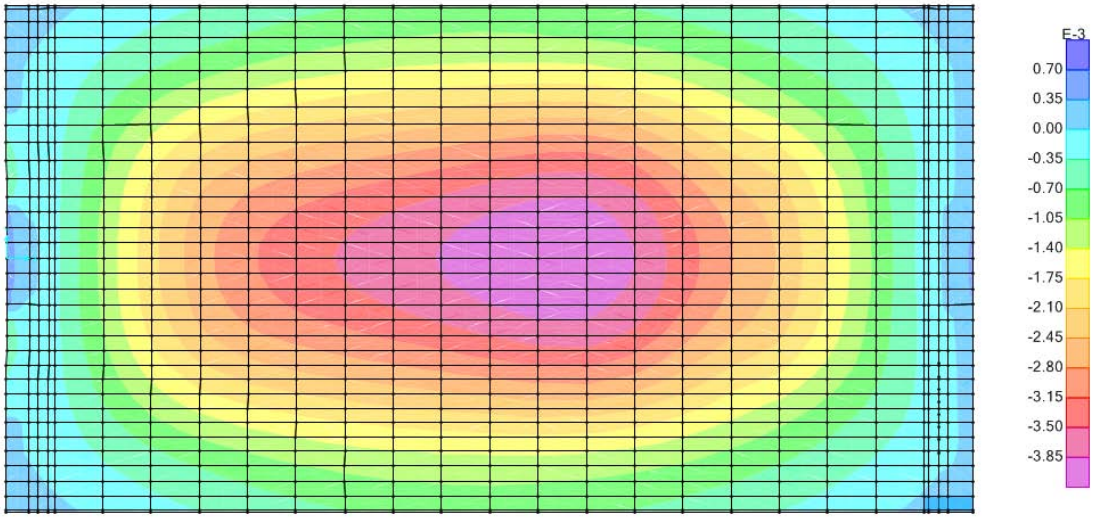

Type D: Speed 53 [m/sec]

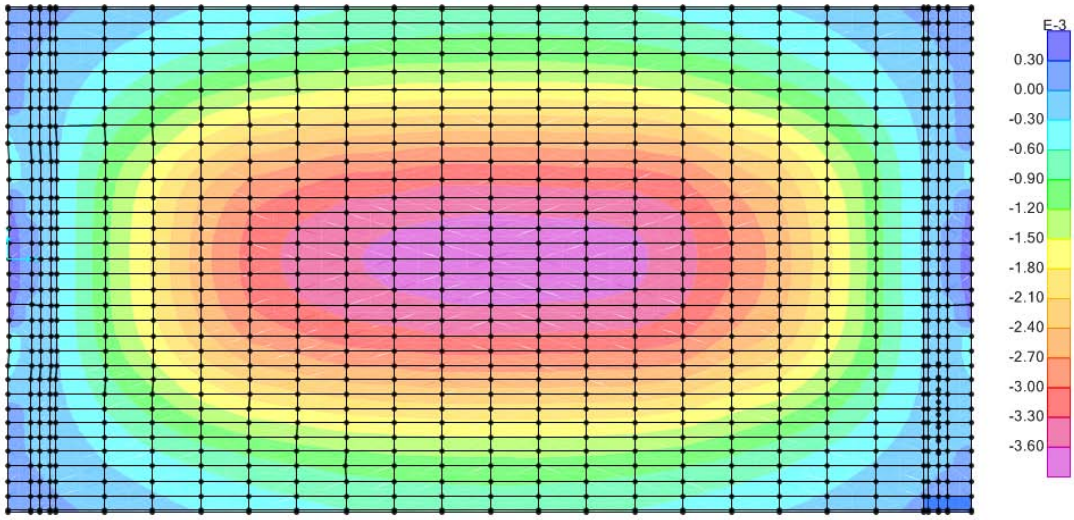

Type E: Speed 10 [m/sec]

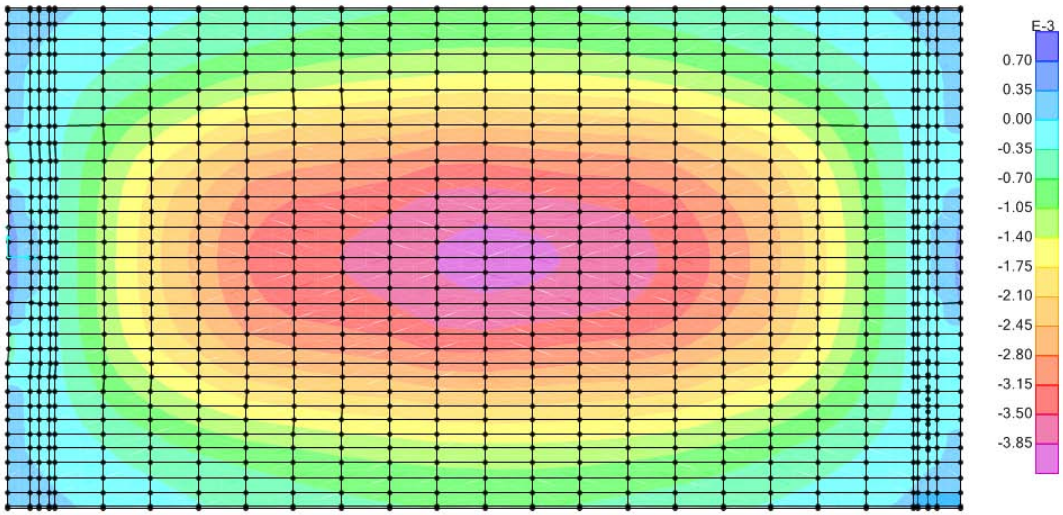

Type E: Speed 20 [m/sec]

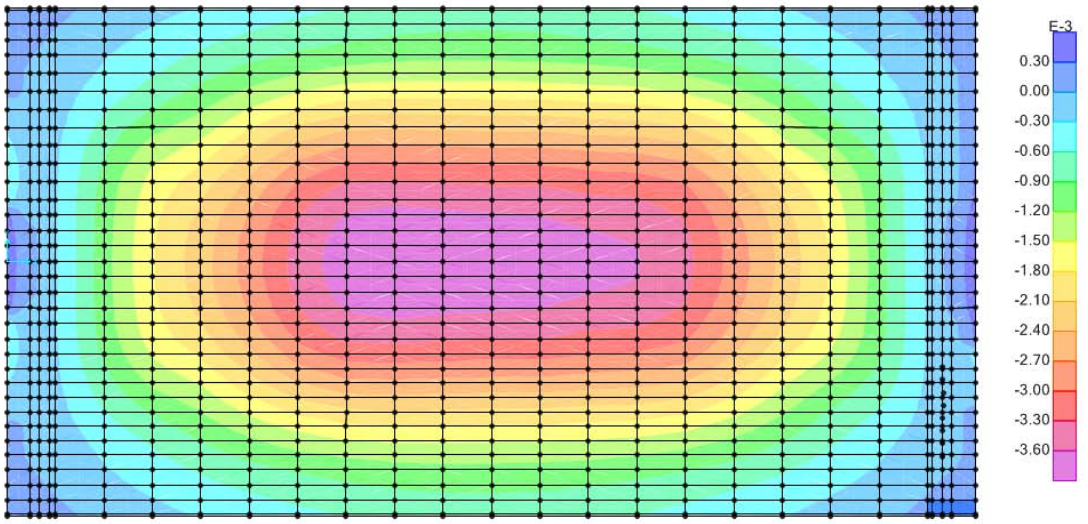

Type E: Speed 30 [m/sec]

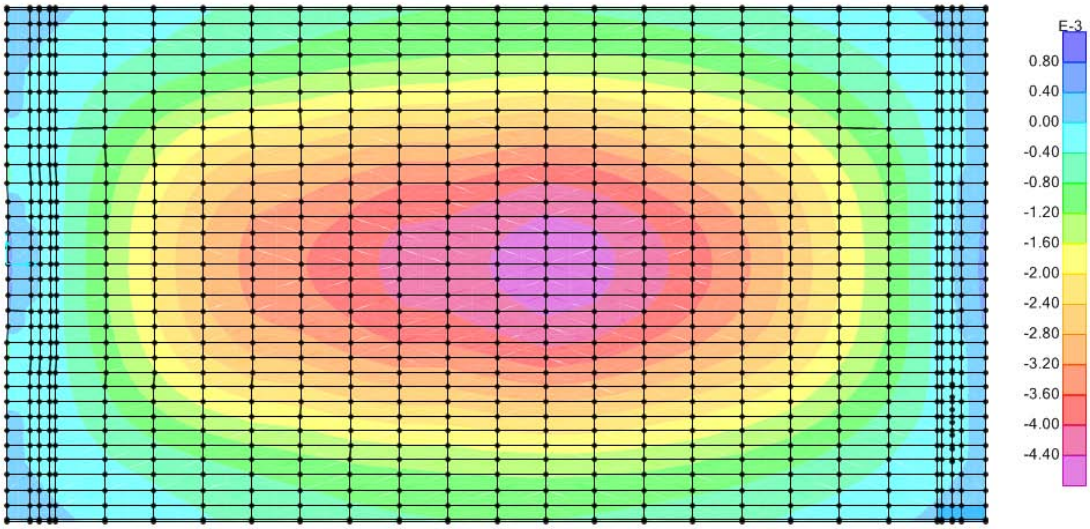

Type E: Speed 40 [m/sec]

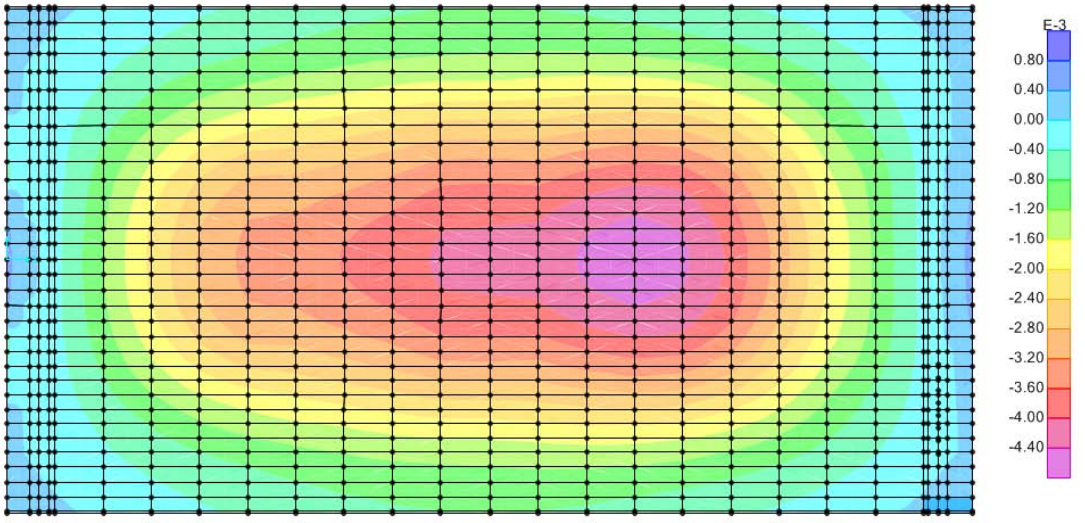

Type E: Speed 46 [m/sec]

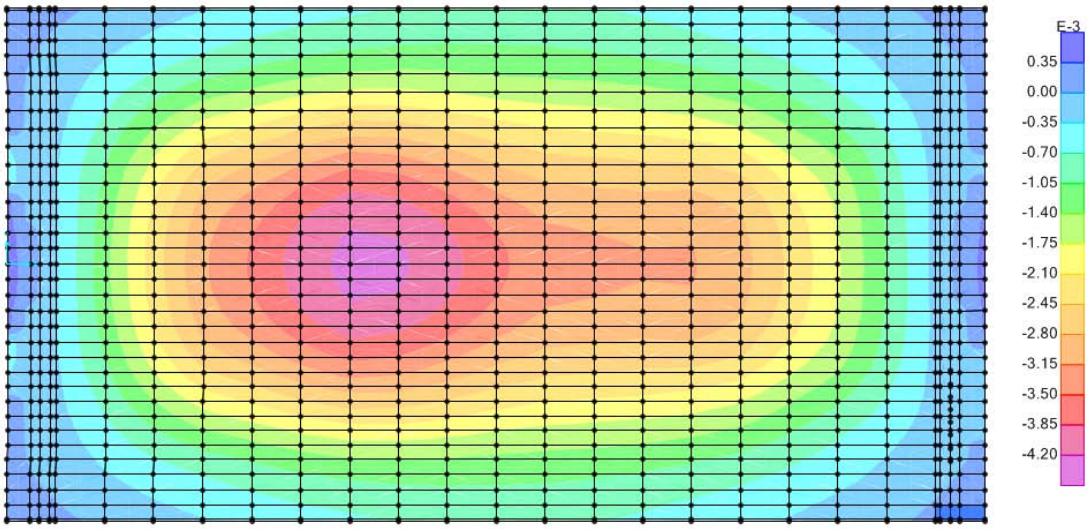

Type E: Speed 53 [m/sec]

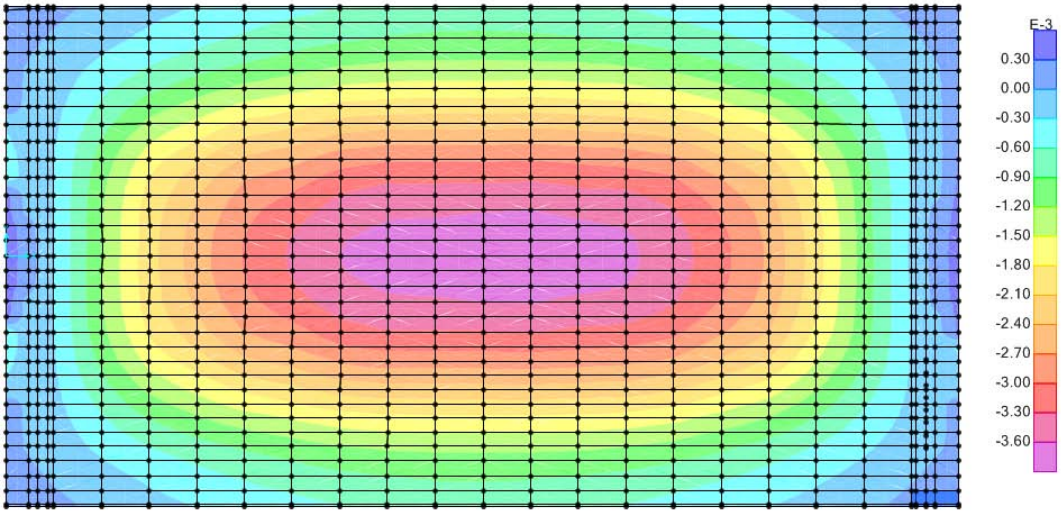

Type F: Speed 10 [m/sec]

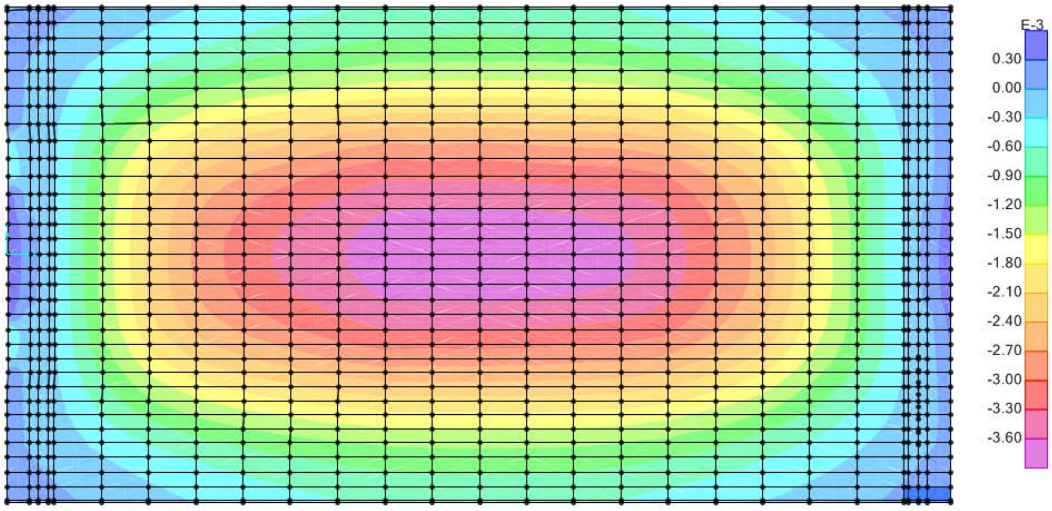

Type F: Speed 20 [m/sec]

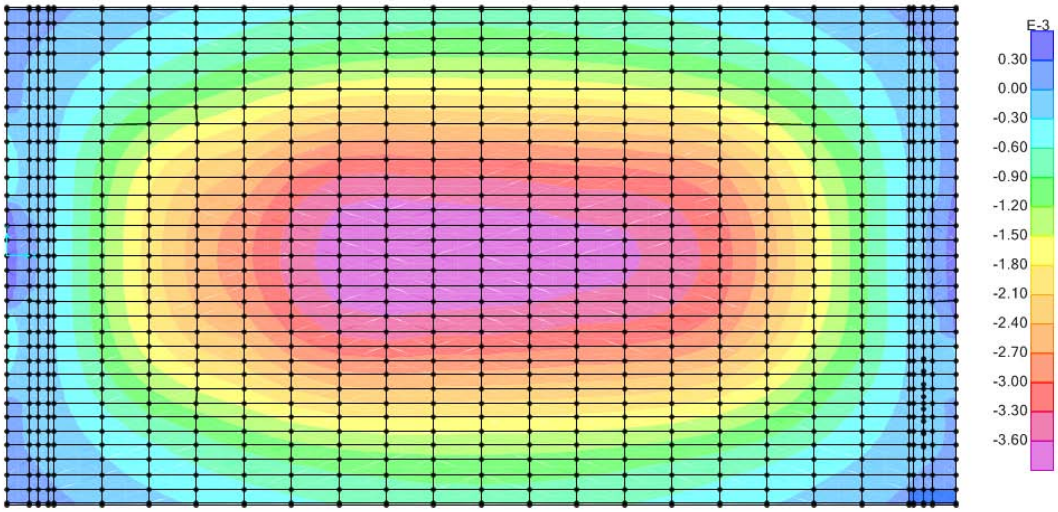

Type F: Speed 30 [m/sec]

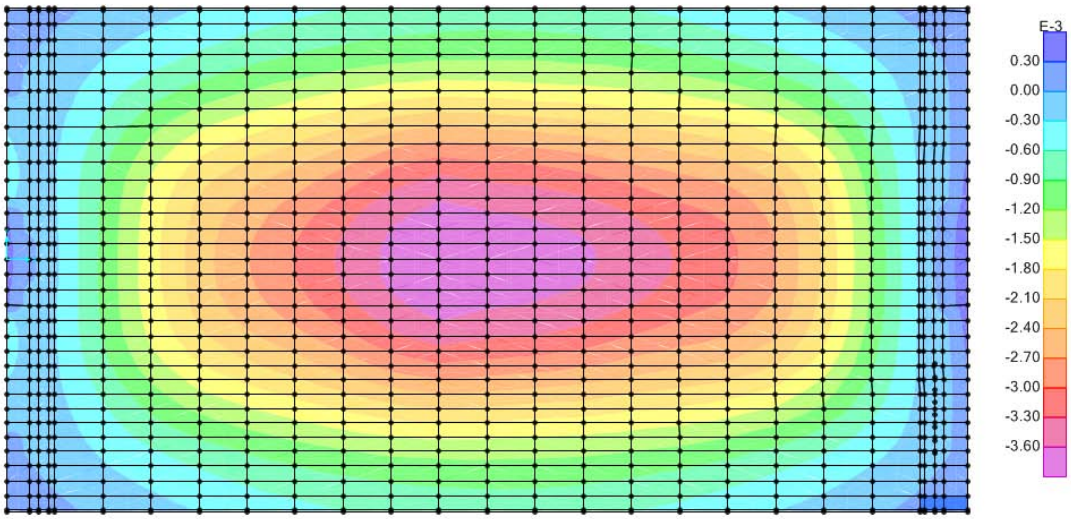

Type F: Speed 40 [m/sec]

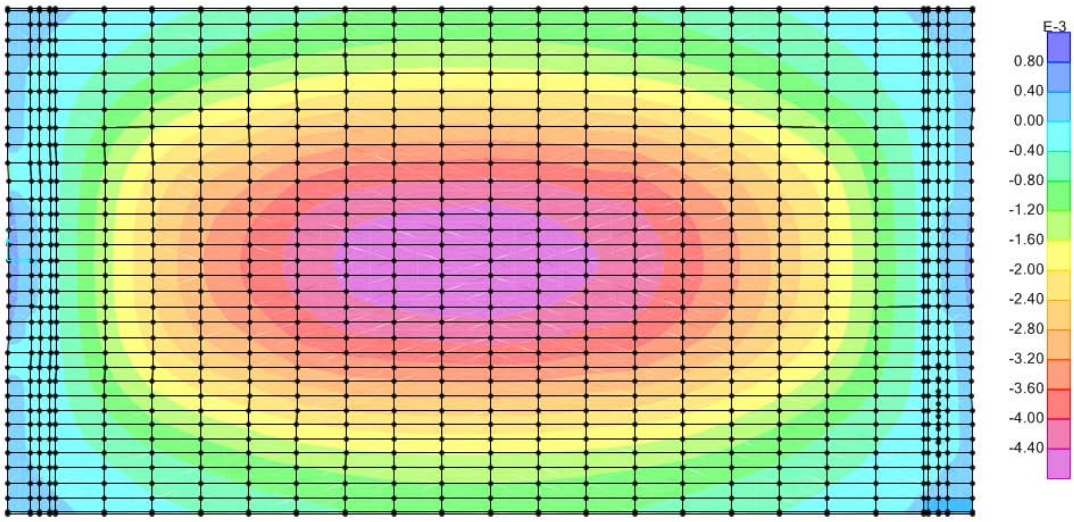

Type F: Speed 46 [m/sec]

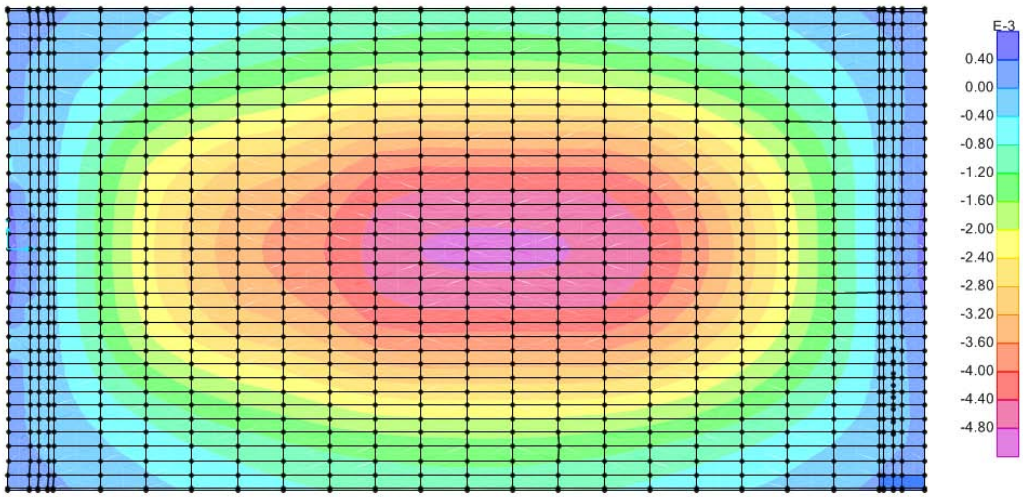

Type F: Speed 53 [m/sec]

9.2) Results for 3 Bearings – Cross End Slab structure:

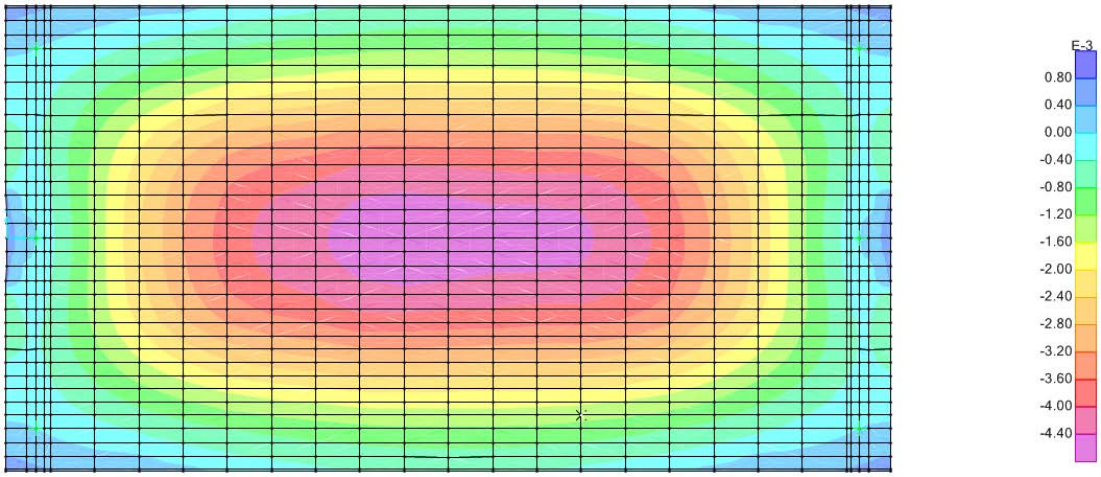

Type A: Speed 10 [m/sec]

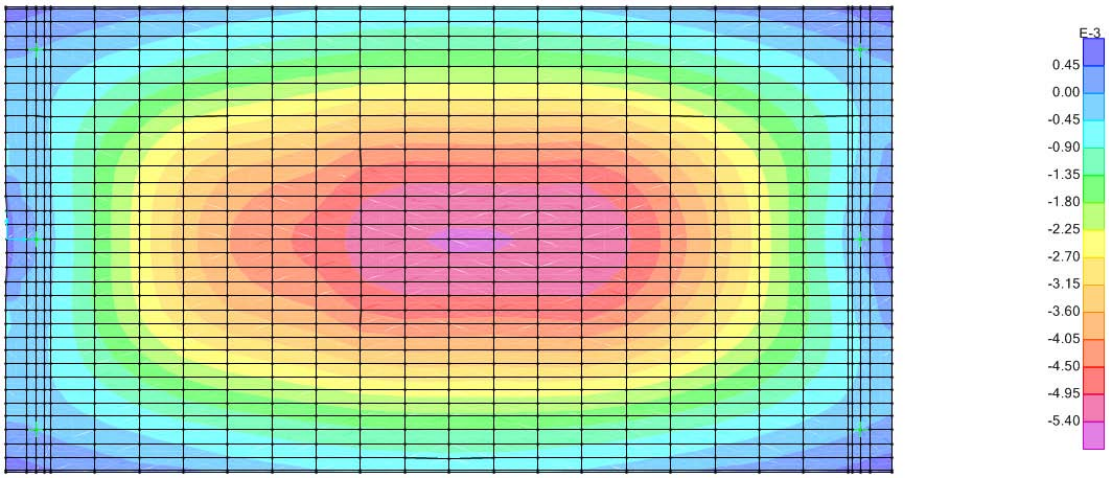

Type A: Speed 20 [m/sec]

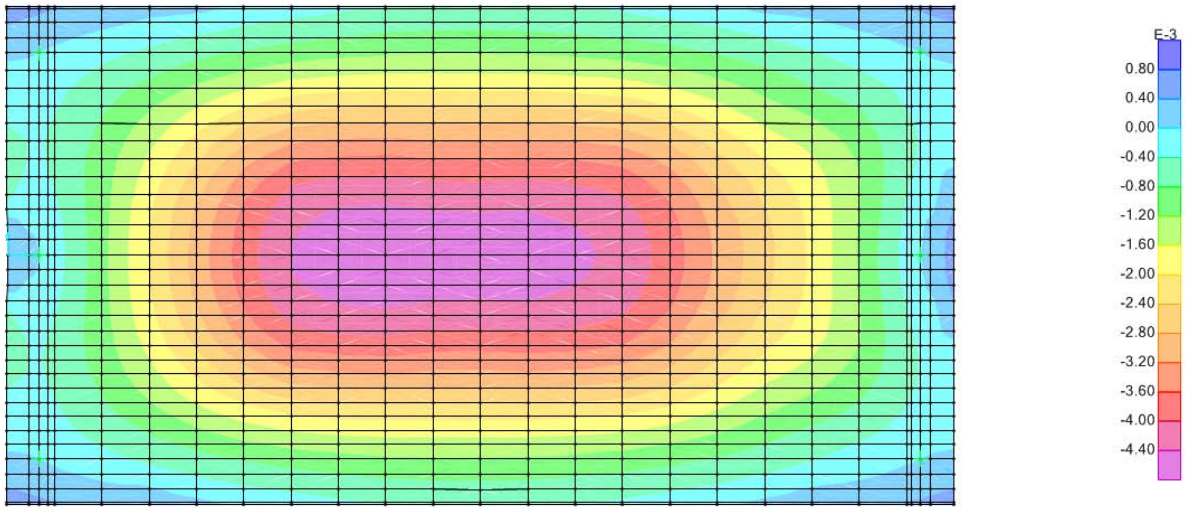

Type A: Speed 30 [m/sec]

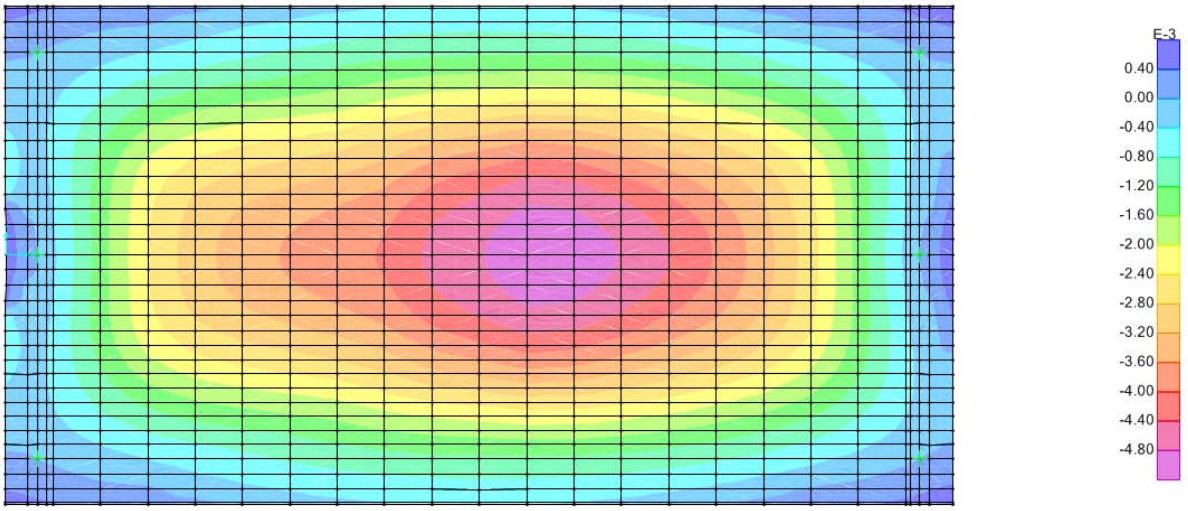

Type A: Speed 40 [m/sec]

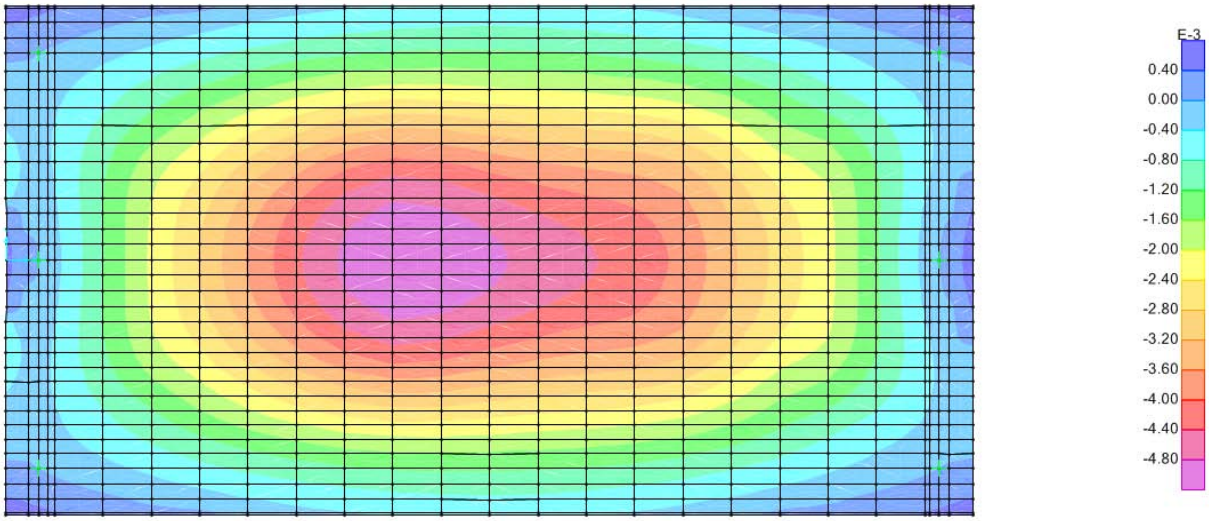

Type A: Speed 46 [m/sec]

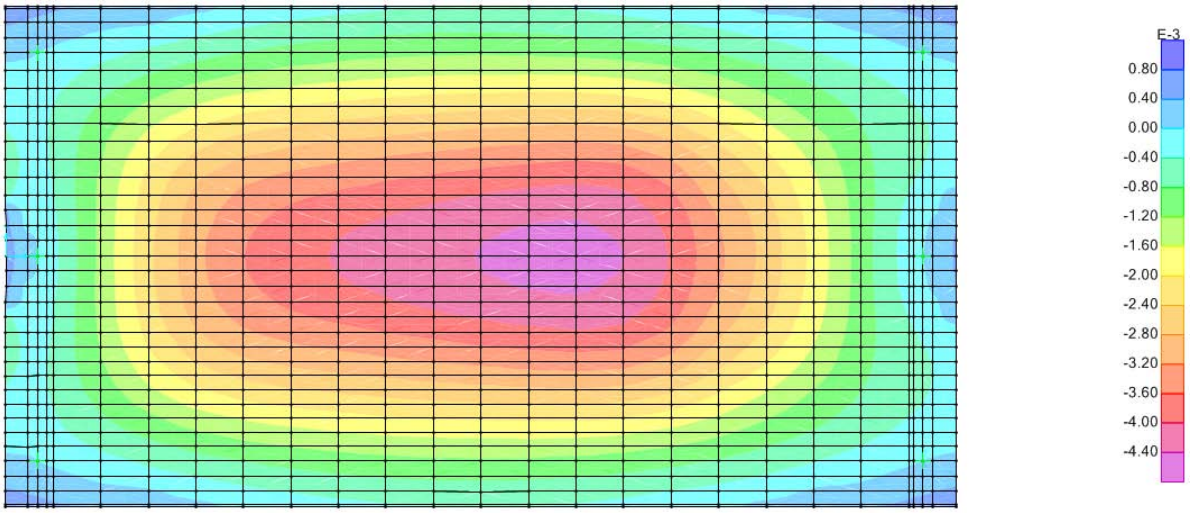

Type A: Speed 53 [m/sec]

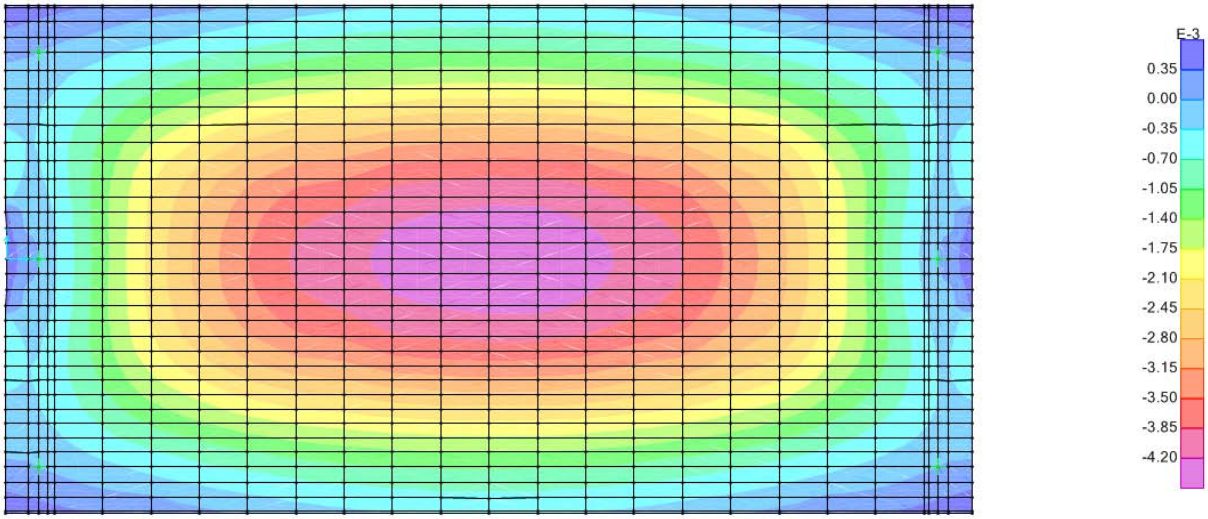

Type B: Speed 10 [m/sec]

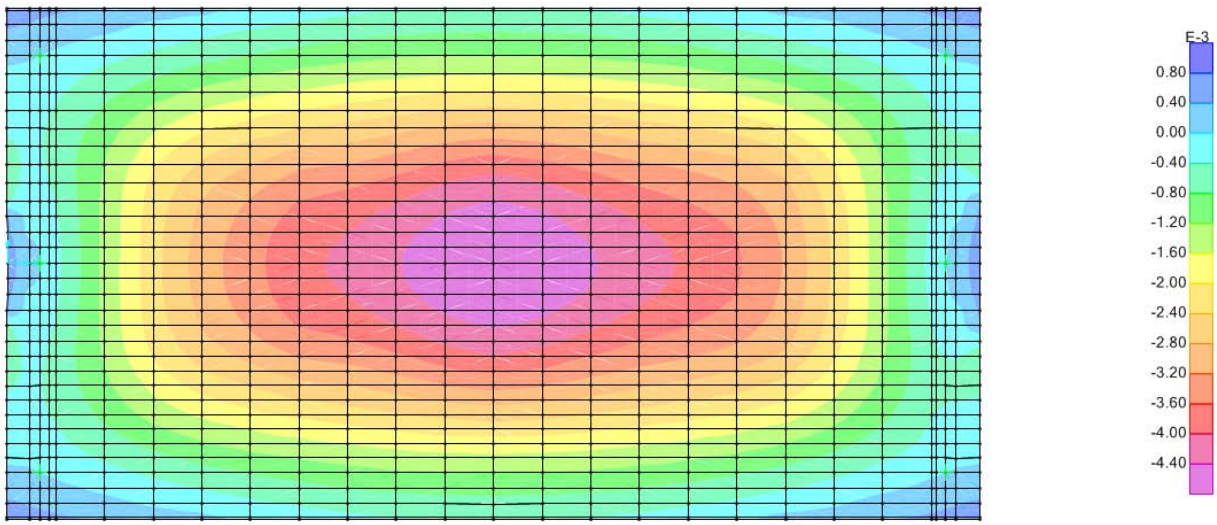

Type B: Speed 20 [m/sec]

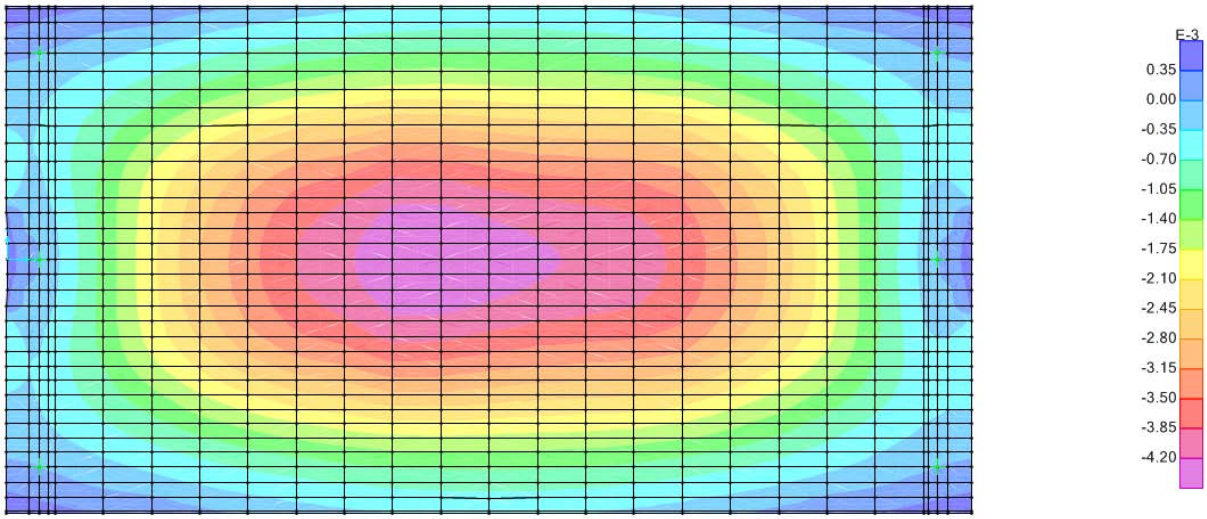

Type B: Speed 30 [m/sec]

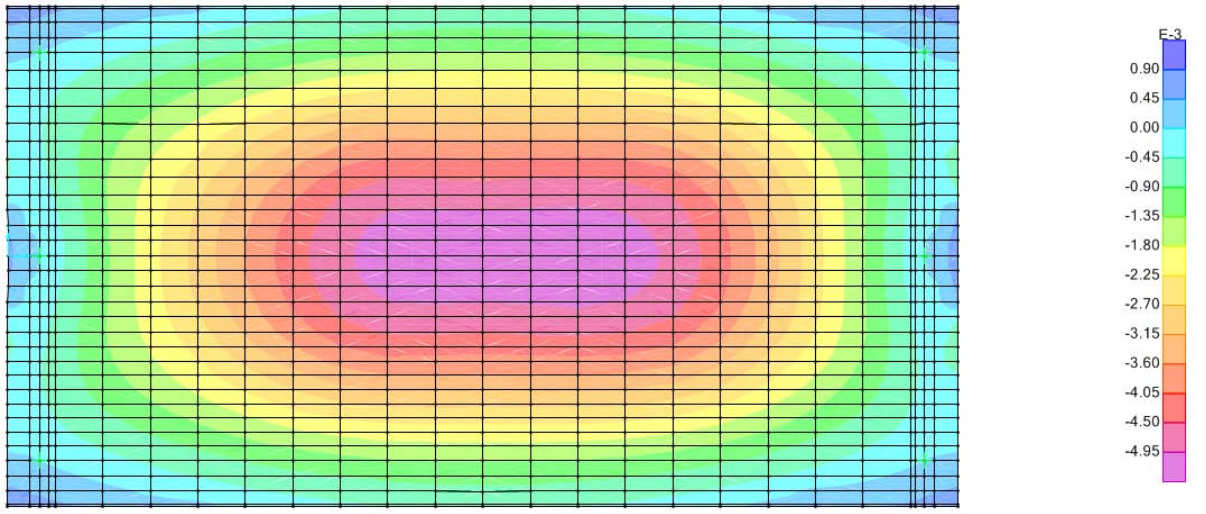

Type B: Speed 40 [m/sec]

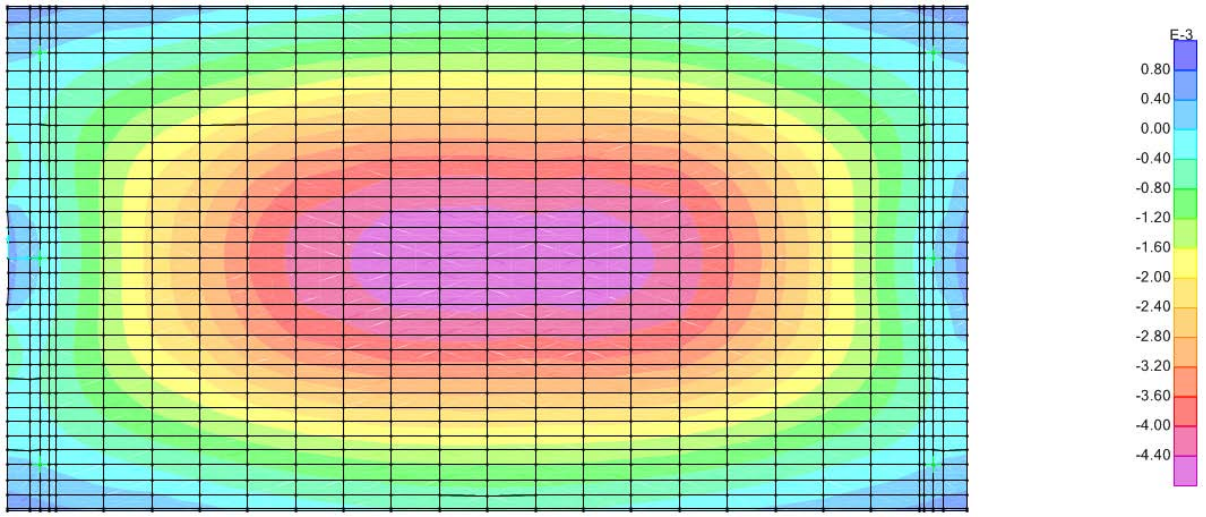

Type B: Speed 46 [m/sec]

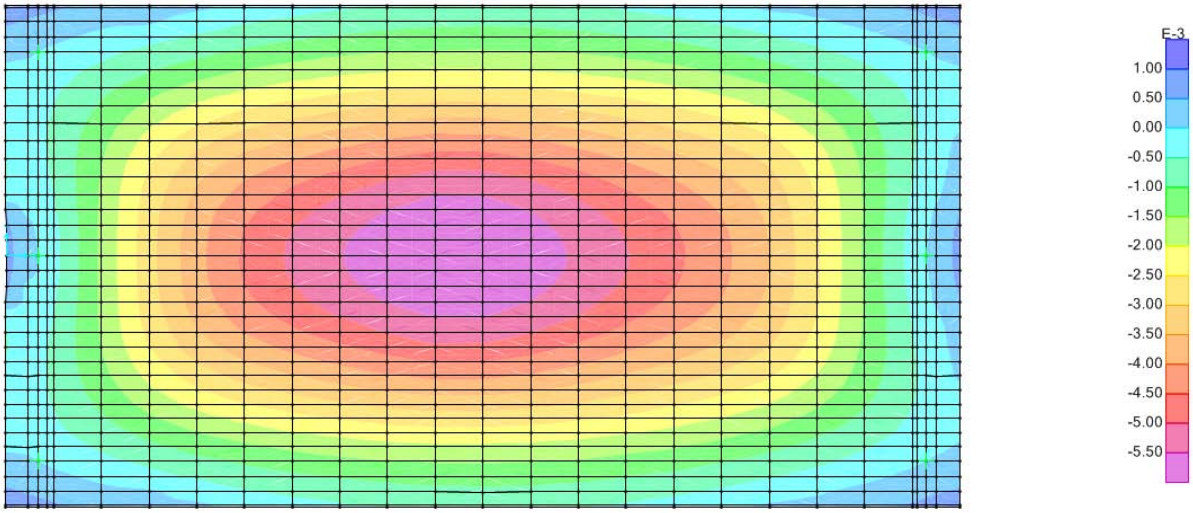

Type B: Speed 53 [m/sec]

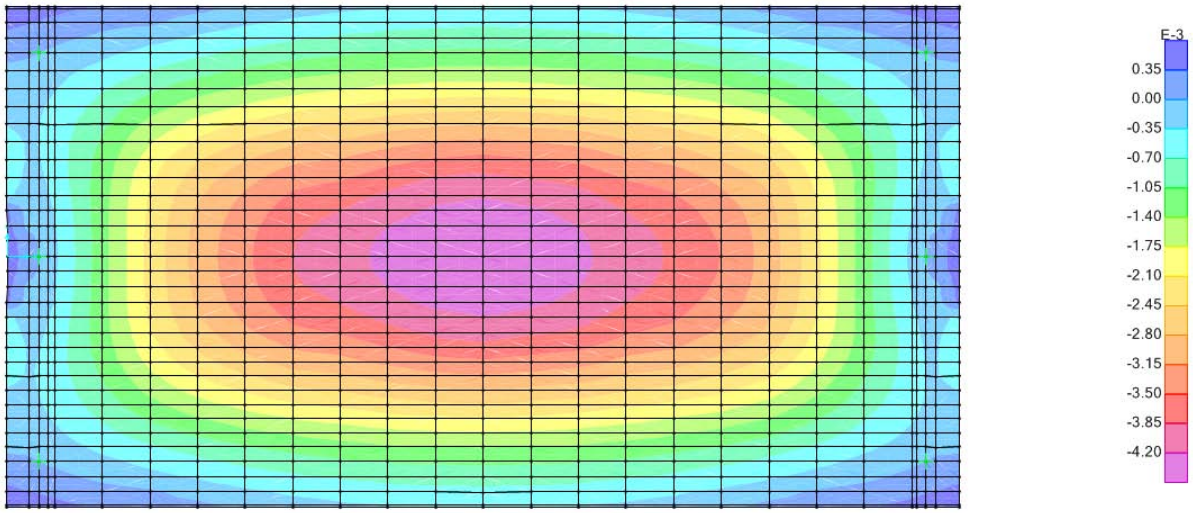

Type C: Speed 10 [m/sec]

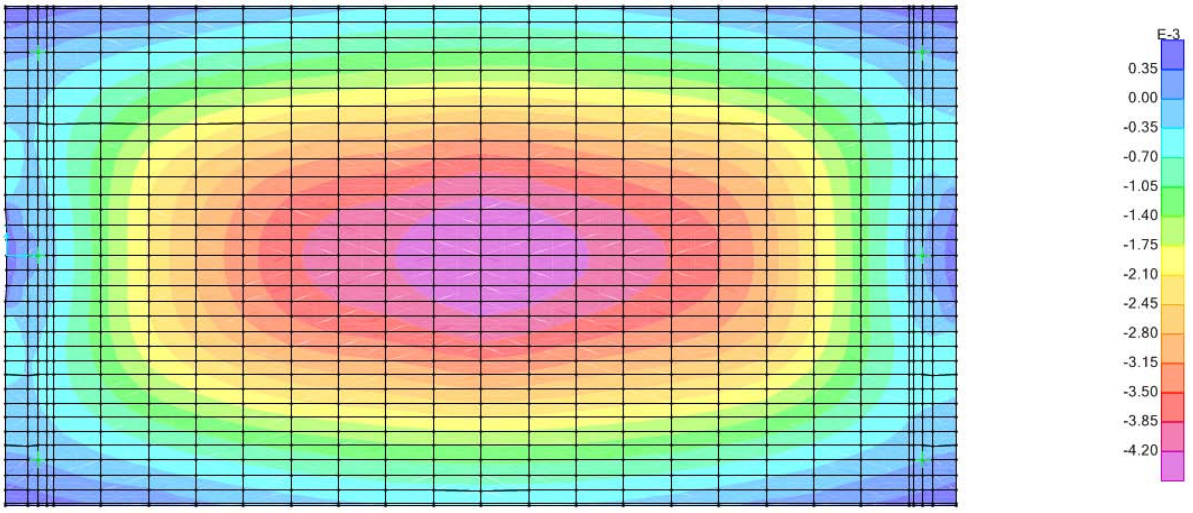

Type C: Speed 20 [m/sec]

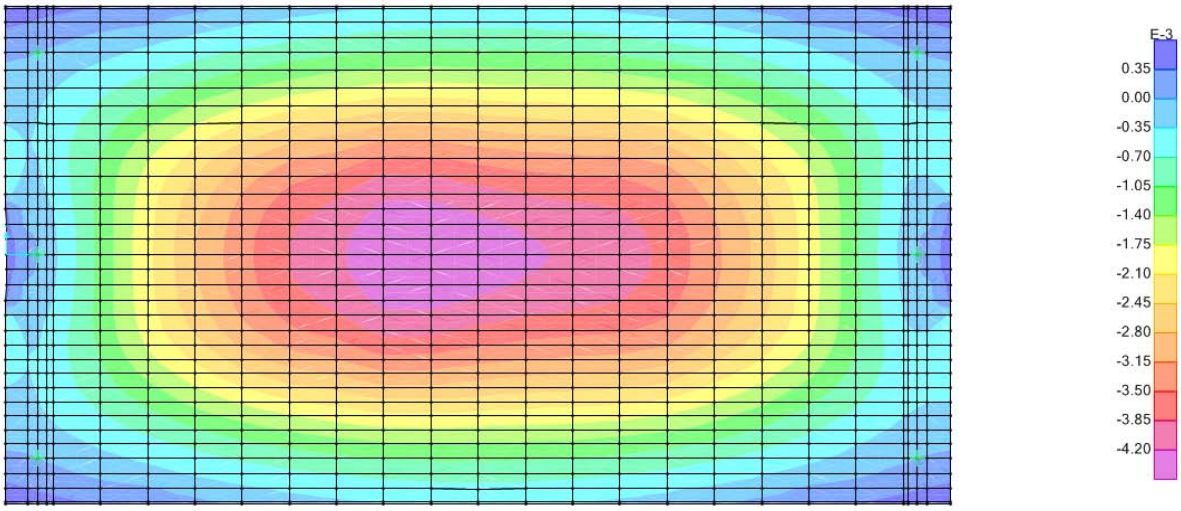

Type C: Speed 30 [m/sec]

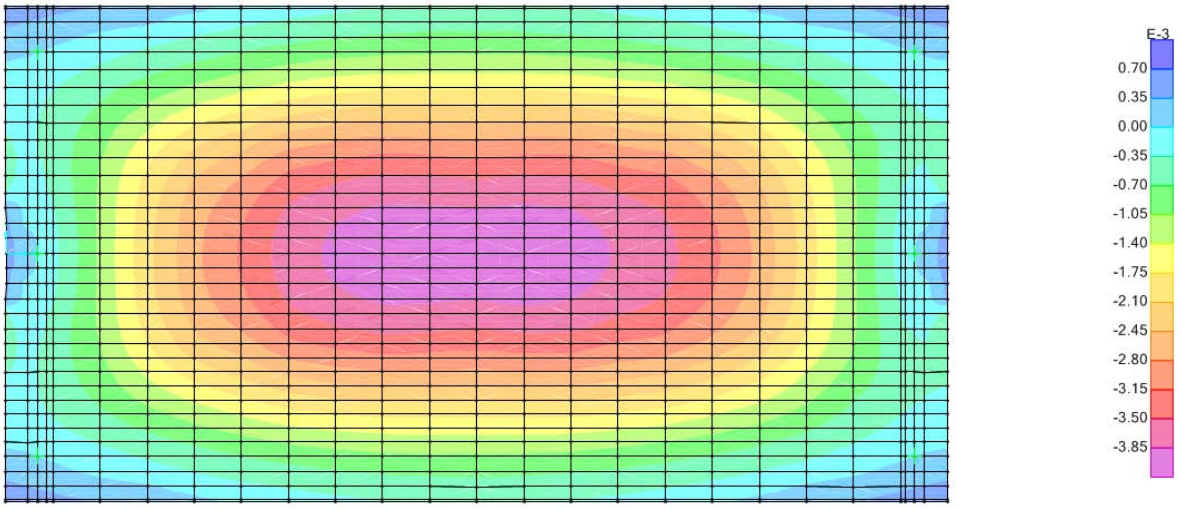

Type C: Speed 40 [m/sec]

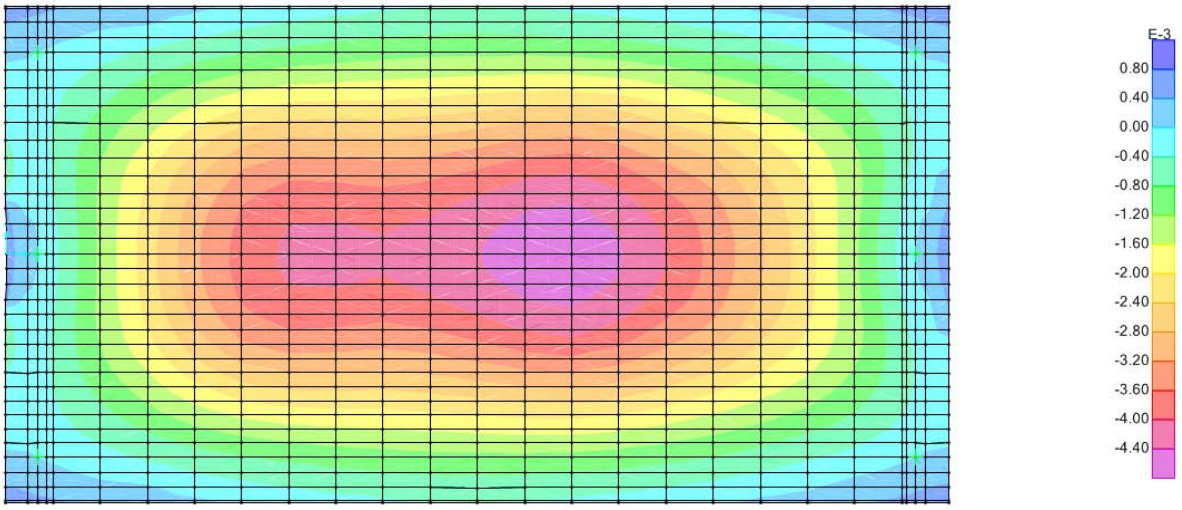

Type C: Speed 46 [m/sec]

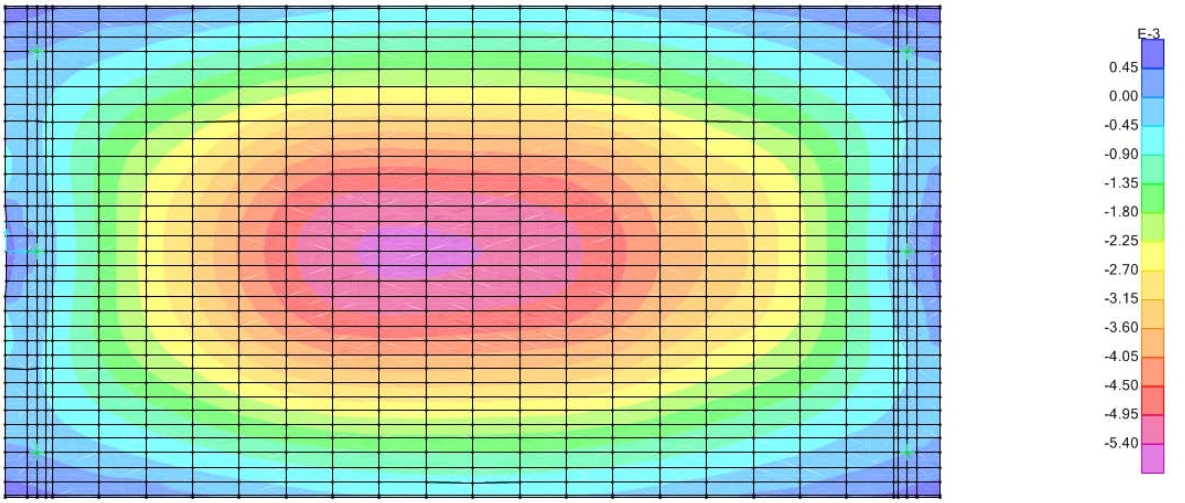

Type C: Speed 53 [m/sec]

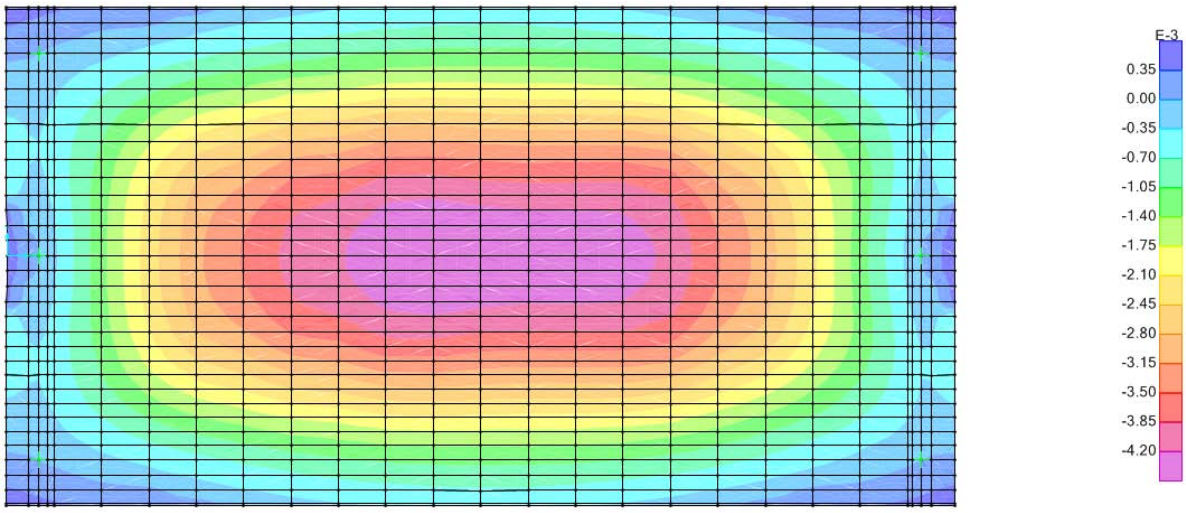

Type D: Speed 10 [m/sec]

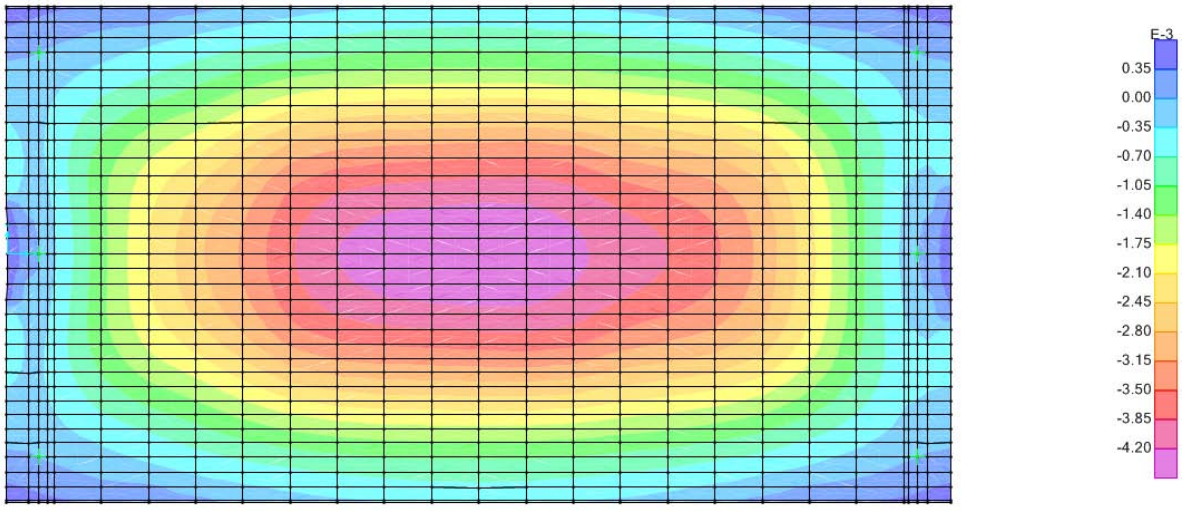

Type D: Speed 20 [m/sec]

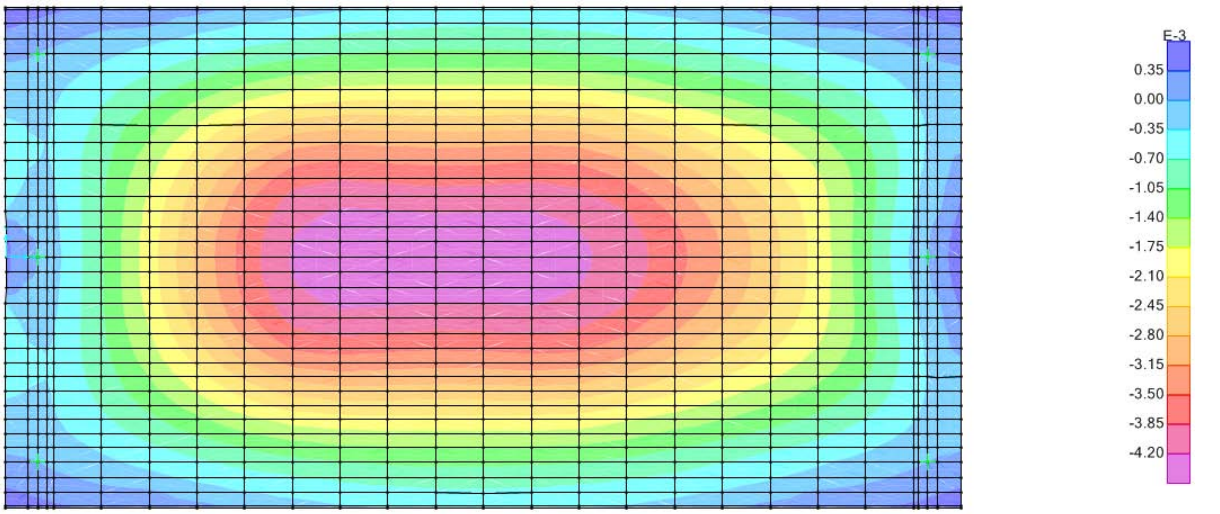

Type D: Speed 30 [m/sec]

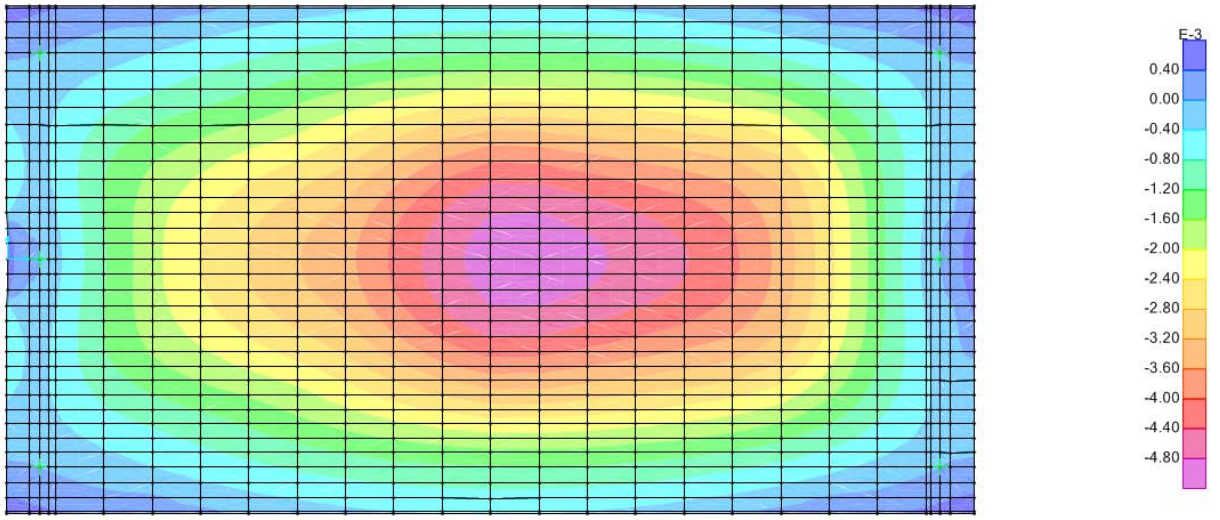

Type D: Speed 40 [m/sec]

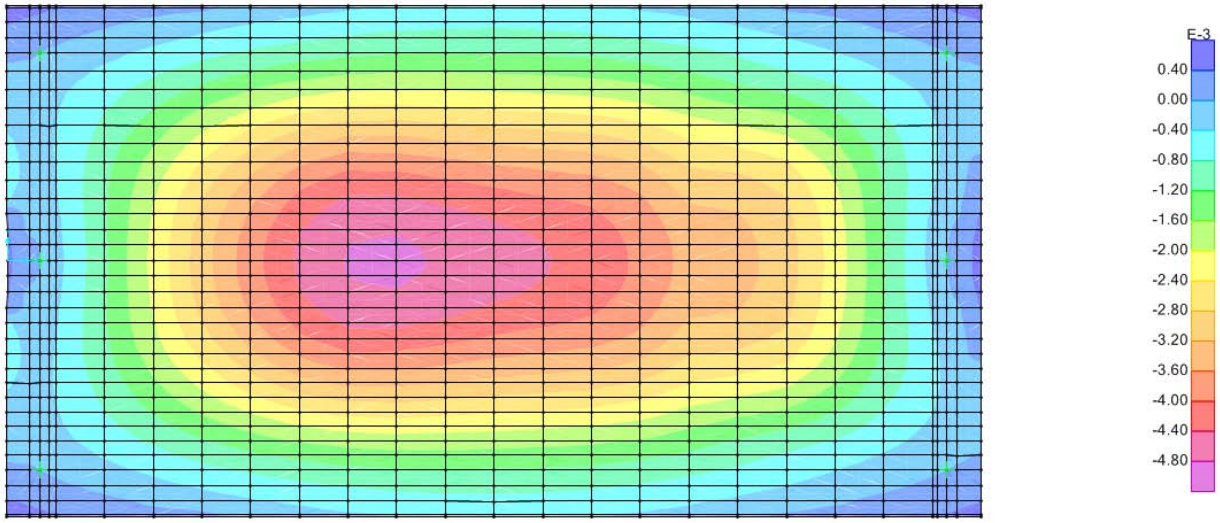

Type D: Speed 46 [m/sec]

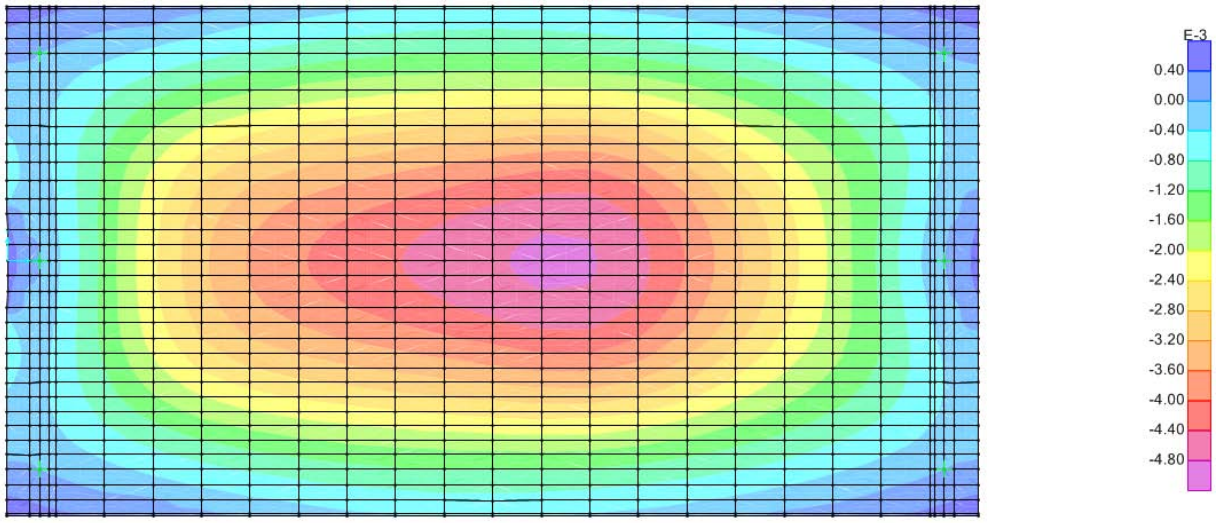

Type D: Speed 53 [m/sec]

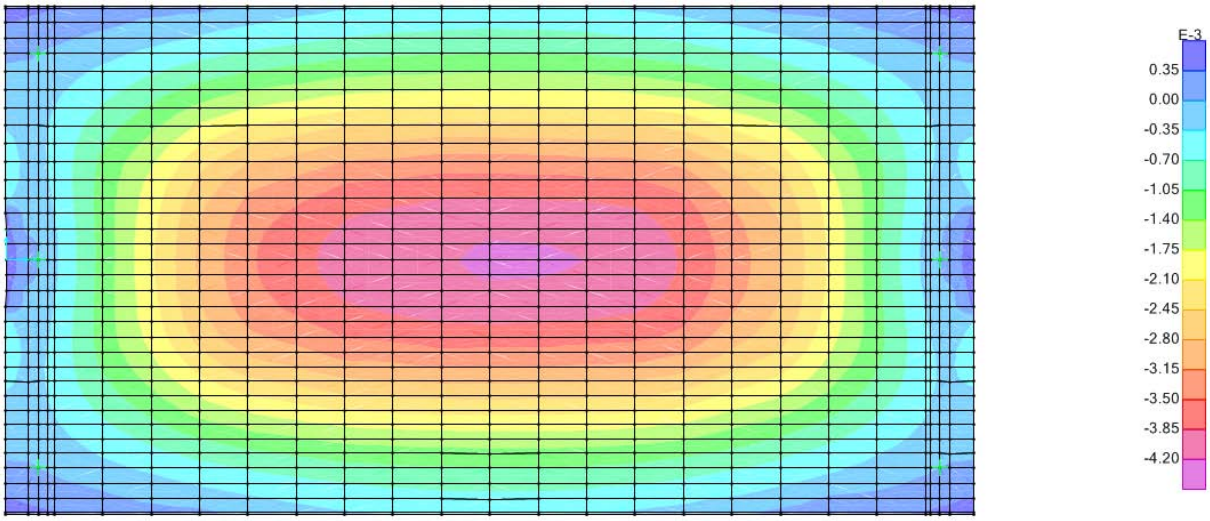

Type E: Speed 10 [m/sec]

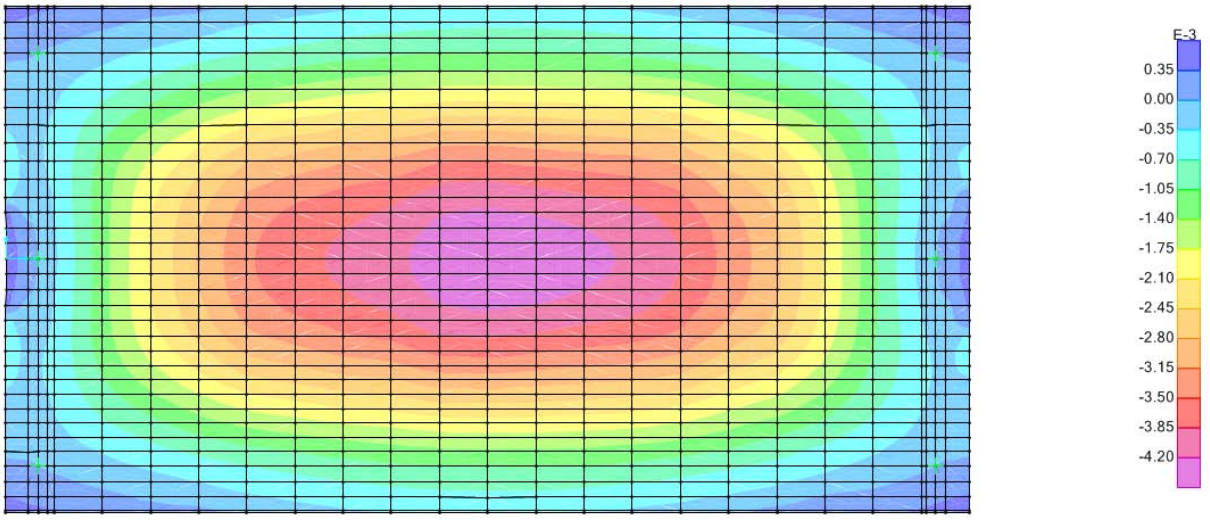

Type E: Speed 20 [m/sec]

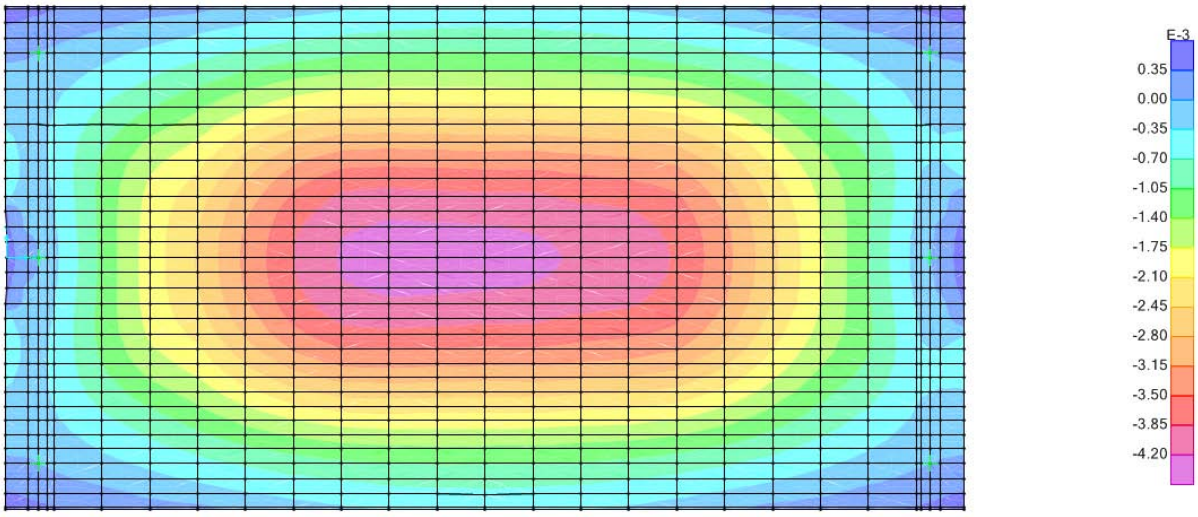

Type E: Speed 30 [m/sec]

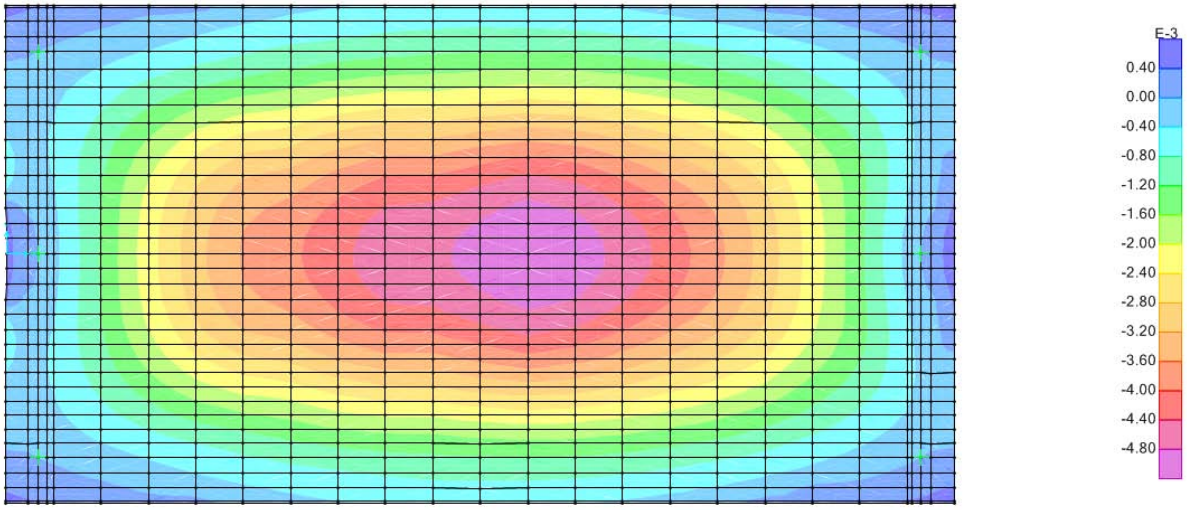

Type E: Speed 40 [m/sec]

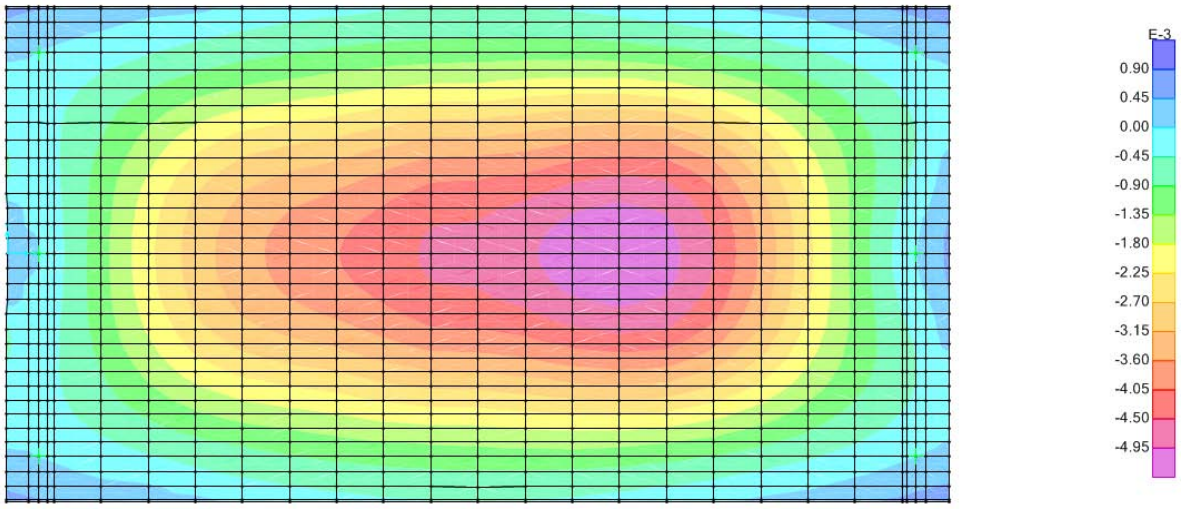

Type E: Speed 46 [m/sec]

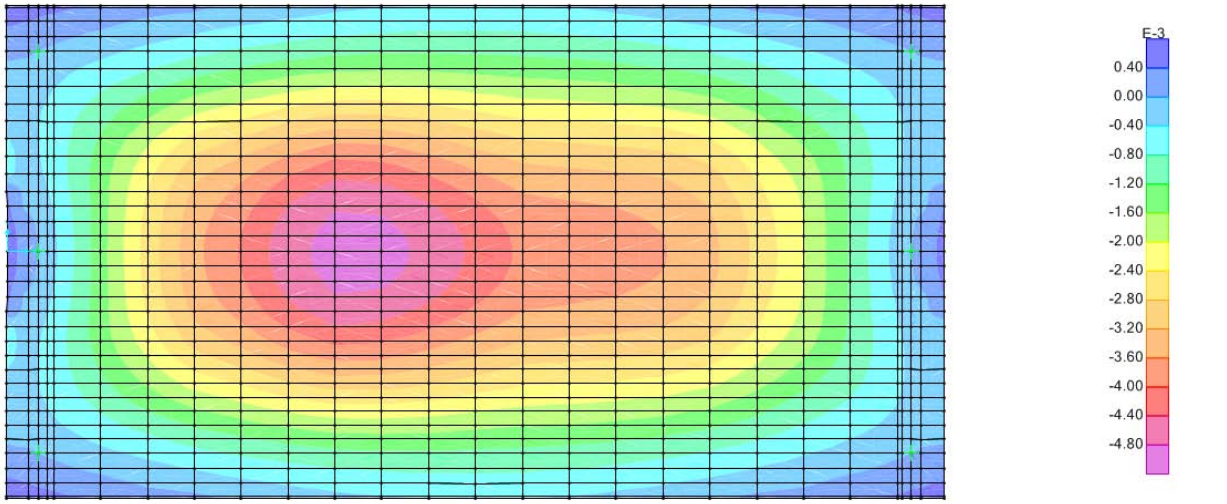

Type E: Speed 53 [m/sec]

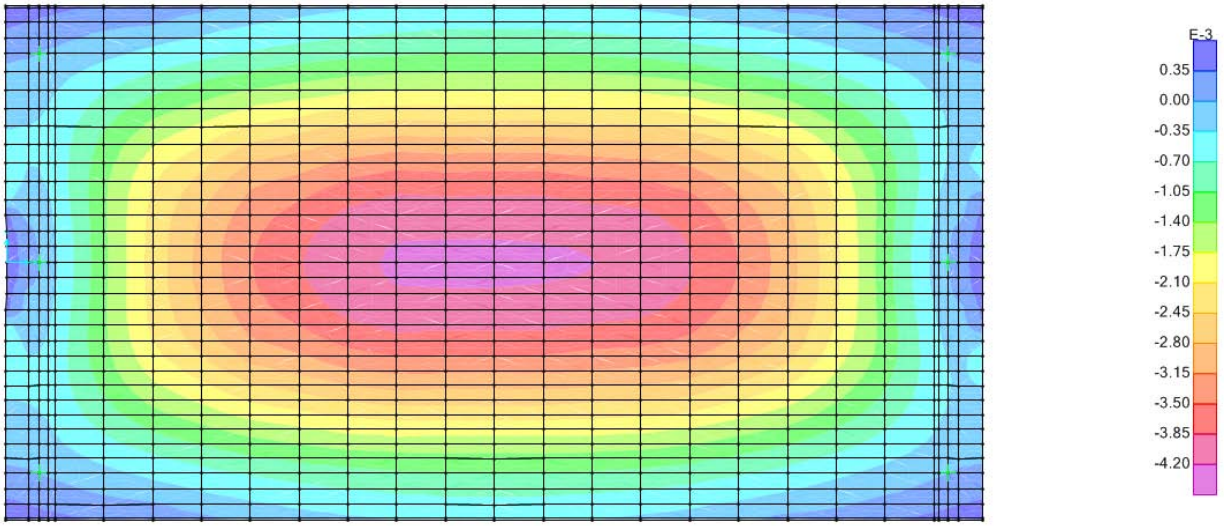

Type F: Speed 10 [m/sec]

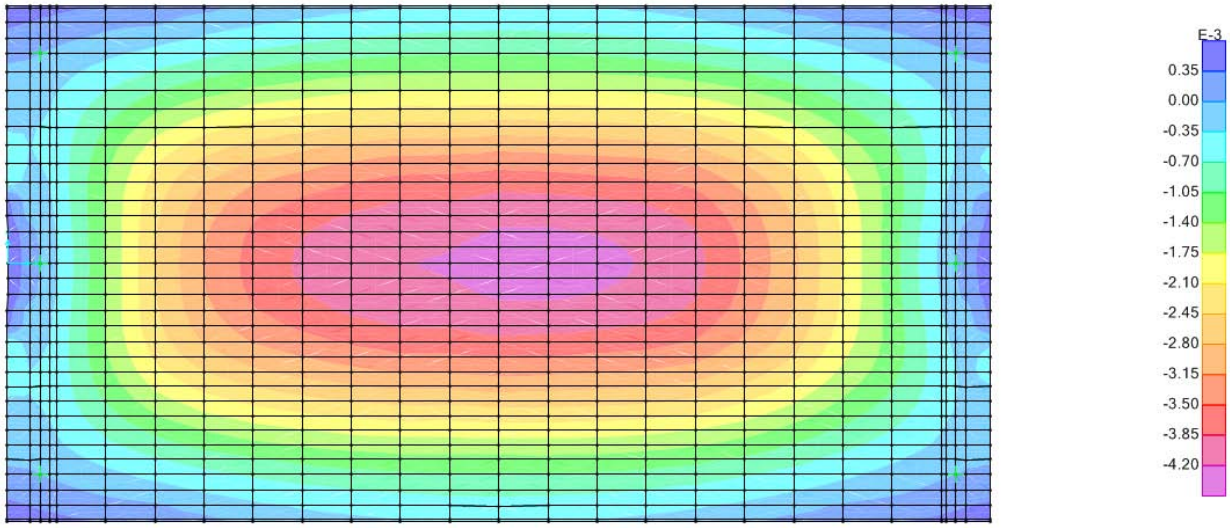

Type F: Speed 20 [m/sec]

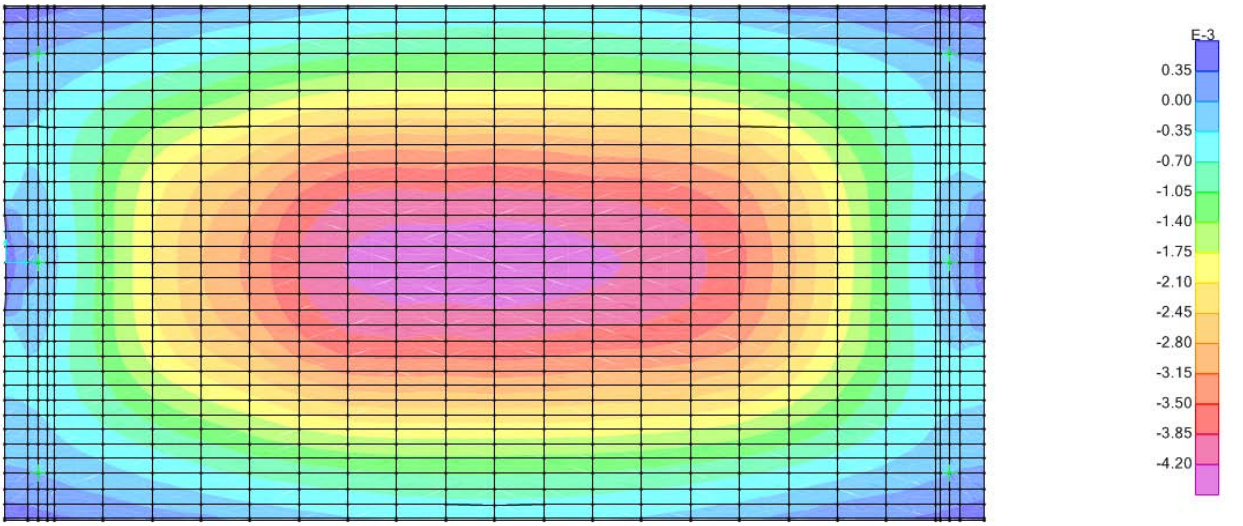

Type F: Speed 30 [m/sec]

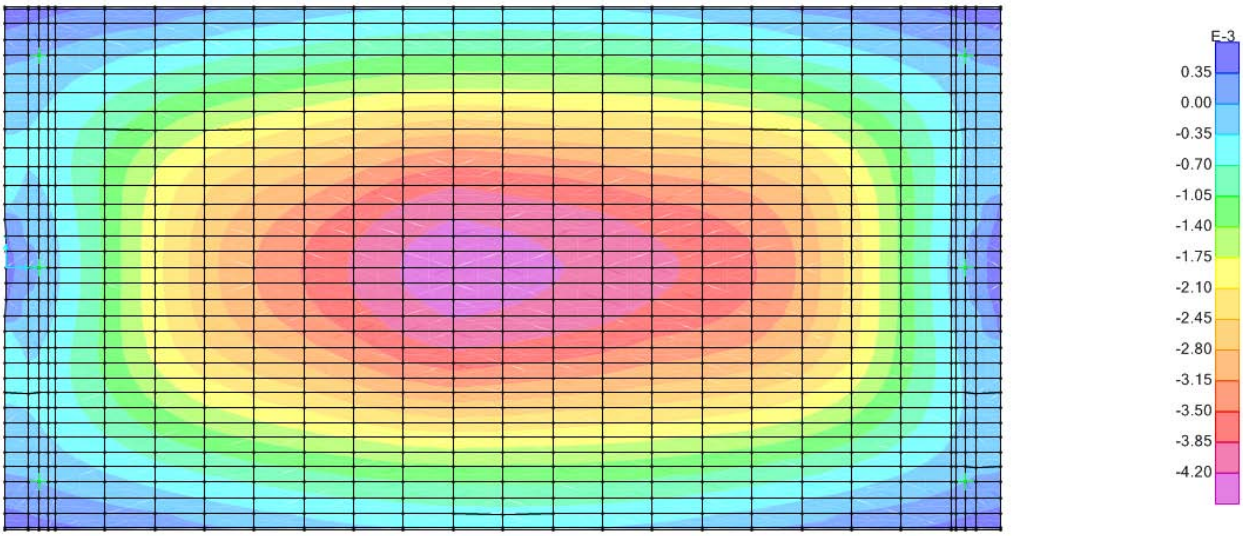

Type F: Speed 40 [m/sec]

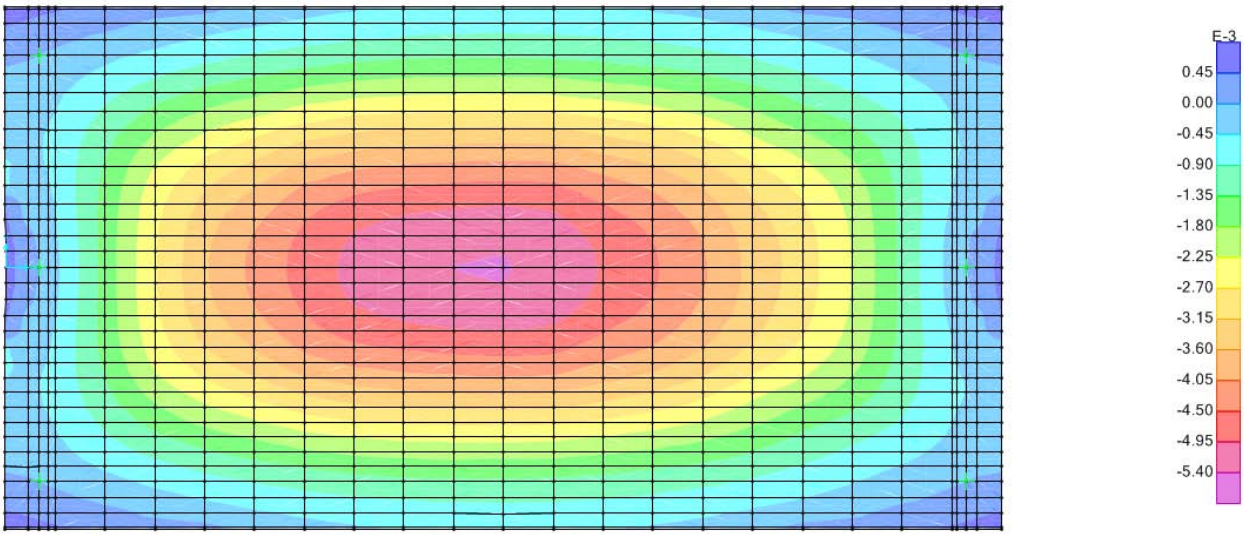

Type F: Speed 46 [m/sec]

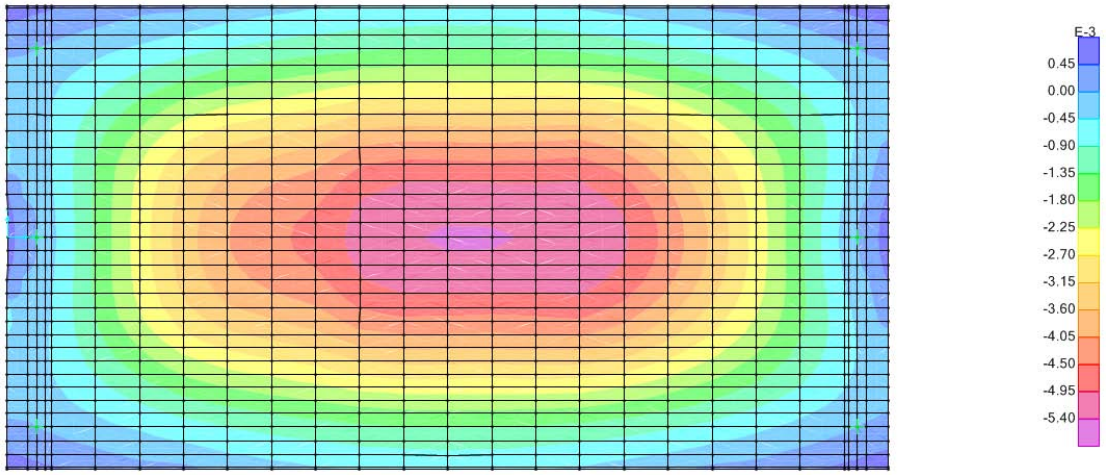

Type F: Speed 53 [m/sec]

9.3) Results for 3 Bearings , 15 meters span

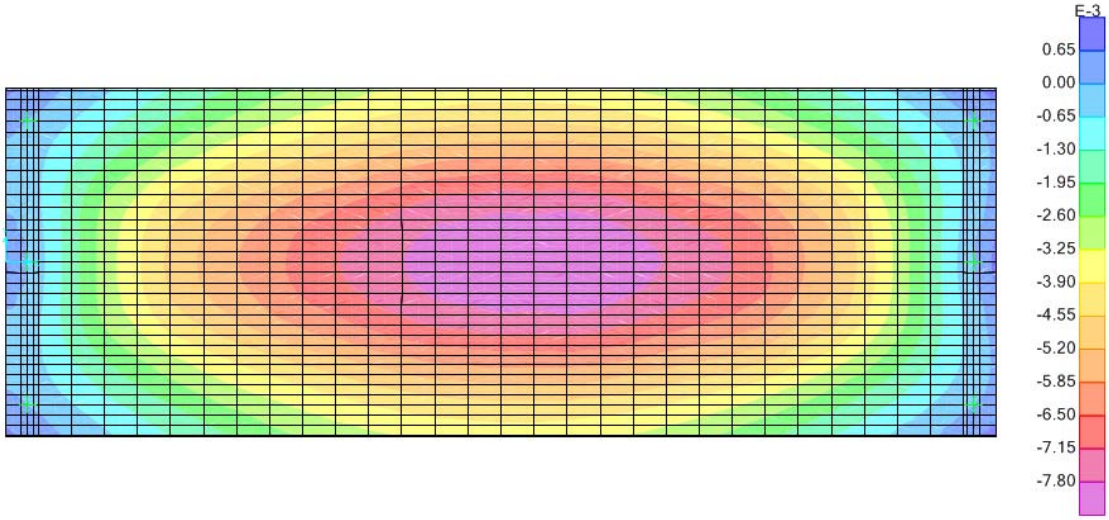

Type A: Speed 10 [m/sec]

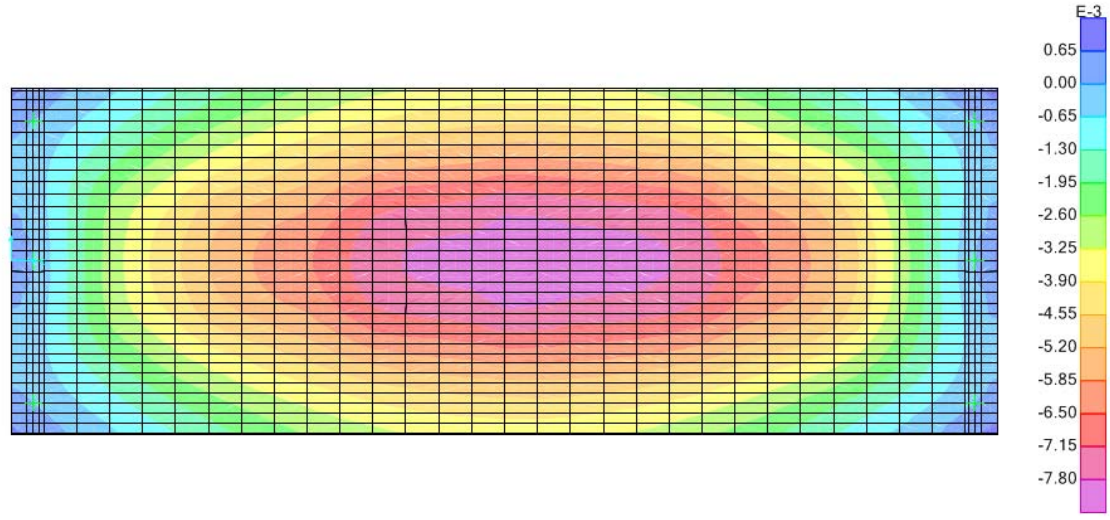

Type A: Speed 20 [m/sec]

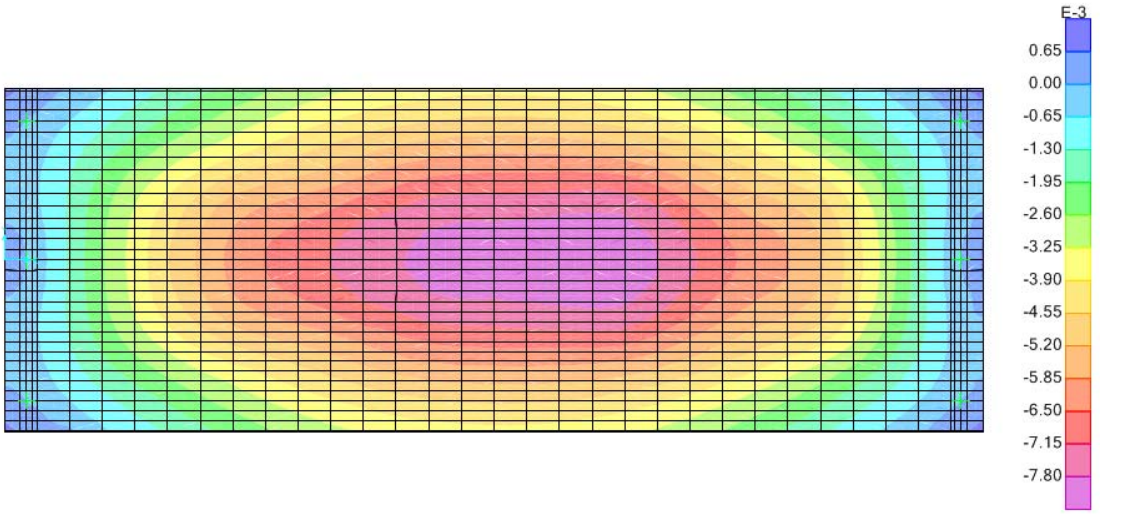

Type A: Speed 30 [m/sec]

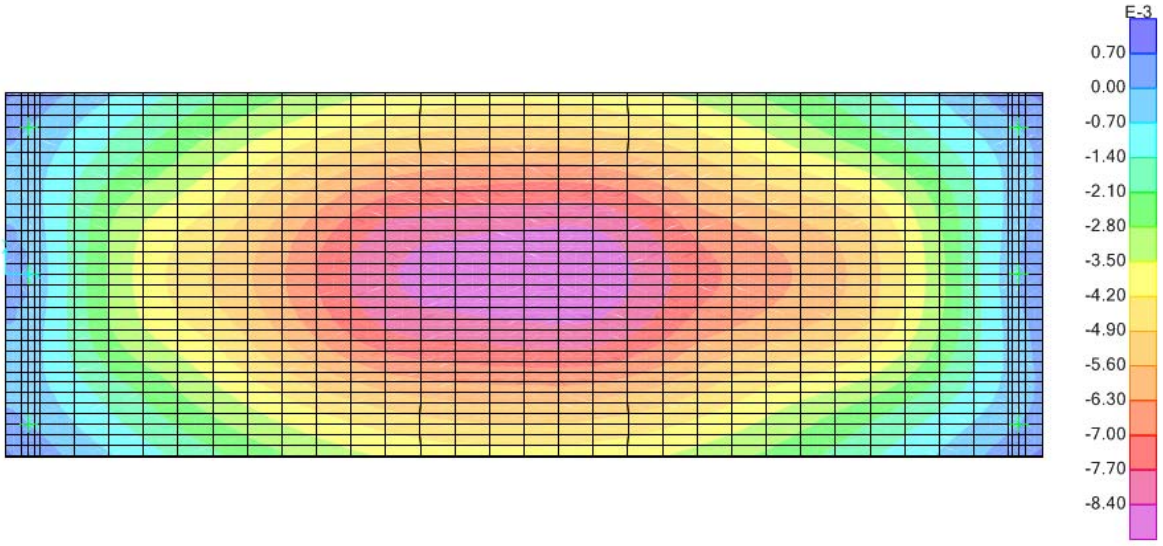

Type A: Speed 40 [m/sec]

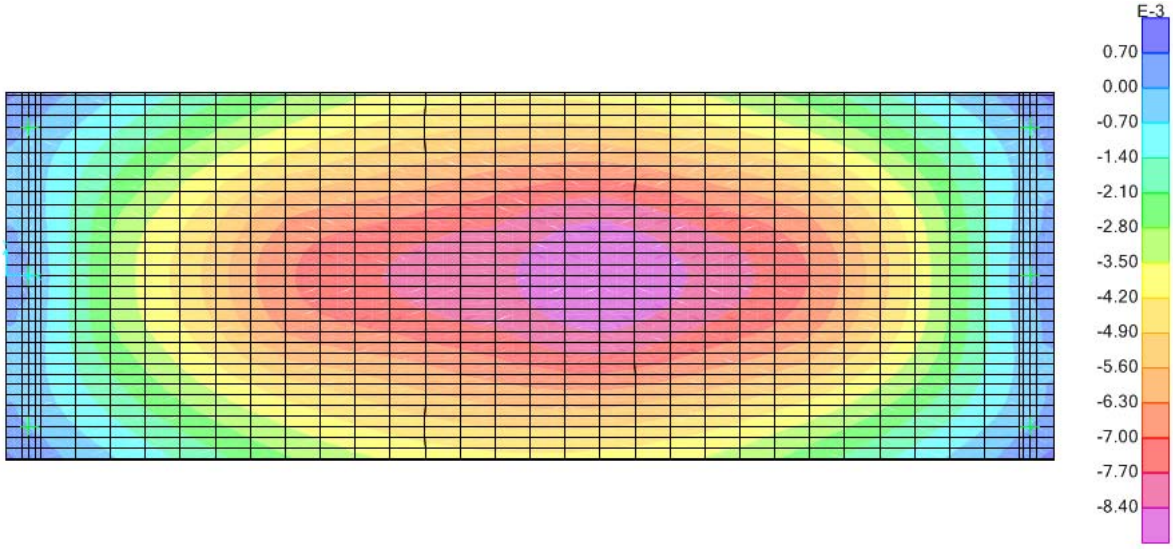

Type A: Speed 46 [m/sec]

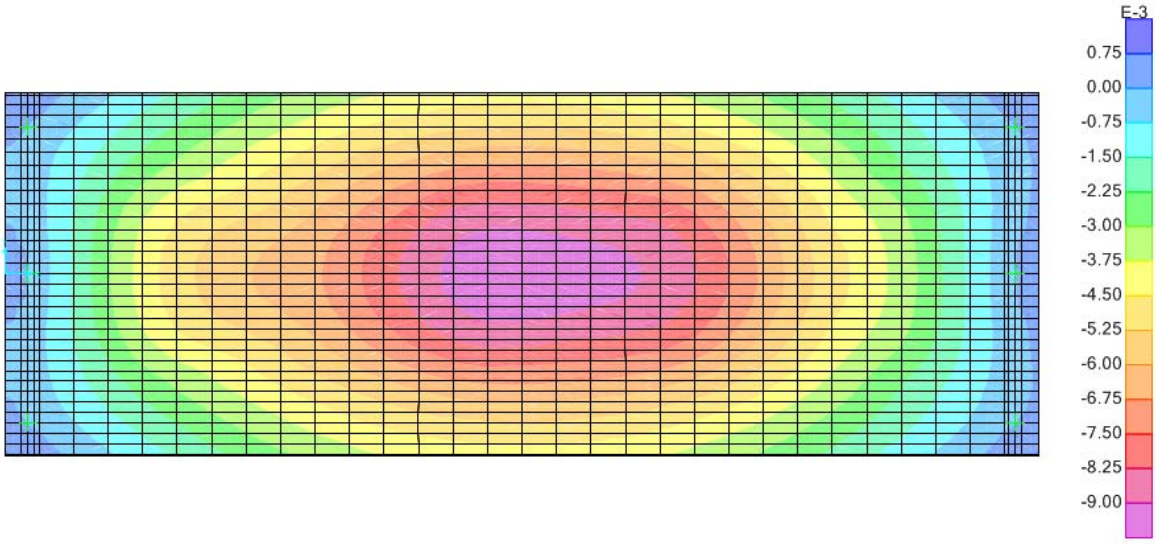

Type A: Speed 53 [m/sec]

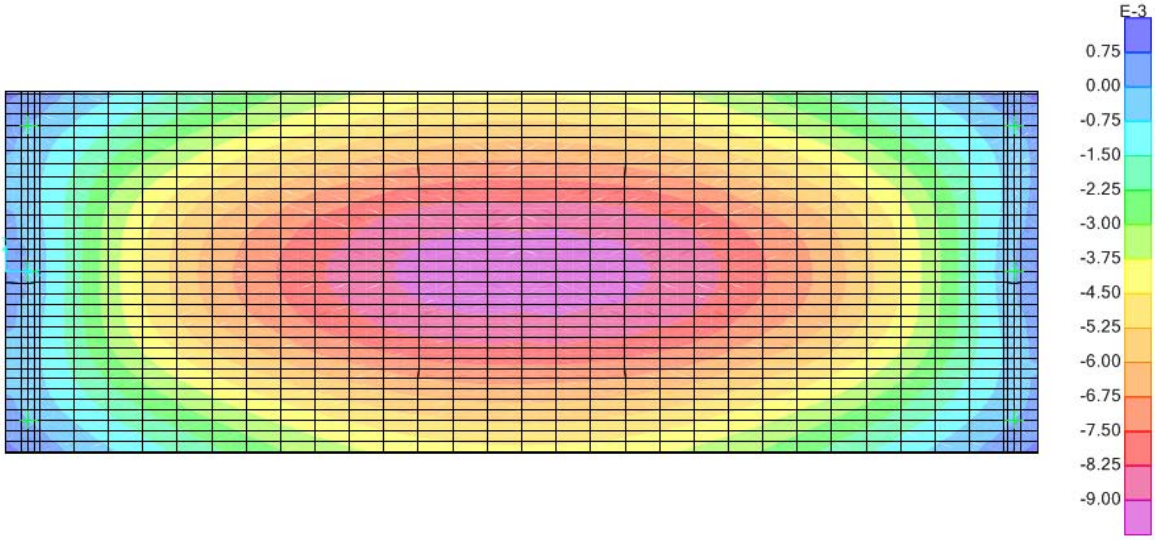

Type B: Speed 10 [m/sec]

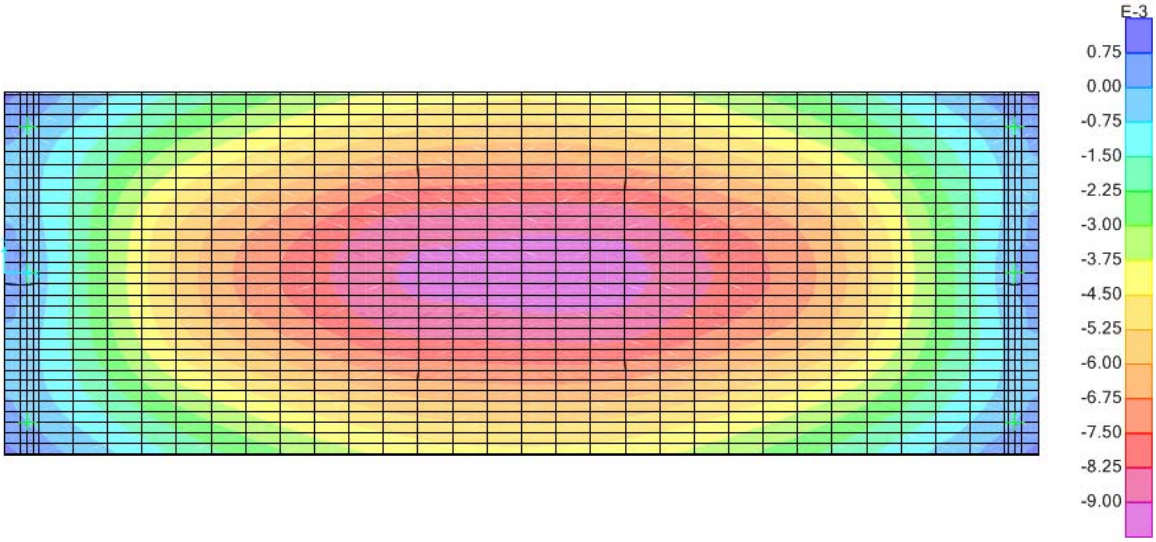

Type B: Speed 20 [m/sec]

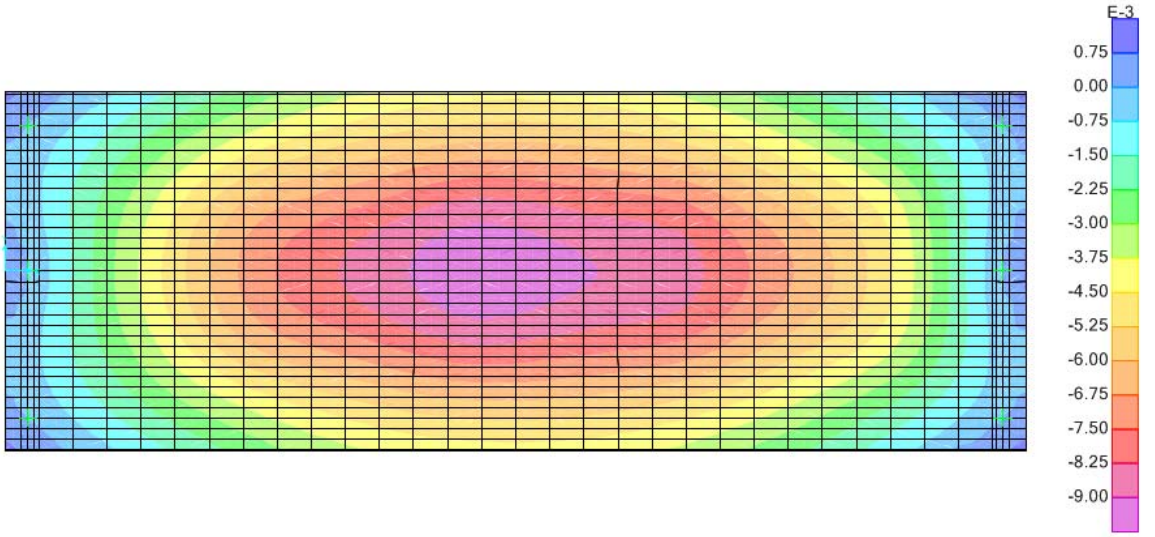

Type B: Speed 30 [m/sec]

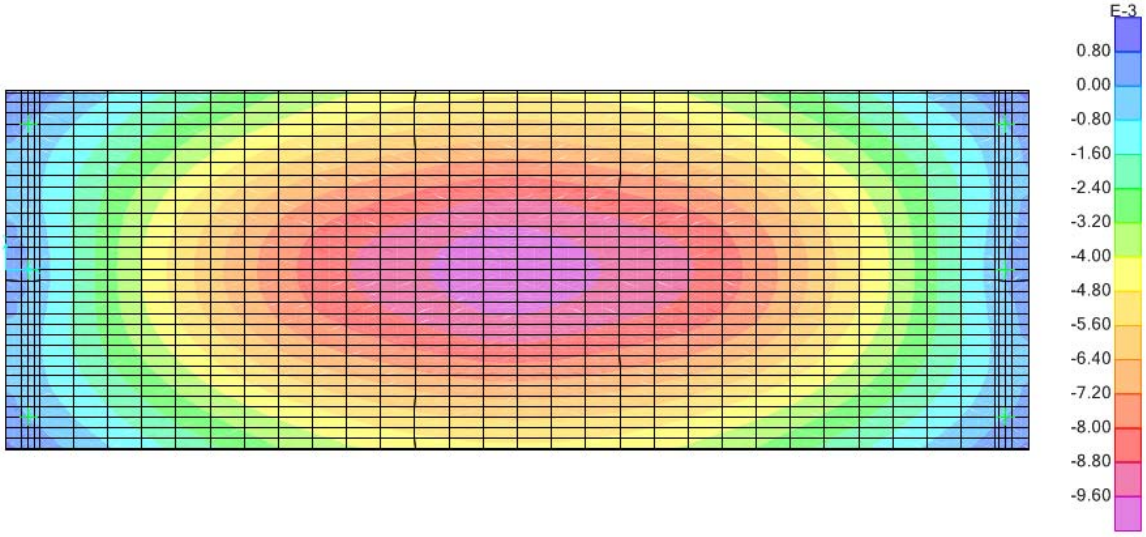

Type B: Speed 40 [m/sec]

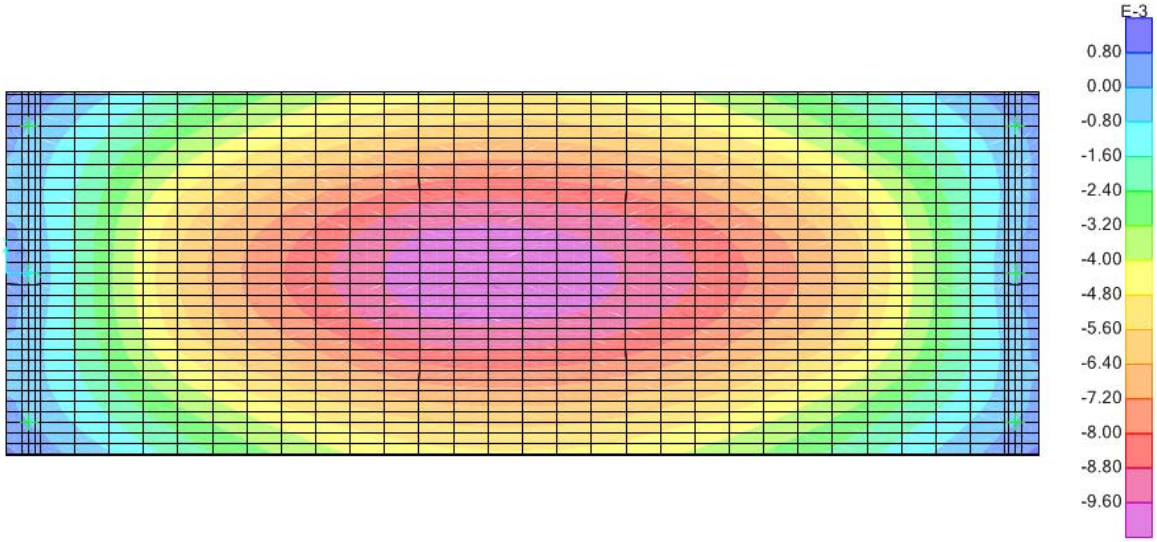

Type B: Speed 46 [m/sec]

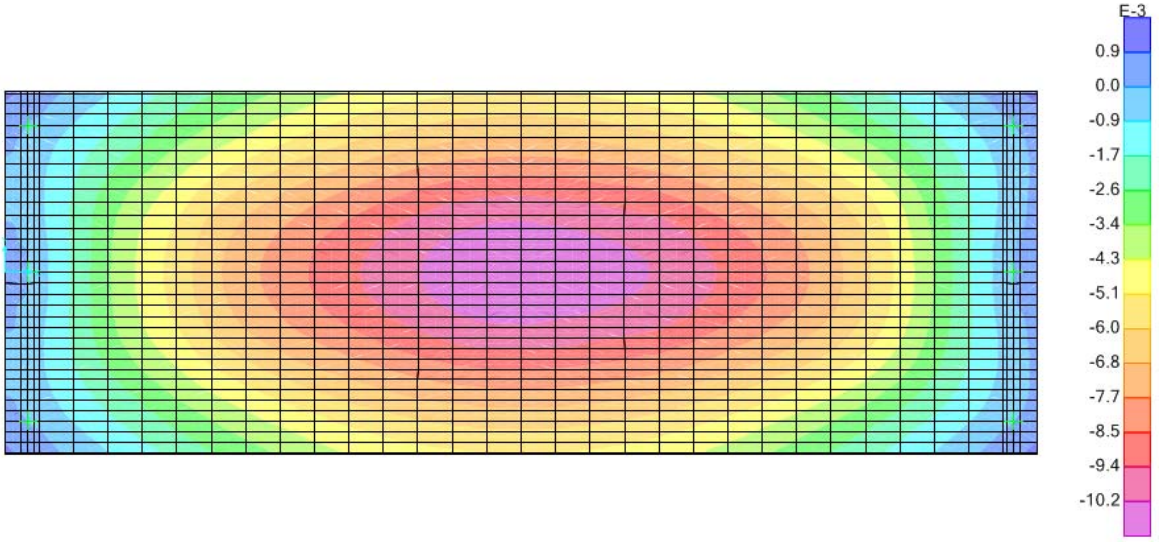

Type B: Speed 53 [m/sec]

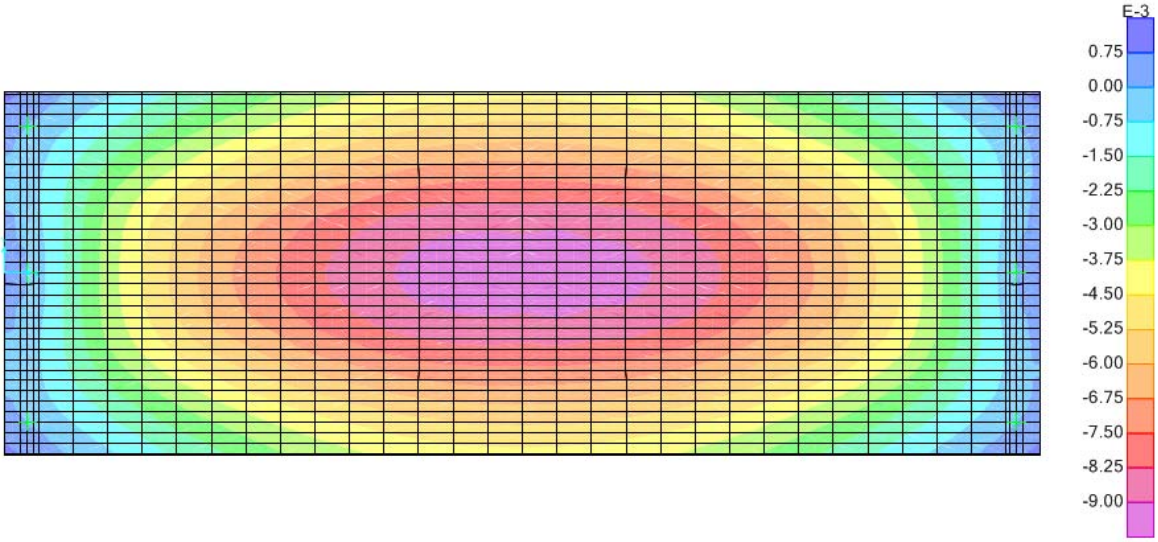

Type C: Speed 10 [m/sec]

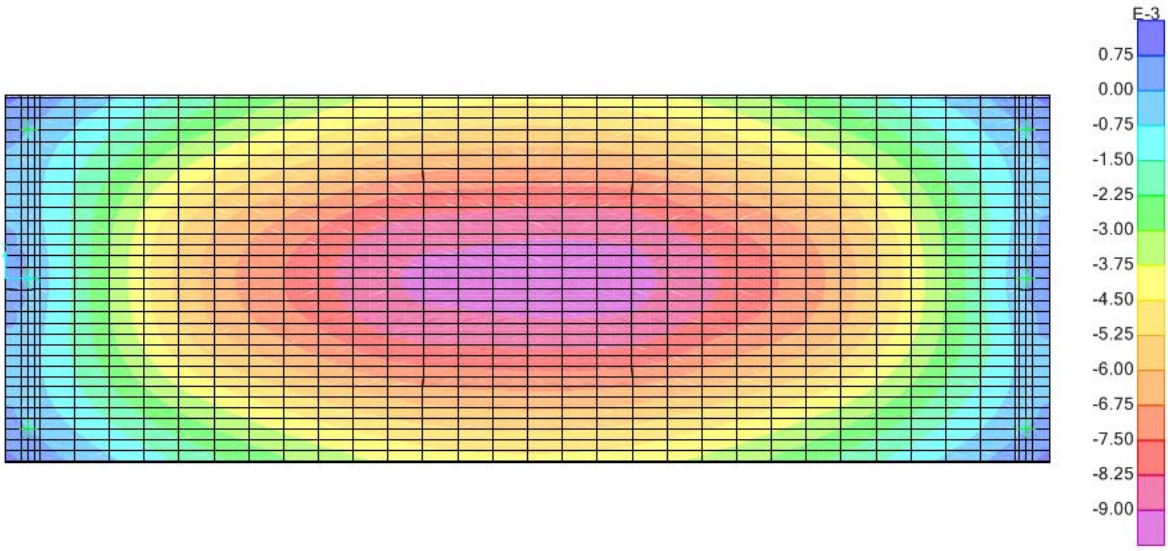

Type C: Speed 20 [m/sec]

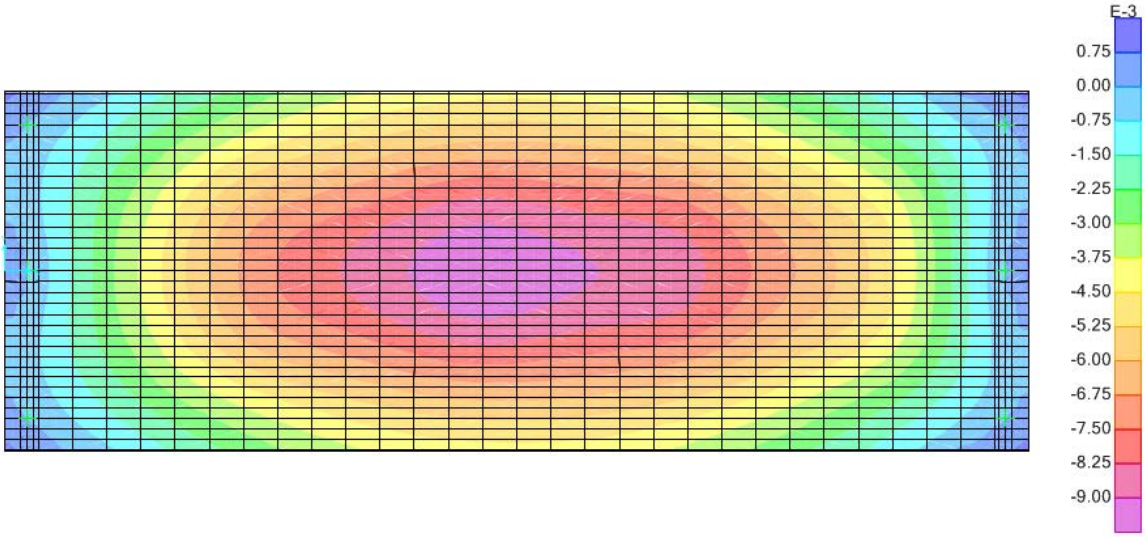

Type C: Speed 30 [m/sec]

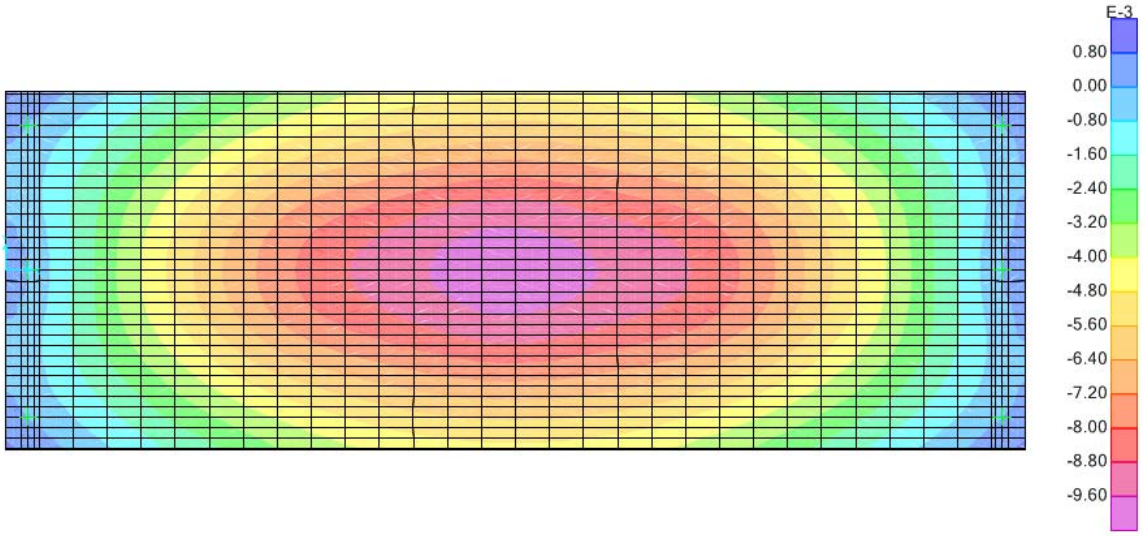

Type C: Speed 40 [m/sec]

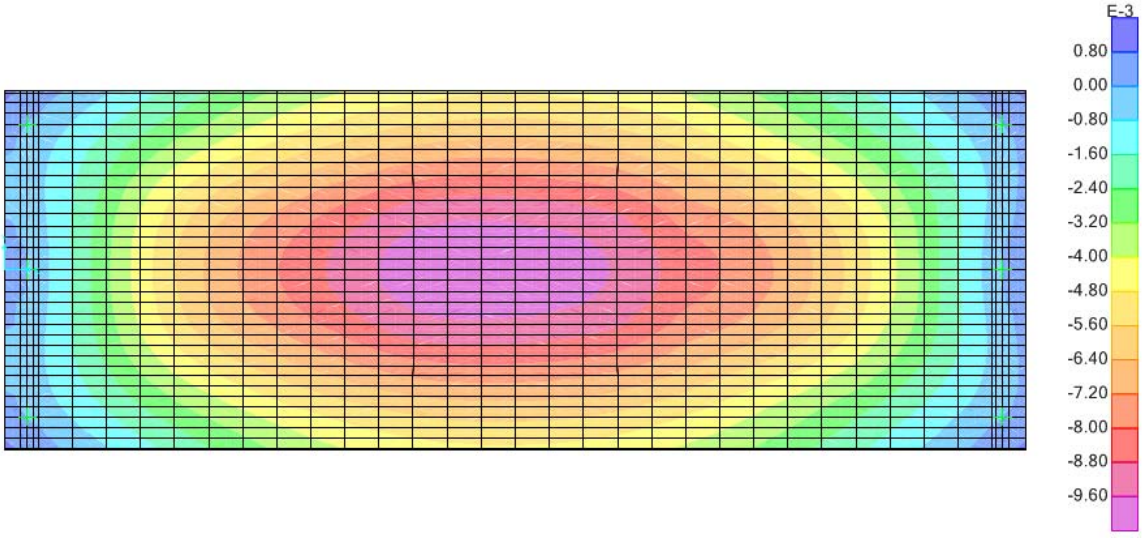

Type C: Speed 46 [m/sec]

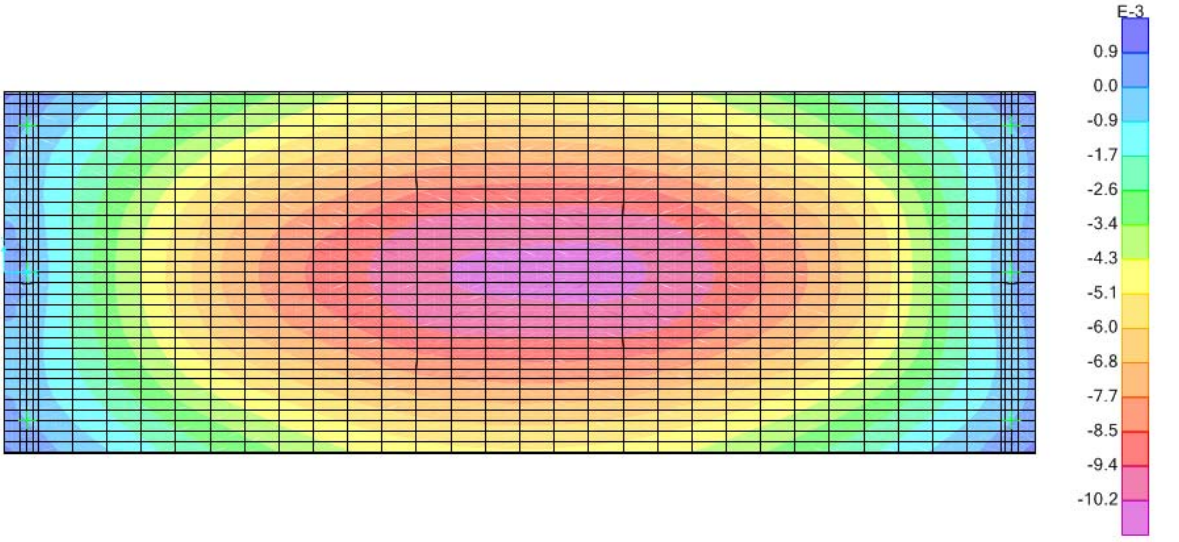

Type C: Speed 53 [m/sec]

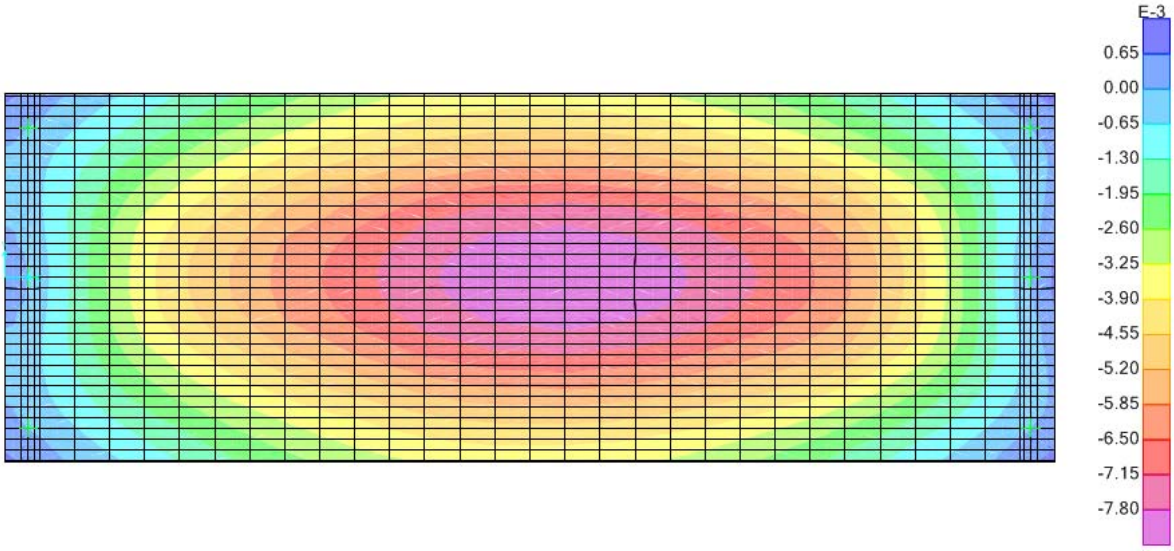

Type D: Speed 10 [m/sec]

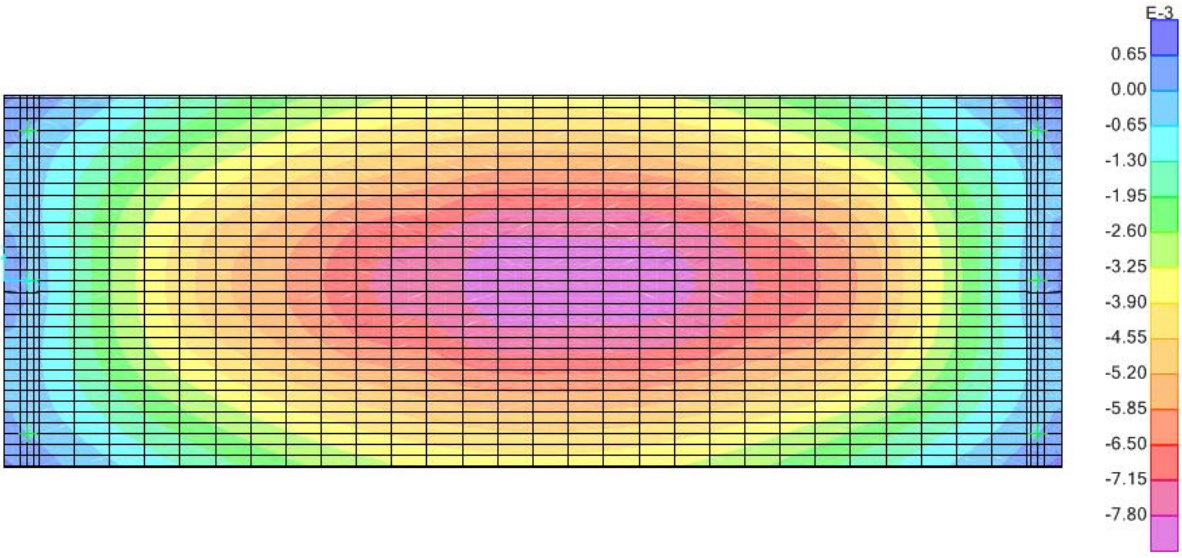

Type D: Speed 20 [m/sec]

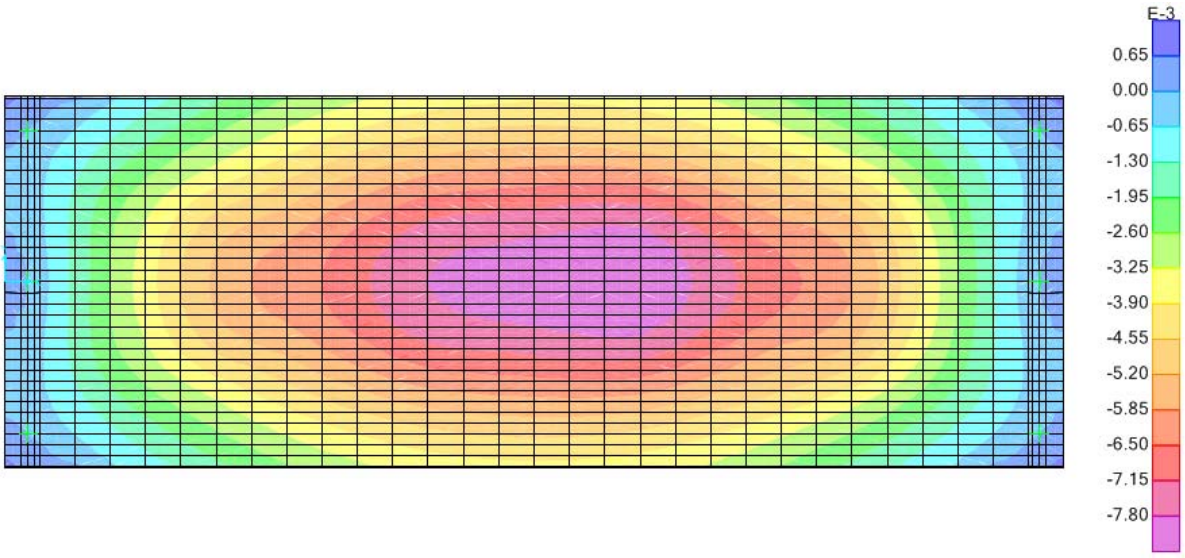

Type D: Speed 30 [m/sec]

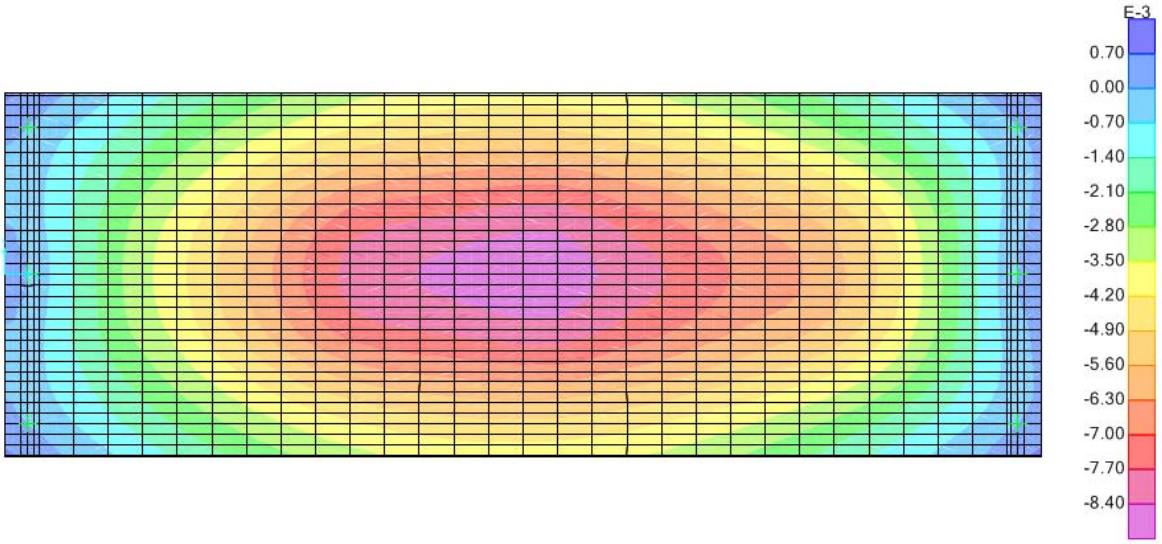

Type D: Speed 40 [m/sec]

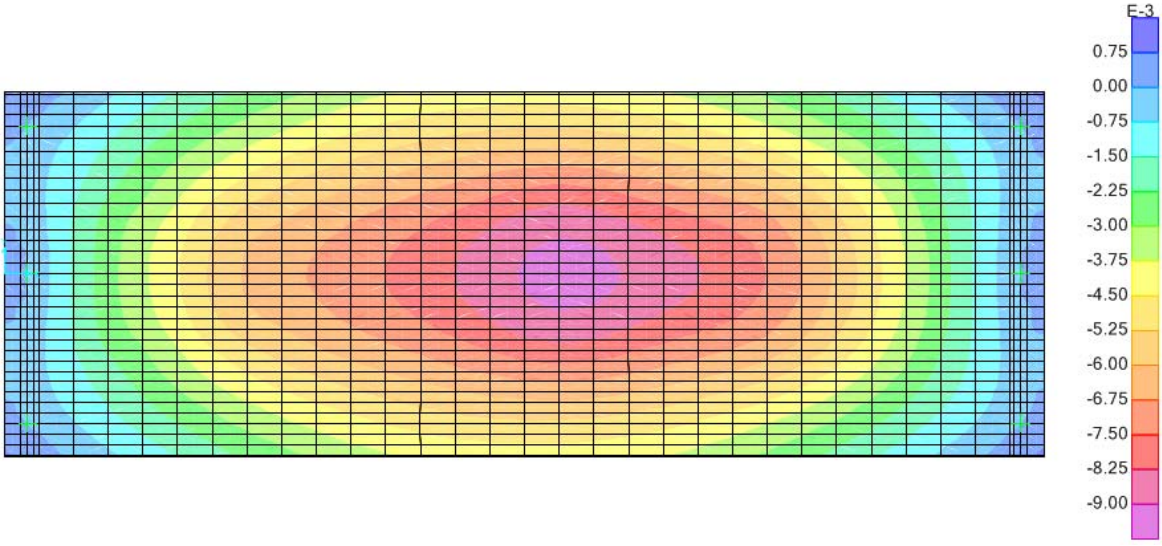

Type D: Speed 46 [m/sec]

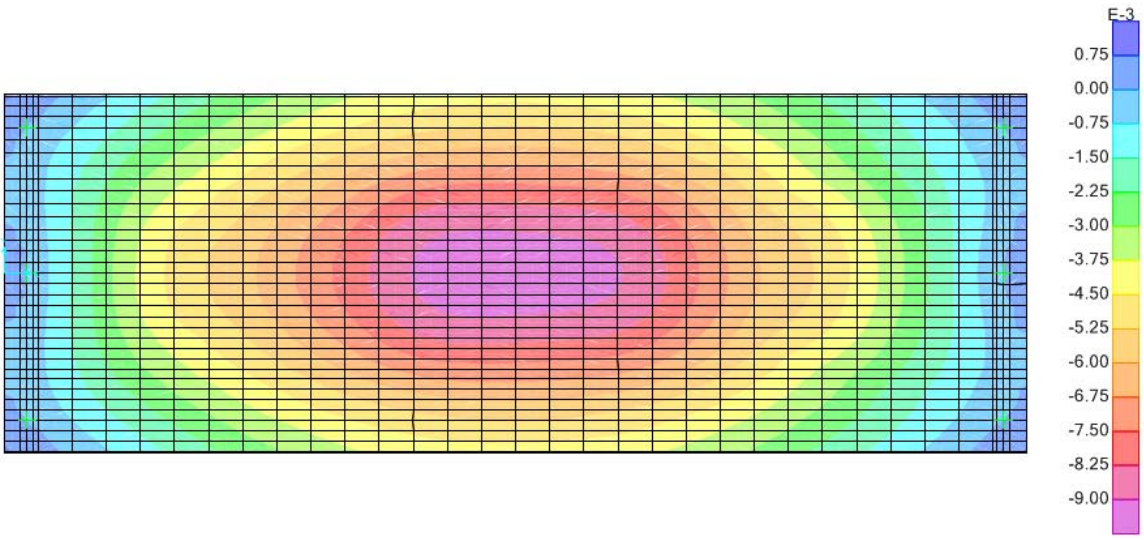

Type D: Speed 53 [m/sec]

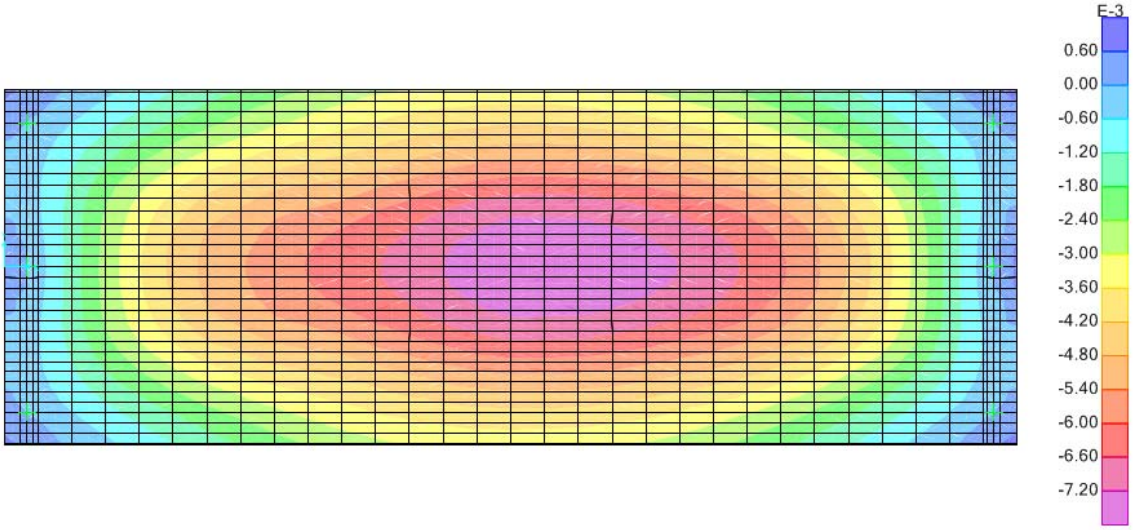

Type E: Speed 10 [m/sec]

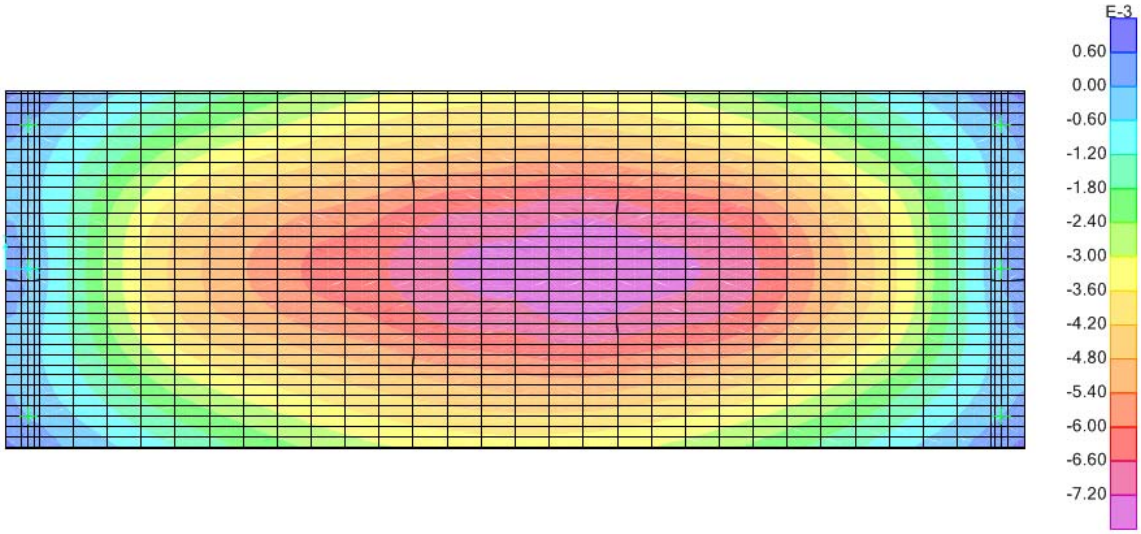

Type E: Speed 20 [m/sec]

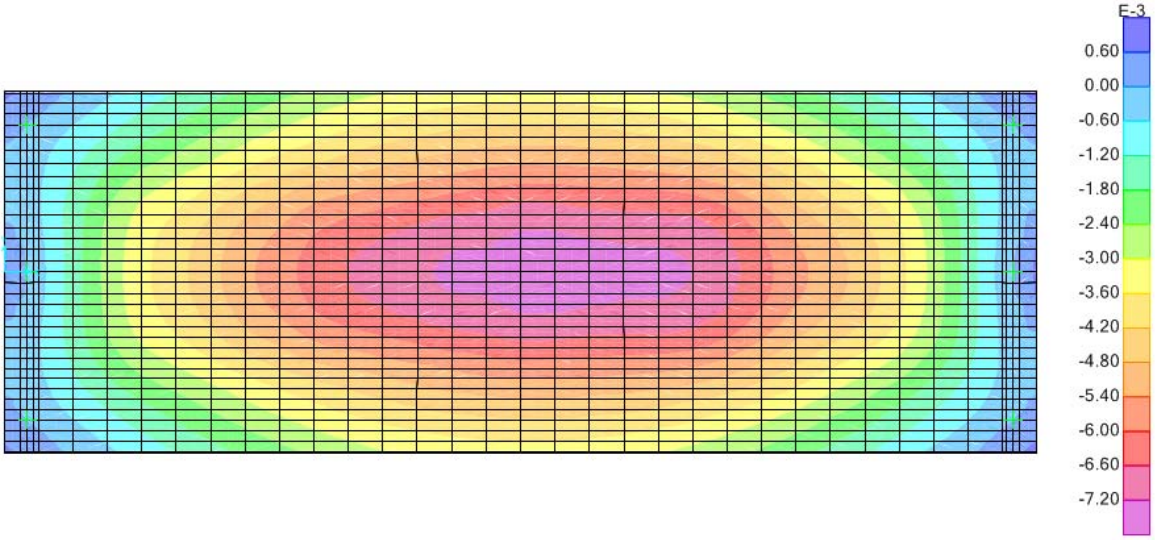

Type E: Speed 30 [m/sec]

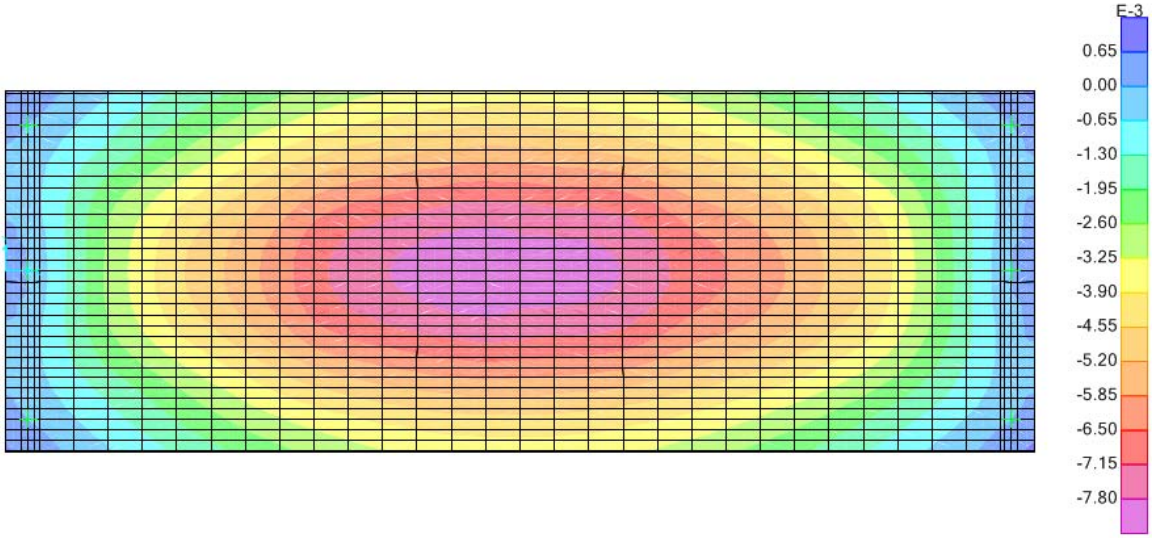

Type E: Speed 40 [m/sec]

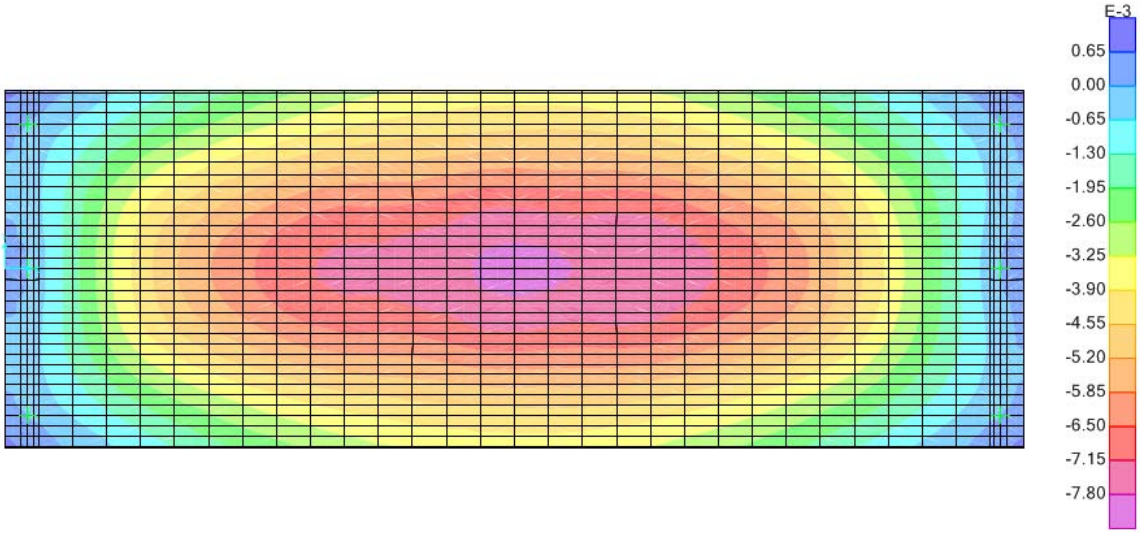

Type E: Speed 46 [m/sec]

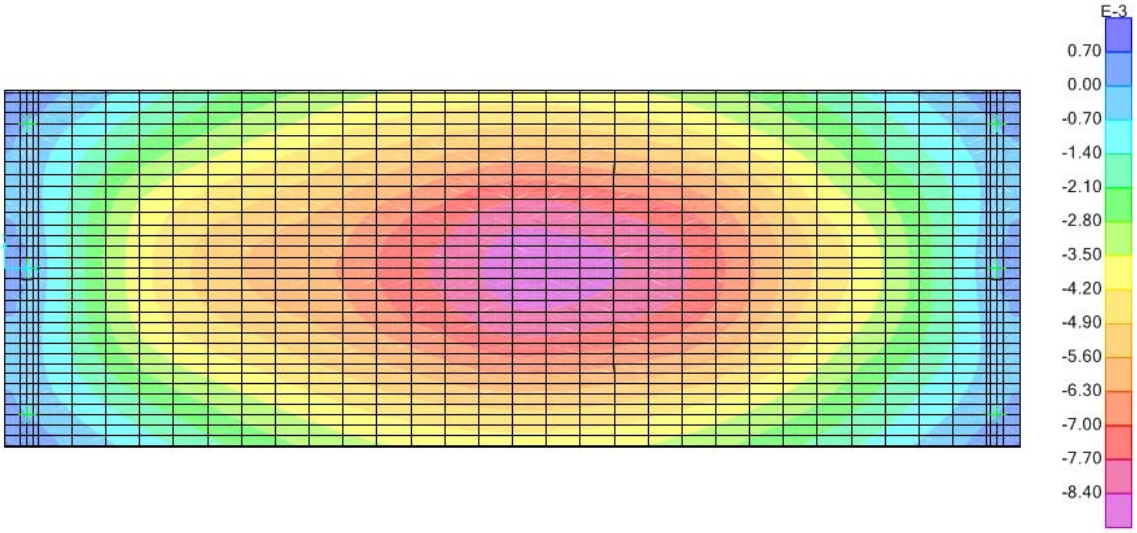

Type E: Speed 53 [m/sec]

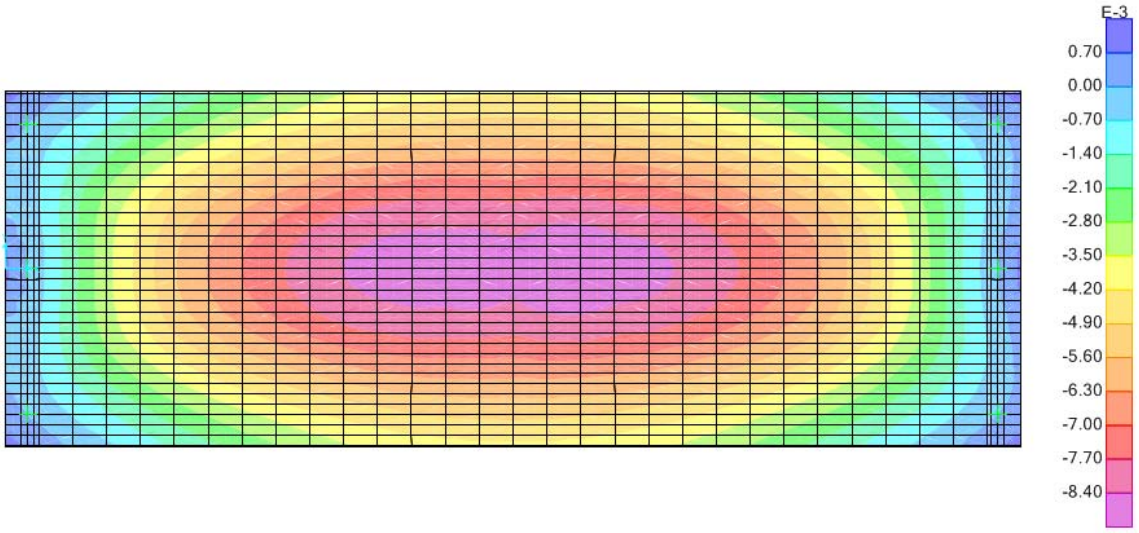

Type F: Speed 10 [m/sec]

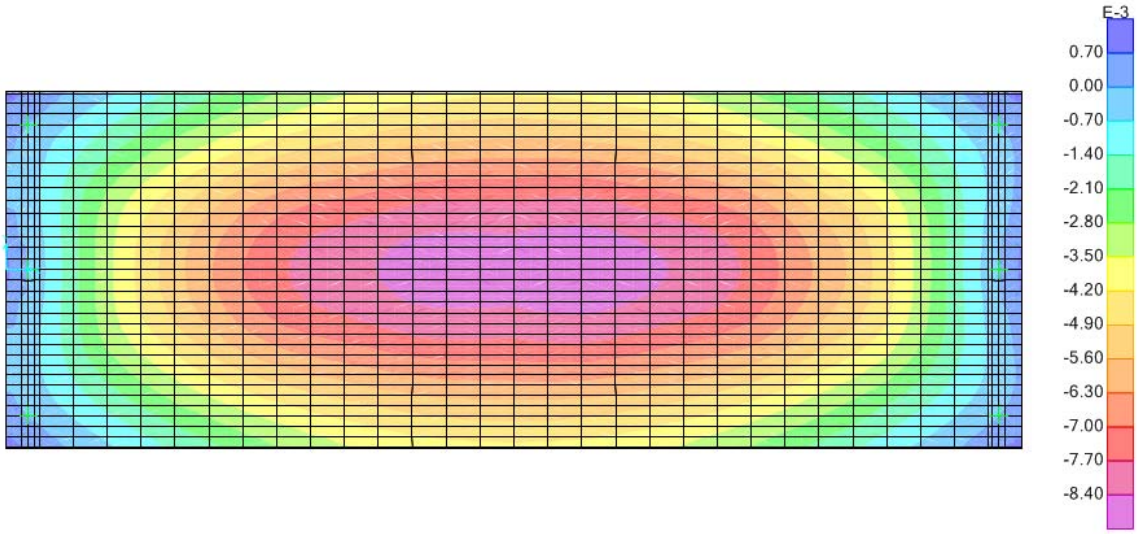

Type F: Speed 20 [m/sec]

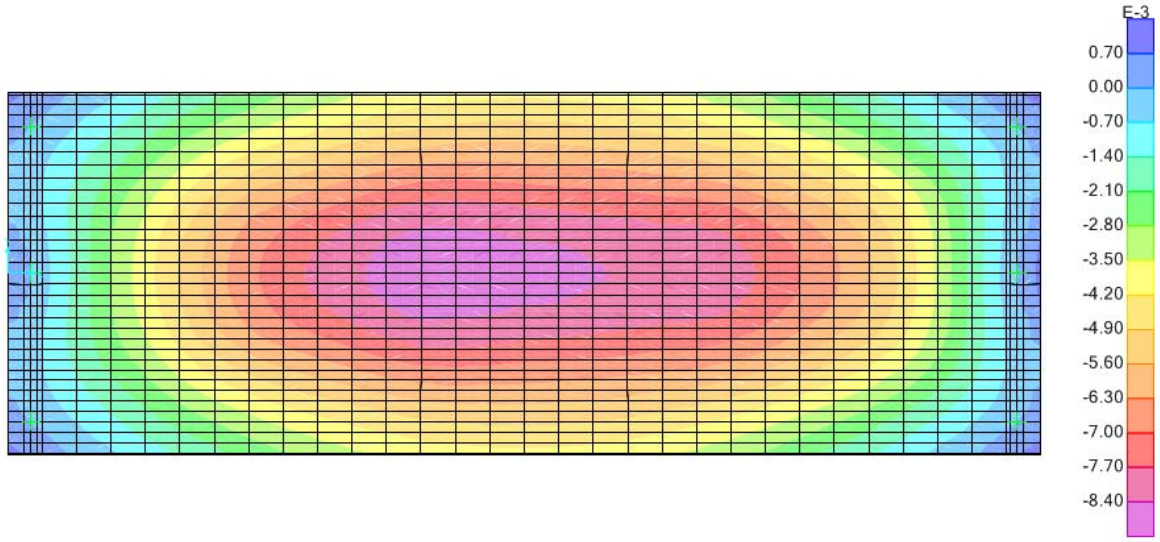

Type F: Speed 30 [m/sec]

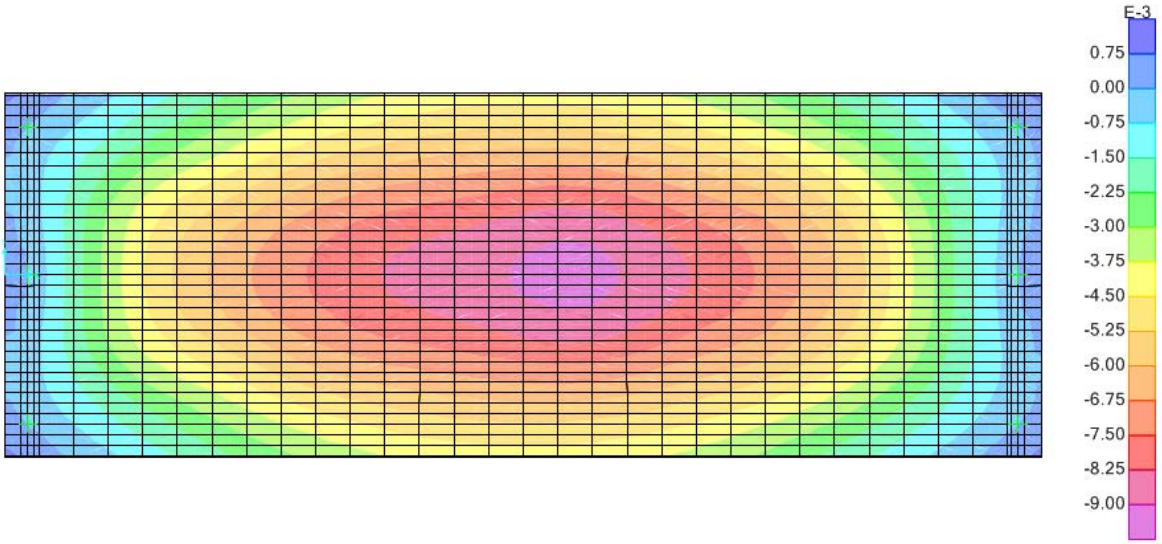

Type F: Speed 40 [m/sec]

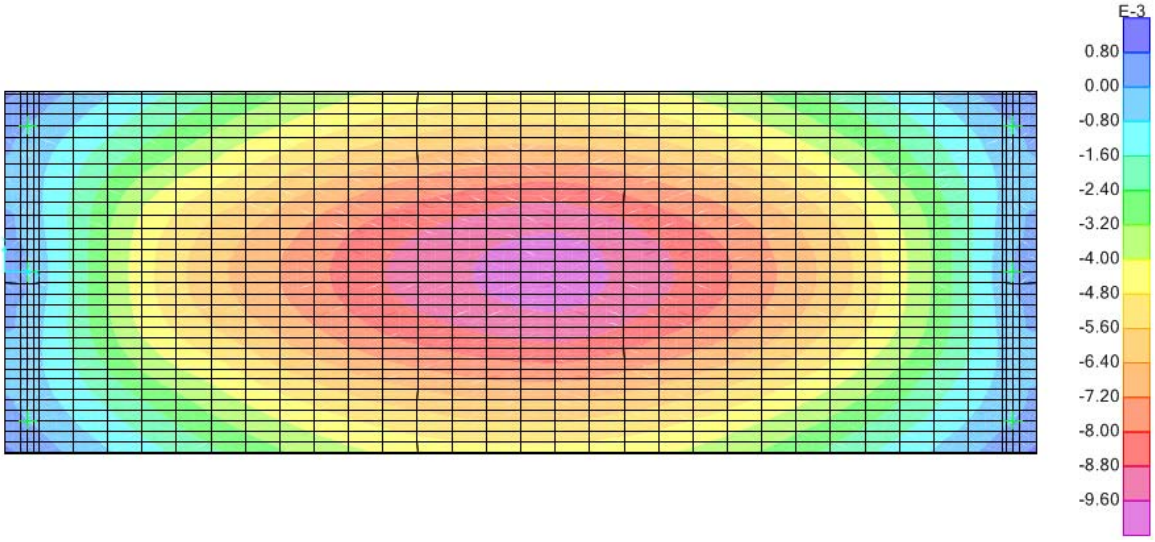

Type F: Speed 46 [m/sec]

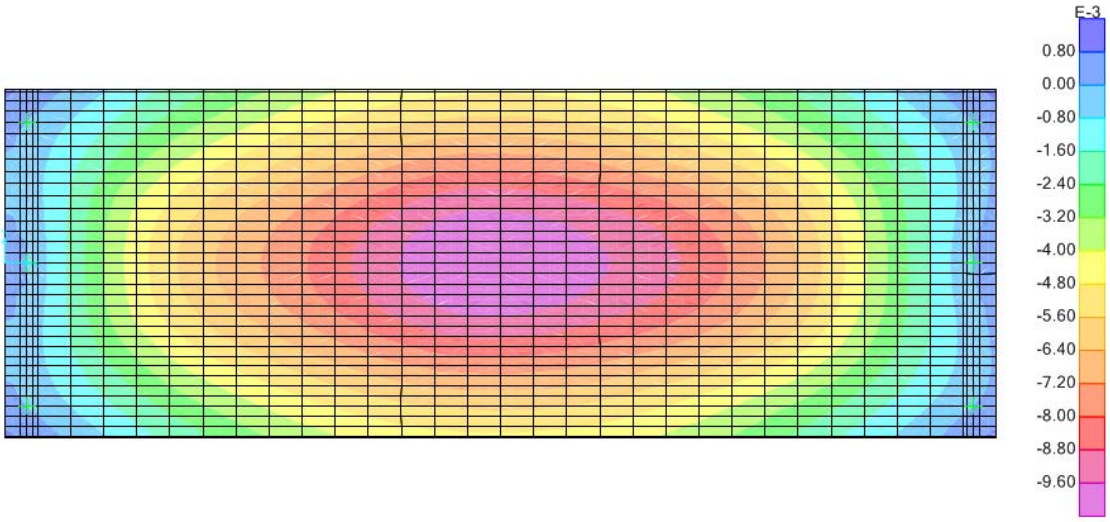

Type F: Speed 53 [m/sec]

9.4) Results for 3 Bearings , 15 meters structure with bigger main girders

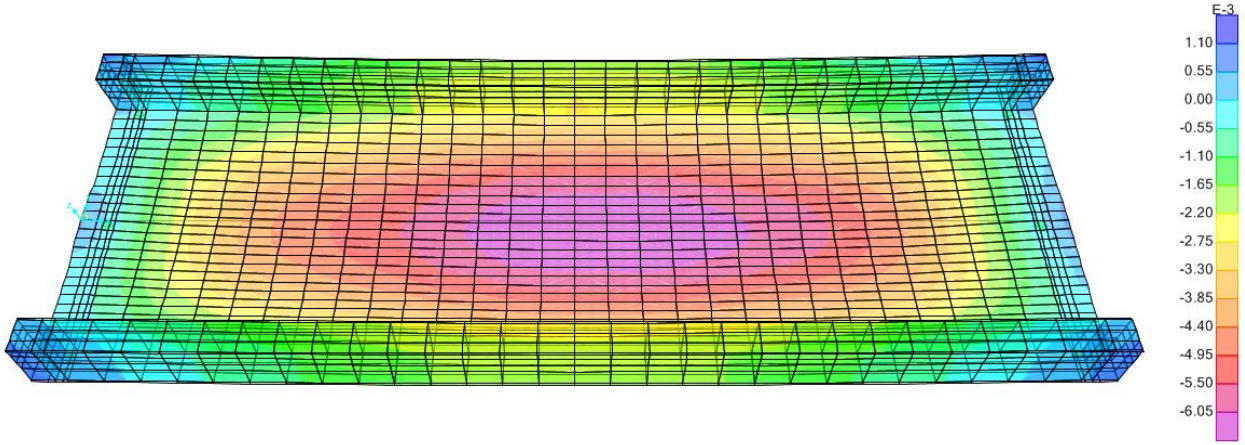

Type A: Speed 10 [m/sec]

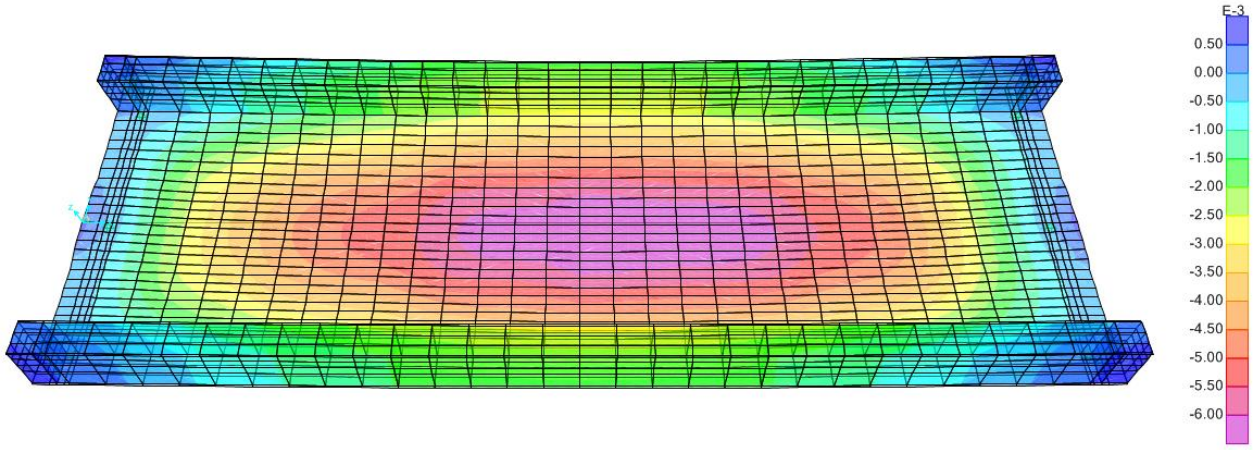

Type A: Speed 20 [m/sec]

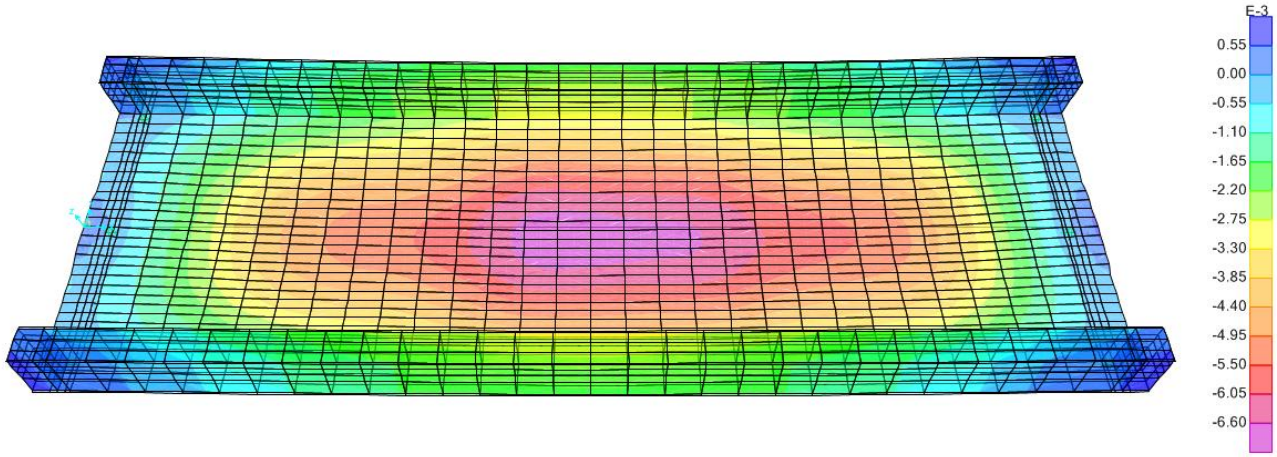

Type A: Speed 30 [m/sec]

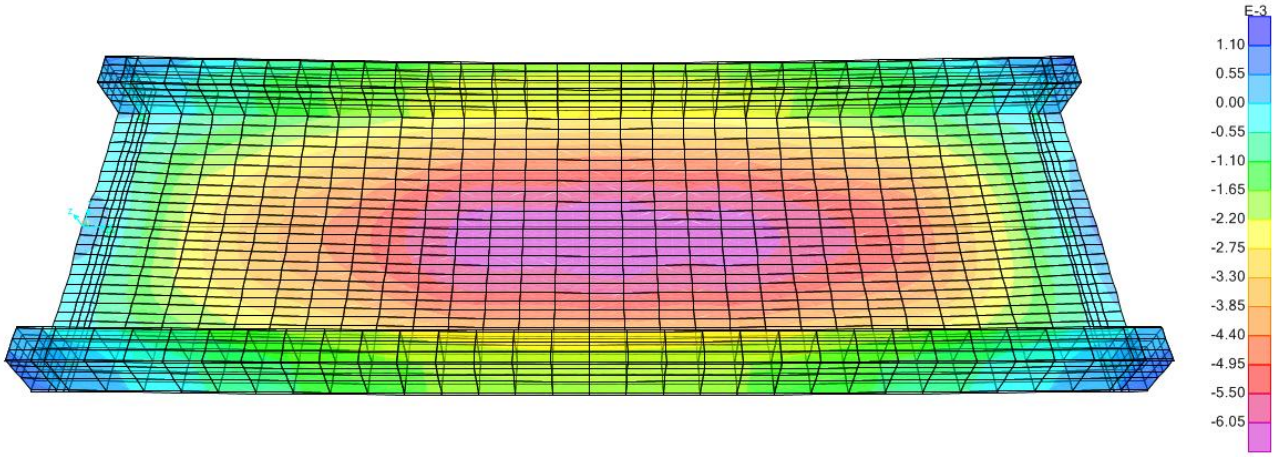

Type A: Speed 40 [m/sec]

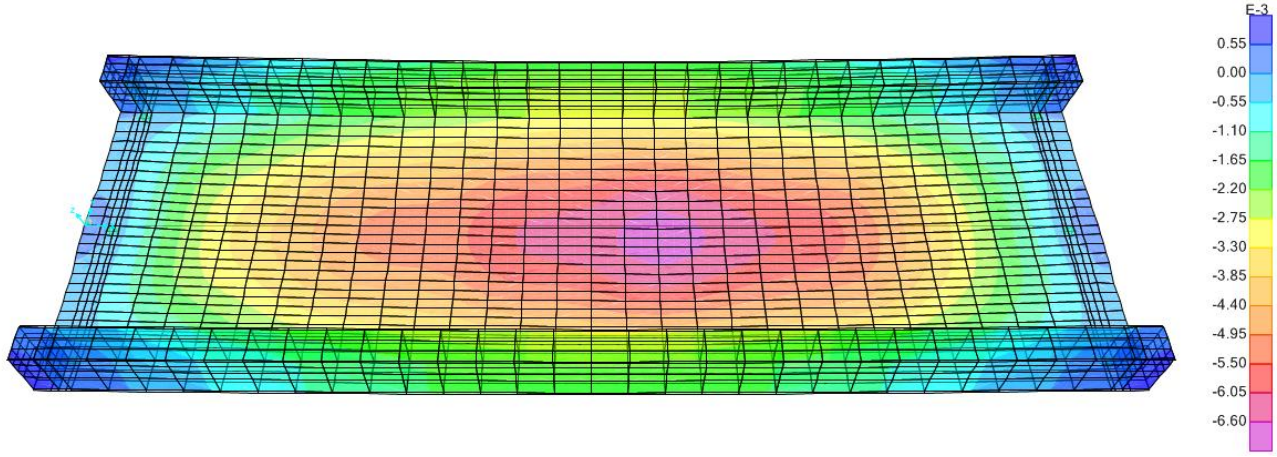

Type A: Speed 46 [m/sec]

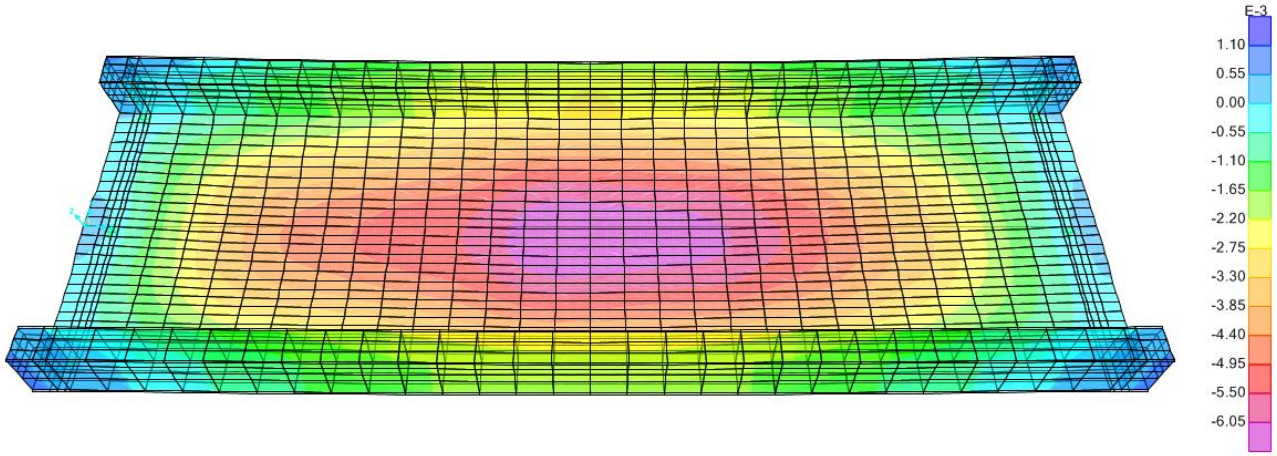

Type A: Speed 53 [m/sec]

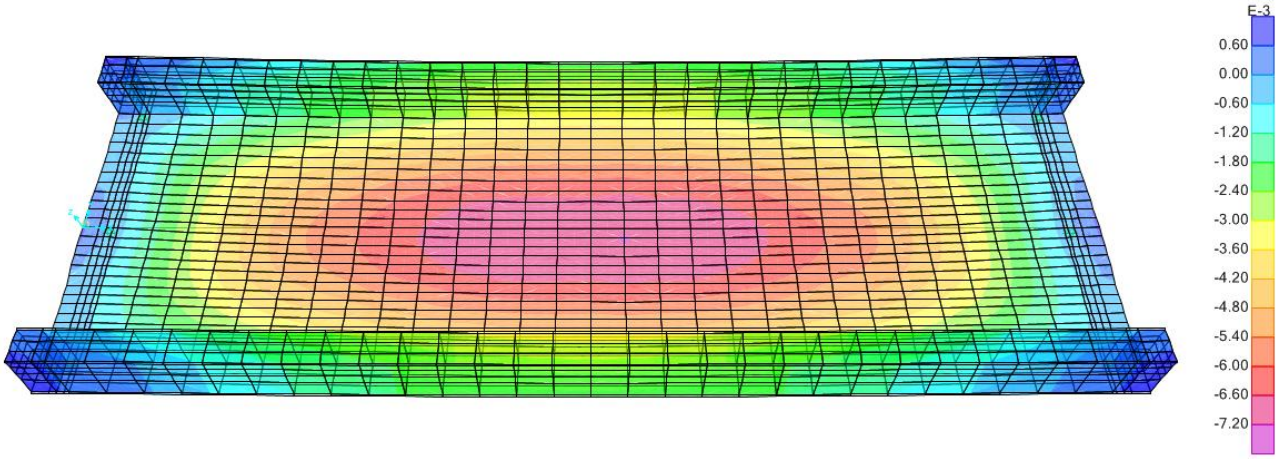

Type B: Speed 10 [m/sec]

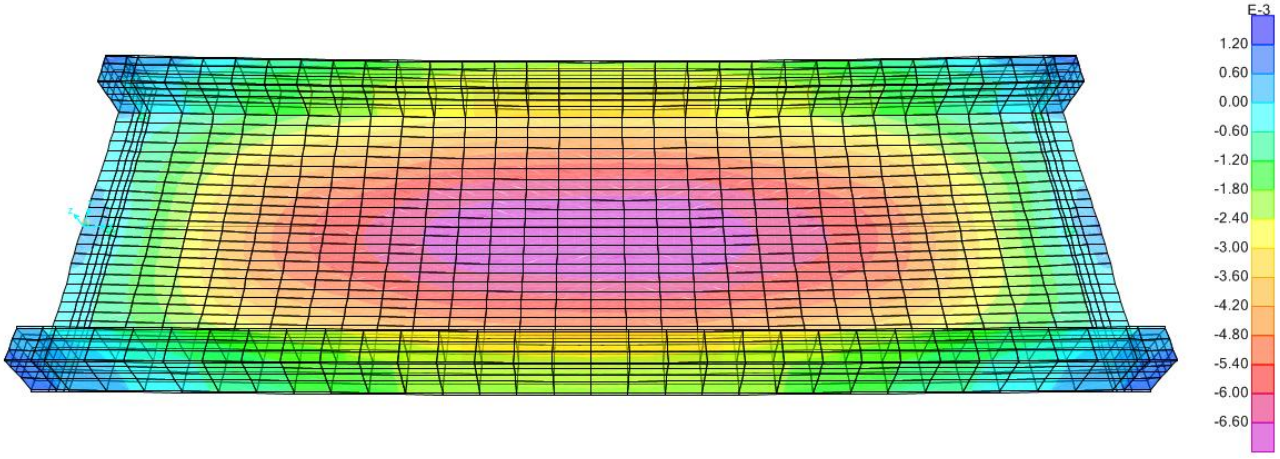

Type B: Speed 20 [m/sec]

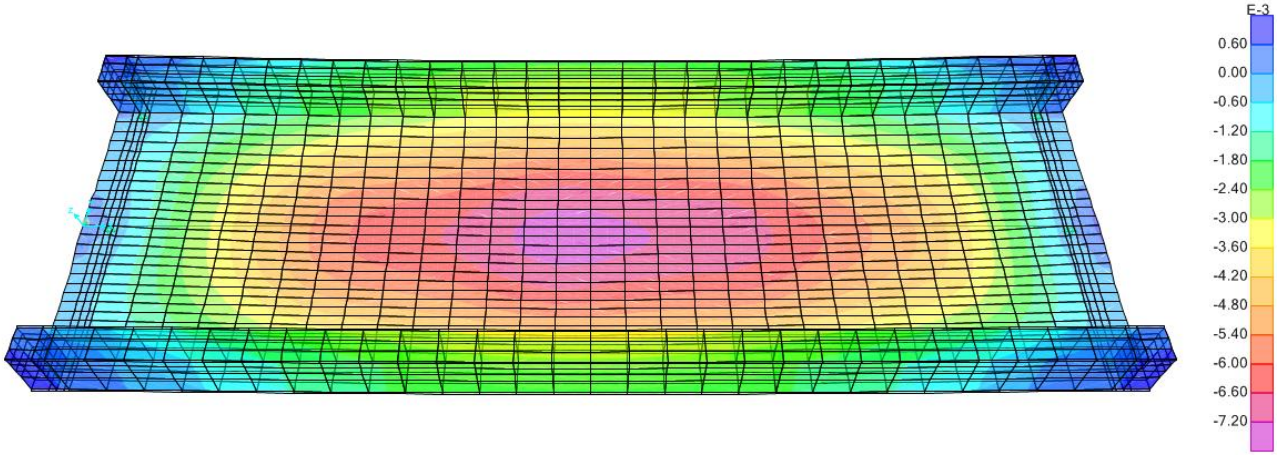

Type B: Speed 30 [m/sec]

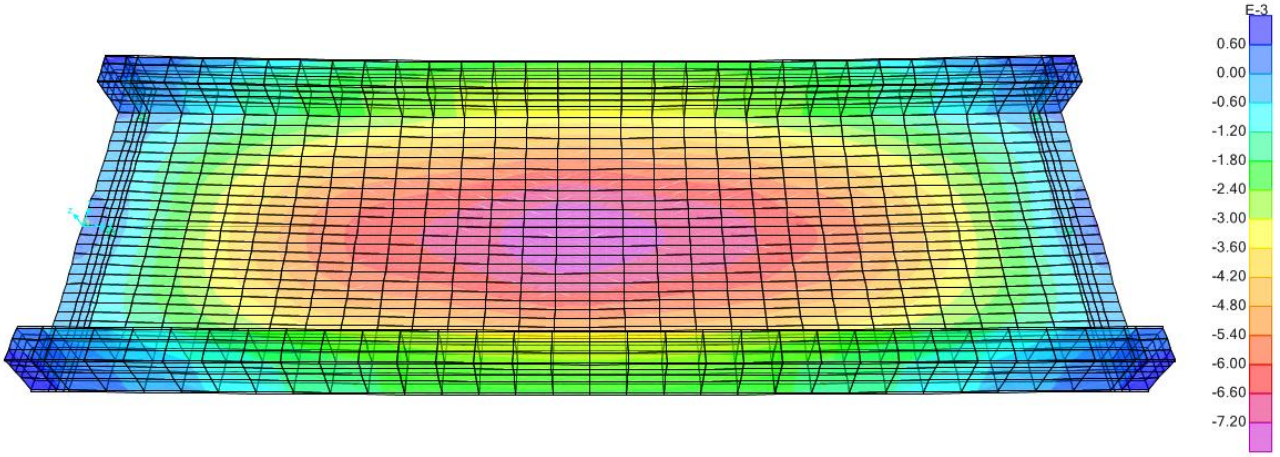

Type B: Speed 40 [m/sec]

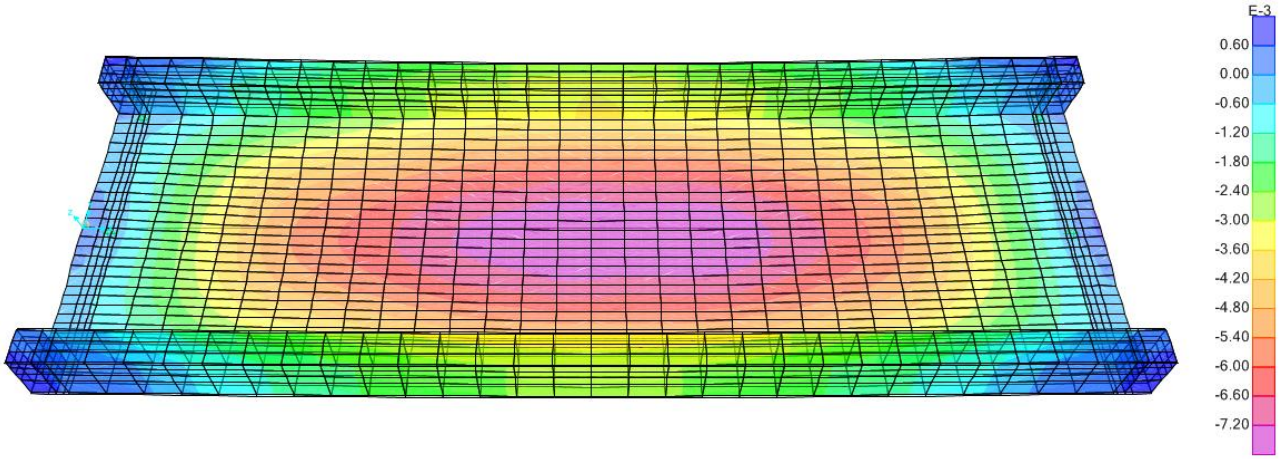

Type B: Speed 46 [m/sec]

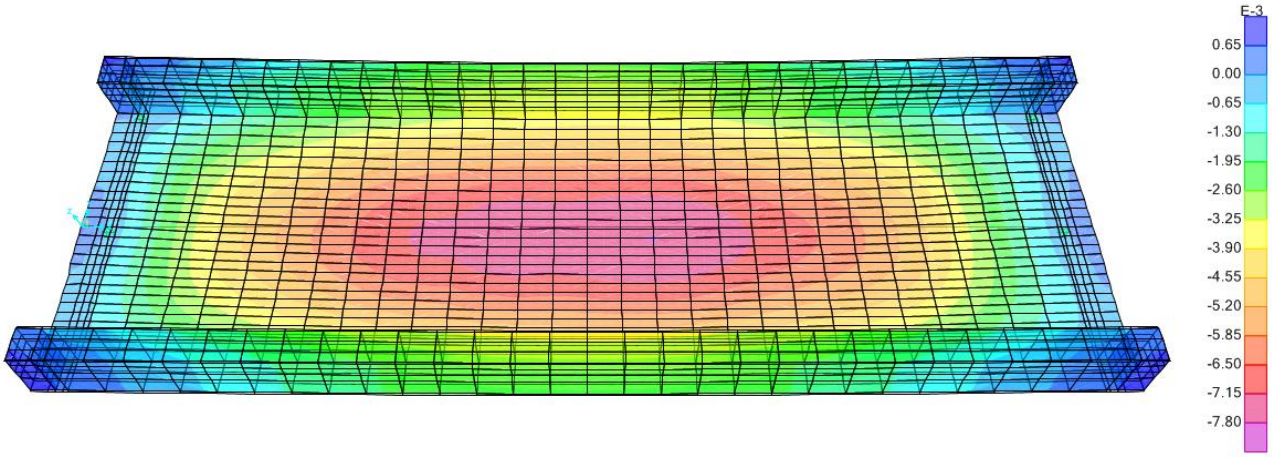

Type B: Speed 53 [m/sec]

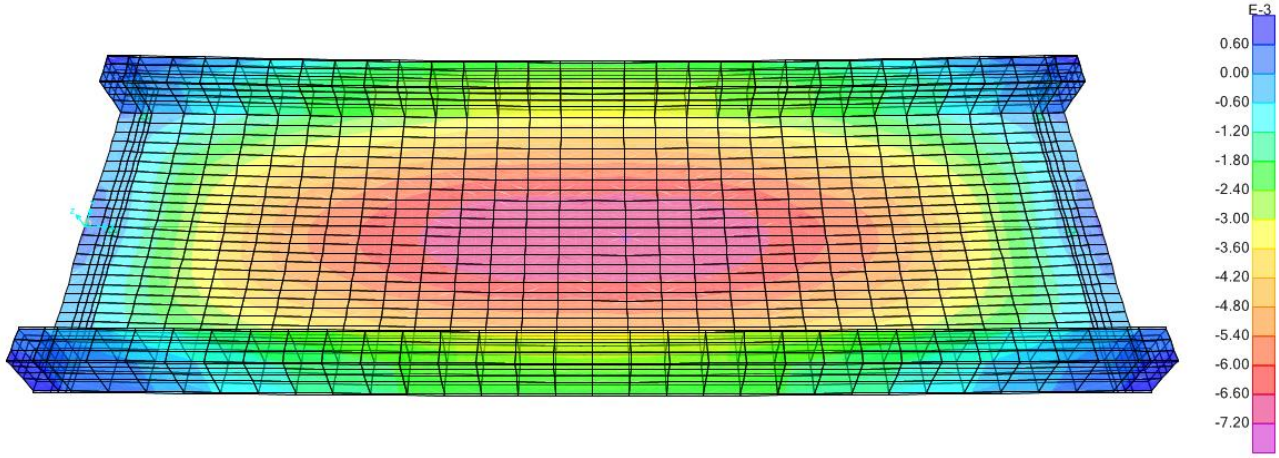

Type C: Speed 10 [m/sec]

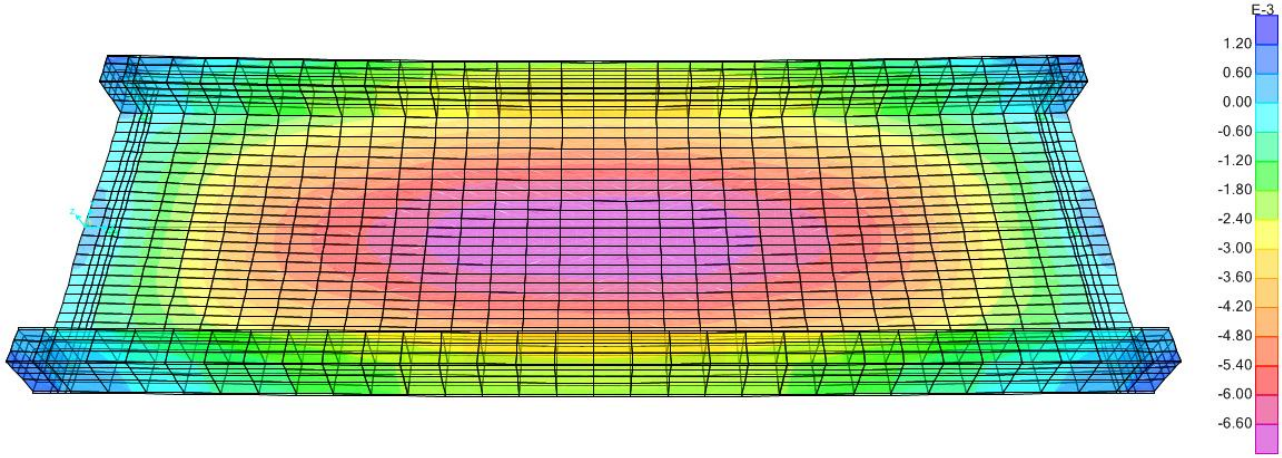

Type C: Speed 20 [m/sec]

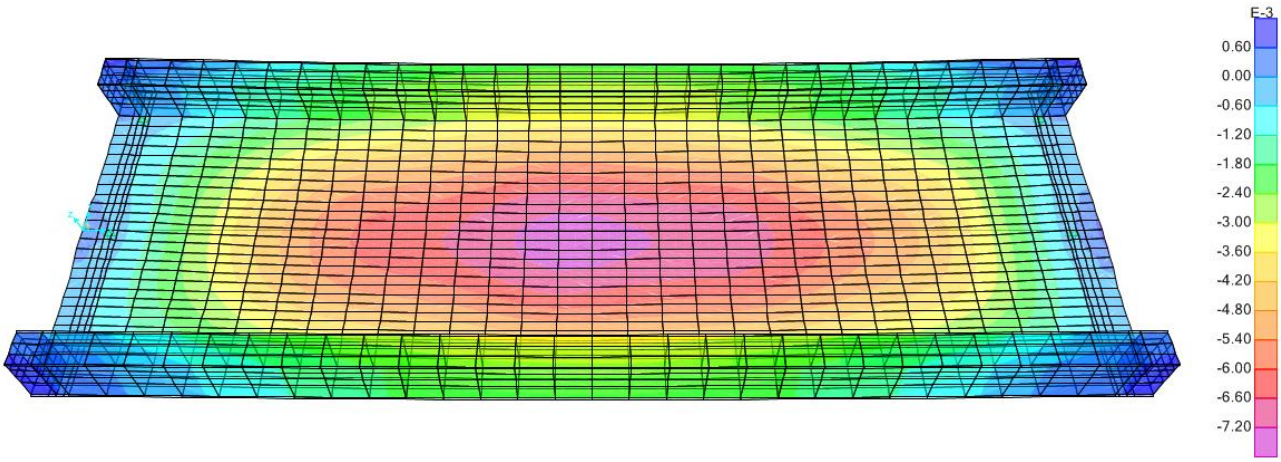

Type C: Speed 30 [m/sec]

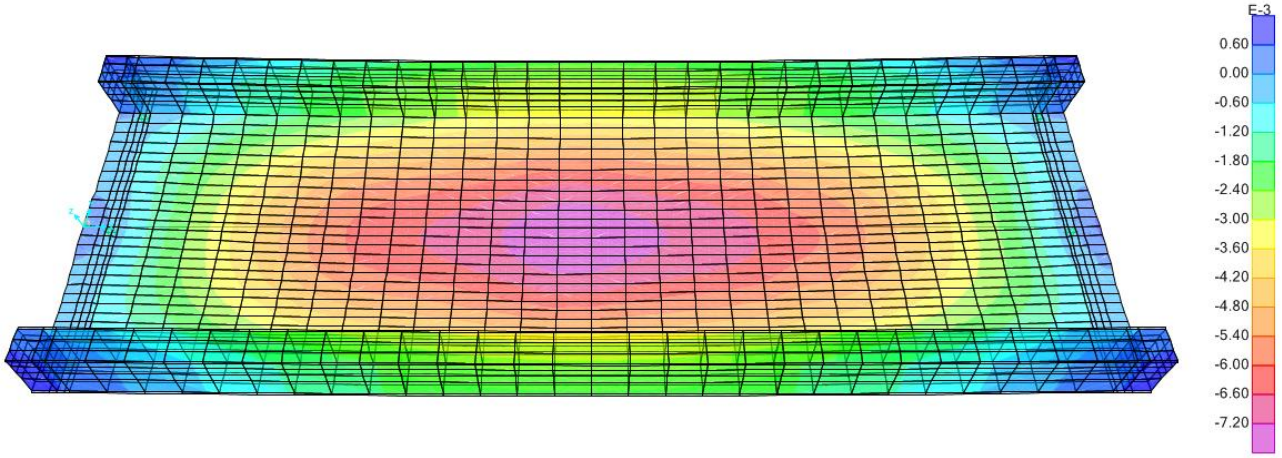

Type C: Speed 40 [m/sec]

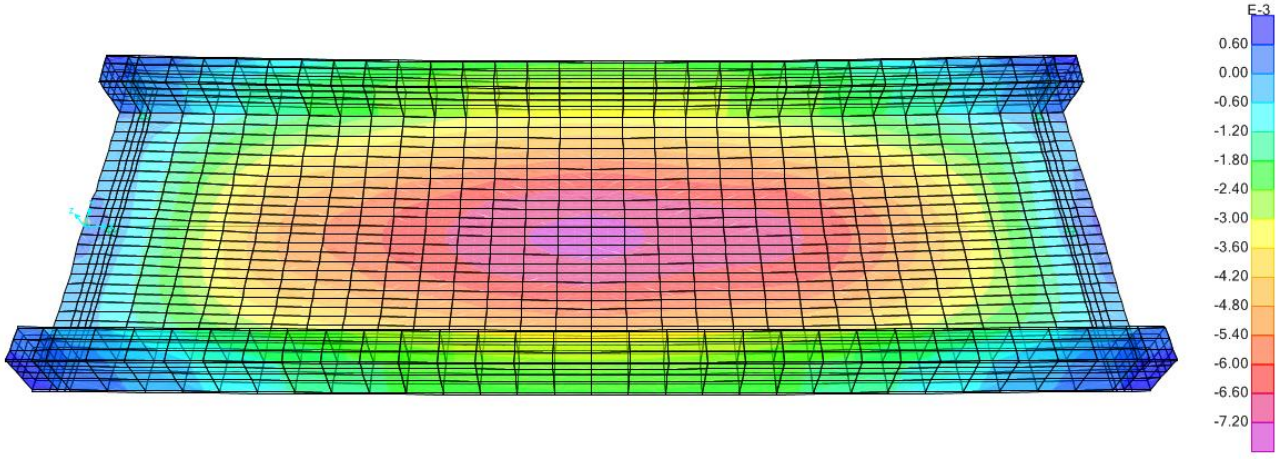

Type C: Speed 46 [m/sec]

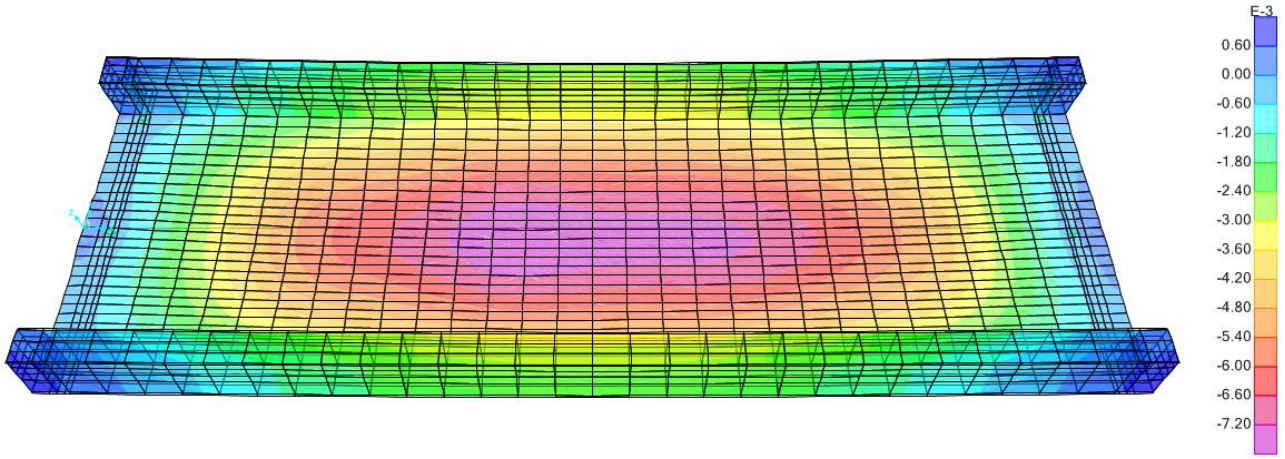

Type C: Speed 53 [m/sec]

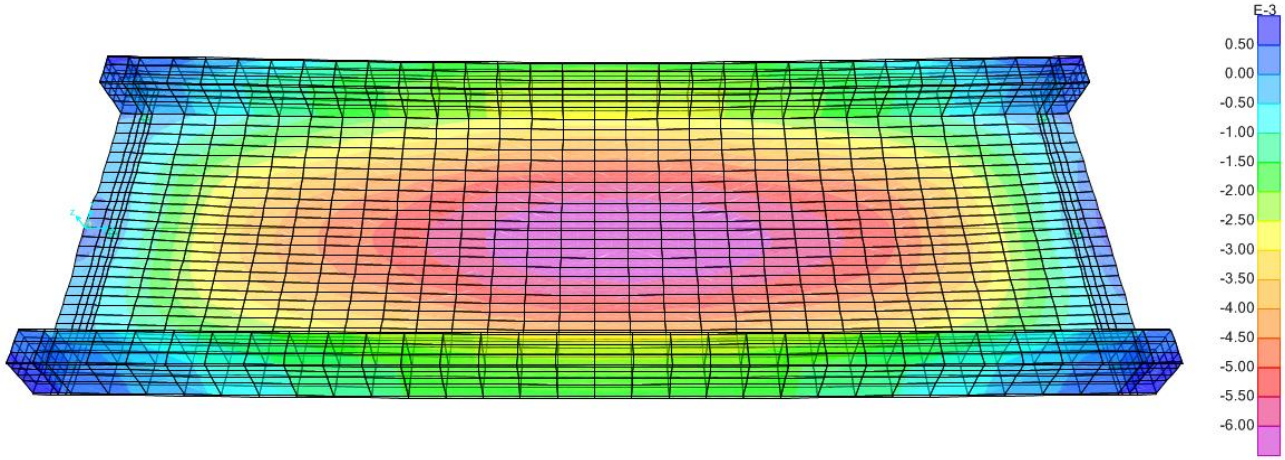

Type D: Speed 10 [m/sec]

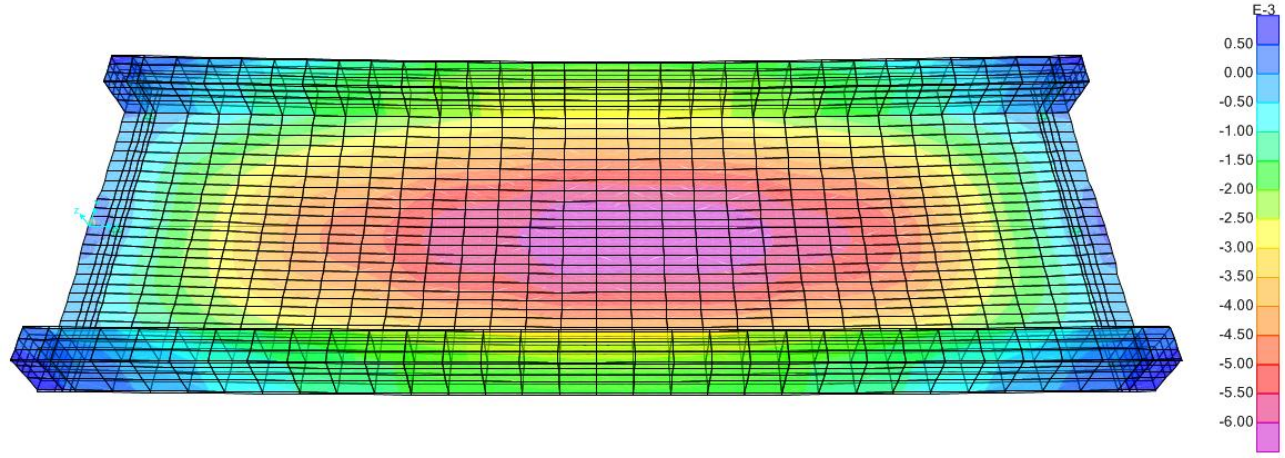

Type D: Speed 20 [m/sec]

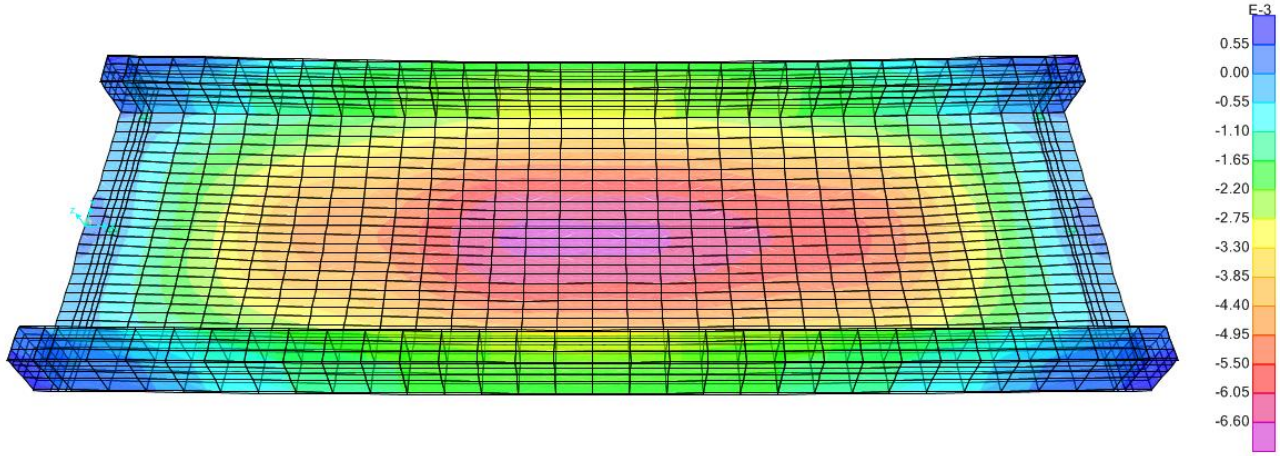

Type D: Speed 30 [m/sec]

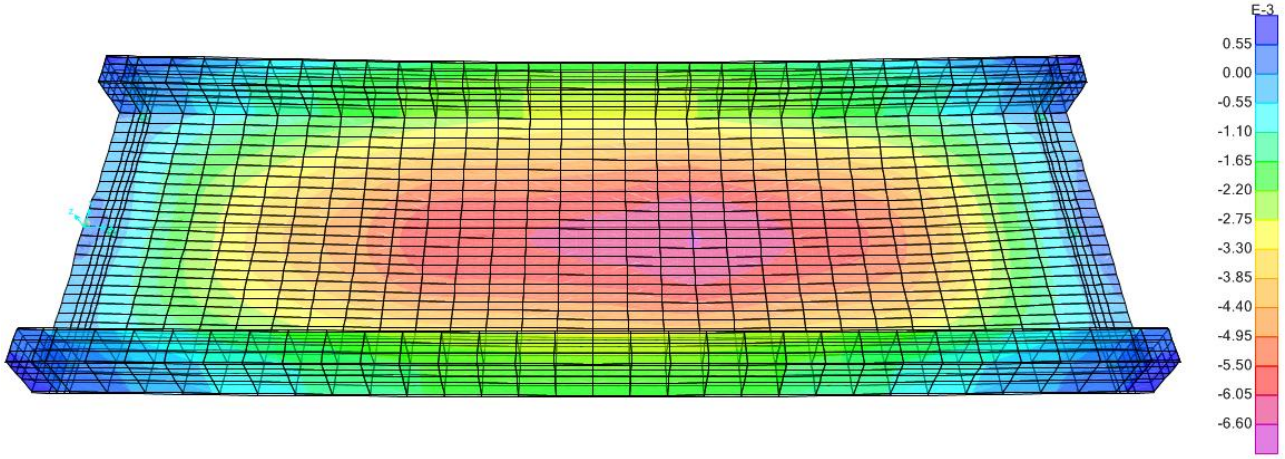

Type D: Speed 40 [m/sec]

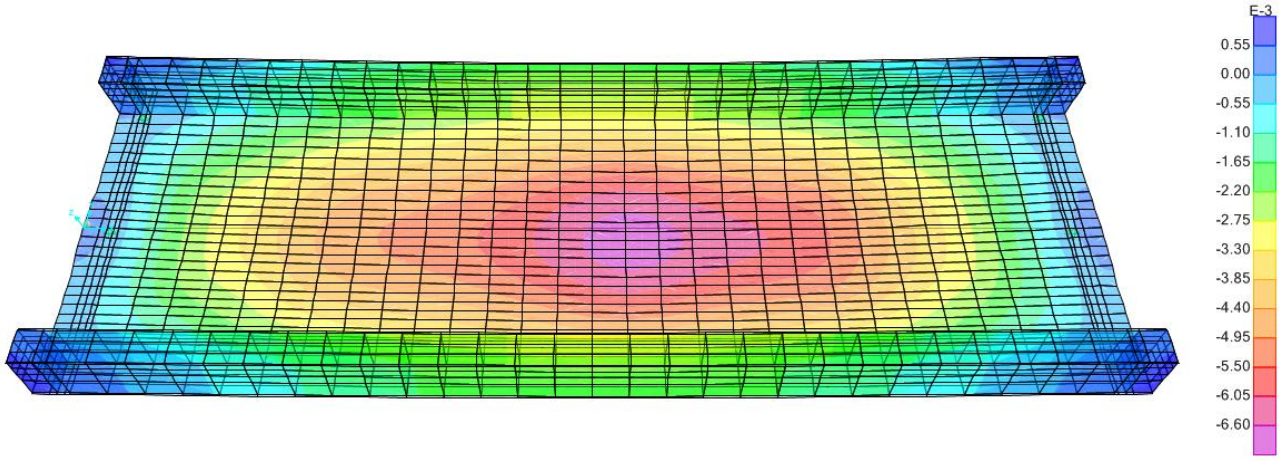

Type D: Speed 46 [m/sec]

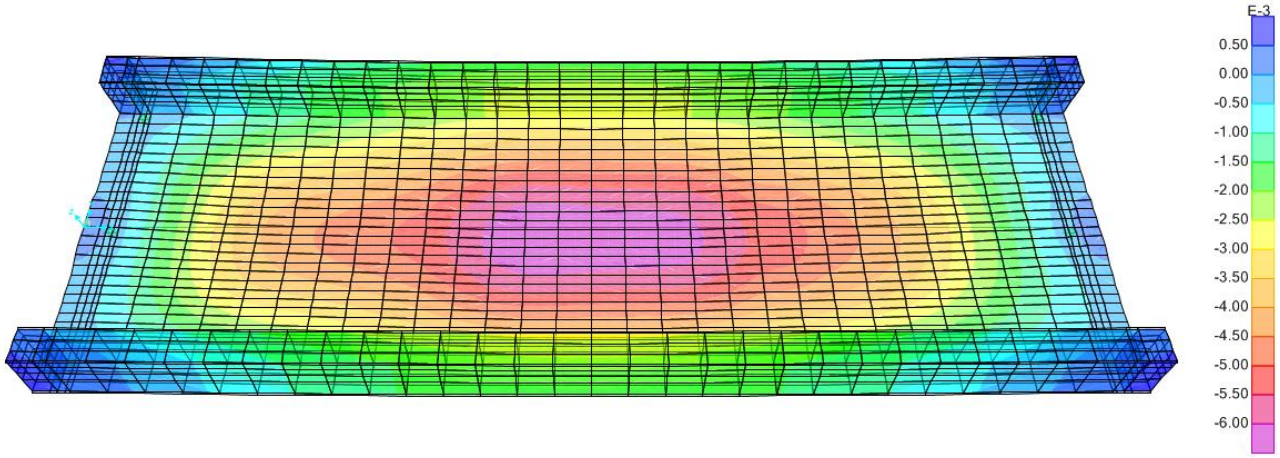

Type D: Speed 53 [m/sec]

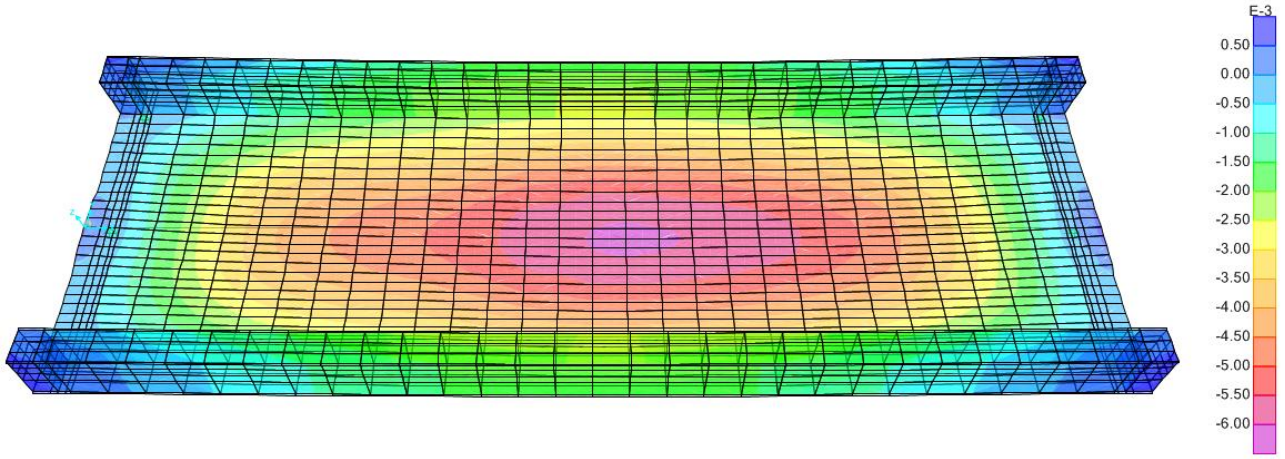

Type E: Speed 10 [m/sec]

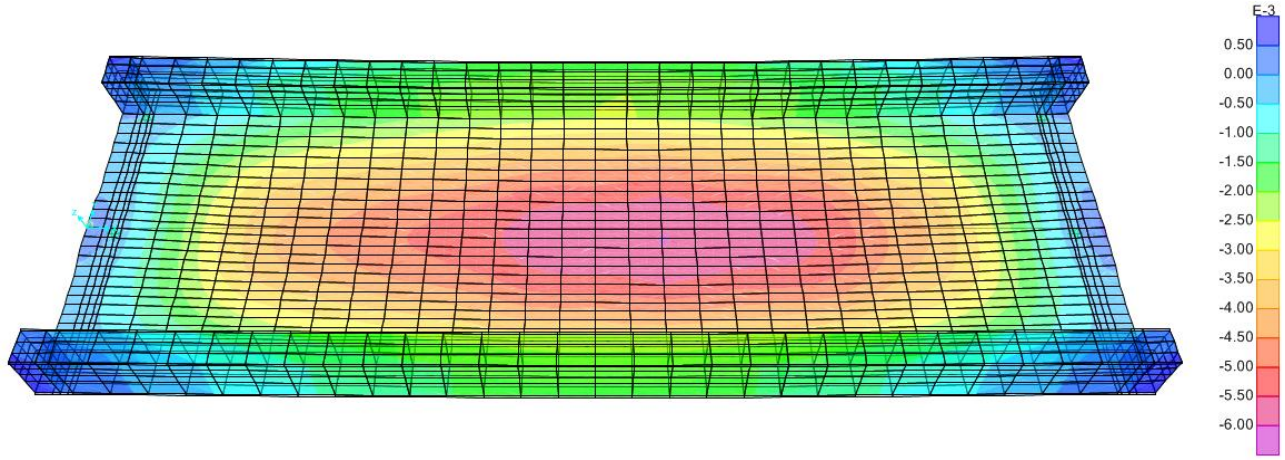

Type E: Speed 20 [m/sec]

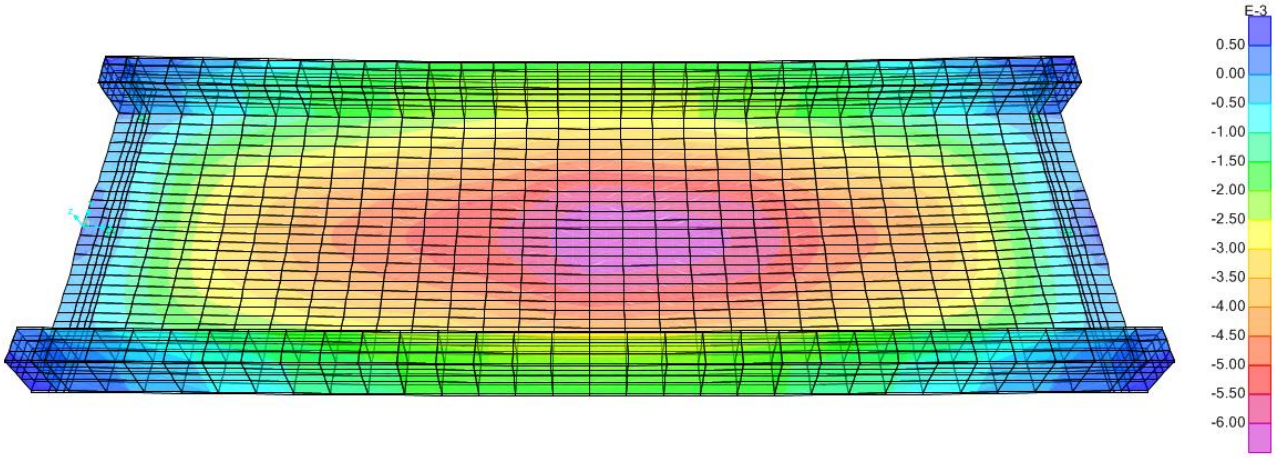

Type E: Speed 30 [m/sec]

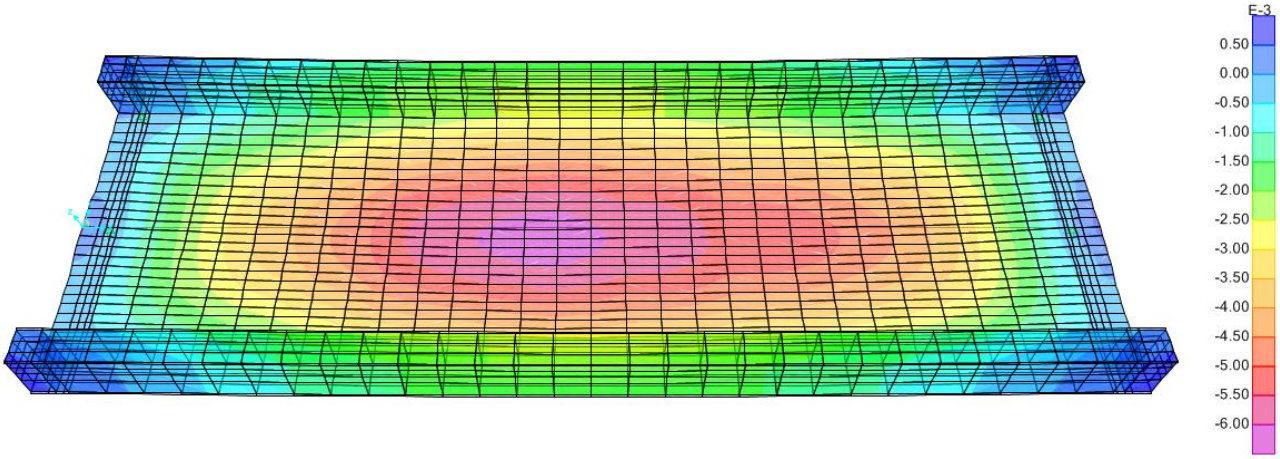

Type E: Speed 40 [m/sec]

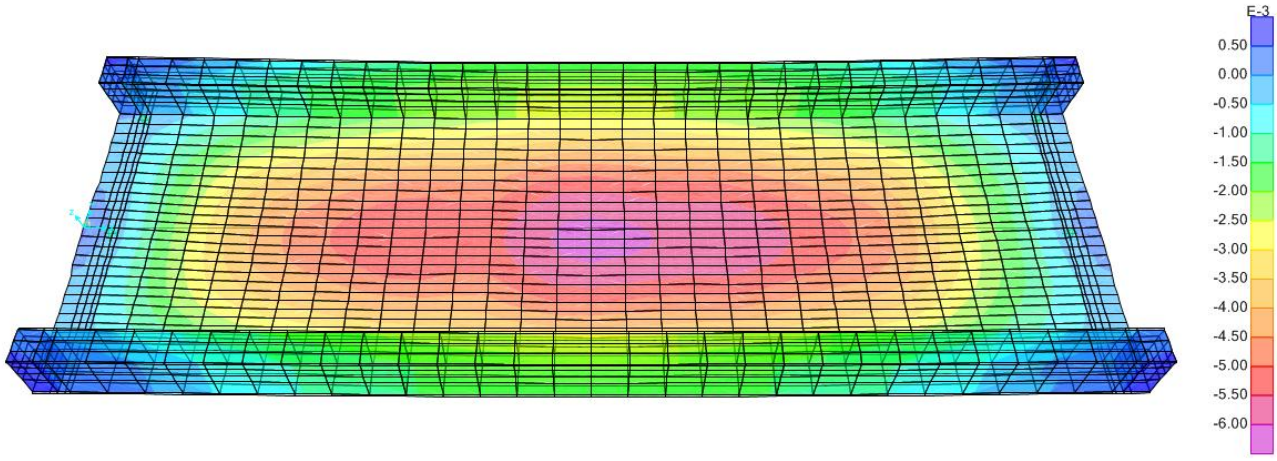

Type E: Speed 46 [m/sec]

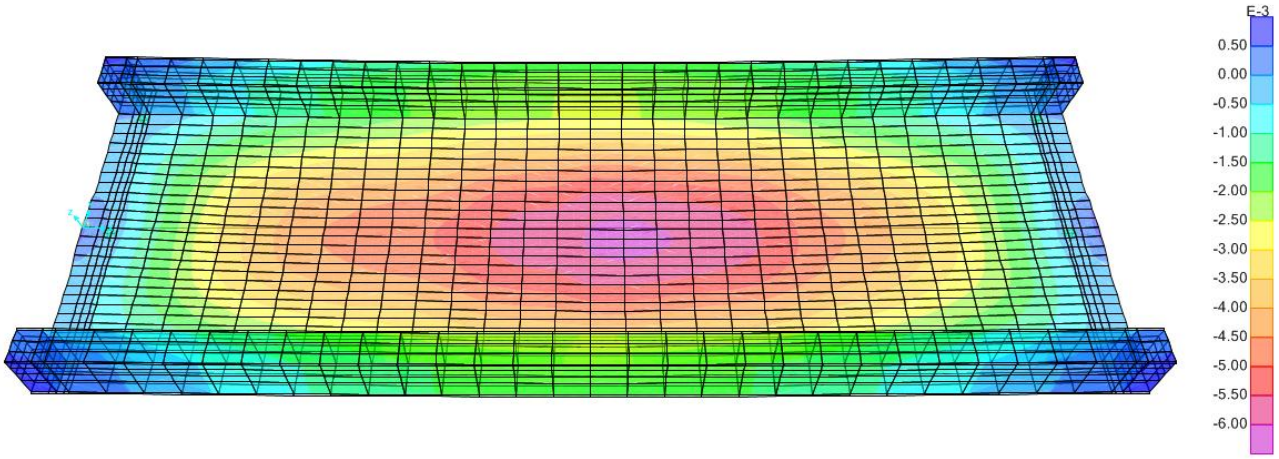

Type E: Speed 53 [m/sec]

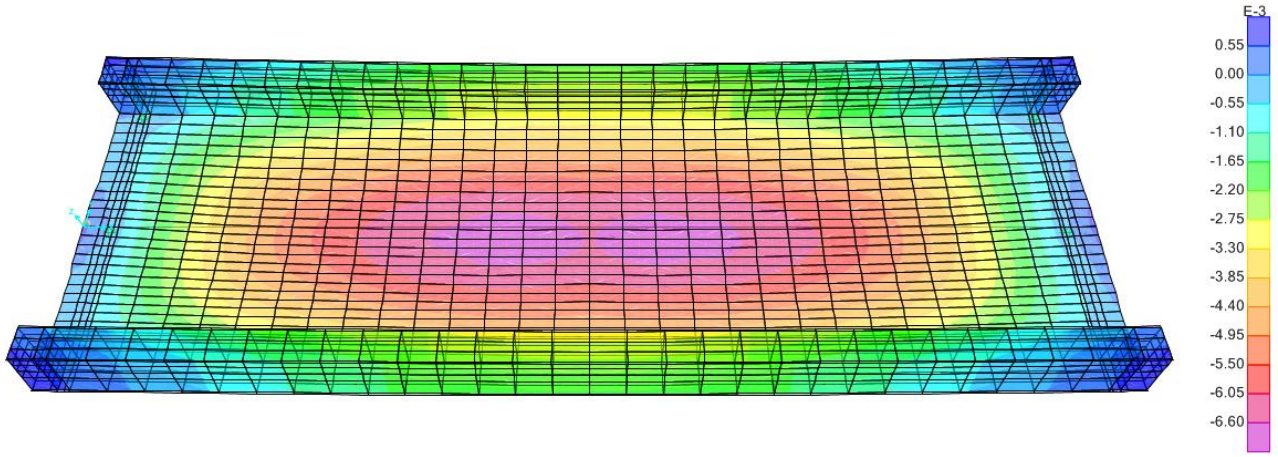

Type F: Speed 10 [m/sec]

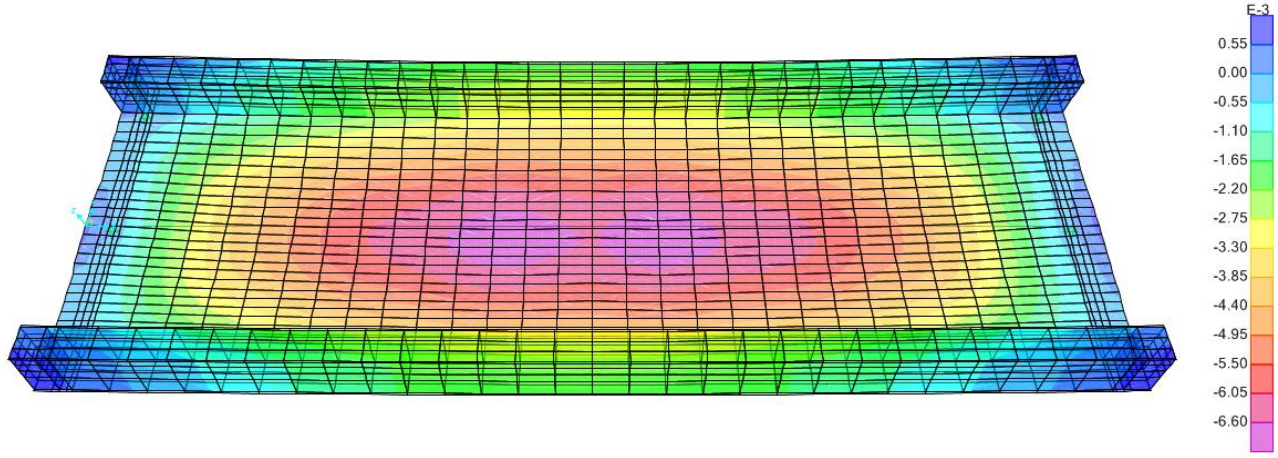

Type F: Speed 20 [m/sec]

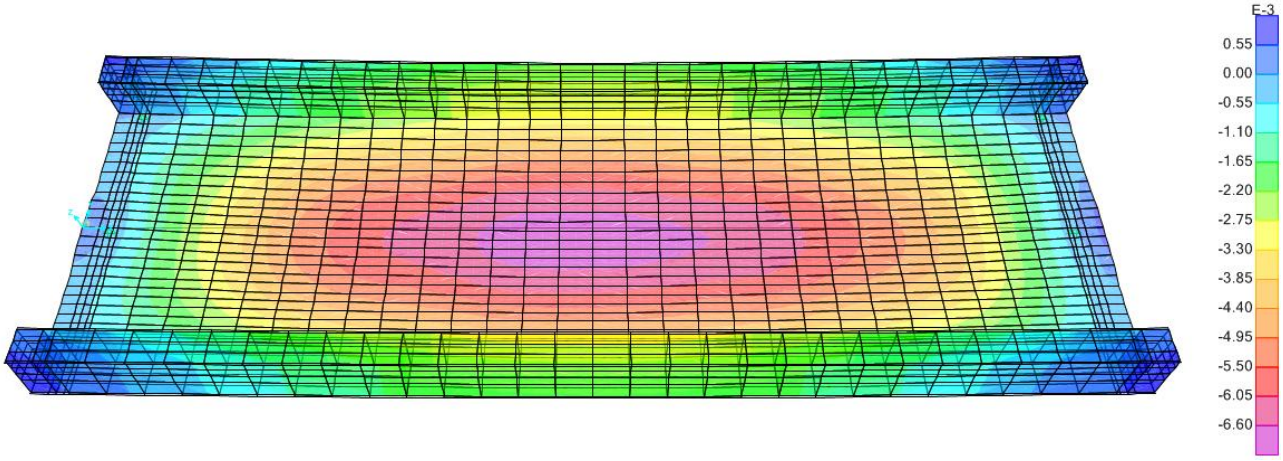

Type F: Speed 30 [m/sec]

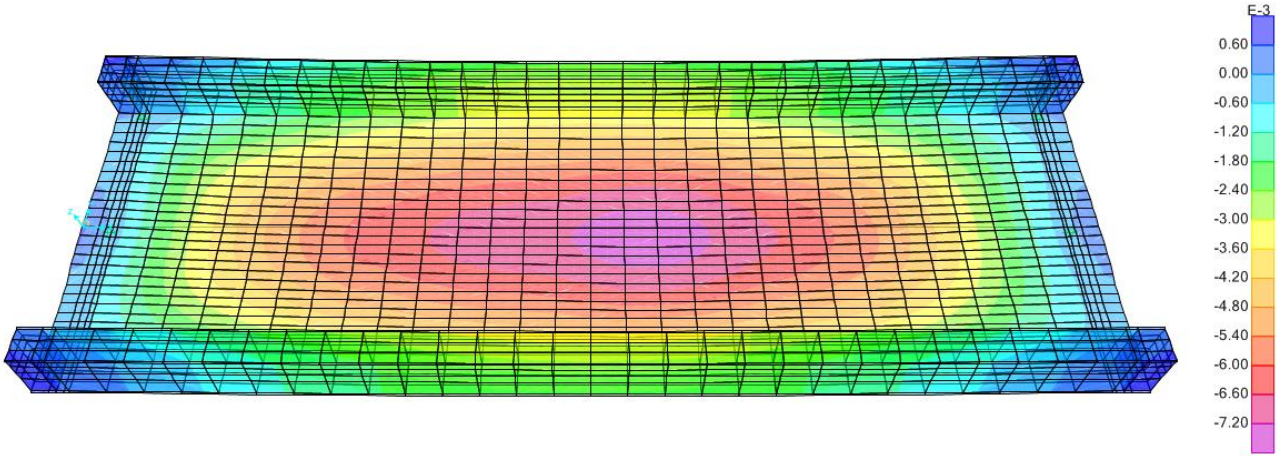

Type F: Speed 40 [m/sec]

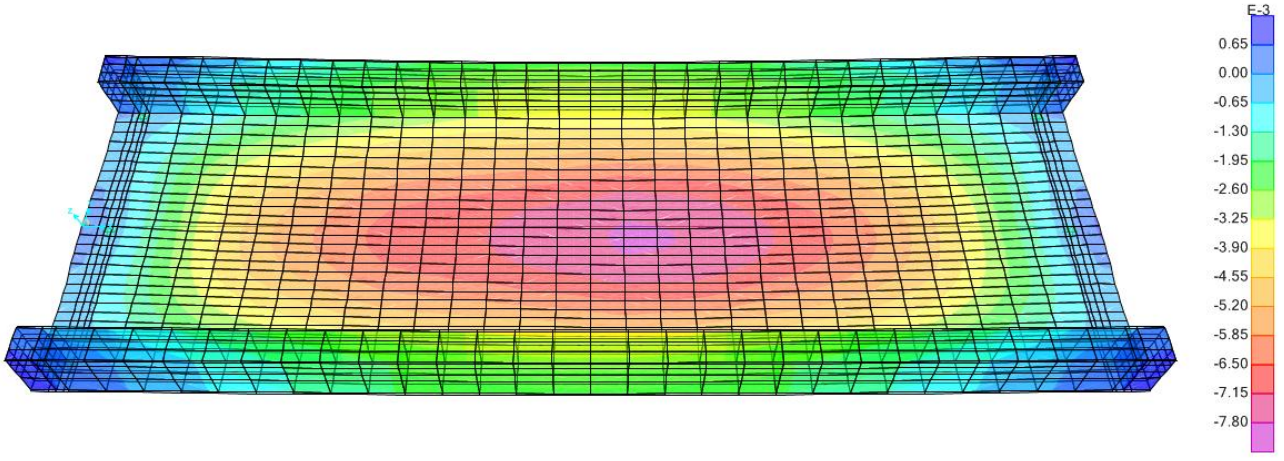

Type F: Speed 46 [m/sec]

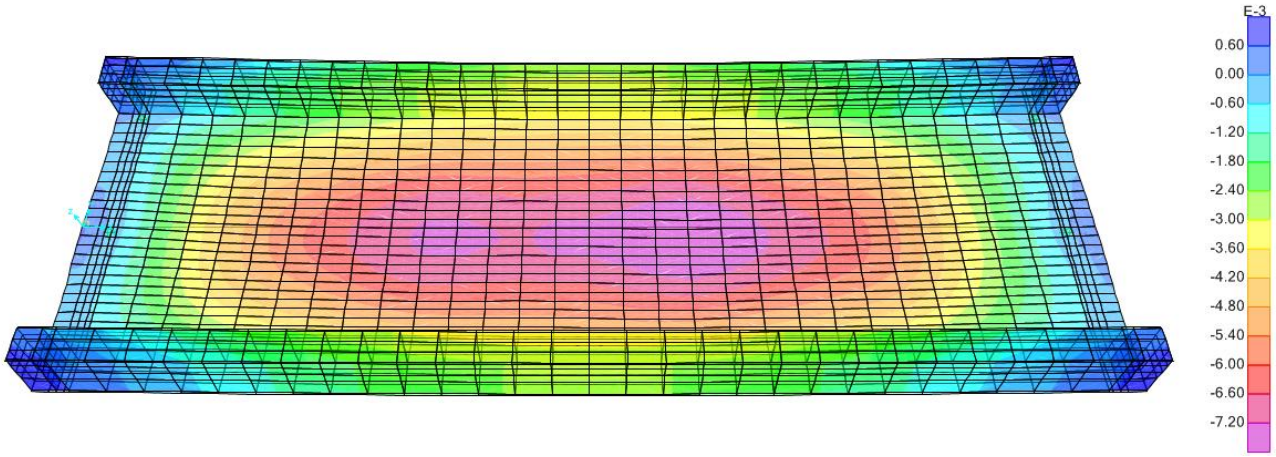

Type F: Speed 53 [m/sec]

9.5) Results for 3 Bearings , 6 meters span

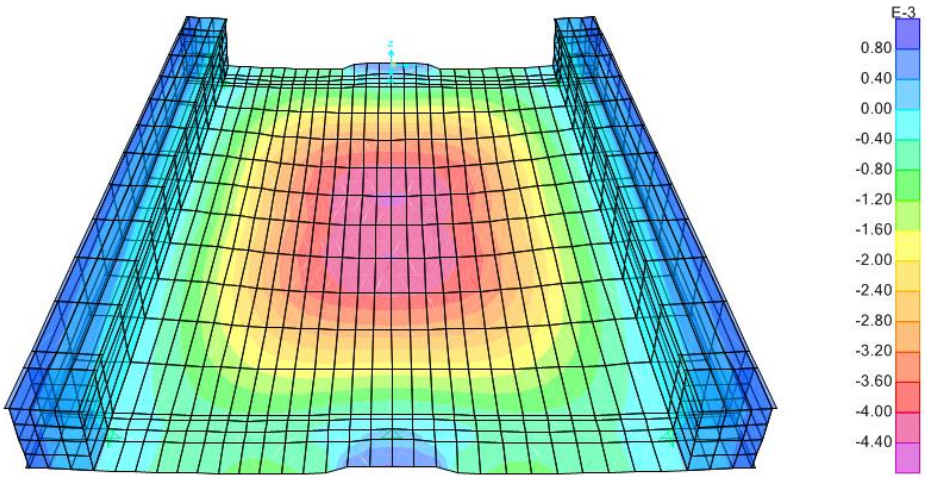

Type A: Speed 10 [m/sec]

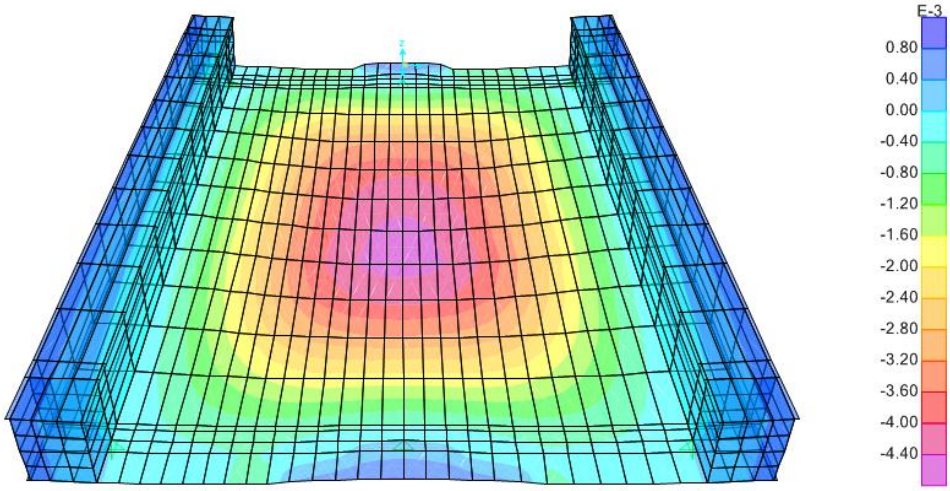

Type A: Speed 20 [m/sec]

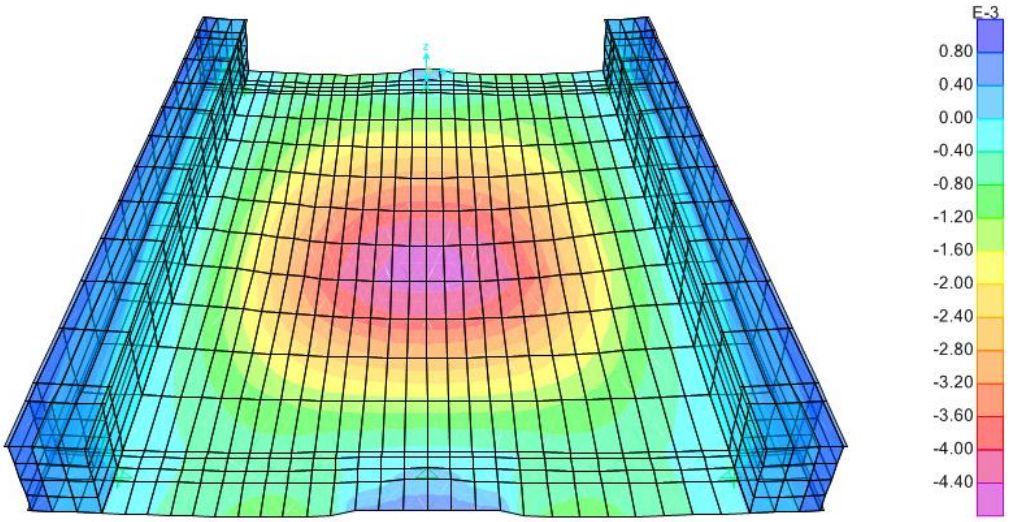

Type A: Speed 30 [m/sec]

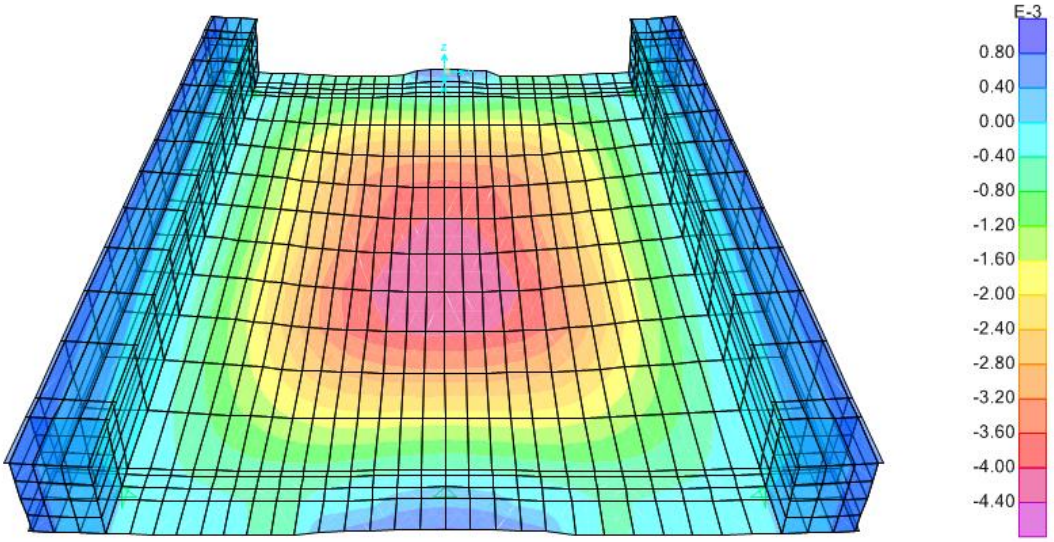

Type A: Speed 40 [m/sec]

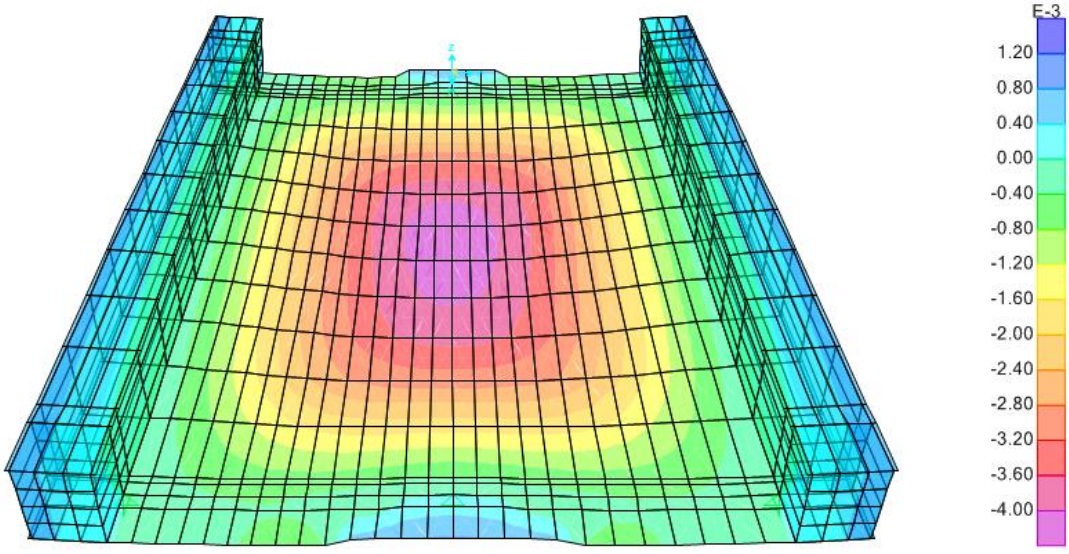

Type A: Speed 46 [m/sec]

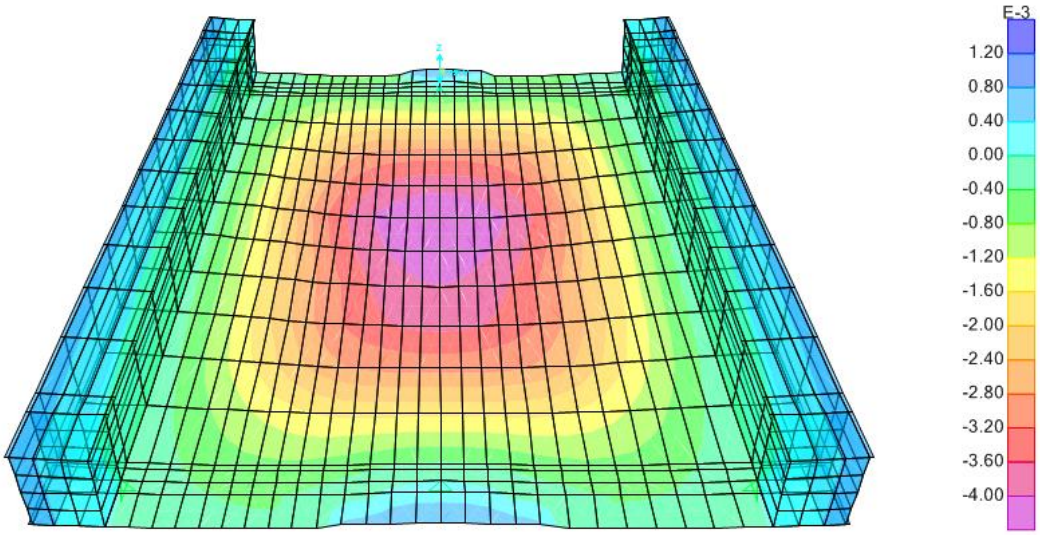

Type A: Speed 53 [m/sec]

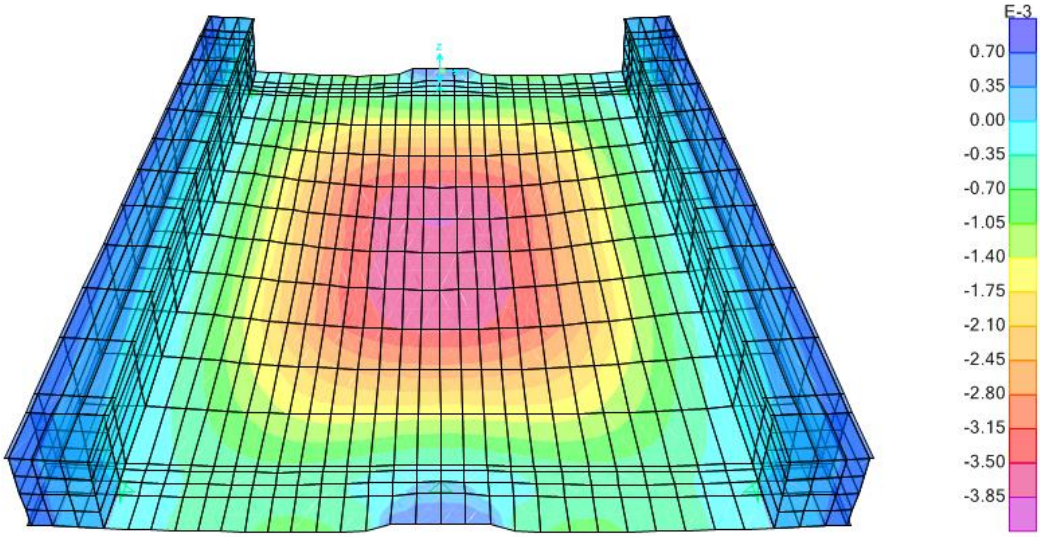

Type B: Speed 10 [m/sec]

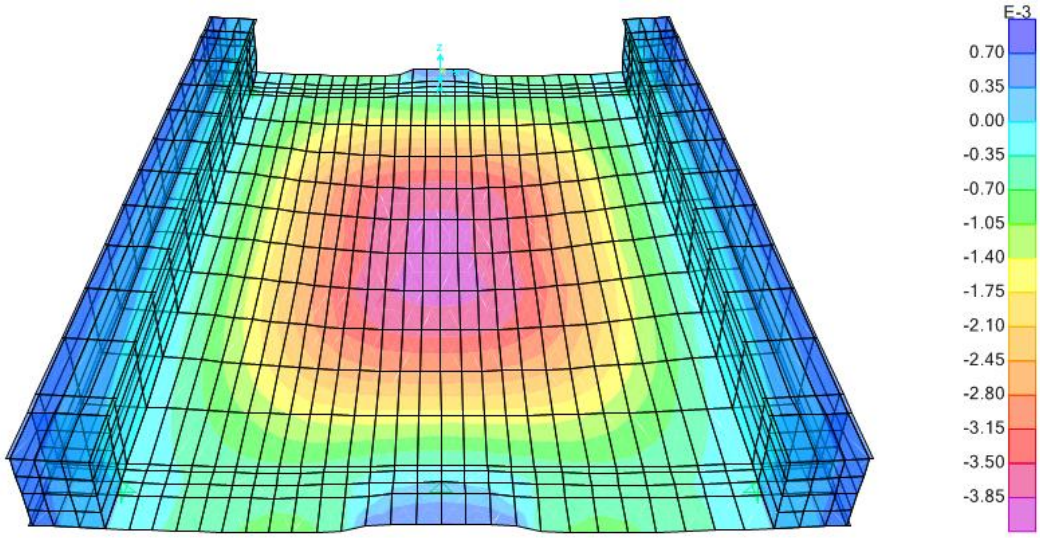

Type B: Speed 20 [m/sec]

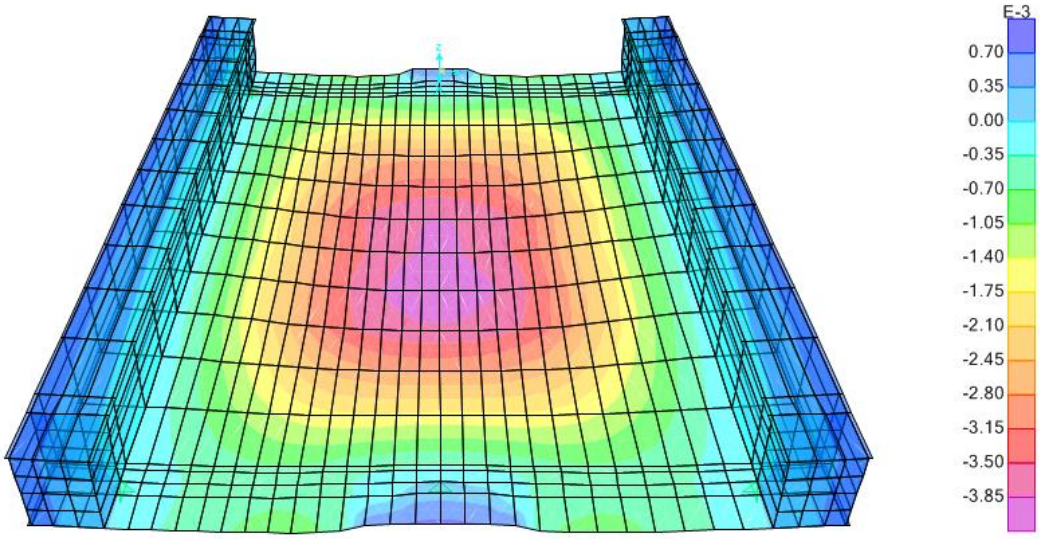

Type B: Speed 30 [m/sec]

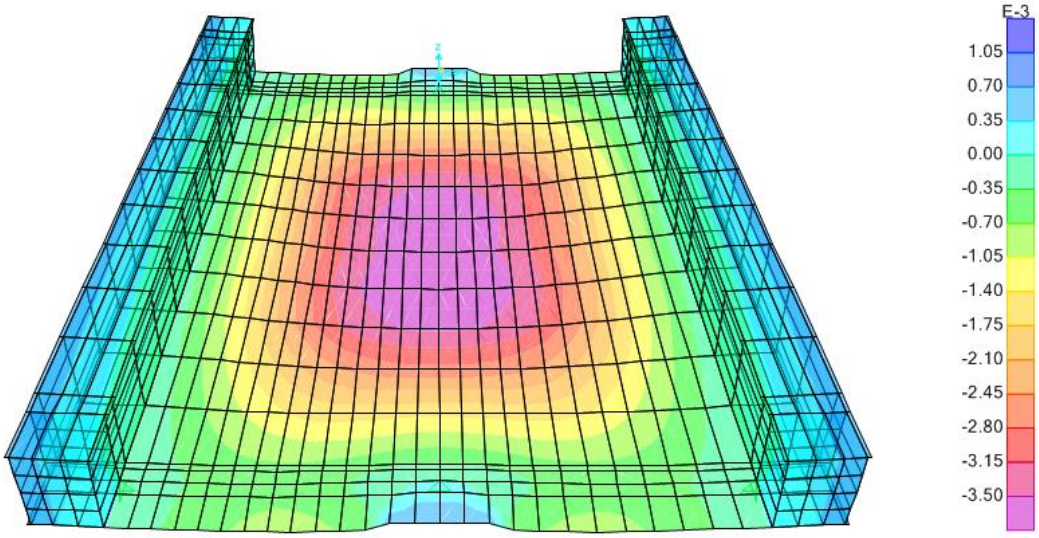

Type B: Speed 40 [m/sec]

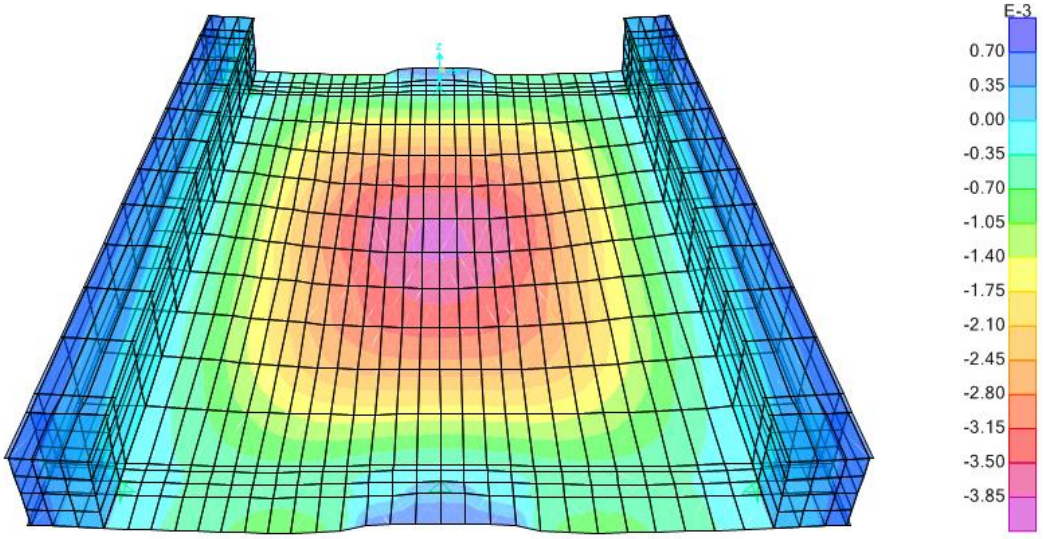

Type B: Speed 46 [m/sec]

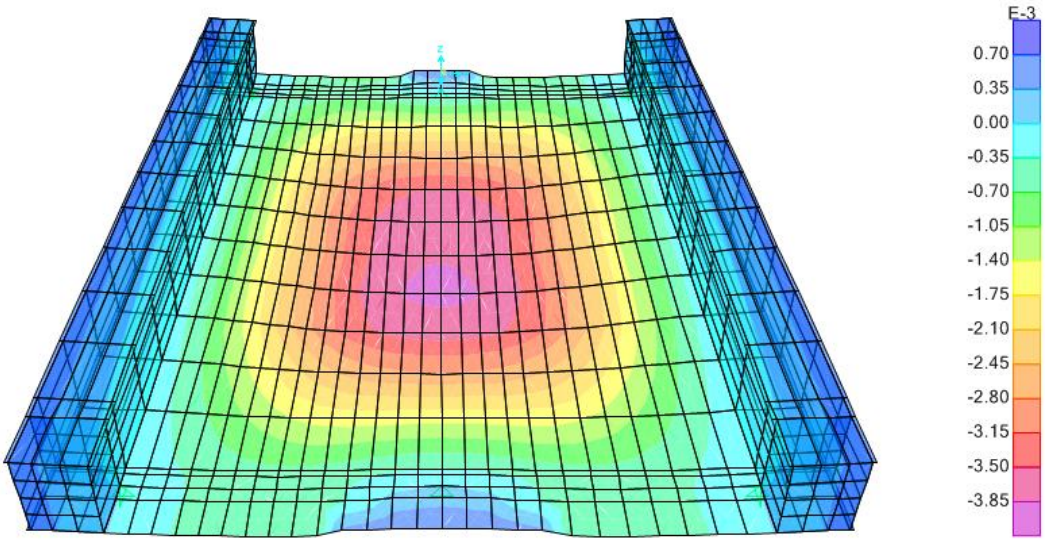

Type B: Speed 53 [m/sec]

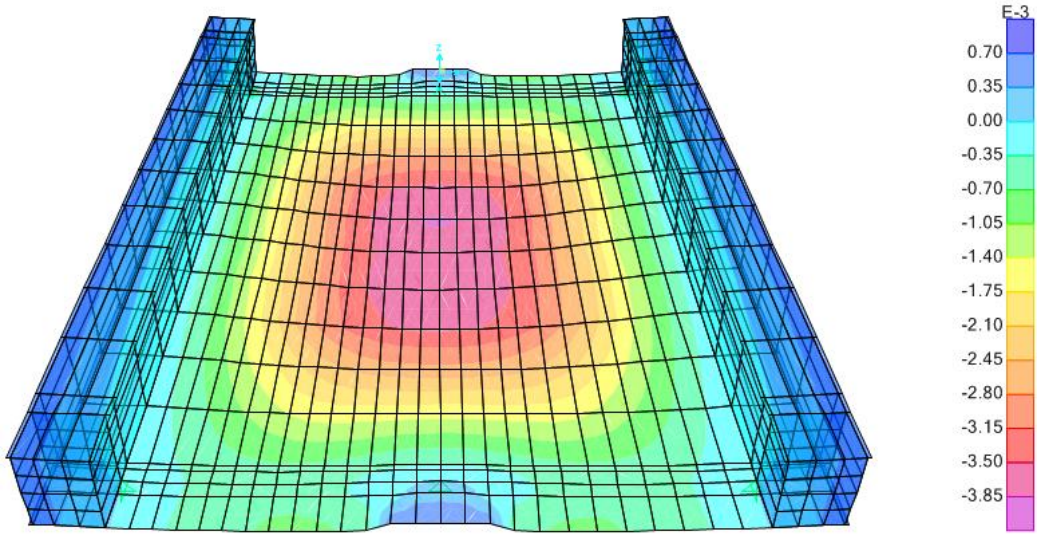

Type C: Speed 10 [m/sec]

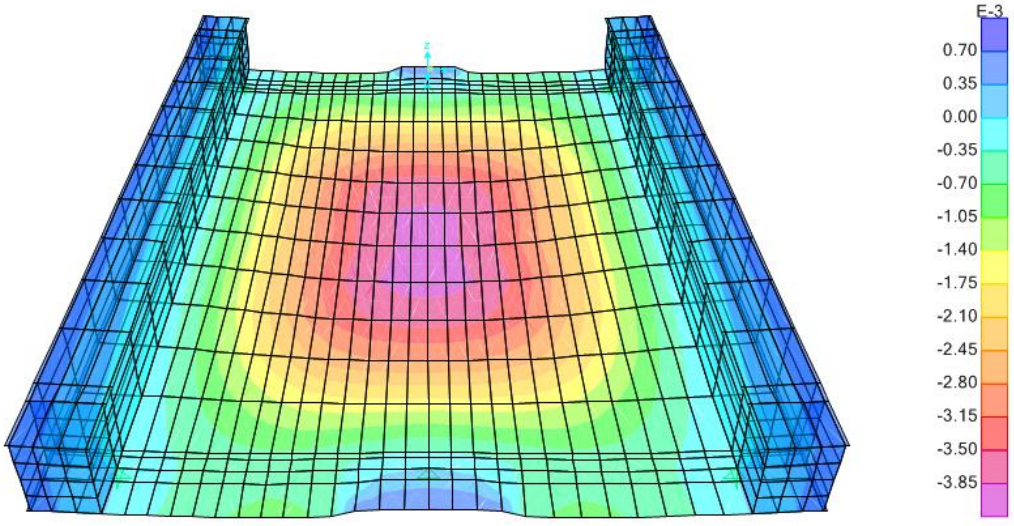

Type C: Speed 20 [m/sec]

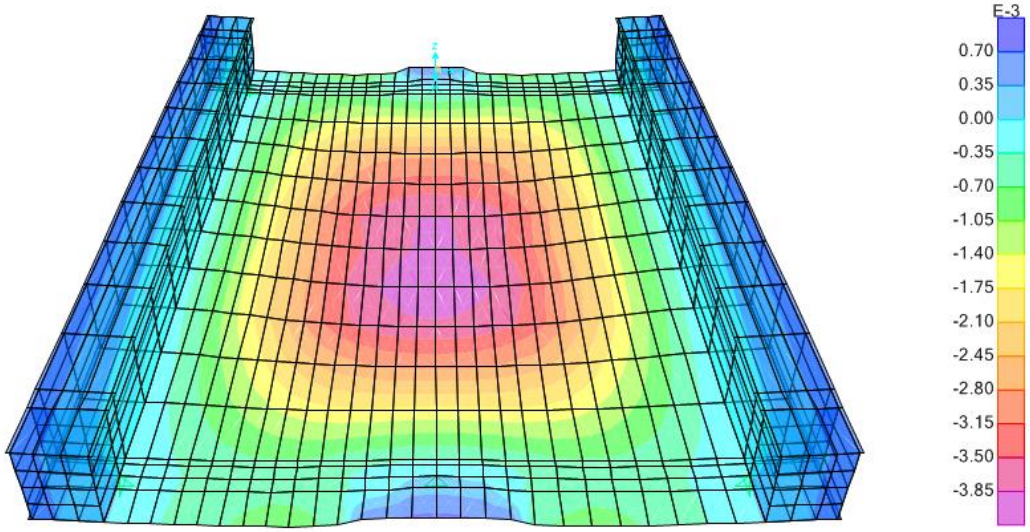

Type C: Speed 30 [m/sec]

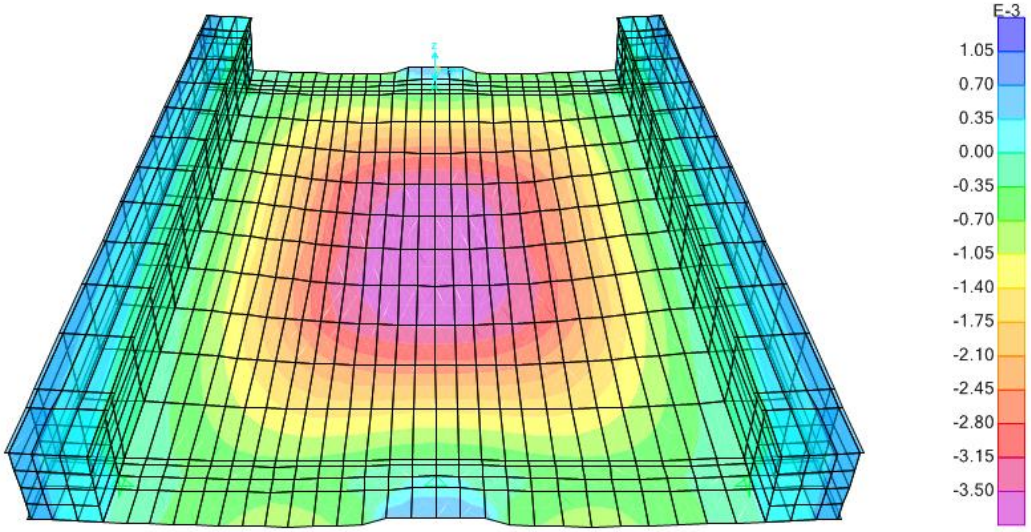

Type C: Speed 40 [m/sec]

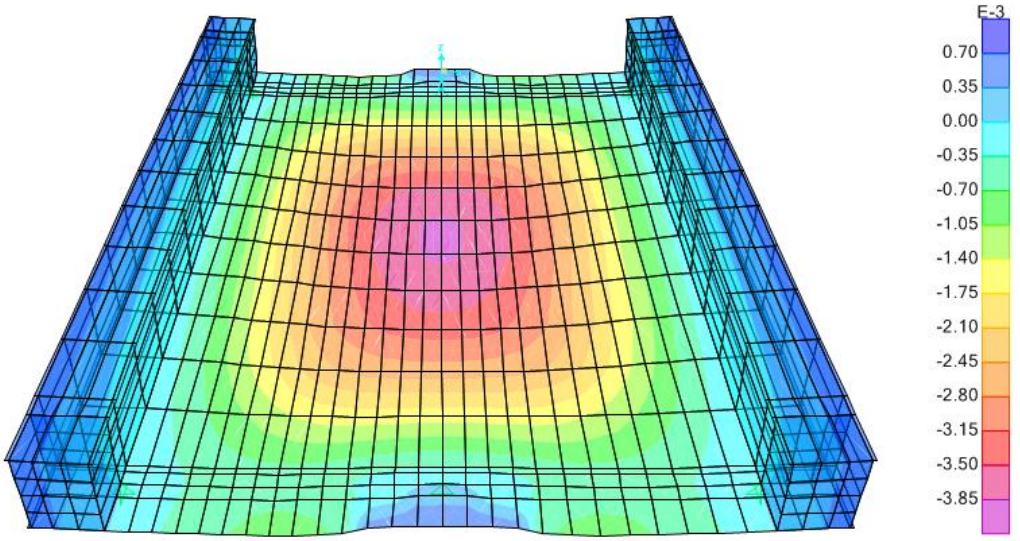

Type C: Speed 46 [m/sec]

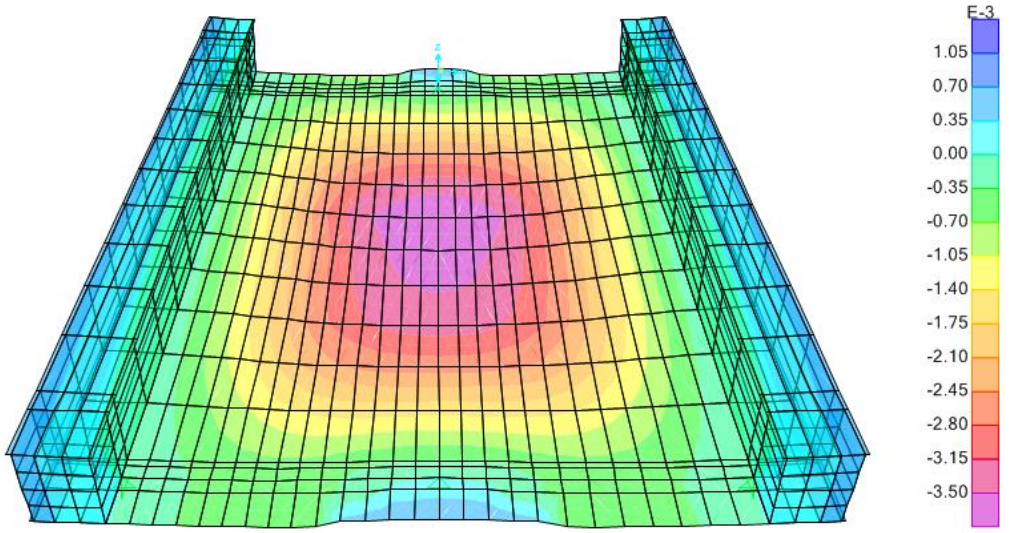

Type C: Speed 53 [m/sec]

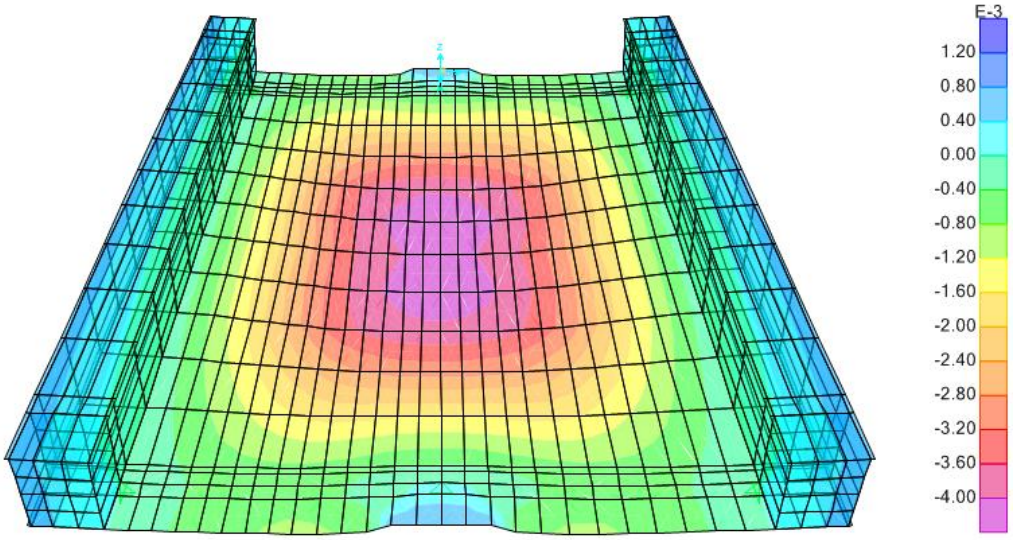

Type D: Speed 10 [m/sec]

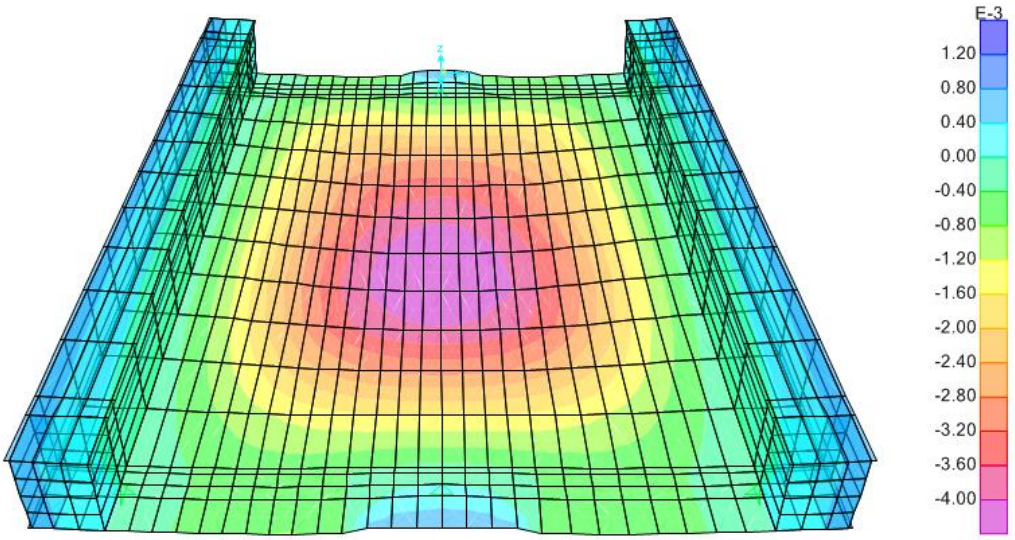

Type D: Speed 20 [m/sec]

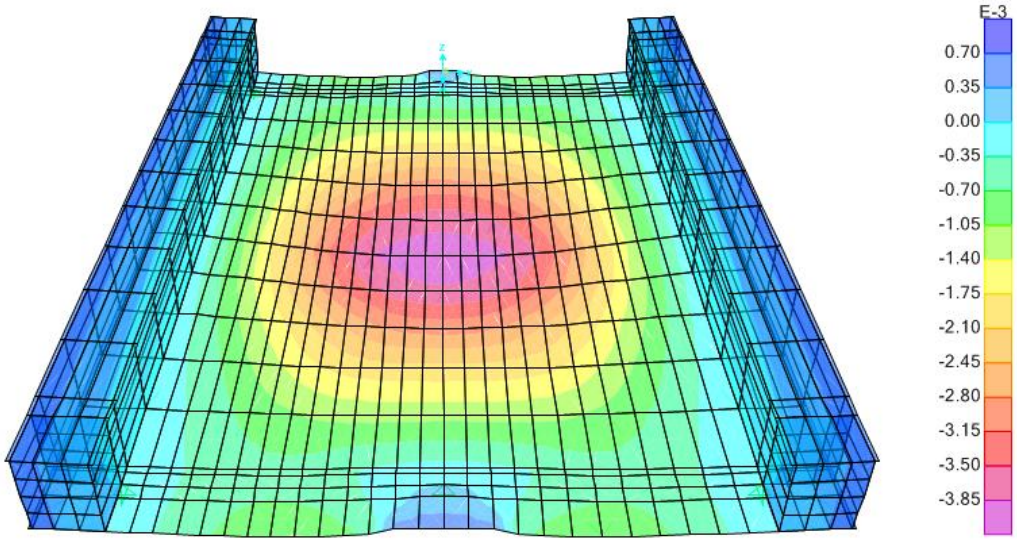

Type D: Speed 30 [m/sec]

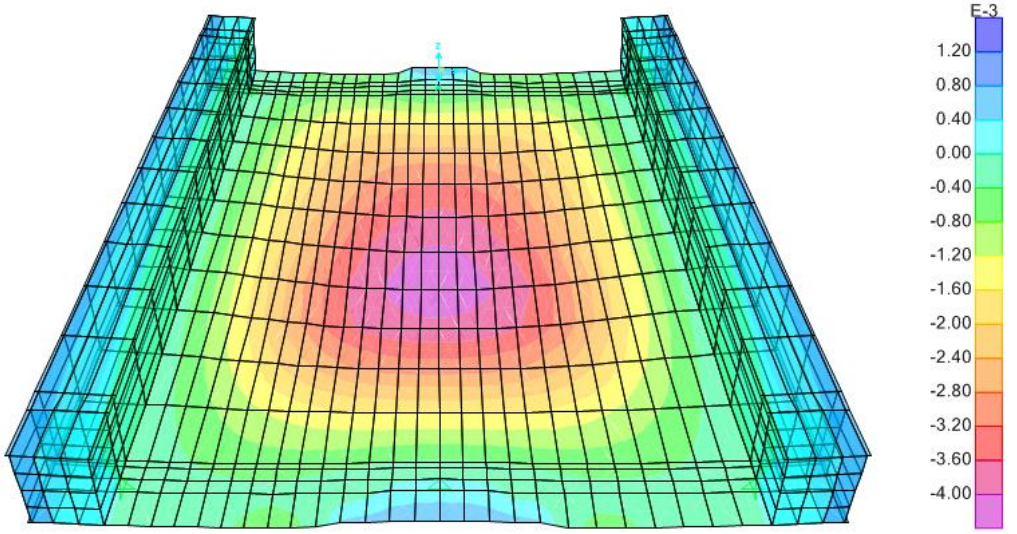

Type D: Speed 40 [m/sec]

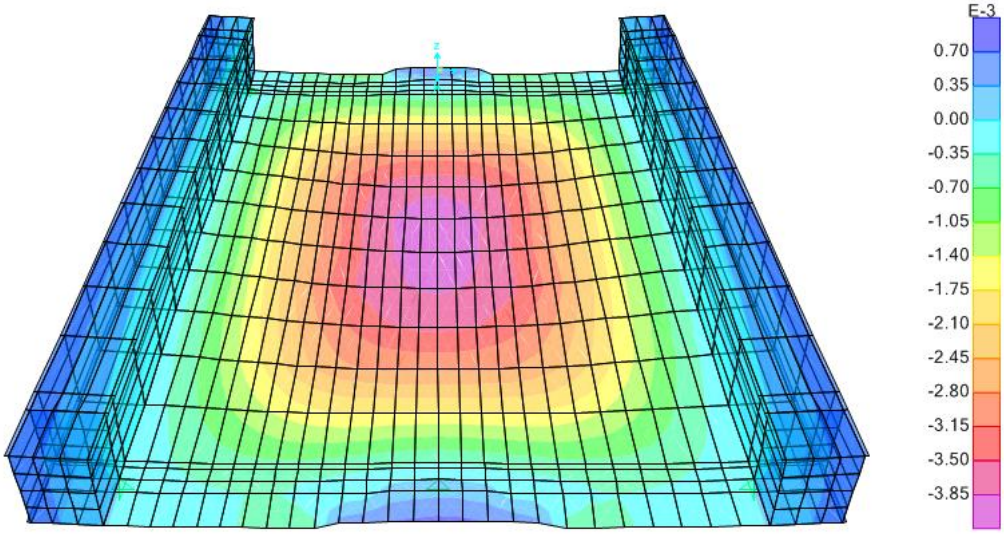

Type D: Speed 46 [m/sec]

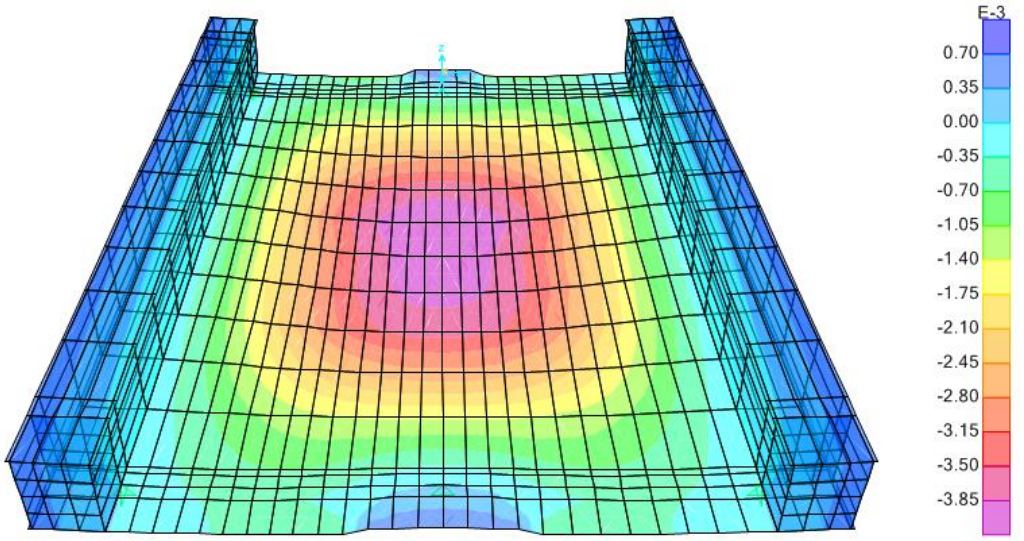

Type D: Speed 53 [m/sec]

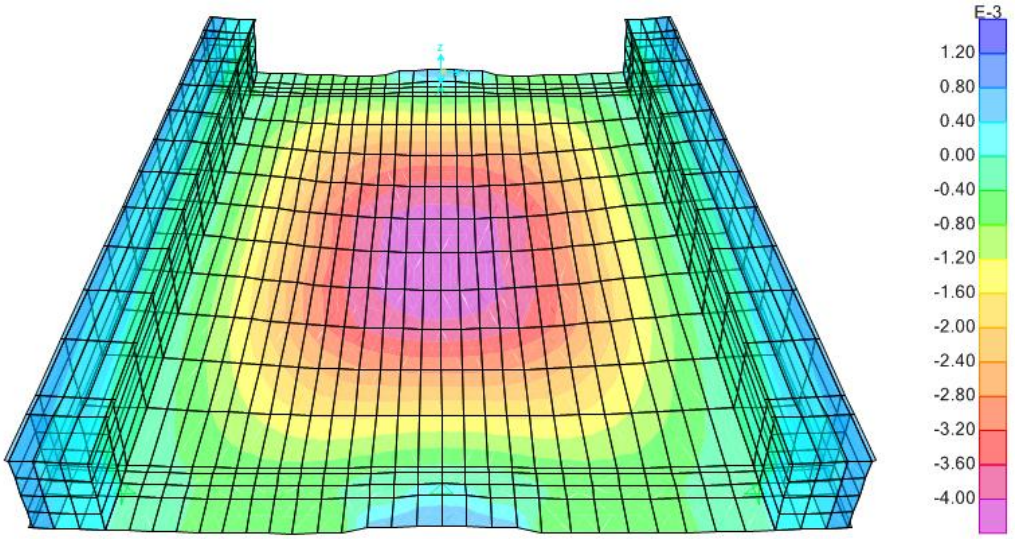

Type E: Speed 10 [m/sec]

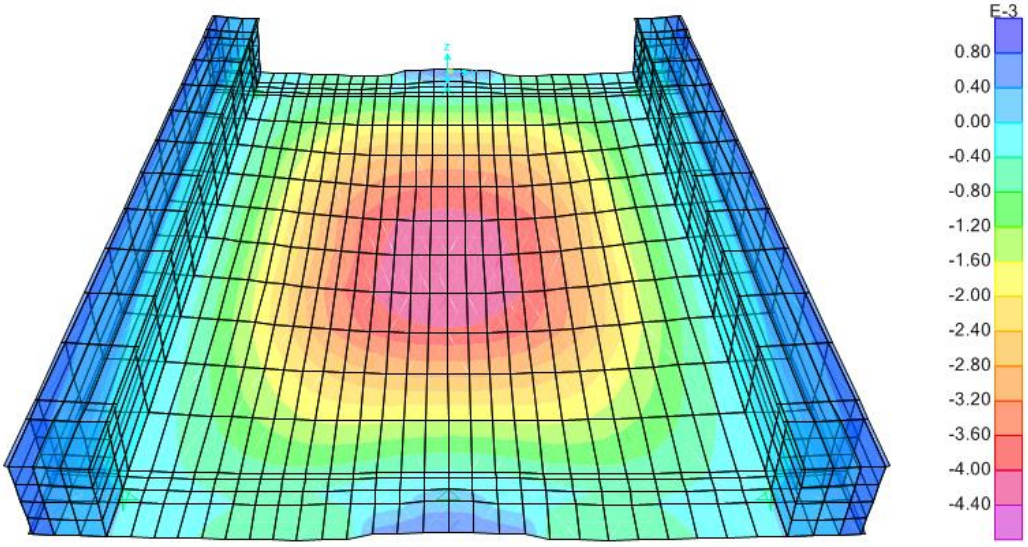

Type E: Speed 20 [m/sec]

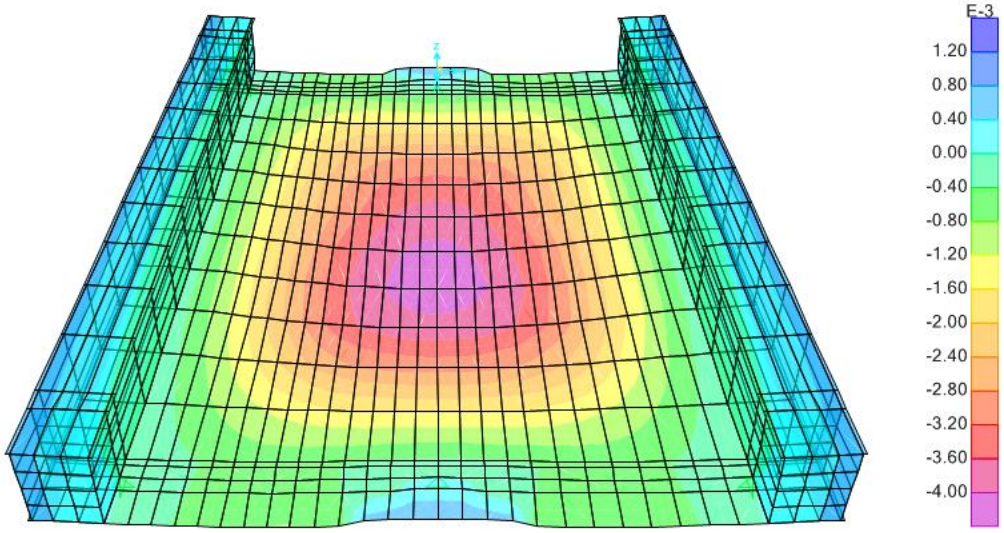

Type E: Speed 30 [m/sec]

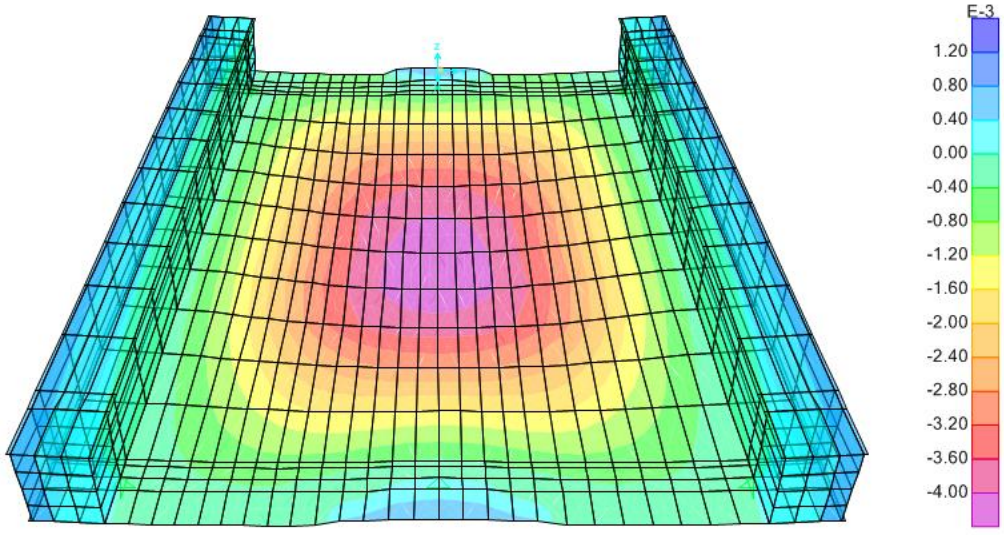

Type E: Speed 40 [m/sec]

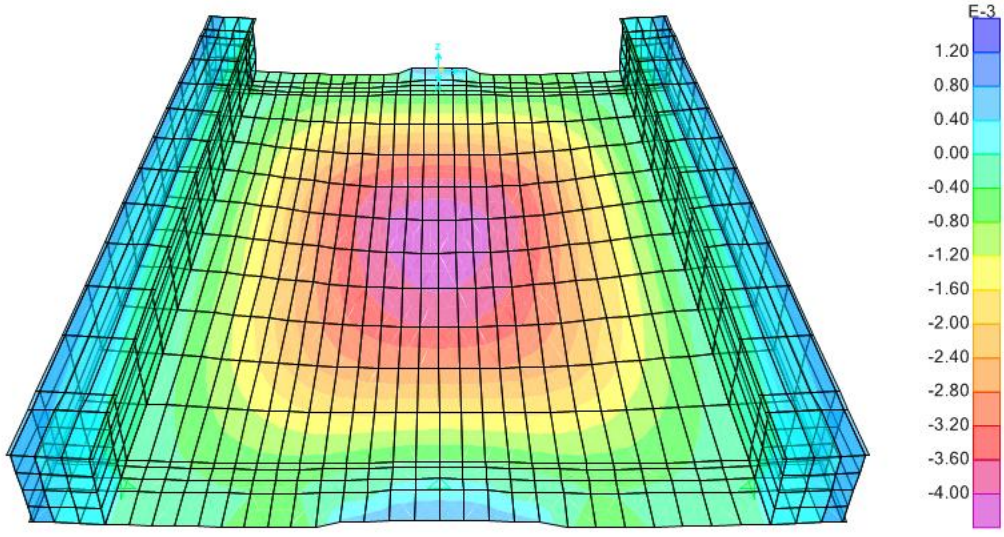

Type E: Speed 46 [m/sec]

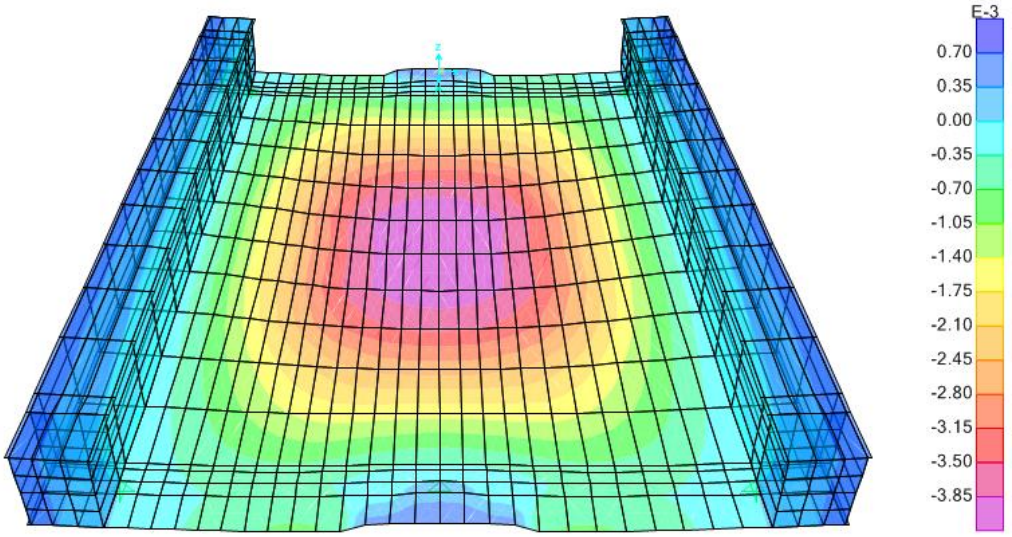

Type E: Speed 53 [m/sec]

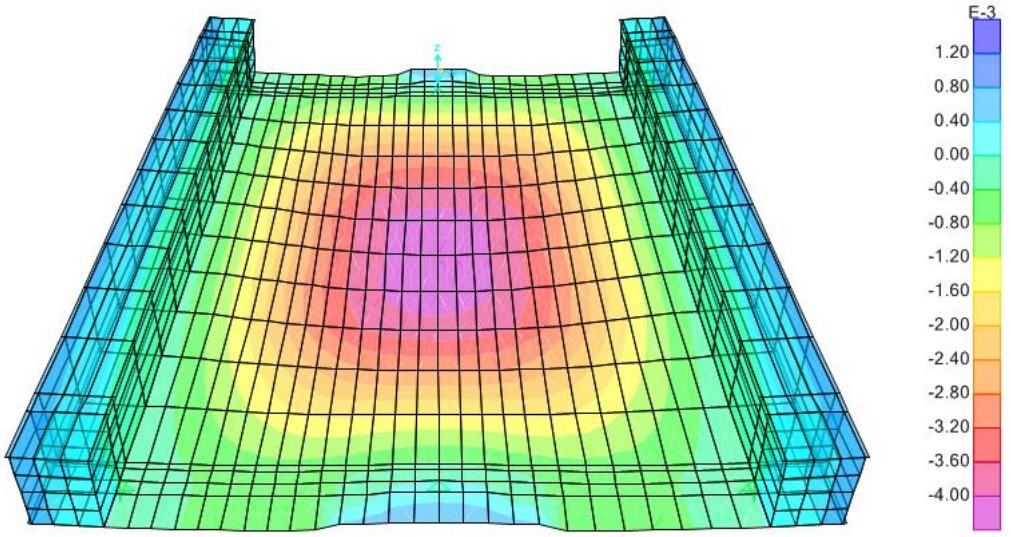

Type F: Speed 10 [m/sec]

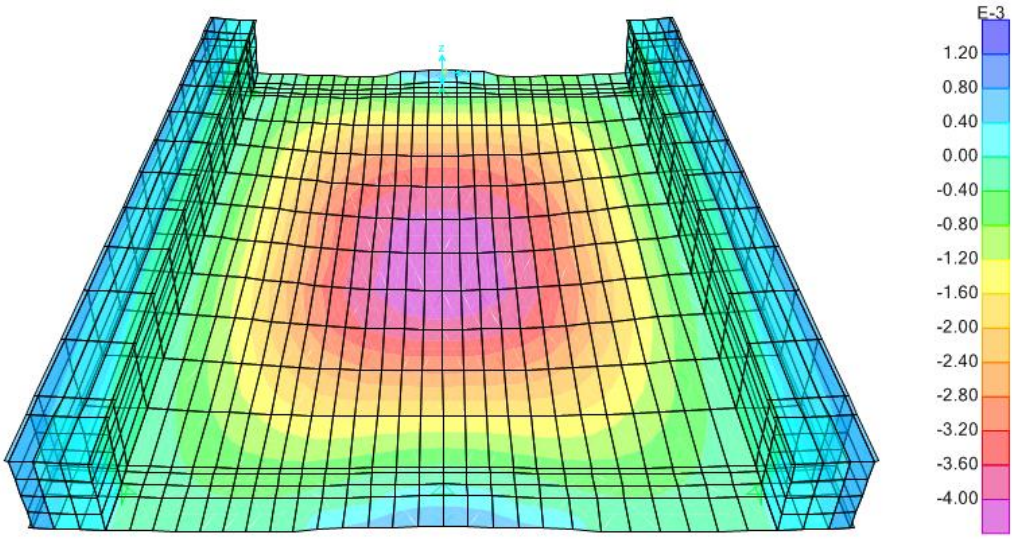

Type F: Speed 20 [m/sec]

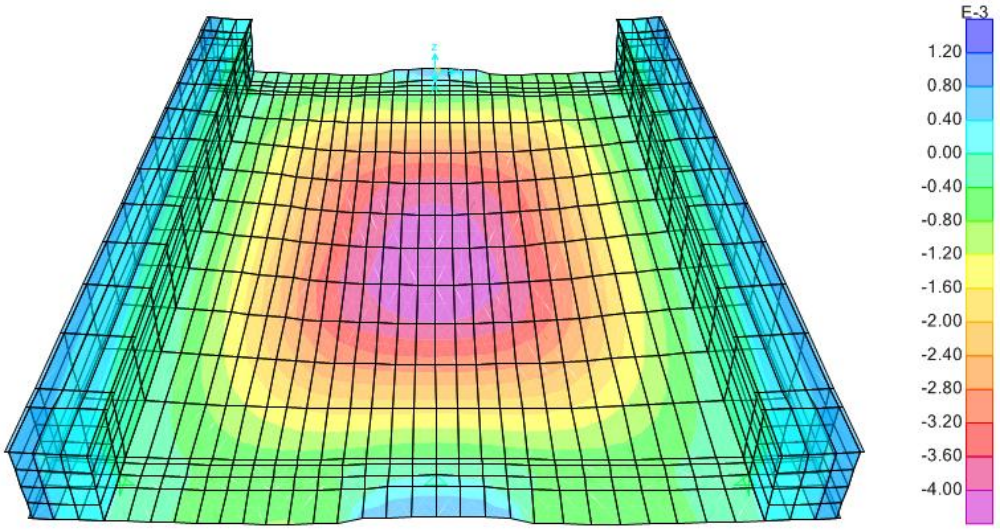

Type F: Speed 30 [m/sec]

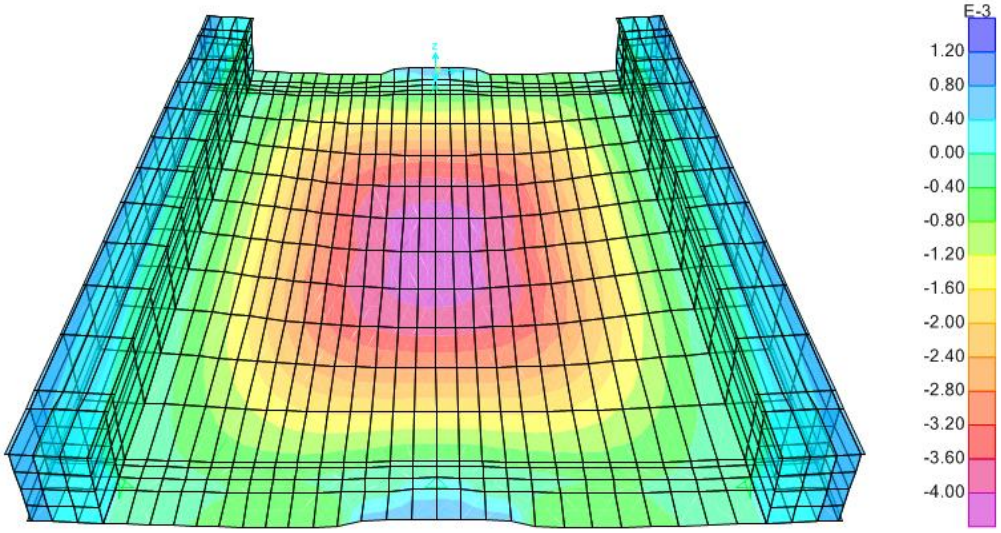

Type F: Speed 40 [m/sec]

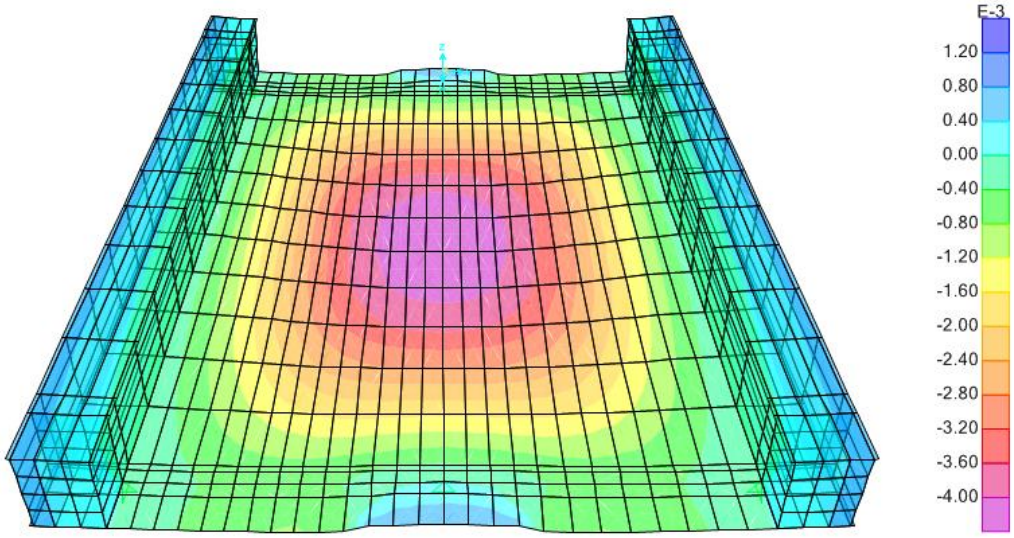

Type F: Speed 46 [m/sec]

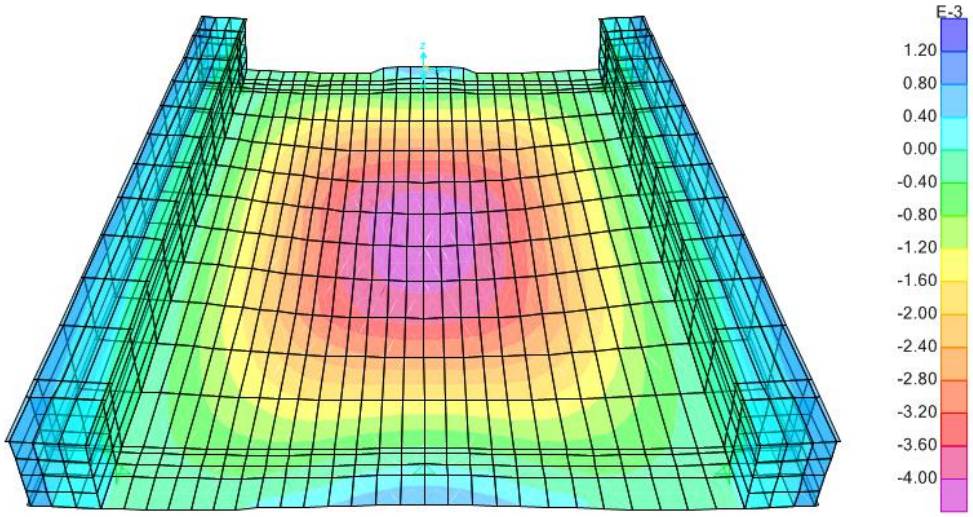

Type F: Speed 53 [m/sec]

10) Annex B

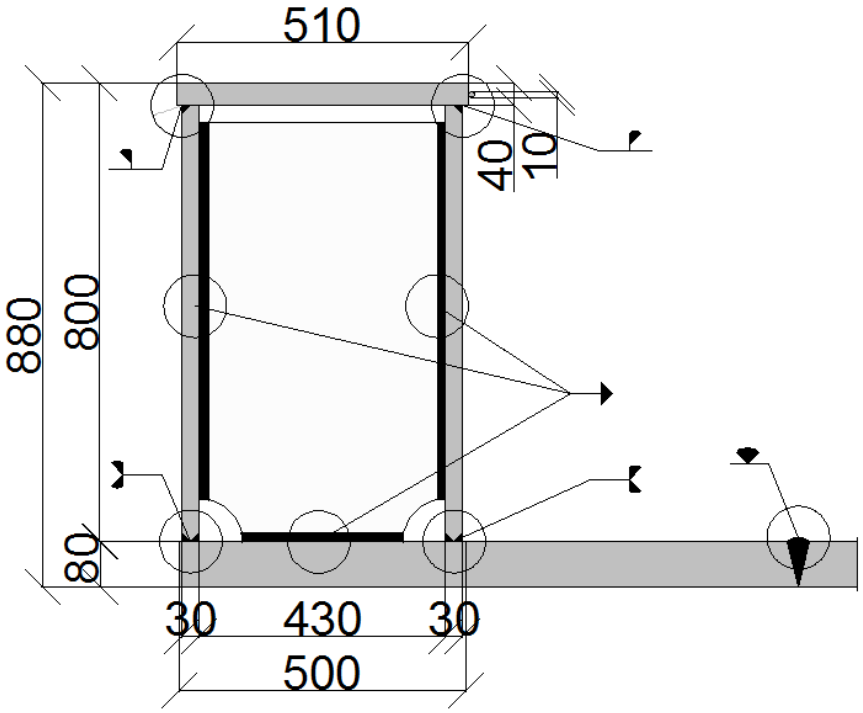

Figure 131 Details of the weldings involved in the assembling of the box girder

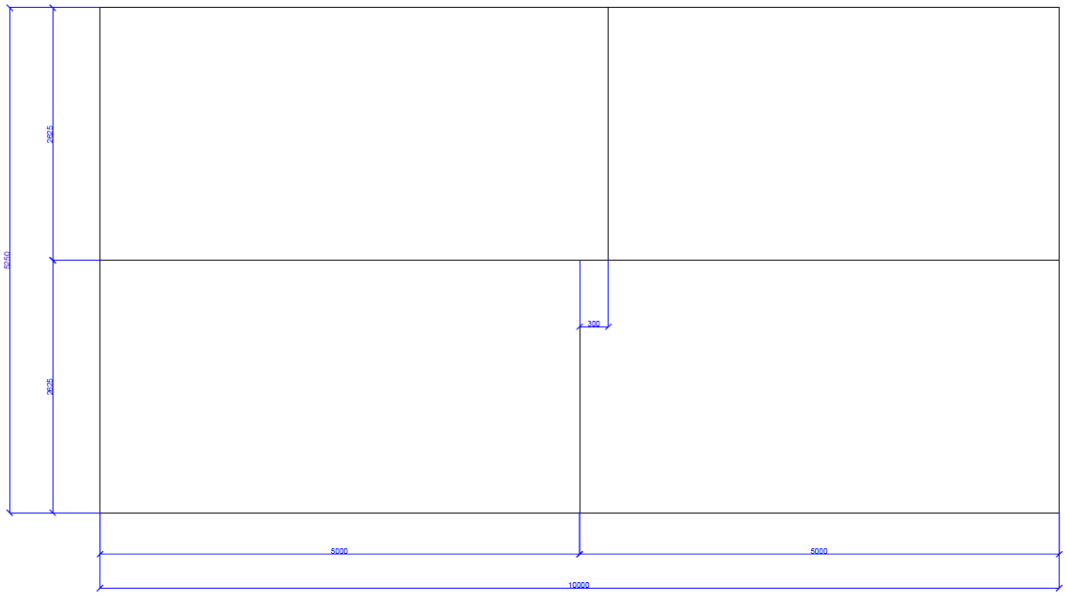

Figure 132 Assembling of the deck

The deck is composed of four smaller plates, all welded together. In the middle, there's a gap of 300 mm to avoid crossing of more weldings that would make them weaker for fatigue.

11) Conclusions

After all this deep static and dynamic analysis, it is possible to draw some conclusions. It was proven that for every structure the best choice to take into the designing of this kind of bridges is using three bearings, due to the fact that two are not enough and the deck will be too thick, resulting far more expensive; as far as the four bearing structure, we can say that the improvement brought by the fourth bearing is not worth the money to install it.

One other thing that is proven to be a better solution, is the use of a end cross slab instead of an end cross beam, since it is far cheaper and faster to produce (it can be obtained from the same plate of the deck since the thickness and material and geometry are the same).

If the purpose is to design a bridge with a 6 meters span, two choices are available and equally valid; this choice is about the thickness of the deck, whether to make it 65mm or 80mm.

The main difference here is the comfort criteria that the designer wants to reach.

In order to have the better comfort, hence $1.00\ [\frac{m}{sec^2}]$ as deck acceleration, the 80mm thick deck has to be used; if the purpose is saving some money and the comfort is not that important ($1.30\ [\frac{m}{sec^2}]$ as deck acceleration) the 65mm thick deck may be used.

In the 10 meters span structure, there are not many choices available in the design, since the structure with end cross slab and three bearings is the only possibility in this context.

Regarding the 15 meters span bridge, there's also a choice to be made.

Since in the first analysis (hence with normal height of the main girders) only 2 cases out of 36 are not verified and those were with high speeds (53 m/sec) , we can decide either to forbid the trains to go through that bridge at high speeds, or we improve the structure with higher main girders.

12) Literature

- *"EUROCODE 1: Actions on structures – Part 2: Traffic loads on bridges"*
- Univ. Prof. DI Dr. techn. Josef Fink - Univ. Ass. DI Paul Herrmann - Univ. Ass. DI Lukas Juen , *"Extremely slender steel-concrete composite deck slab for railway bridges"*
- *"Structurae: the largest database for Civil and Structural engineers"*
- *"Design guide for steel railway bridges"* published by the Steel Construction Institute
- *http://corporate.arcelormittal.com/*
- K.Lundin , A.Magnander , *"CHALMERS: Structural Analysis of a Typical Trough Bridge Using FEM" , 2012*
- *"Serviceability limits and economical steel bridge design"* by U.S Department of transportation, Federal Highway Administration, August 2011
- J.M.Goicolea , J.Dominguez , J.A.Navarro and F.Gabaldòn , *"New dynamic analysis metods for railway bridges in code IAPF and Eurocode 1"*
- L.Sanpaolesi , P.Croce , *"Guide to basis of bridge design related to Eurocodes supplemented by practical examples"*
- X.X.Dai , J.Y.Richard Liew , *"Fatigue performance of lightweight steel-concrete-steel sandwich systems"*
- K.M.A. Sohel, J.Y. Richard Liew , *"Steel–Concrete–Steel sandwich slabs with lightweight core — Static performance"*
- CSi Analysis Reference Manual